The effect of simvastatin on thromboxane-mediated contraction in porcine coronary artery: investigation of the role of mitochondria and extracellular calcium

Mohammed Nathem Saarti, MSc Pharmacology

School of Life Sciences

Faculty of Medicine and Health Sciences

University of Nottingham

Thesis submitted to the University of Nottingham

For the degree of Doctor of Philosophy

June 2019

Abstract

Cardiovascular diseases (CVDs) have a severe impact on human health, increasing the risk of morbidity and mortality. Atherosclerosis is one of the common caused of CVD because the plaques formed cause the affected arteries to narrow, leading to diminished blood flow, ischaemia and hence damage to organs. Statins (3-hydroxymethyl-3-methylglutaryl coenzyme A [HMG-CoA] reductase inhibitors) are one of the most well-known, effective and safe groups of drugs used for treating and preventing the recurrence of this condition. They decrease the incidence of disease (morbidity) and the rate of death (mortality). All statins act by inhibiting the conversion of HMG-CoA to mevalonic acid, which is responsible for the synthesis of cholesterol and consequently associated with a reduction in serum total and low-density lipoprotein (LDL) cholesterol. Statins are effective medications for the primary and secondary prevention of coronary heart disease (CHD). The overall beneficial effects of statins not only come from the reduction of cholesterol, but also come from cholesterol-independent effects known as pleiotropic effects.

Previous studies in the laboratory have indicated the statins, such as simvastatin, cause relaxation of blood vessels through inhibition of mitochondrial complexes. The data also indicated that simvastatin might act to reduce calcium influx through voltage gated calcium channels. However, it is not clear whether the effects on the mitochondria are related to the inhibition of calcium influx. Studies revealed that mitochondria are able to regulate intracellular calcium levels, and, therefore, influx through calcium channels. Furthermore, statins have also been reported to inhibit Rho kinase and ERK, both of which can regulate vascular tone. Although this has been linked to inhibition of isoprenylation, whether this is also related to the effects on the mitochondria is unknown. Therefore, the aim of this study was to determine the effect of simvastatin on U46619-induced contraction in porcine coronary artery (PCA) and to determine whether inhibition of mitochondrial function could underlie effects on calcium, Rho kinase and ERK. Comparisons were made with known mitochondrial complex inhibitors in order to understand how inhibition of mitochondrial complexes could regulate vascular tone.

The study showed that simvastatin inhibits the U46619-induced contraction in PCA only in the presence of calcium possibly via mitochondrial inhibition. The combination of inhibitors of mitochondrial complexes I and III (rotenone-myxothiazol) reduced this inhibitory effect while the combination of mitochondrial inhibitors rotenone-antimycin A enhanced the inhibitory effect of simvastatin. The combination of rotenone-myxothiazol prevented the inhibitory effect of simvastatin on the BAY K8644-induced contraction (L-type Ca^{2+} channel activator) suggesting that the effects of simvastatin on calcium-induced contractions may be due to mitochondrial effects.

The effect of mitochondrial complex III inhibitors, antimycin A and myxothiazol, were examined as a comparison with simvastatin. Antimycin A inhibits the contractile responses in PCA and this effect was mediated through inhibition of calcium influx through L-type calcium channels as well as via a calcium-independent pathway. Unlike simvastatin, the combination of rotenone-myxothiazol had no effect on the antimycin A inhibitory effect, suggesting differences between the mechanism of action of simvastatin and antimycin A. On the other hand, both simvastatin and myxothiazol inhibited the contractile responses in PCA only in the presence of calcium and the data suggest that the anti-contractile effects of both are mediated through inhibition of calcium influx through L-type calcium channels. The study showed that simvastatin, myxothiazol, and antimycin A inhibited $CaCl_2$-induced contraction and BAY K 4668-induced contraction. In addition, the nifedipine-induced relaxation was partially inhibited at the higher concentrations by simvastatin and myxothiazol but not antimycin A. These data suggest that inhibition of complex III at the Qo site, the site that can be blocked with myxothiazol, leads to inhibition of calcium influx through L-type calcium channels.

Finally, experiments on isolated mitochondria showed that simvastatin had no direct effect on the mitochondria, in contrast to previous studies in intact tissues and cells. Antimycin A and myxothiazol (complex III inhibitors) both changed the Rh123 fluorescence, indicating that they decreased the mitochondrial membrane potential.

As a conclusion, the data from the functional studies support the hypothesis that simvastatin produces anti-contractile effects through inhibition of the Qo site at mitochondrial complex III. The data also support the hypothesis that inhibition of complex III at the Qo site leads to inhibition of calcium influx through L-type calcium channels, although how this occurs is yet unknown.

Key words: simvastatin, antimycin A, myxothiazol, rotenone, U46619, ERK, Rho kinase, calcium, and mitochondria.

Abstracts for conferences

1. Saarti M, Roberts R (2016). Inhibition of mitochondrial complex III attenuates thromboxane-mediated contractions of porcine coronary artery through activation of AMP kinase. BPS Winter Meeting, London, Queen Elizabeth II Conference Centre. Poster presentation.

2. Saarti M, Randall M, Roberts R (2017). Simvastatin inhibits thromboxane-induced contraction in porcine coronary artery: role of extracellular calcium. BPS Winter Meeting, London, Queen Elizabeth II Conference Centre. Poster presentation.

3. Saarti M, Randall M, Roberts R (2018). Effect of Mitochondrial Complex Inhibitors Antimycin A, Myxothiazol and Rotenone on the inhibition of thromboxane- mediated contractions by simvastatin in porcine coronary artery. BPS Winter Meeting, London, Queen Elizabeth II Conference Centre. Poster presentation.

4. Saarti M, Randall M, Roberts R (2018). Coenzyme Q10 and Mitoquinol reverse the anti-contractile effect of Antimycin A but not Myxothiazol in porcine coronary artery. BPS Winter Meeting, London, Queen Elizabeth II Conference Centre. Poster presentation.

Acknowledgements

"O My Lord, increase me in knowledge" Quran 20:114

First and above all, I praise ALLAH the Most Gracious, the Most Merciful for providing me with the opportunity and the capability to proceed with my research.

I would like to express my sincere gratitude to my supervisors Dr. Richard Roberts and Dr. Michael Randall for the continuous support throughout my Ph.D. study, for their patience, motivation, enthusiasm, and immense knowledge. Their guidance helped me all the time of research and during the writing of the thesis. I could not have imagined having better supervisors for my Ph.D. study.

My deepest gratitude is also to Dr. Michael Garle, Liaque Latif, and Jagdish Heer, for being very helpful and for their great advice.

I would like to thanks my fellow lab mates in E34 laboratory: I would thank the opportunity that allows me to meet such friends: Thank you to all friends I have made in Nottingham.

I would like to acknowledge all staff and members in the University of Nottingham, School of Life Sciences.

I would also like to thanks the Higher Committee for Education Development (HCED) in Iraq for granting me a scholarship to pursue my higher education at the University of Nottingham.

I wish to thank my beloved mother, brothers, my aunt and my wife´s family for their continuous encouragement and help who were all patients during our long absence abroad.

A big thanks to my wife, my little children. I will never be able to pay my debt of gratitude in full.

Lastly, but most importantly, May Allah's peace and blessing be upon our Beloved Prophet Muhammad who said, *"Allah makes the way to Jannah easy for him who treads the path in search of knowledge."*

Dedication

To my beloved late father,

Nathem Mohammed Ali Hussein,

Who is his prayers and support had been instrumental in achieving my goals,

Yet had never the opportunity to see his dream comes true,

May his soul rest in peace.

Table of Contents

Table of Abbreviations

ADP	Adenosine diphosphate
AMPK	Adenosine monophosphate-activated protein kinase
ATP	Adenosine triphosphate
BSA	Bovine serum albumin
CHD	Coronary heart disease
CoQ	Co-enzyme Q
CRP	C-reactive protein
CVD	Cardiovascular disease
DMSO	Dimethyl sulphoxide
ER	Endoplasmic reticulum
ERK	Extracellular Signal-Regulated Kinase
ETC	Electron transport chain
FCCP	Carbonyl cyanide-4-(trifluoromethoxy) phenylhydrazone
FADH2	Flavin adenine dinucleotide
FPP	Farnesyl pyrophosphate
GBD	Global Burden of Disease
GPRD	General Practice Research Database
GPP	Geranylgeranyl-pyrophosphate
GPX	Glutathione peroxidase
HCED	Higher Committee for Education Development
HDL	High-density lipoprotein
IMM	Inner mitochondrial membrane
LDL	Low-density lipoprotein
LECA	Leukocyte-endothelial cell adhesion
MAPK	Mitogen-activated protein kinase
MEK	Mitogen extracellular kinase or Mitogen-activated protein kinase kinase
MLC	Myosin light chain
MLCK	Myosin light chain kinase

MLCP	MLC phosphatase
MPT	Mitochondrial permeability transition
MYPT	Myosin phosphatase target
NADH	Nicotinamide adenine dinucleotide, reduced form
NOS	Nitric oxide synthase
OMM	Outer mitochondrial membrane
PCA	Porcine coronary artery
RCA	Rat caudal artery
RNS	Reactive nitrogen species
ROCC	Receptor-operated calcium channel
ROS	Reactive oxygen species
SM	Smooth muscle
SMC	Smooth muscle cells
SOD	Superoxide dismutase
SOCC	Store-operated calcium channel
SR	Sarcoplasmic reticulum
VDAC	Voltage-dependent anion-selective channels
VGCC	Voltage-gated calcium channel
VLDL	Very low-density lipoprotein
VSMC	Vascular smooth muscle cell

Chapter I

General introduction

1.1. Cardiovascular disease (CVD):

Cardiovascular disease is a serious worldwide problem and it is one of the most common caused of death in the world (Van Hemelrijck et al. 2016). There are many types of CVD but the main four types are coronary heart disease (CHD), strokes, peripheral arterial disease, and aortic disease (Criqui et al. 2016). As assessed by the Global Burden of Disease Study (GBD) in 2010, ischaemic heart disease and stroke were the main caused of death (Lozano et al. 2012). The incidence of CVD has decreased in the last few years in high-economic countries (Feigin et al. 2009) while in low and middle- economic countries the rate is still rising and those countries represent about 80% of the worldwide population (O'Flaherty, Buchan, and Capewell 2013). In a comparison study performed in England for the incidence of CHD, which is the most common subtype of CVD, between 1999 and 2007, the General Practice Research Database (GPRD) identified that there was a reduction in the incidence of CHD from 1.74 million CHD patients in 1999 to 1.53 million CHD patients in 2007 in men over 25 years old (Pearson-Stuttard et al. 2012). A recent study showed that the caused of decline in the rate of mortality and morbidity in people with CVD are the better lifestyle of patients, increased admission to hospitals without delay, especially people with high-risk factors, and receiving proper acute treatment as soon as possible after diagnosis followed by prophylaxis treatment (Asaria et al. 2017). Although the rate or the incidence of CVD decreased in the UK by 52% between 1990 and 2013 according to the Global Burden of Disease (GBD) study, CVD is still the second cause of death (Newton et al. 2015).

There are many risk factors for CVD and they are divided into two types; factors that can be modified by changing lifestyle such as smoking, drinking alcohol, diet, and exercise. The second types of risk factors are those that cannot be modified or changed such as a person's age, family history (genetics) and cultural factors, including nationality (ethnicity). Additional, well known caused of CVD are hyperlipidaemia, hyperglycaemia, hypertension, obesity, and others. (Nangia, Singh, and Kaur 2016). Studies showed, using the British Heart Foundation Data and American Heart Association Data that the rate of death from CVD has declined but the disease incidence is still considerably high due to the presence of these risk factors, especially the non-modifiable risk factors (Roger et al. 2011). Age could be considered the most important one for obvious reasons, as older people are usually associated with a higher risk of CVD (Dhingra and Vasan 2012).

CVD has many complications and the most common are chest pain, heart attack, heart failure, and cardiac arrhythmias. The main problem in all of them is the narrowing of blood vessels that lead to inadequate blood flow, which mostly occurs due to an accumulation of fatty deposits inside the walls of blood vessels leading to an atherosclerotic plaque. Furthermore, if a plaque ruptures, it may lead to platelet aggregation that can occlude the

blood vessel, blocking the blood supply to the heart, causing a heart attack, or it can block the blood supply to the brain, causing a stroke (Lewington et al. 2007). Thus, educating healthy people and patients about these predisposing factors and treat the underlying caused or diseases followed with prophylaxis are the key things for saving a life and preventing or reducing the recurrence (Boehme, Esenwa, and Elkind 2017).

1.1.1. Hyperlipidaemia:

Hyperlipidaemia is characterized by an abnormal elevation in fat (lipid) in the blood. This lipid can accumulate in the blood vessels leading to narrowing in blood vessels and reducing blood supply to organs, which then increases the risk for CVD. There are two types of lipid abnormalities in the blood, abnormal elevation of cholesterol (hypercholesterolemia) and abnormal elevation of triglycerides (hypertriglyceridemia) (Sun et al. 2018).

Cholesterol is synthesized mainly in the liver. As it is not soluble in water, a carrier is required to transport cholesterol in the blood stream. Cholesterol is transported to peripheral tissues in low-density lipoprotein (LDL) and is transported back to the liver in high-density lipoprotein (HDL) (Iglesias et al. 1996). Lipoproteins are particles formed in the liver that are composed of triacylglycerol (TAG), cholesterol, phospholipids and amphipathic proteins called apolipoproteins. The centre of a lipoprotein is composed of cholesteryl esters, triglycerides, fatty acids and fat-soluble vitamins, like Vitamin E, while the outer layer is composed of a water-soluble layer of apolipoproteins, phospholipids and cholesterol (Yu and Cooper 2001). They are responsible for transport of cholesterol and other fats in the bloodstream to different organs in the body. They are classified according to the ratio of lipid to protein, the higher the density of a lipoprotein, the less lipid it contains relative to protein. There are four main kinds of lipoproteins: chylomicrons, very low-density lipoprotein (VLDL), LDL, and high-density lipoprotein (HDL) (Cain et al. 2005).

Cholesterol is important for cell membrane synthesis and some hormones, and the liver supplies the body with the amount of cholesterol required, therefore there is no need to take it from the diet (Favari et al. 2015). When cholesterol levels are elevated above the normal (>200 milligrams per decilitre), LDL-cholesterol will deposit in the arterial wall forming a plaque. Enlargement of this plaque caused narrowing of the artery; this is the first stage of what is called atherosclerosis. Unfortunately, hyperlipidaemia is symptomless. Thus, the only way to detect it is by regular checking of serum lipid or lipid profile that includes total cholesterol, LDL cholesterol, HDL cholesterol, and triglycerides in people with high-risk factors (Zarate et al. 2016). Treatment of hypercholesterolaemia requires reducing the cholesterol level either via life style changes such as a healthy diet (reduction in saturated fat intake) and increased exercise or through medical approaches via using

antihyperlipidemic medication such as statins, bile-acid-binding resins, fibrates, niacin, or cholesterol absorption inhibitors (Mytilinaiou et al. 2018).

1.2. Statins:

Statins have grown into one of the most important debated groups of medicines in usage today (Lopez-Jimenez et al. 2014). The discussion of whether statins are harmless to some extent has been raised since their introduction in 1987 (Jukema et al. 2012). Statins are usually well tolerated and are thought to have few side effects. However, separate and specific rare unwanted effects have been reported, such as increased liver enzymes, muscle pains, and very infrequently, rhabdomyolysis (the breakdown of muscle tissue). Termination of the use of the statins generally leads to resolving these unwanted actions. Recently, the discussion has concentrated on the probable negative long-term side effects of statin treatment on the loss of memory and the occurrence of cancer (Sun et al. 2015; Jukema et al. 2012). The U.S. Food and Drug Administration has introduced the possibility of patients developing cognitive impairment due to statins therapy (Schultz, Patten, and Berlau 2018). Another study stated that specific statins could be responsible for the development of cancer in mice (Newman and Hulley 1996).

In contrast, a number of results related to clinical studies found that statins and other groups of anti-hyperlipidaemic drugs have anticarcinogenic effects (Davidson 2001). Moreover, there are many studies that recommend using statins as one of the most effective anti-hypercholesteraemic medications to prevent many CVDs and its consequences in patients with elevated cholesterol but have no history of cardiac diseases (i.e. as primary preventer). Furthermore, in 2013, a Cochrane review established that statins have significant ability in reducing the rate of mortality with minor adverse effects and no evidence of severe side effects (Taylor et al. 2013). Additionally, in a review in 2010 that analysed the use of statins to decrease the level of cholesterol in patients with no history of heart disease showed that there was a substantial inhibition of the development of CVD in males, but not in females and no reduction in the rate of death in both genders (Petretta et al. 2010). On the other hand, Kostis et al., (2012) found that statins have beneficial effects in preventing CVD in both males and females. These results were obtained from a study conducted on 138 patients treated with statins, some of them had no previous history of cardiac problems and others had, and the percentage of efficacy was 60% (Kostis et al. 2012). Recent cohort study included 46 864 participants (mean age 77 years; 63% women; median follow-up 5.6 years) showed that statin have the ability to reduce the rate of atherosclerotic cardiovascular disease and mortality significantly in diabetic patients (Ramos et al. 2018).

Although there is controversy about giving statins to patients without existing heart disease as prophylaxis, statins are considered as one of the well-known medications for the treatment of hypercholesterolemia as their efficacy has been demonstrated in different age groups of patients such as young and elderly patients (Altieri 2001; Soedamah-Muthu et al. 2015). Moreover, their effectiveness has been explored in both males and females through large numbers of studies, for example, case-control and observational studies such as the Heart Protection Study of cholesterol lowering with simvastatin in 20,536 high-risk individuals and the effect of very high-intensity statin therapy on regression of coronary atherosclerosis: the Asteroid trial (Hung et al. 2013). Additionally, statins have a good safety profile because they usually have mild side effects like headache, nausea, fatigue and gastrointestinal disturbance to moderate adverse effects like muscle pain, changes in a liver enzyme and kidney disorder (Orsi, Sherman, and Woldeselassie 2001; Bellosta and Corsini 2018). Most of these side effects can disappear gradually after cessation of statins and the patient would return to normal without any side effect (Dujovne 2002). The possibility of developing these adverse effects is more likely to come from long term use or/and with high doses of the drug (Bleda et al. 2011).

1.2.1. Pharmacokinetics:

All statins are given orally and they are well absorbed through the intestine. All of them, with the exception of pitavastatin, undergo extensive first-pass metabolism which reduces the bioavailability of these drugs to 50% (Gotto and Moon 2010; Garcia et al. 2003). All statins are given as an active metabolite (β-hydroxy-acid), except simvastatin and lovastatin, which are administered as inactive (pro-drugs) that need hepatic enzyme metabolism to convert them to the active form. The metabolic pathway for most statins is mainly through cytochrome P450 (for simvastatin and lovastatin is through isoform CYP3A4) (Schachter 2005). On the other hand, pravastatin is metabolized mostly via sulphation, whilst up to 90% of rosuvastatin is exported through biliary excretion (Garcia et al. 2003; Quion and Jones 1994). Therefore the pharmacological activity of statins mainly depends on the parent agents and the active metabolite (Garcia et al. 2003).

The hydrophobicity of each agent of the statins group plays an important role in explaining the pharmacokinetics. Pravastatin, which is the most hydrophilic compound, usually requires active transport into the liver and therefore the rate of metabolism via the cytochrome P450 (CYP) family is very little and excreted by active renal excretion. In contrast, the more lipophilic compounds are transported by passive diffusion and are better substrates for both CYP enzymes and transporters involved in biliary excretion.

1.2.2. Mechanism of action:

Statins, which are analogues of HMG-CoA, act primarily as anti-hypercholesteraemic drugs by competitive and reversible inhibition of HMG-CoA reductase and thereby preventing HMG-CoA from accessing the active site. HMG-CoA reductase is the enzyme that is responsible for the transformation of HMG-CoA to L-mevalonate (which is the precursor of cholesterol; see figure 1.1) and in that way, statins inhibit the rate-limiting stage in the synthesis of cholesterol (Istvan and Deisenhofer 2001; Schachter 2005). As a result, statins inhibit the endogenous synthesis of cholesterol. The consequence of the reduction of cholesterol concentration within hepatocytes is the up-regulation of LDL-receptor expression, which stimulates the uptake of LDL and LDL-precursors from the body. Accordingly, statins indirectly enhance the removal of LDL from the blood beside their action as inhibitors of cholesterol biosynthesis (Brown and Goldstein 1986; McFarland et al. 2014). Statins also have another mechanism of action, which is the reduction of lipoprotein, through the reduction of both hepatic production of Apo lipoprotein B100, and the synthesis of triglyceride-rich lipoproteins (Ginsberg et al. 1987; Grundy 1998; McFarland et al. 2014). As a result, the effect of statins can be summarized by reductions in total serum level of cholesterol, LDL, and triglycerides, and an increase in HDL. Finally, statins can be divided into one of two groups (although different agents of statins group have the same mechanism of action) which are a group I, fungal-derived statins (lovastatin, pravastatin, simvastatin); or group II, synthetically-derived statins (fluvastatin, cerivastatin, atorvastatin, rosuvastatin, pitavastatin). Group II statins are completely synthetic inhibitors of HMG-CoA reductase and show greatly varied pharmacokinetic properties, including differences in metabolism, excretion, half-lives, bioavailability, dosing times and lipophilicity (McFarland et al. 2014).

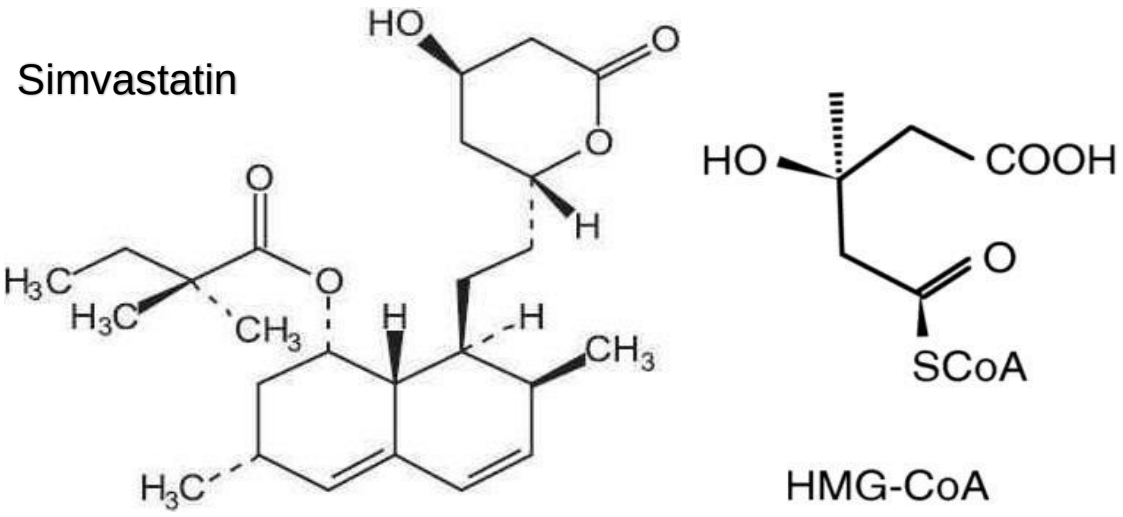

Figure 1.1: Chemical structure of simvastatin: simvastatin (left) have a lactone ring similar to HMG-CoA biologically active moiety (right). Adapted from (Wang and Asgharnejad, 2000).

1.2.3. Pleiotropic effect of statins:

Statins are effective medications for the primary and secondary prevention of CHD (Sever et al. 2003). The overall beneficial effects of statins not only come from the reduction of cholesterol but also come from cholesterol-independent effects known as pleiotropic effects (Alinski and Tsimikas, 2002). All statins act by inhibiting the conversion of HMG-CoA to mevalonic acid, which is an intermediate on the synthesis pathway of cholesterol and consequently associated with a reduction in serum total and low-density lipoprotein (LDL) cholesterol (Andrews et al. 2001). Furthermore, through inhibiting L-mevalonic acid synthesis, other important mediators in the cholesterol synthetic pathway are also prevented from being synthesized by statins (see figure 1.2) such as the isoprenoid intermediates farnesyl pyrophosphate (FPP) and geranylgeranyl pyrophosphate (GGPP) (Goldstein and Brown 1990). These intermediates have a significant role in isoprenylation of proteins, converting them from inactive to active by translocation from the cytoplasm to the cell membrane by working as lipid attachments for the posttranslational modification of a variety of proteins, including the small guanosine triphosphate (GTP)-binding protein Ras; and Ras-like proteins, such as Rho, Rab, Rac, Ral, or Rap (Van Aelst and D'Souza-Schorey 1997). Additionally, both Ras and Rho are examples of small GTP-binding proteins, which reversibly convert from the inactive GDP-bound state to active GTP-bound state (Hall 1998).

Small GTP-binding proteins have essential roles in the regulation of cell growth and differentiation, gene expression, vasoconstriction, inflammation, oxidation, cell motility, protein and lipid trafficking, nuclear transport, and subcellular localization (Takai, Sasaki, and Matozaki 2001; Laufs and Liao 2000). Farnesylation is the key for Ras translocation from the cytoplasm to the plasma membrane, while Rho translocation is reliant on geranylgeranylation (Bellosta et al. 1998; Laufs and Liao 2000).

Some of the pleiotropic effects of statins on the wall of the blood vessels come from the mechanism that involves the inhibition of geranylgeranylation of Rho and therefore inhibition of activation of Rho-kinase (ROCK) (Laufs et al. 1999; Takemoto et al. 2002). Ras is upstream of ERK-MAP kinase activation, which is involved in both smooth muscle contraction and smooth muscle growth. Therefore, prevention of the activation of Ras could lead to inhibition of smooth muscle contraction and growth (Roberts 2012).

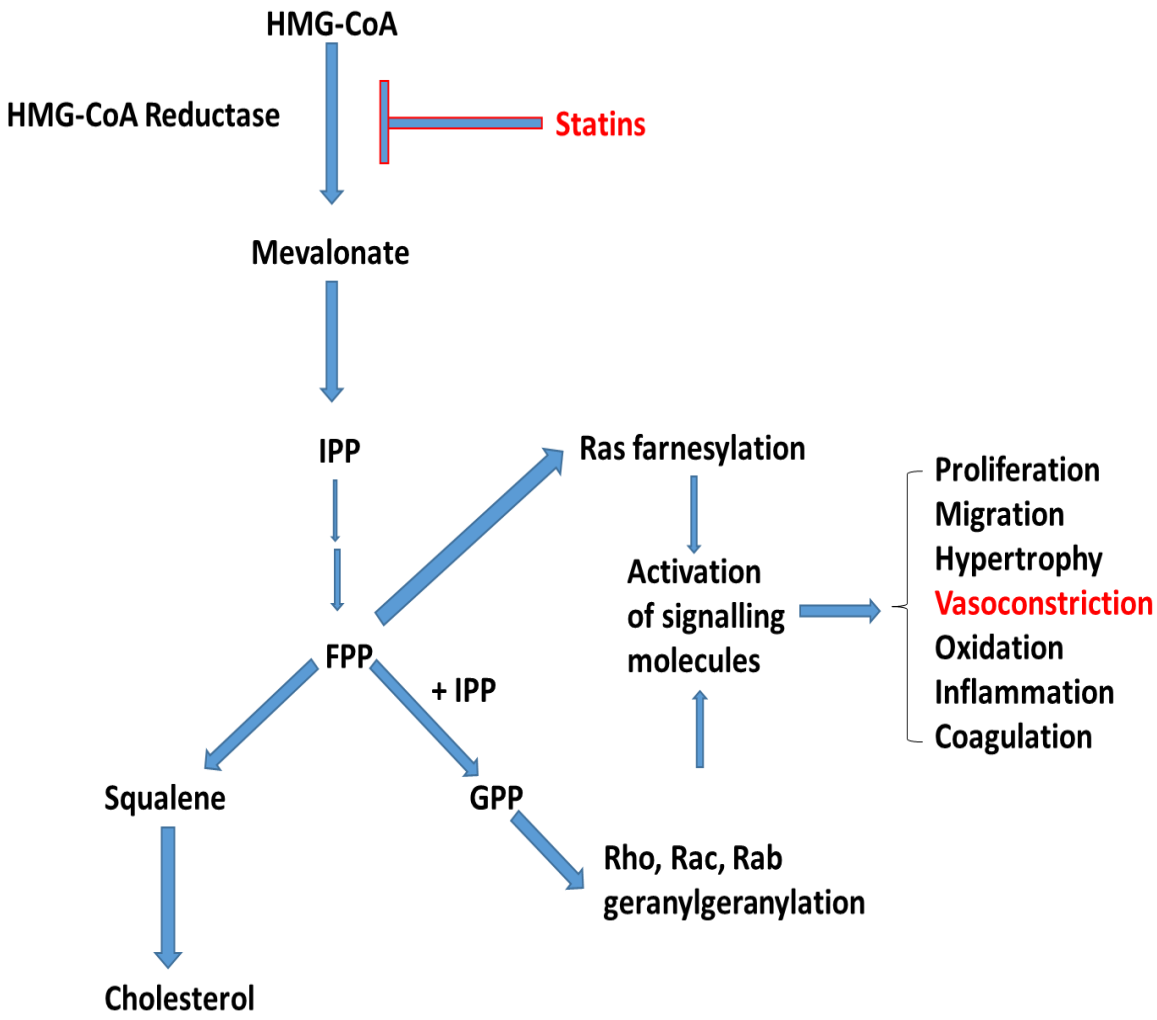

Figure 1.2: Cholesterol biosynthesis pathway and site of statins action. Statins inhibit HMG-CoA reductase. Thus, statins decrease isoprenoid intermediates such as farnesyl pyrophosphate (FPP) and geranylgeranyl-pyrophosphate (GPP), with subsequent inhibition of isoprenylation of the small GTPases such as Ras, Rho, and Rac1. Adapted from (Rikitake and Liao, 2005) with modification.

There are many examples of the pleiotropic effect of statins:

1- The effect of statins on endothelial nitric oxide synthase (NOS), which is a vital enzyme in the physiological and pathophysiological responses of the vascular endothelium (Mihos, Salas, and Santana 2010). It has been revealed by Ming et al. (2002) in human umbilical vein endothelial cells (HUVECs) and human SMCs, that the Rho/Rho kinase pathway inhibits NO production. Using Western blotting, the researchers found that there was a reduction in eNOS expression after enhancing the expression of active Rho (Rho63) or active ROCK (CAT). Another study showed that direct inhibition of ROCK such as using Y27632 caused an enhancement in expression of eNOS mRNA (Rikitake et al. 2005). Studies showed that activity and stability of Rho could be modulated by statins via inhibition of geranylgeranyl pyrophosphate, which is the required isoprenoid for activating

Rho proteins (Pedrini et al. 2005; Rikitake and Liao 2005; Vosper et al. 2015). On the other hand, the bioavailability of NO can be modified by statins by preventing the isoprenylation of Rho that leads to either enhancing eNOS activity (rapid effect) or increasing mRNA expression (late effect). Consequently, chronic use of statins leads to enhancement of NO bioavailability (Koh 2000).

2- The anti-inflammatory effect of statins, which comes from the ability of statins to reduce the concentration of inflammatory biomarkers (Blanco-Colio et al, 2003), such as C-reactive protein (CRP), which is responsible for reduction of NO production from endothelium (Zhou et al. 2010) and increase in the endothelial expression of adhesion molecules (Sadeghi et al. 2000; Dimitrova et al. 2003). The vital step in atherosclerosis (which is a complex inflammatory process) is leukocyte-endothelial cell adhesion (LECA), which is enhanced by adhesion molecules such as P-selectin, and they are responsible for the organ dysfunction and tissue injury associated with these diseases. Furthermore, Wojciak et al (1999) revealed that isoprenylated protein Rho is essential for integrin-dependent adhesion of leukocytes to the endothelium and because the isoprenylation (activation) of Rho is a part of mevalonate pathway, which inhibited by statins, so the statins will inhibit the adhesion (at least partly) and exert its anti-inflammatory effect (Kwak and Mach 2001).

3- The reduction of blood pressure through regulation of dilation or constriction of blood vessels (Ali et al. 2016). Several studies have revealed that statins could modulate the activities of different ion channels of blood vessels such as calcium channels (Kajinami, Mabuchi, and Saito 2000; Bergdahl et al. 2003; Sonmez Uydes-Dogan et al. 2005).

A study performed on rat aorta demonstrated that simvastatin could inhibit VSMC contraction via inhibiting the release of calcium from intracellular stores and via blocking calcium influx. This inhibitory effect could be related to the inhibition of isoprenoid proteins such as Rho and p21 Rac that might involve in the communication between calcium entry and calcium release (Alvarez de Sotomayor et al. 2001). Other study performed on porcine coronary artery smooth muscle cells showed that simvastatin at low concentrations (1-3μM) inhibited BK_{Ca} channels (iberiotoxin-sensitive Ca^{2+}-activated K^+ channels) mediated via isoprenoid inhibitory effect, while statins at higher concentration (10μM) inhibited the BK_{Ca} channels via enhancing the activity of protein kinase C (PKC) (Seto et al. 2007). The insufficient isoprenylation of proteins due to inhibition of mevalonate pathway by statins could lead to inactivation of isoprenoid proteins such as Rho A, Rac and Ras that end with insufficient phosphorylation of myosin light chain (MLC) (Bayguinov et al. 2011). A study that is more recent revealed that adding mevalonate and geranylgeraniol (GGOH) could antagonise the inhibitory effect of simvastatin on voltage gated calcium channels (VGCC)

that regulate Rho A–mediated contraction and intracellular calcium signalling (Kang et al. 2014). The study also confirmed what others previously identified about the contribution of Rho A in simvastatin-inhibited calcium increases (Tesfamariam, Frohlich, and Gregg 1999; Bergdahl et al. 2003) due to the importance of Rho-A/ROCK pathway in the regulation of Ca^{2+} (Pochynyuk et al. 2006; Villalba et al. 2008). Accordingly, statins could inhibit VSMC contraction via affecting calcium channels and/or inhibiting calcium influx.

4- Other important pleiotropic effects of statins, which are valued in CVD, are down-regulation of angiotensin receptor synthesis (Ichiki et al. 2001) reduction of VSMC proliferation and migration (Corpataux et al. 2005), inhibition of platelet aggregation and stabilization of atherosclerotic plaque (Libby 2001).

1.2.4. Statins and co-enzyme Q10:

Inhibition of the mevalonate pathway by statins inhibits the synthesis of important mediator compounds such as ubiquinone (co-enzyme Q10), which has an important role in energy production and regulation oxidative-phosphorylation process in addition to its antioxidant effect (Kumar et al. 2009). Co-enzyme Q10 (CoQ10) can be synthesized in the body but it does not meet the physiological requirement of the body. Thus, the body can get more from oral supplementation and from food rich in cholesterol such as meat, fatty fish, some fruits and vegetables (Acosta et al. 2016). A study showed that treatment with simvastatin and pravastatin reduced CoQ10 levels by 50% after 12 weeks of treatment in both normal people and patients with hypocholesteraemia. On the other hand, the study showed that people respond well to oral CoQ10 replacement therapy and CoQ10 could go back normal (Ghirlanda et al. 1993). Studies showed that the reduction in CoQ10 level due to use of statins could be severe in patients who have an increased rate of lipid peroxidation (Halliwell 2000), and impaired biosynthesis of the quinone moiety (Matthews et al. 1998). An animal study performed on dog, hamster, mini pig and monkey revealed a reduction in tissue and serum level of CoQ10 after statin therapy. Most of these studies were performed on animals with different age groups and on those with and without cardiac problem (Littarru and Langsjoen 2007). Human studies showed that 80 mg oral dose of atorvastatin per day could reduce CoQ10 within 14-30 days (Rundek et al. 2004). Another study showed that there was a 40% reduction in CoQ10 level after treatment with 20 mg simvastatin and/or pravastatin (Ghirlanda et al. 1993). Researchers have also found that the reduction in CoQ10 level after 8 weeks of treatment with 80 mg simvastatin per day could be associated with mitochondrial dysfunction (Paiva et al. 2005). In contrast, a previous study revealed that there was no significant reduction in CoQ10 level after treatment with 20 mg simvastatin for 6 months (Laaksonen et al. 1996). A study performed on hypercholesteraemic patients clarified that the age of patient could have an important role besides the dose and duration of statin treatment. Moreover, animal studies showed that

the reduction in CoQ10 level in response to statins and energy production by mitochondria is more common in older animals (Diebold, Bhagavan, and Guillory 1994). Human studies showed that there is an elevation in demand for CoQ10 in elderly people especially those over 70 years. In a study performed to measure the contractile force in myocardium trabecular tissue, there was a reduction in CoQ10 level, which was associated with a reduction in contractility performance as well (Rosenfeldt et al. 1999).

Accordingly, these studies possibly indicate that the statin medications could routinely result in lower coenzyme Q10 levels in the serum and sometimes in muscle tissue. In addition, the mechanism for a statin to induce myopathy might be the consequence of this reduction in CoQ10 level (Marcoff and Thompson 2007), although, CoQ10 supplementation sometimes could resolve the problem.

1.3. Structure of blood vessels:

Blood is transported in the body inside channels or tubes known as blood vessels. Depending on their structure and function, there are three types of vessels; arteries, veins, and capillaries (Parker et al. 1988). These vessels form two complicated systems that start from the heart and end at the heart. The first one is the pulmonary vessels, which carry the blood from the right ventricle to the lungs while the second is the systemic circulation, which carries the blood from the left ventricle of the heart to all parts of the body then back to the right atrium. The arteries are responsible for transporting the oxygenated blood to all body parts while the veins are responsible for carrying back the non-oxygenated blood from all body tissue to the heart (Smith et al. 1998).

The wall of an artery is composed of three layers; the outer layer is the tunica adventitia (tunica externa) and it is composed of connective tissue with different amount of elastic and collagenous fibres. This layer is usually responsible for connecting the vessel with the surrounding tissues. The middle layer the tunica media is composed mainly of smooth muscle, which is usually the thickest layer. This layer is responsible for changing vessel diameter to regulate blood flow and blood pressure, in addition to providing support to the vessel. The third layer is the tunica intima (tunica interna) and is composed of simple endothelium surrounded by a connective tissue basement membrane with elastic fibres (Nichols et al. 1980; Kieler-Jensen, Lundin, and Ricksten 1995). See figure 1.3.

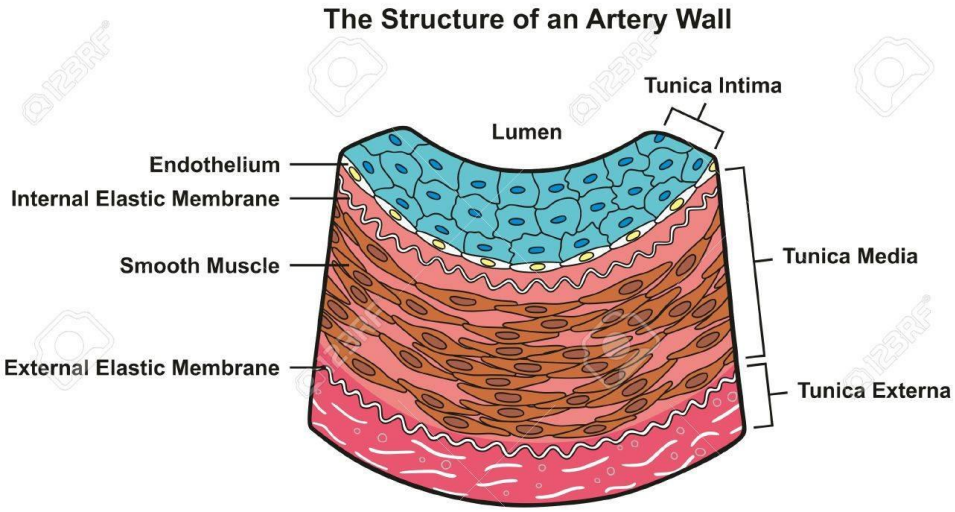

Figure 1.3: Structure and composition of the blood vessel. The innermost layer is made up of endothelial cells, followed by the internal elastic lamina and vascular smooth muscle cells. Figure adapted from anatomy and physiology (2016).

1.3.1. Vascular Smooth muscle cells (VSMCs):

Smooth muscle (SM) is one of the important types of muscles in the body of human and animals. SM cells are longitudinal in shape with central nuclei and are described as non-striated cells because their actin and myosin filaments are not connected to Z lines but organized by connection to dense bodies (figure 1.4). They mainly range from 5 to 10 μm in diameter and 30 to 200 μm in length. They are usually located within the walls of hollow organs such as blood vessels, airways, gastrointestinal tract, and bladder (Gabella 2012).

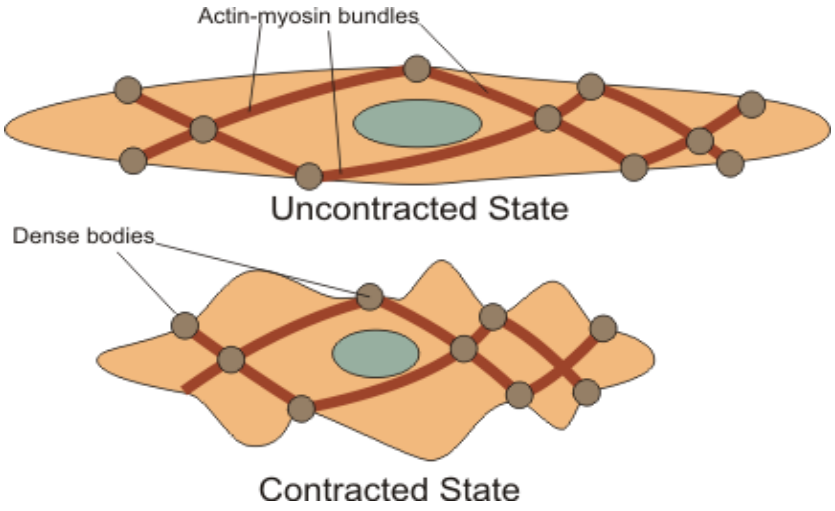

Figure 1.4: Diagram of contraction of smooth muscle fibre. Adapted from (Boundless Anatomy and Physiology 2015).

Smooth muscle cells (SMCs) are organized as thin layers around the tissue as sheets and their contraction is controlled by the autonomic nervous system. The contraction of SMCs is usually slower and more controlled than that with skeletal muscle (Ma et al. 2004). Moreover, they do not have T tubules as in skeletal muscles, which are necessary for signalling pathway. Also, they have less complex sarcoplasmic reticulum (SR), which is responsible for storing of calcium ions (Ca^{2+}) and when there is an appropriate stimulus, the SR will release the Ca^{2+} into the SM. Additionally, SMCs are connected with each other through gap junctions, which help in stimulating adjacent cells by transferring the signal from one cell to another (Nelson 1991). SMCs do not have troponin/tropomyosin complex, but instead, they have a calcium/calmodulin complex important for inducing contraction.

1.3.2. VSMC Phenotypes:

There are two main phenotypes of SMC in the body (Vrancken Peeters et al. 1999; Stegemann, Hong, and Nerem 2005). The most common type in the wall of blood vessels is the contractile or differentiated VSMC which is responsible for regulation of the diameter of blood vessels through contraction and dilatation of them and subsequently controlling the blood flow inside these vessels (Stegemann, Hong, and Nerem 2005; Zalewski, Shi, and Johnson 2002). The second phenotype of SMC is the synthetic, proliferative or migratory cells, which appear in certain conditions such as injury, atherosclerosis and other conditions (Wilden et al. 1998). Contractile SMC converts to the synthetic and migratory SMC phenotype when repair of damaged areas is required. So, the migration and synthesis functions of the non-contractile SMCs are one of the key elements in the treatment of atherosclerosis because they regulate the vascular reconstruction i.e. the inappropriate growth of SMC which can lead to narrowing of the lumen (Su et al. 2001; Enis et al. 2005).

1.3.3. Calcium and smooth muscle cells:

Calcium is involved in the contraction of SMCs (Berridge, Lipp, and Bootman 2000). There are two main sources of calcium; extracellular fluid and intracellular stores. The extracellular space can provide an unlimited influx of Ca^{2+} through Ca^{2+} channels either by depolarization of the cell membrane and/or by messenger molecules, which are either from outside the cell (transmitters) or cytoplasmic second messengers (Kotlikoff, Herrera, and Nelson 1999). Intracellular calcium is released from the sarcoplasmic reticulum (SR) after activation of two receptor-controlled channels—the IP_3R and the RyR receptors. These two sources of calcium are linked and can control each other. For example if the calcium release from SR is depleted this will enhance the activity of store-operated calcium channels leading to calcium influx, while changes in SR calcium release could enhance the activity of other calcium channels on cell membrane to induce calcium influx (McCarron et al. 2004).

1.3.4. Contraction of smooth muscle cells:

One of the main factors that regulate the contractility of SMC is the presence of free intracellular Ca^{2+}, which binds to calmodulin, leading to the formation of a Ca^{2+}/calmodulin complex. This complex is required for activation of myosin light chain kinase (MLC kinase), an enzyme that is responsible for phosphorylation of the myosin light chains (MLC), which in turn allows the formation of cross-bridges with actin, the key element in the contraction of SMC, then contraction occurs through the sliding filament theory (Gao et al. 2013). See figure 1.5

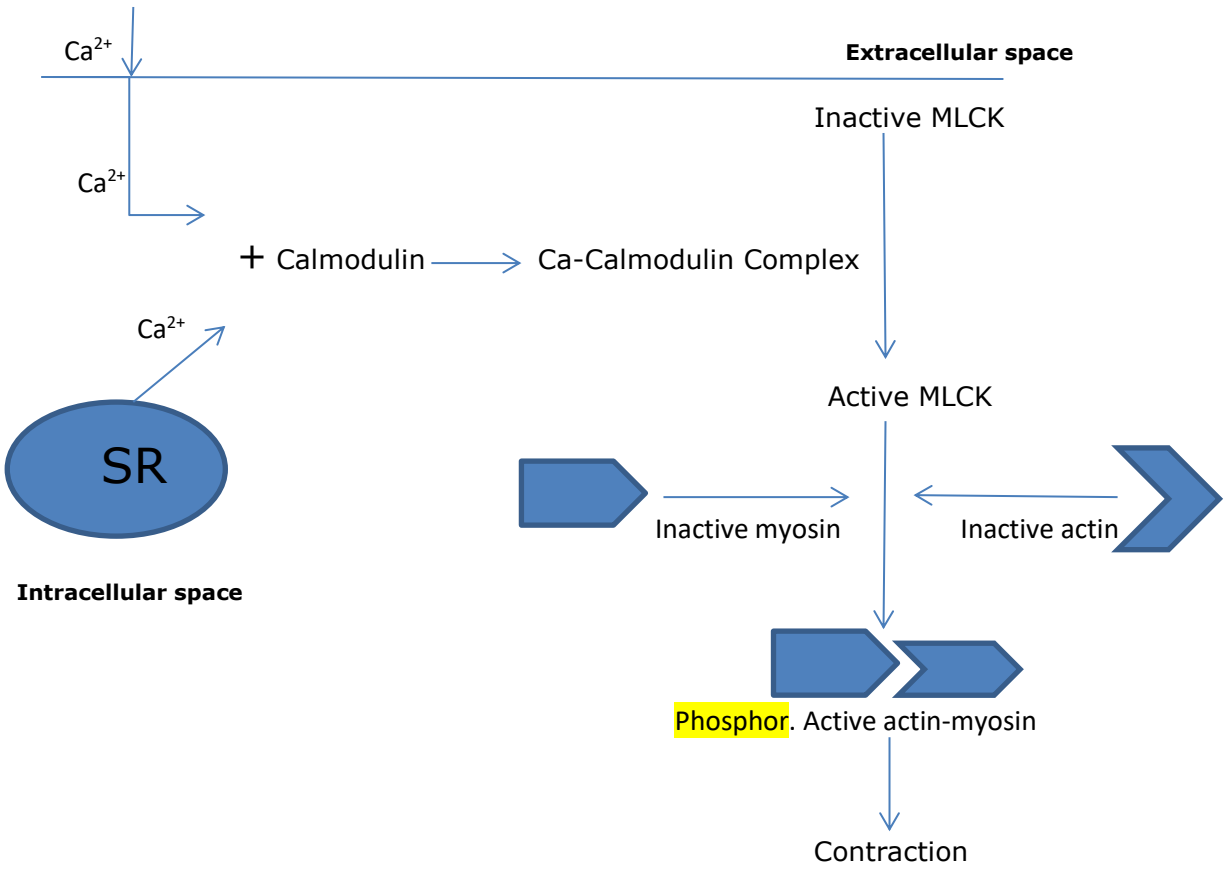

Figure 1.5: signalling pathway of SMC contraction.

The regulation and maintenance of Ca^{2+} levels and phosphorylation of MLC is important for the initiation of contraction in SMC (Somlyo and Somlyo 1994). Compounds such as noradrenaline, angiotensin II, endothelin-1 and vasopressin can activate Gq-proteins and this enhances the release of calcium from SR via inositol 1, 4, 5-trisphosphate (IP_3), which is a second messenger that has the ability to diffuse through the cytoplasm and bind to receptors on the SR. In addition, the uptake of Ca^{2+} by mitochondria may regulate the local Ca^{2+} near the IP_3 receptor, which prevents a Ca^{2+} induced inhibition of Ca^{2+} release, thereby maintaining the release of Ca^{2+} from the SR (McCarron and Muir 1999). Mitochondrial depolarization can inhibit the IP_3-induced Ca^{2+} release (Collins et al. 2000). Activation of Gq-proteins by such compounds can also lead to the conversion of Rho-A from its inactive form (GDP-bound), which is normally found in the cytosol fraction of unstimulated cells, to the active form (GTP-bound) by translocation from cytosol to the membrane. Rho-A activates Rho-kinase, which inhibits MLC phosphatase (MLCP), an enzyme that dephosphorylates MLC and caused relaxation (Kimura et al. 1996). Therefore, inhibition of MLCP by Rho kinase enhances VSM contraction.

1.3.5. Relaxation of smooth muscle cells:

Two important factors regulate the relaxation of SMC which are the phosphorylation of MLC and level of Ca^{2+} inside the cell (Koga and Ikebe 2008). Increases in cyclic AMP (cAMP) levels in the smooth muscle leads to inhibition of myosin light chain kinase (MLCK) and this caused relaxation. Nitric oxide (NO) released from the endothelium activates guanylyl cyclase that caused an increased production of cGMP, which stimulates MLCP and caused relaxation in SMC (Palizvan et al. 2013). Reducing intracellular calcium levels will also cause relaxation of smooth muscle. cAMP can activate calcium-activated potassium (BK_{Ca}) channel via cross-activation of protein kinase G (PKG). This leads to inhibition of calcium influx and caused relaxation as the BK_{Ca} channels is sensitive to intracellular calcium increase (White et al. 2000). The plasma membrane Na^+/ Ca^{2+} exchanger enhances the entrance of Na^+ in exchange for Ca^{2+} and therefore decreases Ca^{2+} inside the cell (Campbell and Paul 1992).

Mitochondria can regulate Ca^{2+} levels through supplying the energy required firstly, for refilling the SR via sarcoplasmic reticulum Ca^{2+} ATPase which drives Ca^{2+} into the SR and secondly, for removing Ca^{2+} from inside to outside the cell via membrane Ca^{2+} ATPase. So, in both cases, the level of Ca^{2+} inside the cell will decrease and this will lead to the relaxation of SMC (Demaurex, Poburko, and Frieden 2009).

1.3.6. Rho kinase and vascular smooth muscle cells:

Rho A is a small G-protein Rho that plays an important role in a number of major cell functions such as contraction, motility, proliferation, and apoptosis in addition to its role on actin organization (Etienne-Manneville and Hall 2002).

1.3.6.1. Role of ROCK in the regulation of vascular smooth muscle contraction:

As stated above, phosphorylation of MLCs is performed mainly through Ca^{2+} dependent pathways that involve activation of MLCK. Therefore, an increase in cytosolic Ca^{2+} will increase the rate of contraction by increase formation of calcium-calmodulin complex, which activates MLCK. De-phosphorylation of MLC is carried out by enhancing the activity of MLCP (Somlyo and Somlyo 2003). Inhibition of MLCP by Rho-kinase leads to enhancement of MLC phosphorylation in a Ca^{2+}-independent mechanism and this underlies the calcium-sensitization mechanism of smooth muscle contraction, which means increase the gain or sensitivity of myosin light chain kinase to calcium (Mizuno et al. 2008).

Agonist such as noradrenaline, endothelin and thromboxane contract the SMC after binding to their G-protein-coupled receptors by increasing both cytosolic Ca^{2+} and Ca^{2+} sensitivity. Moreover, it has been found that this contractile effect is attributed to ROCK activation by Rho A which in turn, phosphorylates myosin phosphatase target subunit (MYPT-1), the regulatory subunit of MLCP, and inhibits its activity (Uehata et al. 1997). It has been documented that Ca^{2+} sensitization is mainly controlled by ROCK activity rather than other contractile proteins (Uehata et al. 1997; Fu et al. 1998). Finally, a group of researchers used ROCK inhibitors in pressurized small arteries to show that the Rho-ROCK pathway is active in the absence of vasoconstrictors and is involved in the maintenance of basal tone (VanBavel, van der Meulen, and Spaan 2001; Lagaud et al. 2002).

1.3.7. Extracellular Signal-Regulated Kinase (ERK):

ERK is a protein kinase from the family of mitogen-activated protein kinases (MAPK). There are six isozymes of ERKs (ERK1, ERK2, ERK3/4, ERK5, and ERK7). ERK1 and ERK2 are thought to have a role in contraction and proliferation of VSMC (Cargnello and Roux 2011). The activation of the MAPK family occurs via a successive phosphorylation steps, which consists of three protein kinases; MAPK kinase, MEK, and MAP kinase kinase kinase. Activation of ERK1 and ERK2 is performed through activation of the G protein Ras that activates the MEK kinase Raf, which in turn activates MEK, and finally phosphorylates ERK1 and ERK2 (Cobb 1999) (figure 1.6). Phosphorylation of ERK at threonine 202 and tyrosine 204 by MEK is necessary for activation of the protein kinase. Therefore, inhibition of MEK by protein kinase inhibitors, such as PD98059 lead to inhibition of ERK activation (Whelchel, Evans, and Posada 1997; Ostrakhovitch and Cherian 2005). It has been found that the

contraction of differentiated VSMC is regulated to some extent by ERK1 and ERK2 (Raman, Chen, and Cobb 2007).

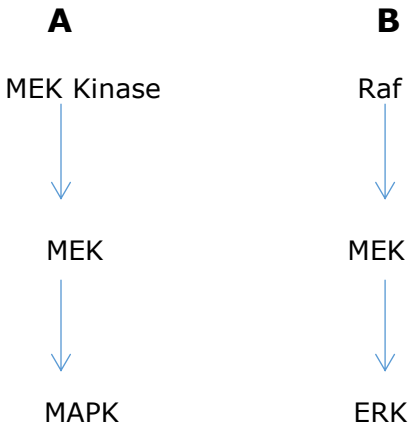

Figure 1.6: Schematic diagram showing (A) the general signalling pathway for activation of mitogen-activated protein kinases and (B) the specific pathway for activation of extracellular signal-regulated kinase.
Abbreviations: ERK, extracellular signal-regulated kinase; MAPK, mitogen-activated protein kinase; MEK, mitogen extracellular kinase.

1.3.7.1. Role of ERK in the regulation of vascular smooth muscle contraction:

It has been found in a number of studies that the elevation in ERK activity is accompanied by an increased contraction of blood vessels, which occurs either as a response to activation of certain G-protein receptors (Dessy et al. 1998; Roberts 2001) or as a response to stretch, which also induces contraction (Oeckler, Kaminski, and Wolin 2003a). In addition, studies have shown that there is a reduction in the contraction of blood vessels after inhibition of ERK activation by inhibiting MEK (Dessy et al. 1998; Roberts 2001). Regulation of the contraction of blood vessels via ERK seems to be dependent upon the receptor activated and/or the blood vessel as in case of the α_2-adrenoceptor, which caused a contraction of blood vessels mainly via ERK compared to the α_1-adrenoceptor, which mediates contraction of ferret aorta mainly by another pathway (Roberts 2001; Dessy et al. 1998).

There are number of suggested mechanisms by which ERK can cause contraction of VSMC. One of them is the phosphorylation of the actin-binding protein caldesmon. Caldesmon inhibits the ATPase activity of myosin. By phosphorylation of caldesmon, this inhibitory effect is blocked (Ngai and Walsh 1984). It has been found that the vasoconstrictor effect of phosphorylated caldesmon is inhibited by the MEK inhibitor PD98059 that prevents ERK activation (Xiao et al. 2004). In contrast, another study suggested that the ERK phosphorylation of caldesmon is involved in cell division rather than contraction because

ERK can only phosphorylate l-caldesmon, which is only present in dedifferentiated smooth muscle (D'Angelo et al. 1999). Another mechanism by which ERK can induce contraction is the phosphorylation of myosin light chains (MLC) by activation of myosin light-chain kinase (MLCK) (Klemke et al. 1997). This is supported by studies in the porcine palmar lateral vein showing that inhibition of ERK activation caused a reduction in myosin light-chain phosphorylation (Roberts 2004).

1.4. Mitochondria:

Mitochondria are the powerhouse responsible for supplying energy in the form of adenosine triphosphate (ATP) in cells to maintain their normal functions. They regulate nearly every part of cell function by providing a continuous supply of ATP, controlling Ca^{2+} signalling, manipulating reactive oxygen species (ROS) levels and maintaining redox status (Hajnoczky, Hager, and Thomas 1999; Chalmers et al. 2007). In general, mitochondria travel along cytoskeletal paths to places of high-energy demand and then change their overall morphology by fusion (merging) and fission (division) according to the cellular environment. This differentiation and proliferation of mitochondria is vital for maintaining mitochondrial number and function (Li et al. 2004; Chang, Honick, and Reynolds 2006).

The mitochondrial organelle is composed of four barriers, which are the outer, the inner, inter-membrane space and the matrix and each one of them have specific function depending on its properties. The outer is a permeable membrane that allows passing ions and this property is attributed to voltage-dependent anion-selective channels (VDAC) (Liu and Colombini 1992). The VDAC allows anions and cations to pass through at low potential while at high potential, it is allow just cations (Das, Steenbergen, and Murphy 2012). Additionally, it has been found that calcium movement between mitochondria and endoplasmic reticulum could happen via VDAC depending on cytosolic and organelle [Ca2+] (Rapizzi et al. 2002). The inner membrane is an impermeable membrane and most ions and molecules need transporters to pass through. Also, it comprises a large component (20%) of the total mitochondrial protein composition such as transporters for carrying proteins into the matrix and the enzymes of the electron transport chain (Murphy and Smith 2000). The inter-membrane space, which is located between the outer and inner membrane, usually contains proteins such as cytochrome c that performs main roles in mitochondrial energetics and apoptosis. Finally, the matrix that mainly contains the enzymes that participate in the citric acid cycle (Goglia and Skulachev 2003).

The generation of ROS by mitochondria is performed via oxidative phosphorylation (OXPHOS) pathway, which is involved in energy production (Cai and Jones 1999). OXPHOS consists of 5 multiple subunit complexes implanted in the inner mitochondrial membrane. Electrons are moved from NADH to molecular oxygen via an electron transport chain (ETC)

which consisting of complexes I (NADH dehydrogenase), II (succinate-ubiquinone oxidoreductase), III (ubiquinol cytochrome oxidoreductase), and IV (cytochrome c oxidase). Electrons are given to complex I from NADH to complex II via succinate and passed to ubiquinol via coenzyme Q and then ubisemiquinone. Ubiquinol gives electrons to complex III, which, in turn, transfers electrons to cytochrome c. From cytochrome c, electrons transfer to complex IV and in this process molecular oxygen is reduced to H_2O (figure 1.7). The movement of electrons through the ETC caused pumping of protons across the mitochondrial inner membrane at complexes I, III, and IV, creating a transmembrane electrochemical gradient. The proton motive force, which drives the re-entry of protons into the matrix, is used by complex V (ATP synthase) to condense ADP and inorganic phosphate to synthesize ATP. Matrix ATP is then exchanged for cytosolic ADP by the adenine nucleotide translocase (Holtzman and Moore 1973, 1975).

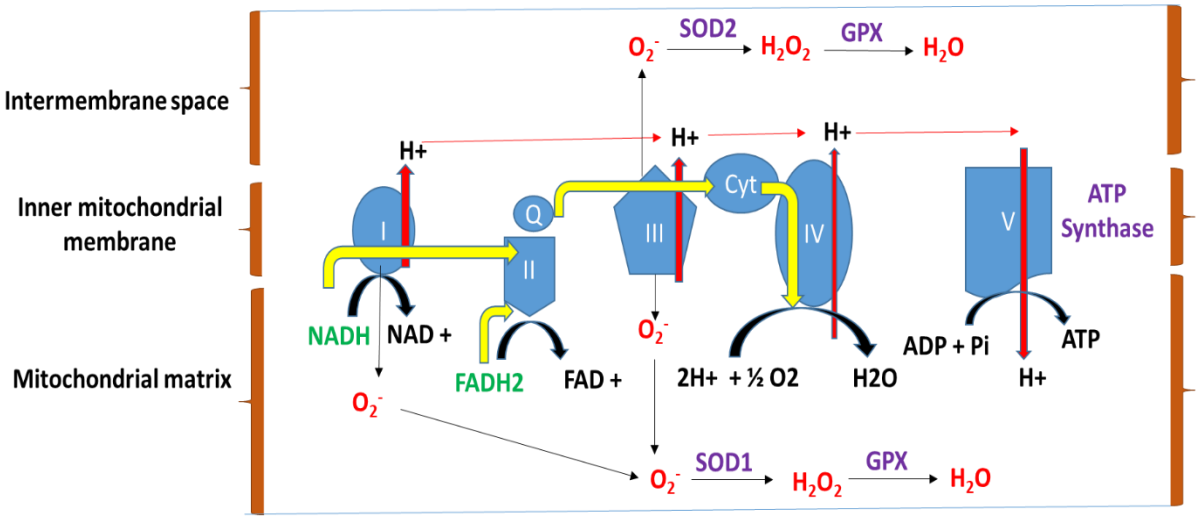

Figure 1.7: schematic diagram showing the electron transport chain and production of ROS in mitochondria. superoxide dismutase (SOD), glutathione peroxidase (GPX), superoxide (O_2^-), Nicotinamide adenine dinucleotide, reduced form (NADH), Flavin adenine dinucleotide, reduced form (FADH2) and adenosine triphosphate (ATP).

1.4.1. Mitochondria and ROS in the regulation of vascular tone:

There are two levels for the presence of ROS in cells and blood. The first one is the pathological level, in which the level of ROS is very high and this has an effect on nitric oxide production (NO) and results in loss of endothelial protective effect. Lower levels of ROS have a physiological role, in which the ROS show beneficial effect through activation of phosphatidylinositol 3-kinase–Akt–endothelial NO synthase axis. This is followed by the production of nitric oxide, which caused coronary relaxation (Feng et al. 2010). Another mechanism by which ROS (H_2O_2) can cause a relaxation of coronary vessels is via activation of BK_{ca} channel which involves the phospholipase A(2) (PLA(2))/arachidonic acid (AA)

signalling cascades suggested indirect effect (Barlow, El-Mowafy, and White 2000; Thengchaisri and Kuo 2003) or K_v channels (Rogers et al. 2006).

Mitochondria possibly have an important role in cell signalling pathways since most of the ROS produced in cells come from mitochondrial metabolism (Zhang and Gutterman 2007). In 2005, Gutterman found that the Ca^{2+} sparks, which are found in endothelial cell of large vessels, could be activated by mitochondrial ROS. These activated Ca^{2+} sparks could, in turn, activate eNOS, which is responsible for producing endothelial-dependent relaxation (Gutterman, Miura, and Liu 2005). In contrast, mitochondrial ROS (specifically H_2O_2) was found to be responsible for producing flow-mediated vasodilatation in the small vessels and it was NO-independent (Cai 2005). Moreover, Xi et al. (2005) revealed that an increase in ROS production and calcium spark activation can cause cerebral vasodilatation through stimulation of BK_{Ca} channels, occurred in a state of mild mitochondrial depolarization. A reduction in ROS production and calcium spark activation with subsequent blockade of BK_{Ca} channels happened in a state of severe depolarization of the mitochondria. Finally, it has been found that the mitochondria of SMC produce ROS that plays an important role in cold-induced cutaneous artery vasoconstriction via activation of the RhoA/Rho kinase pathway (Bailey et al. 2005).

1.4.2. Mitochondria and statins:

Statins have been found to have an effect on mitochondria causing alteration and modulation in their functions (Herrero-Martin and Lopez-Rivas 2008). A number of studies have demonstrated that inhibition of the mevalonate pathway by statins can lead to inhibition of ubiquinone and co-enzyme Q10, which is needed for oxidative phosphorylation and synthesis of ATP. Therefore, blocking this pathway can result in impairment of mitochondrial bioenergetics such as in the case of co-enzyme Q10 deficiency caused by simvastatin that mainly found to cause hepatotoxicity (Tavintharan et al. 2007a). Moreover, it has been found that simvastatin is responsible for worsening of myocardial mitochondrial respiration during ischaemia by decreasing myocardial coenzyme Q10 levels (Satoh et al. 1995).

Studies revealed that statins could cause toxicity in the skeletal muscle and smooth muscle via alteration mitochondrial respiration and calcium homeostasis (Kwak et al. 2012; Galtier et al. 2012). It has been found that simvastatin and lovastatin (lipid soluble drugs) but not pravastatin (water soluble) have an inhibitory effect on complex I, II, III, IV and complex V of heart and liver mitochondria. This difference in the effect between those two groups may be attributed to the structural difference of the latter i.e. β-hydroxy acid in pravastatin in comparison to lactone ring in simvastatin (Nadanaciva et al. 2007). A study performed on human hepatocellular carcinoma cells showed that fluvastatin could cause

depolarization of the mitochondrial membrane (Zhang et al. 2010). In another study, it has been found that simvastatin, lovastatin, and atorvastatin could cause cytotoxic effects in rat hepatocytes because of the production of ROS and mitochondrial depolarization (Abdoli et al. 2013).

On the other hand, a study performed on neonatal rat cardiac myocytes revealed that simvastatin could attenuate the reduction in mitochondrial membrane potential, caused by exposure of myocytes to H_2O_2, when added 1 hr before exposure. Thus, simvastatin reduced the depolarization of the mitochondrial membrane after exposure to oxidative stress (Jones et al. 2003). A study that is more recent showed that simvastatin and lovastatin have an antioxidant effect on the mitochondria derived from the liver of rat as both could lower intra-mitochondrial ionized calcium that decreases activity of mitochondrial nitric oxide synthase (mtNOS), which then lowers oxidative stress (Parihar et al. 2012).

Recent studies in our laboratory have demonstrated that simvastatin alters mitochondrial membrane potential in an intact coronary artery. Simvastatin caused relaxation of the coronary artery, and this relaxation was inhibited by inhibition of mitochondrial complex inhibitors. Almukhtar (2015) found that the relaxant effect of simvastatin on PCA was attenuating by inhibition of mitochondrial complexes I via using rotenone and III via using myxothiazol. This indicates that the relaxation produced by simvastatin is dependent upon the activity of complexes I and III. This finding is consistent with the previous findings of others (Brandt, Schagger, and von Jagow 1988) and (Schirris et al. 2015) who revealed that statin lactones, in which simvastatin is one of the best examples for widely used statin lactones medication, exert their mitochondrial inhibitory effect mainly via inhibition at the Q_o site of complex III rather than Q_i . In intact artery, Almukhtar (2015) demonstrated that simvastatin caused an increase in Rh123 fluorescence, which indicates a change in mitochondrial membrane potential ($\Delta\psi m$). This was also seen in cultured aortic smooth muscle cells, demonstrating that simvastatin can depolarize the mitochondrial membrane potential in whole cells. On the other hand, pravastatin showed no effect on the mitochondrial potential in SMC, which associates with the absence of relaxation with pravastatin.

1.4.3. Mitochondria and calcium:

Studies have shown that mitochondria are able to regulate intracellular calcium via their ability to uptake and sequester calcium from the cytoplasm in a huge amount with buffer power reach to about three folds that in the cytoplasm (Duchen 2000). The presence of about 5 mM phosphate within the mitochondria is the reason for this large buffering power. Calcium uptake by mitochondria is maintained by the slow export via Na^+-(or H^+-) Ca^{2+}

antiporter mechanism (Chalmers and McCarron 2009). This means that mitochondrial calcium uptake could regulate calcium release from SR under the control of IP_3R or RyR or Ca^{2+} entry across the outside membrane via voltage-gated channels through regulation of cytosolic levels. Accordingly, these calcium-signalling pathways could be enhanced or inhibited depending on the mitochondrial function activity and types of cells. Studies showed that the mitochondrial uptake of calcium could enhance IP_3-induced Ca^{2+} release so that stopping mitochondria from taking up more Ca^{2+} as in smooth muscle and astrocytes reduces the amplitude of the Ca^{2+} signal (Collins et al. 2000; Drummond and Tuft 1999a; Chalmers and McCarron 2009). Other studies performed in guinea-pig colonic smooth muscle and rat adrenal chromaffin cells showed that mitochondrial calcium uptake reduced the rate of calcium transition across voltage-dependent calcium entry but inhibition of calcium uptake returned the calcium entry to the normal rate (Drummond and Fay 1996; Herrington et al. 1996; McCarron et al. 2000).

It has been found that mitochondria could regulate calcium signalling with wide range of cytoplasmic Ca^{2+} concentration $[Ca]_c$ (200 nM to 10 μM) and the mitochondria have high affinity towards calcium signalling with $[Ca]_c$ range 200–600 nM (McCarron, Olson, and Chalmers 2012; Pitter et al. 2002).

Studies performed on vascular smooth muscle cells showed that when the mitochondrial calcium uptake is inhibited (using complex I inhibitor or uncoupler) the mitochondria exert dramatic effect on calcium waves and repetitive calcium rises (oscillations). This effect is beyond the control of calcium rise and gives mitochondria the ability to decide if some of these waves or oscillations could happen or not (Boitier, Rea, and Duchen 1999; Rizzuto, Bernardi, and Pozzan 2000; McCarron et al. 2013).

A study performed on pancreatic acinar cells, which identified to have three independent mitochondrial pools in different region, showed that when the calcium signal (waves) escaped from granular region towards the nucleus, the perinuclear mitochondria worked as a shelter and prevented waves invasion from entering the basal part of endoplasmic reticulum (ER) tunnel, thus, stopped proceeding the signal (Park et al. 2001). In SMCs, the effect is different, as mitochondrial activity could regulate the production of calcium waves inside the cell. The calcium signal (waves) progress when the mitochondrial membrane potential is polarized but the signal could be stopped from propagation throughout the cell if the mitochondrial membrane potential becomes depolarized as in case of a reduction in ATP production (Balemba et al. 2008; Olson, Chalmers, and McCarron 2010).

1.4.4. AMP Kinase and regulation of vascular tone:

AMPK is a major regulator for cellular energy homeostasis as it balances the metabolic rate and body requirement of energy. It is acts as a sensor of energy because when the ATP: AMP ratio decreases, this leads to the activation of AMPK (Suter et al. 2006; Gowans et al. 2013). One potential mechanism by which mitochondria could regulate smooth muscle tone is through activation of AMP-activated protein kinase (AMPK) (Moral-Sanz et al. 2016). In a study performed on aortic rings from rat, the researchers found that AMPK attenuated the SMC contraction via inactivating MLCK and this contributed to lower ATP turnover in the tonic phase of contraction (Horman et al. 2008). In smooth muscle cells, AMPK has a direct anti-contractile effect via inhibition the activity of Rho A at Ser188 and this leads to dephosphorylating MLC and inducing relaxation (Gayard et al. 2011; Wang et al. 2011). Inappropriate production of ROS from uncoupled mitochondria could also interact with NO thus reducing its activity (Siragusa and Fleming 2016).

Studies have shown that metformin (antidiabetic medication) could cause vasodilatation through activation of AMPK. A study performed on cultured bovine aortic endothelial cells identified that metformin increases AMPK activity possibly via mitochondrial reactive nitrogen species (RNS) (Zou et al. 2004). Other studies identified the ability of metformin to inhibit complex I in the mitochondria, which leads to inhibition of ATP production and reduction in the ATP: AMP ratio, and hence activation of AMPK (Owen, Doran, and Halestrap 2000; Madiraju et al. 2014). In another recent study, researchers found that metformin and AICAR (an AMPK activator) could cause vasodilator effects in retinal arteries from rat eyes by enhancing the activity of AMPK, followed by activation of eNOS and NO, which exerts a relaxant response. This finding was confirmed by using compound C, an inhibitor of AMP-activated protein kinase (AMPK), and N^{G}-nitro-L-arginine methyl ester, an inhibitor of nitric oxide (NO) synthase, which both abolished the vasorelaxant effect when applied (Mori et al. 2017). Other compounds such as statins could also activate AMPK to induce relaxation. Lovastatin in the bovine aorta and atorvastatin in human umbilical vein endothelial cells and mouse aorta have been shown to activate AMPK that may be related to the pleiotropic effect of statins (Sun et al. 2006). Accordingly, inhibition of mitochondrial complexes by statins could lead to AMPK activation, which could be the mechanism by which statins have their anti-contractile effect.

1.5. Aim of the study:

Previous study in the laboratory have indicated that statins, such as simvastatin, cause relaxation through inhibition of mitochondrial complexes (Almukhtar et al. 2016). The data also indicated that simvastatin might act to reduce calcium influx through voltage gated calcium channels. However, it is not clear whether the effects on the mitochondria are related to the inhibition of calcium influx. As discussed above, mitochondria are able to regulate intracellular calcium levels, and, therefore, influx through calcium channels. Furthermore, statins have also been reported to inhibit Rho kinase and ERK, both of which can regulate vascular tone. Although this has been linked to inhibition of isoprenylation, whether this is also related to the effects on the mitochondria is unknown.

Therefore, the aim of this study was to determine the effect of simvastatin on U46619-induced contraction in PCA and to determine whether inhibition of mitochondrial function could underlie effects on calcium, Rho kinase and ERK. Comparisons were made with known mitochondrial complex inhibitors in order to understand how inhibition of mitochondrial complexes could regulate vascular tone.

Chapter II

The effect of simvastatin on U46619 (thromboxane A2 agonist)-induced contraction in porcine coronary arteries (PCAs)

2.1. Introduction:

Cardiovascular diseases (CVDs) have a severe impact on human health, increasing the risk of morbidity and mortality. Atherosclerosis is one of the common caused of CVD because the plaques formed caused the affected arteries to narrow, leading to diminished blood flow, damage to organs and stopping them working appropriately (Lewington et al. 2007). Statins (3-hydroxymethyl-3-methylglutaryl coenzyme A reductase inhibitors) are one of the most well-known, effective and safe groups of drugs used for treating and preventing the recurrence of this condition. They decrease the incidence of disease (morbidity) and the rate of death (mortality) (An et al. 2017). All statins act by inhibiting the conversion of HMG-CoA to mevalonic acid, which is responsible for the synthesis of cholesterol and consequently associated with a reduction in serum total and low-density lipoprotein (LDL) cholesterol (Andrews et al. 2001). Statins are effective medications for the primary and secondary prevention of coronary heart disease (CHD) (Sever et al. 2003). The overall beneficial effects of statins not only come from the reduction of cholesterol, but also come from cholesterol-independent effects known as pleiotropic effects (Barone, Di Domenico, and Butterfield 2014).

Through inhibiting L-mevalonic acid synthesis, other important mediators in the cholesterol synthetic pathway are also prevented from being synthesized by statins. These are isoprenoid intermediates such as farnesyl pyrophosphate (FPP) and geranylgeranyl pyrophosphate (GGPP)(Goldstein and Brown 1990). These intermediates have a significant role in isoprenylation of proteins and converting them from inactive to active forms by translocation from the cytoplasm to the cell membrane through working as lipid attachments for the posttranslational modification of a variety of proteins. These proteins include the small guanosine triphosphate (GTP)-binding protein Ras and Ras-like proteins, such as Rho, Rab, Rac, Ral, or Rap (Van Aelst and D'Souza-Schorey 1997). See figure 1.2 in the introduction (Cholesterol biosynthesis pathway and site of statins action).

Rho A is the prototype of the small G-protein Rho that plays an important role in a number of major cell functions such as contraction, motility, proliferation, and apoptosis (Etienne-Manneville and Hall 2002). Rho A has a vital role in conversion of inactive GDP-bound to an active GTP-bound conformation, which is needed for activation of Rho kinases (ROCKs), and other downstream or effectors (Sahai and Marshall 2002). Activated Rho-kinase inhibits MLC phosphatase (MLCP), an enzyme that dephosphorylates MLC and thereby caused relaxation (figure 2.1) (Kimura et al. 1996). Therefore, inhibition of MLCP by Rho kinase enhances vascular smooth muscle contraction. Inhibition of the synthesis of isoprenoids, therefore, could lead to prevention of vascular smooth muscle contraction

through inhibition of Rho A geranylgeranylation and hence inhibition of Rho kinase activation (Takemoto et al. 2002)

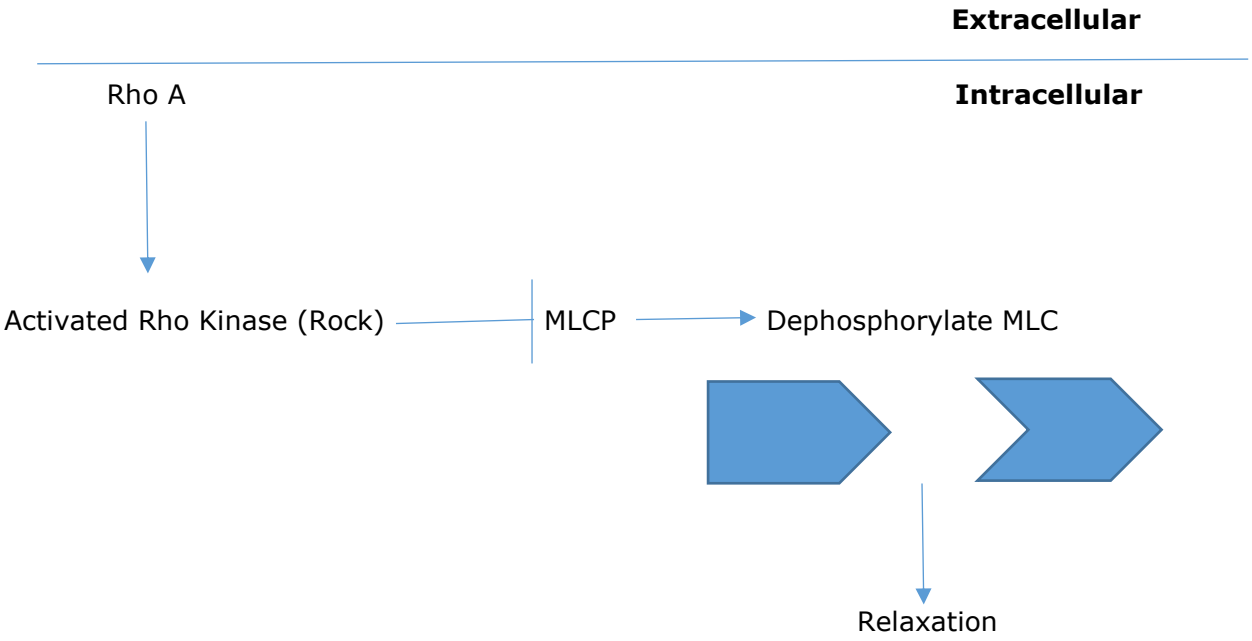

Figure 2.1: Activated Rho-kinas and smooth muscle cells relaxation.

ERK is a protein kinase from the family of mitogen-activated protein kinases (MAPK). ERK1 and ERK2 are thought to have a role in the contraction and proliferation of VSMC (Roberts 2012). Phosphorylation of ERK at threonine 202 and tyrosine 204 by MEK is necessary for activation of the protein kinase (Butch and Guan 1996). It has been found in a number of studies that the elevation in ERK activity is accompanied by an increased contraction of blood vessels, which occurs as a response to activation of certain G-protein-coupled receptors (Dessy et al. 1998; Roberts 2001). These studies demonstrated that there is a reduction in the contraction of blood vessels after inhibition of ERK activation by inhibiting MEK.

Recent studies in our laboratory have demonstrated that simvastatin alters mitochondrial membrane potential in an intact coronary artery (Almukhtar et al., 2016). Simvastatin caused relaxation of the coronary artery and this relaxation was reduced in the presence of inhibitors of mitochondrial complex I or III inhibitors, suggesting that the inhibitory effect of simvastatin on mitochondria may underlie the relaxation.

A number of studies have demonstrated that inhibition of the mevalonate pathway by statins can lead to inhibition of ubiquinone and Coenzyme Q10, which are needed for

oxidative phosphorylation and synthesis of ATP. Therefore, blockage of this pathway can result in impairment of mitochondrial bioenergetics (Tavintharan et al. 2007b). In a study performed by (Satoh et al. 1995), they found that simvastatin is responsible for worsening of myocardial mitochondrial respiration during ischemia by decreasing myocardial coenzyme Q10 levels. Additionally, statins can cause toxicity in the skeletal muscle via alteration mitochondrial respiration and calcium homeostasis (Galtier et al. 2012; Kwak et al. 2012). Other study showed that simvastatin has an inhibitory effect on complex I, II, III, IV and complex V of heart and liver mitochondria (Nadanaciva et al. 2007). In addition, it has been found that simvastatin has an anti-oxidative effect on rat mitochondria via lowering intra-mitochondrial ionized calcium (Parihar et al. 2012). This inhibited mitochondrial NOS activity, which is responsible for releasing NO and cytochrome c. This, in turn, prevents mitochondrial permeability transition opening and resulting in a lowering of oxidative stress. Therefore, statins could alter mitochondrial activity through inhibition of CoQ10.

One potential mechanism by which mitochondria could regulate smooth muscle tone is through activation of AMP-activated protein kinase (AMPK), which is considered a sensor of energy because when the ATP: AMP ratio decreases, this leads to the activation of AMPK (Suter et al. 2006; Gowans et al. 2013). Lovastatin in bovine aorta and atorvastatin in human umbilical vein endothelial cells and mouse aorta have been shown to activate AMPK that may be related to the pleiotropic effect of statins (Sun et al. 2006).

Mitochondria can also have effects on intracellular signaling through control of Ca^{2+} signaling and manipulating reactive oxygen species (ROS) levels (Chalmers et al. 2007). Mitochondria are responsible for uptake, accumulate, store or release of calcium depending on calcium level in the cytosol, cell type and cell condition (Drummond and Tuft 1999b; Roux and Marhl 2004). This means that mitochondrial calcium uptake could regulate calcium release from SR under the control of IP_3R or RyR or Ca^{2+} entry across the outside membrane via voltage-dependent channels through regulation of cytosolic levels.

In summary, a number of signalling pathways may be involved in the anti-contractile effect of simvastatin, including inhibition of calcium influx, activation of AMPK, and inhibition of Rho kinase/ ERK. We hypothesised that the effects of simvastatin on these signalling pathways are downstream of inhibition of mitochondrial respiratory complexes. Therefore, the aim of this study was to determine the effect of simvastatin on smooth muscle tone in the PCA and to determine the relative role of each of these signaling pathways in the anti-contractile response.

2.2. Material and Method:

2.2.1. Tissue Preparation:

Hearts from large white hybrid pigs of both sexes, 4-6 months old, and weighing about 50 kg were obtained from a local abattoir and transferred to the laboratory in modified Krebs'-Henseleit solution (NaCl 118, KCl 4.8, $CaCl_2.H_2O$ 1.3, $NaHCO_3$ 25.0, KH_2PO_4 1.2, $MgSO_4.7H_2O$, glucose 11.1 in mM) on ice. The porcine coronary artery (PCA) was then dissected out.

2.2.2. Isolated organ bath experiments:

For organ bath experiments, the PCA was put in Krebs'-Henseleit solution pre-gassed with 5% CO_2 and 95% O_2 for overnight storage at 4°C. The following day, PCAs were cleaned of fat, finely dissected, and then cut into rings of approximately 5 mm in length and suspended in 5 ml organ baths. Vessels were attached to two metal hooks placed through the lumen, ensuring that the hooks were not overlapping. One hook was attached to a glass rod and the other was attached to a silk thread. Each bath was filled with 5 ml of Krebs-Henseleit solution and maintained at 37°C and constantly gassed with carbogen (95% O_2, 5% CO_2). The tension was added to each segment, 8-10 g. Previous experiments have indicated that this is the optimum level of tone for the porcine coronary artery. This tension was measured and recorded using a Power-Lab data acquisition system (AD Instruments) via an amplifier. Transducers were calibrated with a 10 g weight daily. Once a stable baseline was reached, 60 mM KCl was added for two consecutive responses to obtain standardization. After about 10 min, the KCl was washed out with fresh Krebs'-Henseleit solution. Following the return to a stable baseline and, after a further 20-30 min, exposure to KCl was repeated. Once again, the tissue was washed out with Krebs'-Henseleit solution, to allow the segment tone to re-stabilize to baseline.

2.2.3. Effect of Simvastatin on U46619-induced tone:

In order to determine the effect of simvastatin on U46619-induced tone, tissues were exposed to simvastatin (1-10 μM) or vehicle control (0.1% v/v DMSO) for 2 h. Previous studies in the laboratory have demonstrated that this is the optimal incubation time for maximum effect (Almukhtar et al. 2016). After the incubation period, the thromboxane mimetic U46619 was added in a cumulative manner (1-300nM). Contractile responses were expressed as a percentage of the response to 60 mM KCl. In some experiments, the Krebs-Henseleit buffer was replaced with calcium-free Krebs solution in which the calcium was replaced with 2 mM ethylene glycol bis (β amino ethyl ether)-N,N,N,N-tetra acetic acid (EGTA). In other experiments, the Krebs-Henseleit buffer was replaced with glucose-free Krebs.

The contractile response to U46619 is well maintained and is likely to involve different pathways in the initiation of contraction compared to the maintenance of contraction. In order to determine whether simvastatin alters the contractile profile to U46619 over time, tissues were incubated with a single concentration of simvastatin (10 μM) for 120 min, followed by a single concentration of U46619 (30 nM) in order to look at the effects of the drugs on the time profile of the contraction.

Previous studies in the laboratory have demonstrated that simvastatin caused a time-dependent relaxation of the PCA (Almukhtar et al. 2016; Seto et al. 2013).In order to confirm these studies; PCAs were contracted with U46619 to about 40-60% of the KCl contraction. After the contraction had reached a plateau, a single concentration of simvastatin (10μM) was added then tension recorded for up to 120 min.

2.2.4. Effect of Rho kinase, MEK, calyculin A and L-type calcium channel inhibition on U46619-induced contraction:

It has been proposed that simvastatin inhibits Rho kinase, ERK-MAP kinase, L-type calcium channels, and myosin phosphatase. Therefore, in order to determine whether inhibition of these pathways could underlie the inhibitory effects of simvastatin on the U46619-induced contraction, it was first necessary to determine if these pathways are involved in the contractile response. After the KCl responses, tissues were exposed to one of the following compounds: Y27632 (1-10 μM), a selective inhibitor of Rho kinase, PD98059 (5-50 μM), a selective inhibitor of MEK, verapamil (10 μM) or, nifedipine (5 μM), calcium channel blockers. Control tissues received vehicle only (distilled water for Y27632, 0.1% v/v DMSO for the other compounds). Cumulative concentration-response curves to U46619 were then carried out in the presence or absence of extracellular calcium.

In other experiments, tissues were incubated with a single concentration of PD98059 (50 μM) or Y27632 (10 μM) for 60 min, followed by a single concentration of U46619 (30 nM) to determine the effects of the drugs on the time profile of the contraction to U46619.

In order to determine the role of myosin phosphatase and/or L-type calcium channels in the U46619-induced contractions, tissues were incubated with a single concentration of simvastatin (10μM) for 120 min, then contracted with U46619 to about 40-60% of the KCl contraction. This was followed by adding either a single concentration of calyculin or cumulative additions of nifedipine (1-3000nM) to induce relaxation.

2.2.5. Effect of mitochondrial inhibitors on the simvastatin-induced inhibition of thromboxane contraction:

The previous study in the laboratory indicated that relaxation responses to simvastatin are mediated through effects on the mitochondria (Almukhtar et al. 2016). In order to determine whether the inhibition of the U46619-induced contraction by simvastatin involves the mitochondria, the effects of the mitochondrial inhibitors rotenone (complex I inhibitor), antimycin A (complex III inhibitor at Qi site), myxothiazol (complex III inhibitor at Qo site), were determined. Tissues were pre-incubated with simvastatin (10 μM), rotenone (10μM), antimycin A (10 μM), myxothiazol (10 μM) individually or in combination. Control tissues received vehicle only (0.1% v/v DMSO). Cumulative concentration-response curves to U46619 were then carried out in the presence or absence of extracellular calcium and in the presence or absence of glucose.

2.2.6. Effect of FCCP and AMP Kinase inhibitor on the simvastatin-induced inhibition of thromboxane contraction:

In further experiments to determine whether the inhibition of the U46619-induced contraction by simvastatin involves the mitochondria, the effect of FCCP (potent mitochondrial oxidative phosphorylation uncoupler) was determined (Kadenbach 2003). Inhibition of the electron transport chain in the mitochondria can lead to activation of AMP kinase(Im et al. 2015). Therefore, the effect of dorsomorphin (AMPKinase inhibitor) was also determined. Tissues were pre-incubated with simvastatin (10 μM) in the absence or presence of FCCP (1 μM) (Hogan et al. 2014) or dorsomorphin (10 μM) (Liu et al. 2014). Control tissues received vehicle only (ethanol 0.1% v/v for FCCP and 0.1% v/v DMSO for the rest). Cumulative concentration-response curves to U46619 were then carried out in the presence of extracellular calcium.

2.2.7. Effect of mitochondrial stimulants on the simvastatin-induced inhibition of thromboxane contraction:

If simvastatin inhibits the electron transport chain at complex I, the effects should be prevented by co-enzyme Q10 or mitoquinol (a reduced form of coenzyme Q10). Alternatively, H_2S can support the mitochondrial electron transport chain (Kimura, Shibuya, and Kimura 2012). Therefore, AP39 (mitochondria-targeted H_2S donor) would be expected to prevent the effect of simvastatin. Tissues were exposed to coenzyme Q10 (5 μM) or mitoquinol (1 μM). Control tissues received vehicle only (ethanol 0.1% v/v for coenzyme Q10 and 0.1% v/v DMSO for the rest). Cumulative concentration-response curves to U46619 were then carried out in the presence of extracellular calcium.

For AP39, tissues were pre-incubated with simvastatin (10 μM) and AP39 (30 μM), this concentration was determined by pilot studies. Control tissues received vehicle only (0.1%

v/v DMSO). After the incubation period, tissues were exposed to a single concentration of U46619 (30 nM) then tension recorded for up to 120 min.

2.2.8. Effect of simvastatin and mitochondrial inhibitors on $CaCl_2$ and Bay K 8644-induced contraction:

Previous studies in the laboratory have indicated that simvastatin reduces calcium influx. Therefore, in order to determine whether the inhibition of the U46619-induced contraction by simvastatin involves the presence of extracellular calcium, tissues were pre-incubated for 2 h with simvastatin (10 μM) in the absence of extracellular calcium. Control tissues received vehicle only (0.1% v/v DMSO). After the incubation period, tissues were exposed to a maximum concentration of U46619 (300 nM). $CaCl_2$ was then added cumulatively (10 μM-3 mM) to induce a contraction. In order to determine whether the inhibitory effect of simvastatin to calcium-induced contraction could be prevented by mitochondrial inhibitors, the experiment was repeated in the absence or presence of antimycin-rotenone combination (10 μM) or myxothiazol-rotenone combination (10 μM).

In other experiments, to determine and confirm the involvement of L-type calcium channel in the inhibitory effect of simvastatin, tissues were pre-incubated with simvastatin (10 μM). Control tissues received vehicle only (0.1% v/v DMSO). After the incubation period, the L-type calcium channels opener Bay K8644 was then added cumulatively (1-300 nM). Contractile responses were expressed as a percentage of the response to 60 mM KCl. In order to determine if the inhibitory effect of simvastatin could be prevented by mitochondrial inhibitors, the experiment was repeated in the presence of a myxothiazol-rotenone combination (10 μM each).

2.2.9. Western blotting:

It has been proposed that statins can reduce the activity of Rho Kinase and ERK. Therefore, activity of these enzymes was determined by measuring changes in phosphorylation of MYPT1 (Rho kinase substrate) or ERK using Western blotting.

2.2.9.1. Tissue preparation:

PCA segments were set up in 5 ml organ baths linked to an isometric force transducer for recording tissue tone, as above. After two successive KCl (60 mM) challenges, two segments were incubated with 10μM simvastatin, the third was incubated with 0.1% v/v DMSO as a solvent control while the fourth segment left without any treatment for 2 h. After the incubation period, one of the segments treated with simvastatin and the segment without any treatment received a single concentration of U46619 (30 nM). After a steady contractile tone was achieved, ring segments from all channels were removed at the same time and frozen quickly on dry ice. The rings were homogenized using a glass homogeniser

(Fisher Brand 0.1 ml glass-glass homogeniser) in ice-cold buffer composed of 80 mM sodium β-glycerophosphate, 20 mM imidazole, 1 mM dithiothreitol (DTT), 1 mM sodium fluoride (NaF) [pH 7.6] with a protease inhibitor cocktail (Calbiochem). A sample of homogenate was removed for a protein assay. The remaining homogenised samples were diluted (1:2) in 2x Laemmli sample buffer [4% (w/v) SDS, 20% (w/v) glycerol, 10% (v/v) 2-mercaptoethanol, 0.004% (v/v) bromophenol blue and 0.125 M Tris HCl pH 6.8] then heated at 95 ºC for 5 min.

2.2.9.2. Bradford Protein Assay:

This assay was used to estimate the protein concentration in the tissue homogenates using a bovine serum albumin (BSA) standard curve (0 to 2 mg/ml). The protein assay was carried out in a 96-well plate using Bio-Rad protein assay dye reagent, following the protocol from Bio-Rad. Absorbance at 595 nm was read using a Spectromax plate reader.

2.2.9.3. Western blotting protocol:

Equal amounts of each sample (~10µg protein) were carefully loaded into wells of pre-cast 4-20% (w/v) acrylamide SDS-PAGE gels (Bio-Rad). Loaded gels were fitted into an electrode tank having electrophoresis buffer (25 mM Tris, 192 mM glycine and 0.1% (w/v) SDS in distilled H_2O at pH 8.3). Gels were run at 150 V for 45 min. Proteins were then transferred onto nitrocellulose membrane (GE Healthcare Life Sciences, Amersham, UK) using a Bio-Rad mini Transblot apparatus. Proteins were transferred in 25 mM Tris, 192 mM glycine and 20% methanol in distilled H_2O at pH 8.3 at a voltage of 100 V for 60 min.

After that, non-specific protein binding sites on the nitrocellulose membrane were 'blocked' by incubating the membrane for 60 min in 5% (w/v) BSA solution (in the case of MYPT1 detection) or 5% (w/v) non-fat dairy milk (Marvel) solution (in the case of ERK detection). Both were dissolved in Tris-buffered saline [25 mM Tris, 125 mM NaCl to pH 7.6 in distilled H_2O] containing 0.1% Tween-20 (TBS-Tween). Then, membranes were incubated overnight at 4 ºC with primary antibodies against phosphorylated MYPT1, total MYPT1, phosphorylated ERK and total ERK, as indicated in table 2.1.

Antibody	Species	Dilution	Catalogue Number	Source	Secondary Antibody
Phospho-MYPT1 Thr696	Rabbit	1:1000 in 5% BSA	ABS45	Merck	Goat anti-Rabbit IRDYE/680LT/Licor 926-68021
Phospho-MYPT1 Thr850	Rabbit	1:1000 in 5% BSA	36-003	Merck	Goat anti-Rabbit IRDYE/680LT/Licor 926-68021
Total MYPT1	Rabbit	1:1000 in 5% BSA	ab70809	Abcam	Goat anti-Rabbit IRDYE/680LT/Licor 926-68021
Phospho-p44/42 MAPK (ERK1/2) (Thr202/Tyr204)	Mouse	1:2000 in 5% milk	9106S	Cell Signaling Technology	Goat anti-Mouse IRDYE/680RD/Licor 926-68070
Total-p44/42 MAPK (ERK 1/2)	Mouse	1:2000 in 5% milk	9107S	Cell Signaling Technology	Goat anti-Mouse IRDYE/680RD/Licor 926-68070

Table 2.1: primary and secondary antibodies for western blotting.

The next day, blots were washed in TBS-Tween 4 times over 1 h, then incubated with a fluorescently-labelled secondary antibody, as indicated in table 1. Antibodies were diluted 1:10,000 in 5% (w/v) BSA solution (in the case of MYPT) and 5% (w/v) milk solution (in the case of ERK). After that, blots were washed again for 4x 15 min in TBS-Tween then washed with distilled water. Finally, the blots were then scanned at 700 and 800 nm wavelengths using an Odyssey Infrared Imaging System (LI-COR Biotechnology Ltd., Cambridge, UK). To analyze the optical densities and molecular weights of the visualized bands Odyssey software (LI-COR Biotechnology Ltd., Cambridge, UK) was used. In order to identify if there was a difference in the level of total and phosphorylation of ERK and/or MYPT, the density of the bands was normalized to a control band derived from PCA ring treated with 0.1 v/v DMSO. Statistical significance between simvastatin, U46619 and simvastatin-U46619 combination treated PCA rings was determined using One-way ANOVA followed by Tukey post-hoc test with $p<0.05$ determining significance.

2.2.10. Drugs and Chemicals:

Simvastatin, U41669, Y27632, PD98059, verapamil and Bay K 8644 were purchased from Tocris Bioscience. Antimycin A, myxothiazol, rotenone, dorsomorphin, coenzyme Q10, FCCP, EGTA, and nifedipine were purchased from Sigma Aldrich. Mitoquinol and AP39 were purchased from Cayman Chemical Company. Finally, calyculin A was purchased from Cell Signaling Technology.

A stock solution of Y27632 was dissolved in distilled water. A stock solution of co-enzyme Q10 was dissolved in ethanol. The stock solutions of U46619 were made to 10mM in ethanol. All further dilutions of the stock solutions were made using distilled water. Stock solutions of all remaining chemicals were dissolved in dimethyl sulfoxide (DMSO).

All stocks were kept frozen at -20 ^{o}C, except for KCl and $CaCl_2$, which were kept at room temperature.

2.2.11. Statistical Analysis:

Data were expressed as mean ± SEM where n = the number of different animals. The concentration-response curves were fitted to a sigmoidal curve with a variable slope using four parameters (Top, bottom, log EC50 and slope) logistic equation using Graph-Pad Prism software. The maximum percentage contraction (R_{max}) and the negative log of concentration required to produce half the response to that ligand (pEC_{50}) were derived from the fitted curves where appropriate. Data were analyzed using 2-tailed, paired (dependent) for one group sample tested twice or unpaired (independent) Student's t-test to compare the means of 2 groups-tested once. Differences between 3 or more groups were assessed using one-way ANOVA or two-way ANOVA in conjunction with the Sidak's post-hoc test or Tukey post-hoc test to assess possible difference at individual concentrations. The P-value <0.05 was considered statistically significant. Statistical analysis was performed by Graph-Pad Prism (Version 7).

2.3. Results:

2.3.1. The effects of simvastatin on U46619 (thromboxane A_2 mimetic) induced contraction in porcine coronary arteries (PCAs):

In order to determine whether simvastatin inhibited the contractile response to thromboxane receptor activation, the effect of pre-incubation with simvastatin on U46619-induced contractions was determined in the presence of extracellular calcium (Fig.2.2) and in the absence of extracellular calcium (Fig.2.3). In the presence of calcium, control tissues reached an R_{max} of 118 ± 8% of the KCl response with a pEC_{50} value of 8.0 ± 0.1 (n= 6). Pre-incubation with increasing concentrations of simvastatin caused a significant inhibitory effect on the contractile response with 10 μM simvastatin. Table 2.2 shows the R_{max} and pEC_{50} values in the presence of simvastatin.

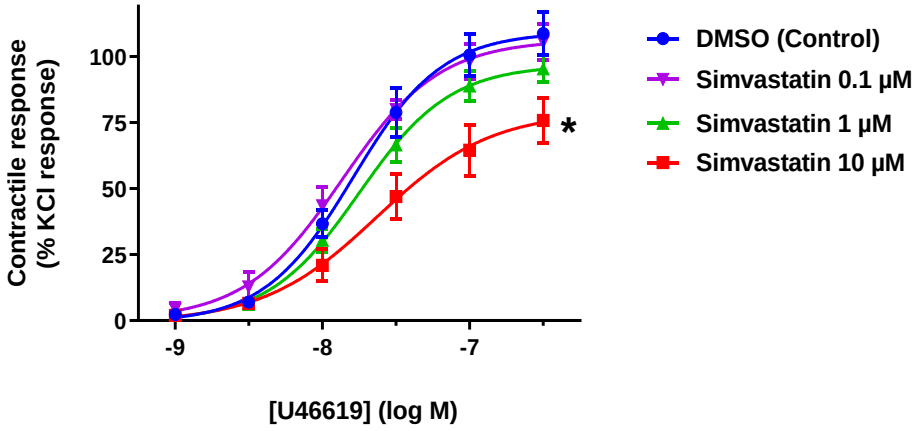

Figure 2.2: Log concentration-response curves for the vasocontraction effects of U46619 with pre-incubation of simvastatin (100 nM, 1 and 10 μM). Control is vehicle only (0.1% v/v DMSO). Data are expressed as a percentage of the contraction to 60 mM KCl and are mean ± SEM of 6 experiments. *P<0.05, One-way ANOVA v control followed by Sidak post-hoc test.

	R_{max} (% KCl response, mean ± SEM)	pEC_{50} (mean ± SEM)
Control	110 ± 7	7.76 ± 0.06
0.1 μ M simvastatin	106 ± 8	7.94 ± 0.11
1 μM simvastatin	97 ± 5	7.74 ± 0.07
10 μM simvastatin	84 ± 6*	7.51 ± 0.14

Table 2.2: Maximum contraction (R_{max}) expressed as a percentage of the response to 60mM KCl and log EC_{50} (pEC_{50}) for U46619 in the absence (control, 0.1% v/v DMSO), or presence of simvastatin (100 nM, 1, and 10 μM) in PCAs. Data are expressed as mean ± SEM of 6 experiments. *p<0.05 v control, One-way ANOVA followed by Sidak post-hoc test.

On the other hand, in the absence of calcium, pre-incubation with 10 μM simvastatin had no effect on U46619 induced contraction of the PCA (Response at maximum concentration = 14 ± 1%, n=6) compared to the control (Response at maximum concentration = 13 ± 2%, n=6). See figure 2.3.

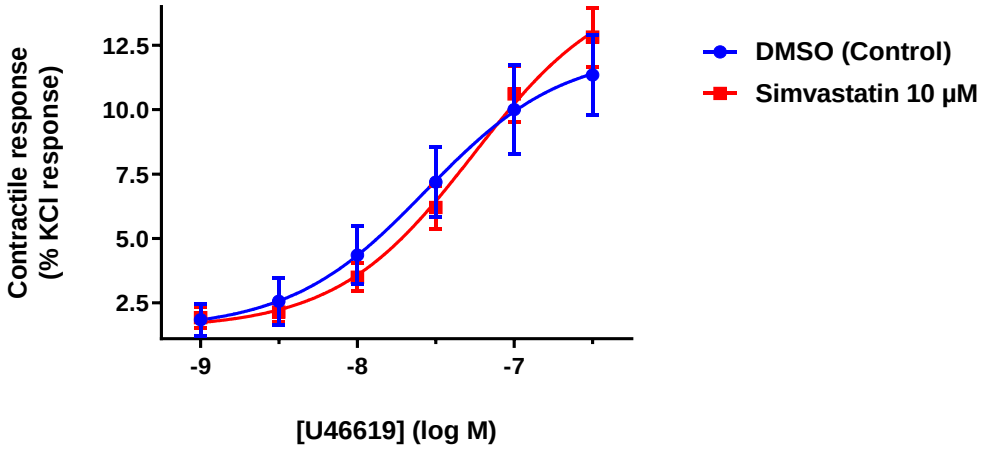

Figure 2.3: Log concentration-response curves for the vasocontraction effects of U46619 with pre-incubation simvastatin (10 μM) in the absence of calcium. Control is vehicle only (0.1% v/v DMSO). Data are expressed as a percentage of the contraction to 60 mM KCl and are mean ± SEM of 6 experiments. Non-significant p>0.05 v control.

2.3.1.1. The effects of simvastatin on the time profile of the contraction to U46619 in PCA:

Previous studies have demonstrated that simvastatin produces a time-dependent relaxation of the porcine coronary artery. As there was an apparent effect of simvastatin on the U46619-induced concentration-response curve, we determined the effect of simvastatin on the time profile of the contraction to U46619 in order to establish whether simvastatin affects the initiation of the contraction or the maintained response. Tissues were pre-contracted with 30 nM U46619 in the presence of 10 μM simvastatin and contractions measured for 2 h. Simvastatin caused significant inhibition of U46619-induced contraction at all-time points as shown in figure 2.4.

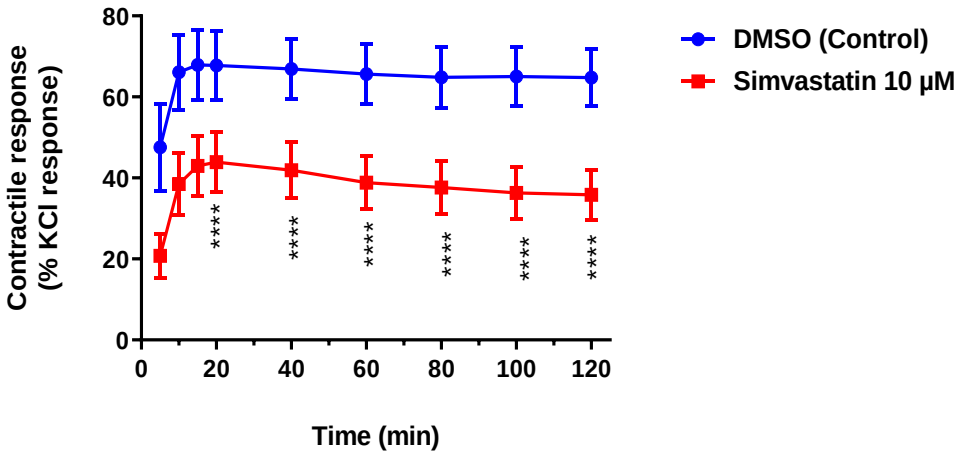

Figure 2.4: Time-response curves for the vasocontraction effects of 30 nM U46619 on PCA pre-incubated with 10 μM simvastatin. Control is vehicle only (0.1% v/v DMSO). Data are expressed as a percentage of the contraction to 60 mM KCl at different time points and are mean of 6 experiments. **** $p<0.0001$ v control, 2-way ANOVA followed by Sidak post-hoc test.

On the other hand, in the absence of calcium, pre-incubation with a single concentration (10 μM) of simvastatin had no effect on the single concentration of U46619 induced contraction of the PCA at different time points except, the last one (figure 2.5). Contractions to U46619 were a lot smaller in the absence of extracellular calcium compared to the presence of calcium.

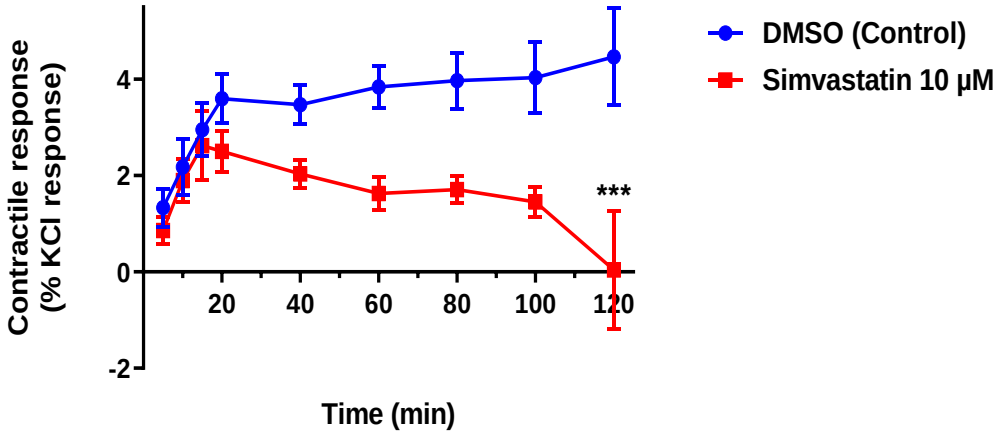

Figure 2.5: Time-response curves for the vasocontraction effects of 30 nM U46619 on PCA pre-incubated with 10 μM simvastatin in the absence of calcium. Control is vehicle only (0.1% v/v DMSO). Data are expressed as a percentage of the contraction to 60 mM KCl at different time points and are mean of 6 experiments. *** $p<0.001$ v control, 2-way ANOVA followed by Sidak post-hoc test.

2.3.1.2. The effects of simvastatin on tissues pre-contracted with U46619:

Previous studies have demonstrated that simvastatin produced a time-dependent relaxation of porcine coronary artery pre-contracted with U46619. In order to confirm these studies, the effect of 10 μM simvastatin on tissues pre-contracted with 300 nM U46619 was determined in coronary artery segments. As expected, 10 μM simvastatin caused a time-dependent relaxation of pre-contracted PCA as shown in figure 2.6.

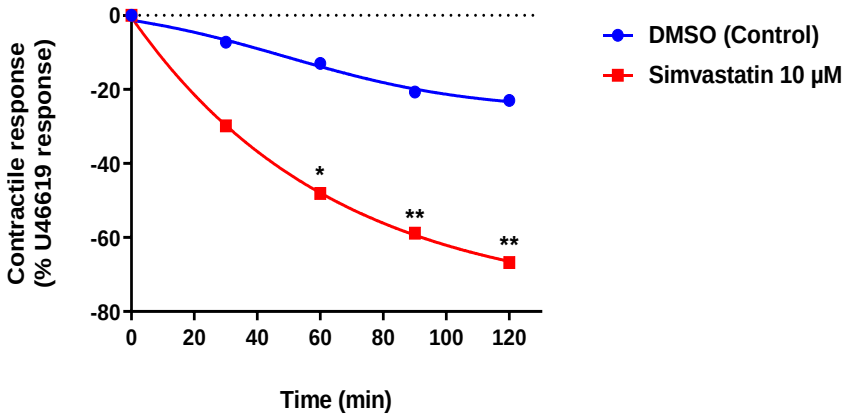

Figure 2.6: Effect of simvastatin (10 μM) on porcine coronary artery pre-contracted with U46619. Control is vehicle only (0.1% v/v DMSO). Data are expressed as a percentage of relaxation to 300 nM U46619-induced contraction and are mean of 6 experiments. *p<0.05, **p<0.01 v control, 2-way ANOVA followed by Sidak post-hoc test.

2.3.2. The effects of Y27632 (Rho kinase inhibitor) on U46619 induced contraction in PCA:

To examine the hypothesis that Rho kinase is involved in the contractile response evoked by activation of thromboxane receptors, the effect of the Rho kinase inhibitor Y27632 on concentration-response curves to U46619 was determined in coronary artery segments from the pig in the presence of calcium (Fig.2.7) and in the absence of calcium (Fig.2.8). In the presence of calcium and absence of Y27632, U46619 produced a large contraction of the PCA (R_{max} = 87 ± 9% KCl response, pEC_{50} = 8.4 ± 0.04, n=6). Y27632 caused a concentration-dependent inhibition of the U46619-induced contraction. Table (2.3) shows the R_{max} and pEC_{50} values in the presence of Y27632.

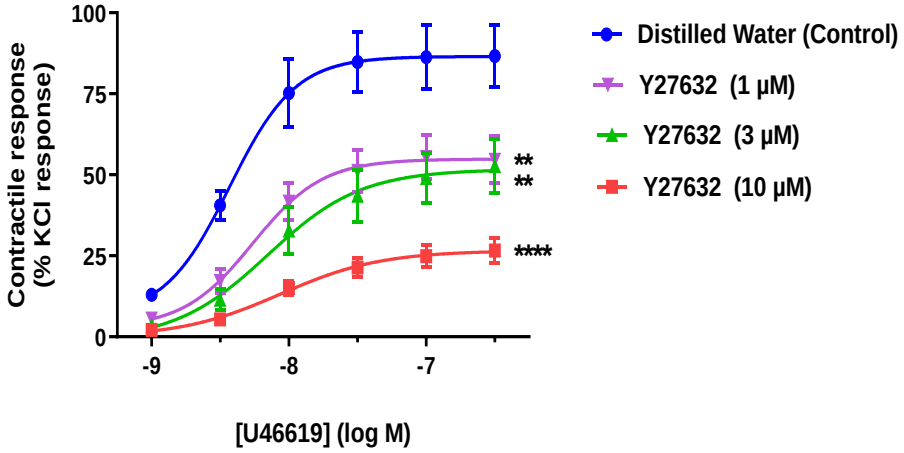

Figure 2.7: Log concentration-response curves for the vasocontraction effects of U46619 with pre-incubation of Y27632 (1, 3, 10 µM). Control is Distilled water. Data are expressed as a percentage of the contraction to 60 mM KCl and are mean ± SEM of 6 experiments. **p<0.01, and ****p<0.0001 v control, One-way ANOVA followed by Sidak post-hoc test.

	R_{max} (% KCl response, mean ± SEM)	pEC50 (mean ± SEM)
Control	87 ± 9 %	8.4 ± 0.04
1 µM Y27632	55 ± 7 %**	8.3 ± 0.1
3 µM Y27632	52 ± 8 %**	8.1 ± 0.1
10 µM Y27632	27 ± 4 %***	8.0 ± 0.1

Table 2.3: Maximum contraction (Rmax) expressed as a percentage of the response to 60 mM KCl and log EC_{50} (pEC_{50}) for U46619 in the absence (control, which is distilled water), or presence of Y27632 (1, 3, and 10 µM) in PCAs. Data are expressed as mean ± SEM of 6 experiments. **p<0.01 and ****p<0.0001 v control, One-way ANOVA followed by Sidak post-hoc test.

In the absence of calcium and absence of Y27632, U46619 also produced contraction of the PCA, although the maximum response was reduced compared to addition of U46619 in the presence of calcium (Response at maximum concentration = 18 ± 1%, n=6). In the presence of Y27632, U46619-induced contraction was almost completely inhibited (Response at maximum concentration = 2 ± 0.5 %).

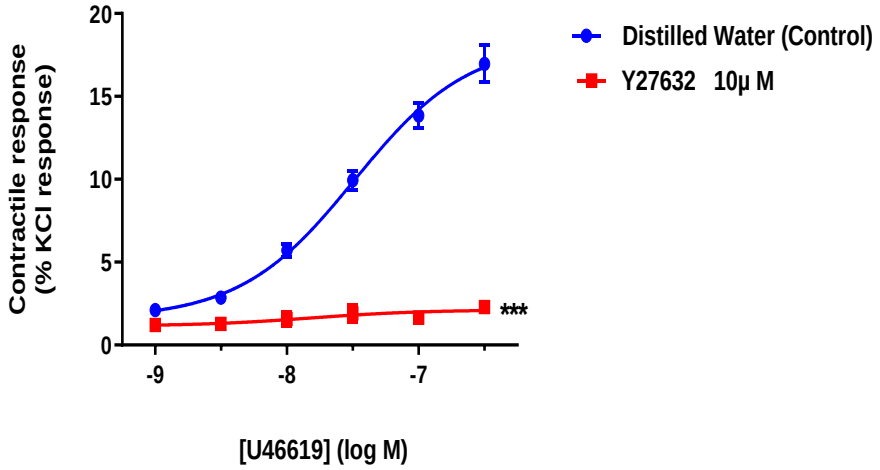

Figure 2.8: Log concentration-response curves for the vasocontraction effects of U46619 with pre-incubation of Y27632 (10 µM) in the absence of calcium. Control is distilled water. Data are expressed as a percentage of the contraction to 60 mM KCl and are mean ± SEM of 6 experiments. ***p<0.001 v control, Student's 2-tailed paired t-test.

2.3.2.1. The effects of Y27632 on the time profile of the contraction to U46619 in PCA:

In order to determine the effect of inhibition of Rho kinase on the time-dependent contraction profile to U46619, tissues were pre-incubated with a single concentration of Y27632 (10 μM) for 60 min, prior to exposure to a single, sub-maximum effective concentration of U46619 (30 nM). In the presence of 10 μM Y27632, there was a significant inhibition of U46619-induced contraction with most time points as shown in figure 2.9.

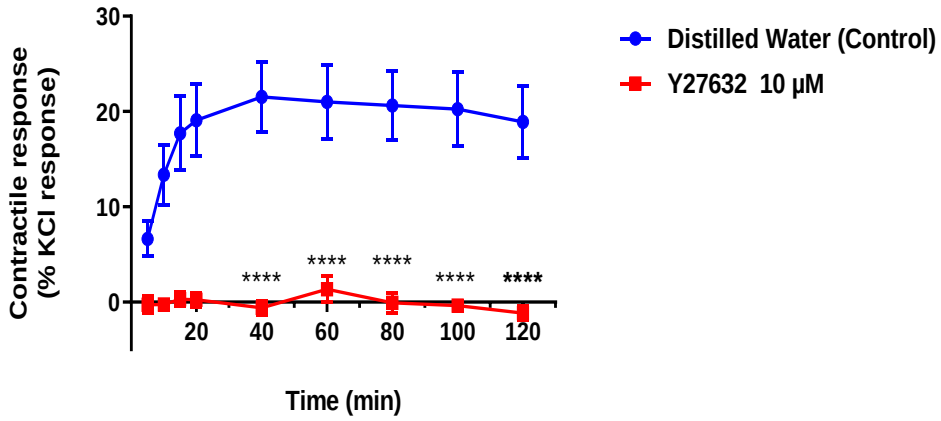

Figure 2.9: Time-response curves for the vasocontraction effects of 30 nM U46619 on PCA pre-incubated with 10 μM Y27632. Control is distilled water. Data are expressed as a percentage of the contraction to 60 mM KCl at different time points and are mean of 6 experiments. ****p<0.0001 v control, 2-way ANOVA followed by Sidak post-hoc test.

2.3.2.2. The effects of Y27632 on PCA pre-contracted with U46619:

In order to determine the time profile of the relaxant effect of Y27632, the effect of 10 μM Y27632 on tissues pre-contracted with 300 nM of U46619 was determined in coronary artery segments from pig over time. Y27632 caused complete relaxation of pre-contracted PCA through all time points as in figure 2.10.

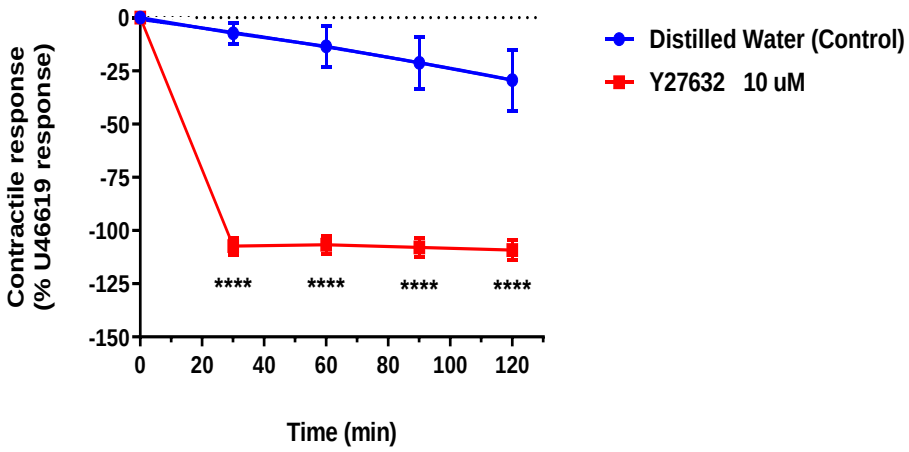

Figure 2.10: Effect of Y27632 (10 uM) on porcine coronary artery pre-contracted with U46619. Control is distilled water. Data are expressed as a percentage of relaxation to 300n M U46619-induced contraction and are mean of 6 experiments. ****p<0.0001 v control, 2-way ANOVA followed by Sidak post-hoc test.

2.3.2.3. The combined effect of simvastatin and Y27632 on U46619-induced contraction in PCA:

We hypothesised that, if simvastatin inhibited Rho kinase activation, inhibition of Rho kinase activation with Y27632 would prevent the inhibitory effect of simvastatin. In order to determine the combined inhibitory effect of simvastatin (10 μM) and Y27632 (10 μM) on concentration-response curves to U46619, tissues were pre-incubated with and without simvastatin (10 μM) for 2 h then with Y27632 (10 μM) for 1 h. The inhibitory effect of simvastatin and Y27632 together was larger than that produced by Y27632 and DMSO (control). (Response at maximum concentration = 15 ± 5%, mean ± SEM, n=6) compared to the control (Response at maximum concentration = 41 ± 3.4 %, mean ± SEM, n=6). Table (2.4) and figure (2.11).

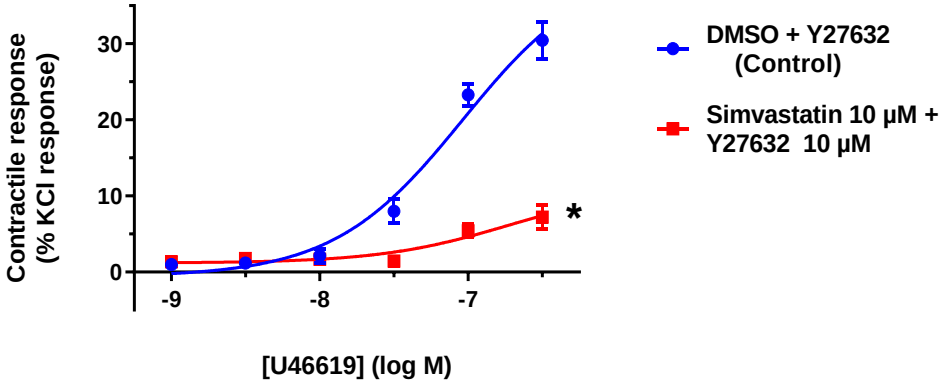

Figure 2.11: Log concentration-response curves for the vasocontraction effects of U46619 with pre-incubation of Simvastatin and Y27632 (10 μM). Control is DMSO+Y27632. Data are expressed as a percentage of the contraction to 60 mM KCl and are mean ± SEM of 6 experiments. *p<0.05 v control at 300 nM of U46619, Student's 2-tailed paired t-test.

	Response at 300 nM U46619 ± SEM
DMSO+Y27632 (Control)	41 ± 3.4 %
Simvastatin+Y27632 (10 μM)	15 ± 5 % *

Table 2.4: Response at maximum concentration expressed as a percentage of the response to 60 mM KCl for U46619 in the absence (control, which is DMSO+Y27632), or presence of simvastatin and Y27632 (10 μM) in PCAs. Data are expressed as mean ± SEM of 6 experiments. *p<0.05 v control at 300 nM U46619, Student's 2-tailed paired t-test.

2.3.2.4. Effect of simvastatin on MYPT1 phosphorylation in porcine coronary artery:

In order to determine the Rho kinase activity, changes in phosphorylation of the Rho kinase substrate MYPT1 were determined using Western blotting. Representative blots are shown in figure 2.12 C of Western blotting experiment assessing the effect of simvastatin incubation and U46619 on MYPT1 phosphorylation in isolated PCA rings. The antibody against total MYPT1 detected a band at ~140 kDa, which is close to the predicted molecular weight of 115 KDa. The antibody against phosphorylated MYPT1 at Thr696 detected a faint band at ~140 kDa, whereas the antibody against phosphorylated MYPT1 at Thr850 did not detect any band at ~140 kDa but did detect a strong band at just over 75 kDa (figure 2.12 C). Although there was an apparent increase in the intensity of the 75 kDa band with simvastatin and U46619, it is questionable whether this is MYPT1.

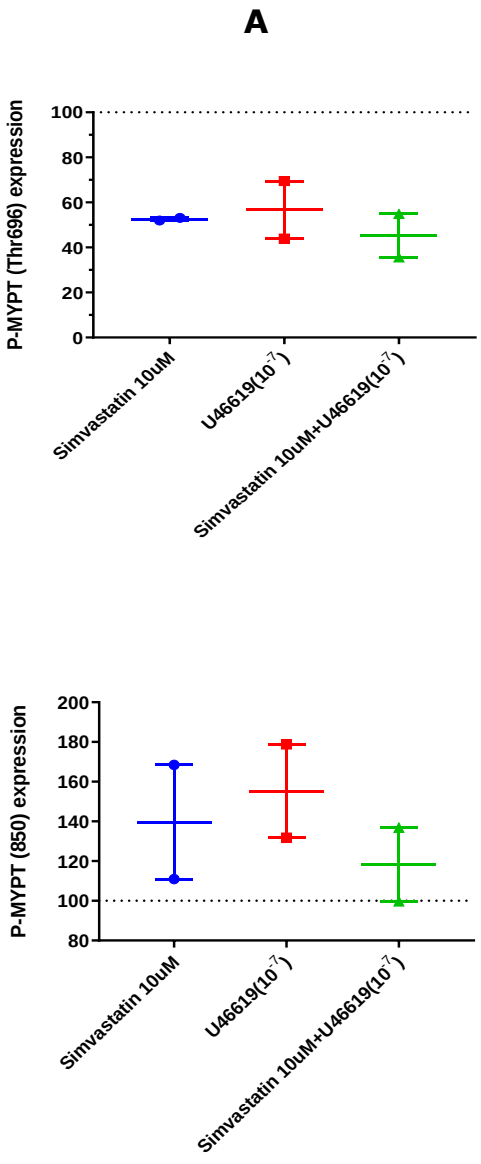

B

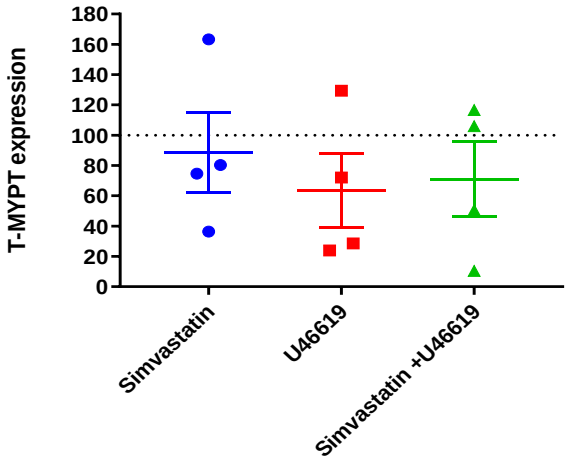
T-MYPT expression
180
160
140
120
100
80
60
40
20
0
Simvastatin
U46619
Simvastatin +U46619

C

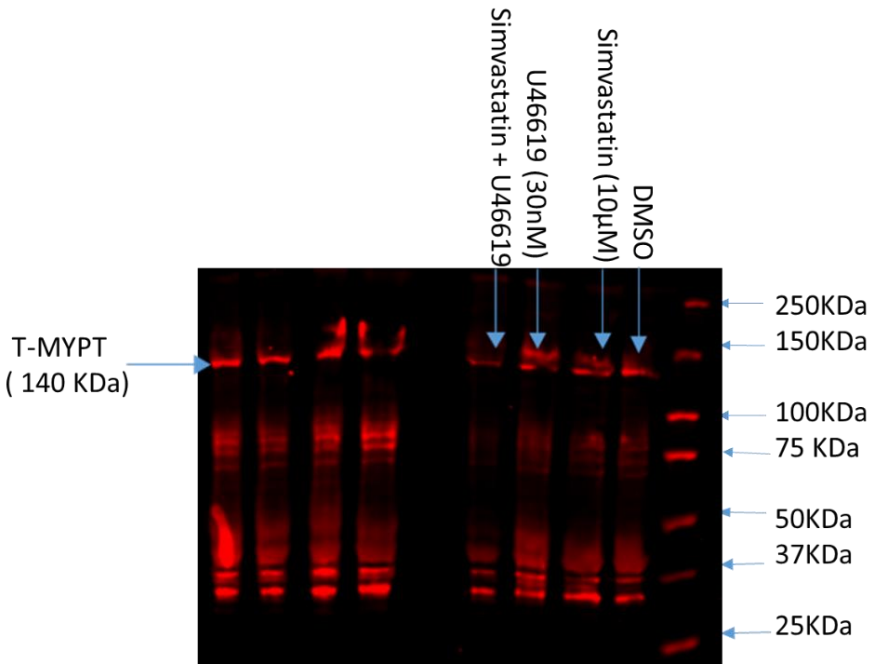
Simvastatin + U46619
U46619 (30nM)
Simvastatin (10µM)
DMSO
T-MYPT
(140 KDa)
250KDa
150KDa
100KDa
75 KDa
50KDa
37KDa
25KDa

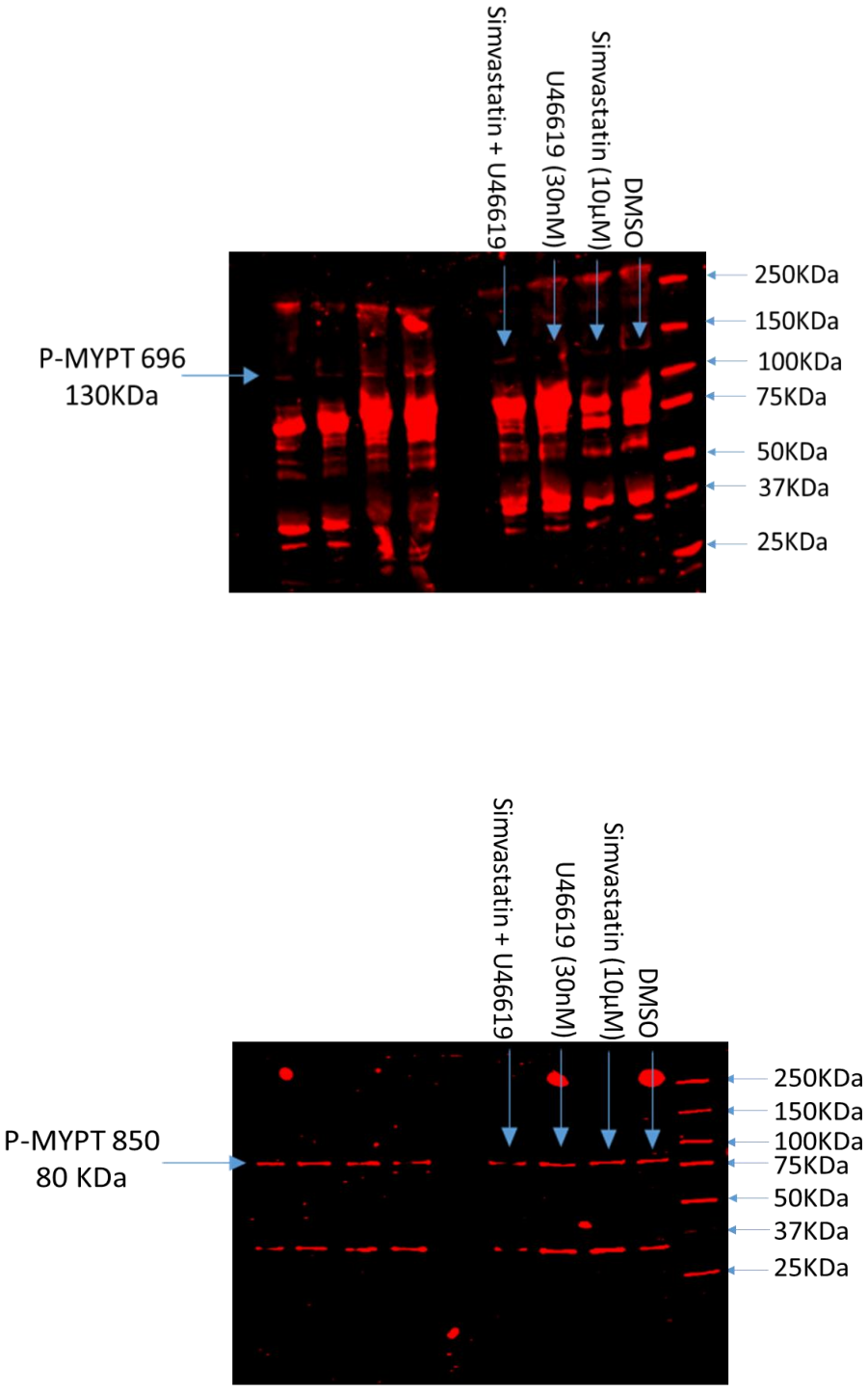

Figure 2.12: A and **B** Bar charts showing the levels of phosphorylated and total -MYPT1 (Thr696 and Thr850 sites) from simvastatin and U46619 treated segments of 2 different tissues. Data are presented as a percentage of the control (untreated tissues) and are presented as scatterplots, One-way ANOVA followed by Tukey post-hoc test. **C** Representative Western blots assessing the effect of simvastatin on MYPT1 phosphorylation in PCA. Prior to freezing and homogenisation, PCA rings were incubated in tissue baths for 2 h in the absence or presence of simvastatin (10 µM) and U46619 (30 nM).

2.3.3. The effects of PD98059 (MEK inhibitor) on the cumulative contraction of U46619 (thromboxane A2 agonist) in the PCA:

In order to determine whether ERK is involved in the contraction in response to thromboxane receptor activation, the effect of the MEK inhibitor PD98059 on U46619-induced contractions was determined (figure 2.13). In these experiments, control tissues reached an R_{max} value of 104 ± 9% KCl response with a pEC_{50} value of 8.1 ± 0.1 (n = 6). Pre-incubation with increasing concentrations of PD98059 had no significant effect on the contractile response. Table (2.5) shows the R_{max} and pEC_{50} values in the presence of PD98059.

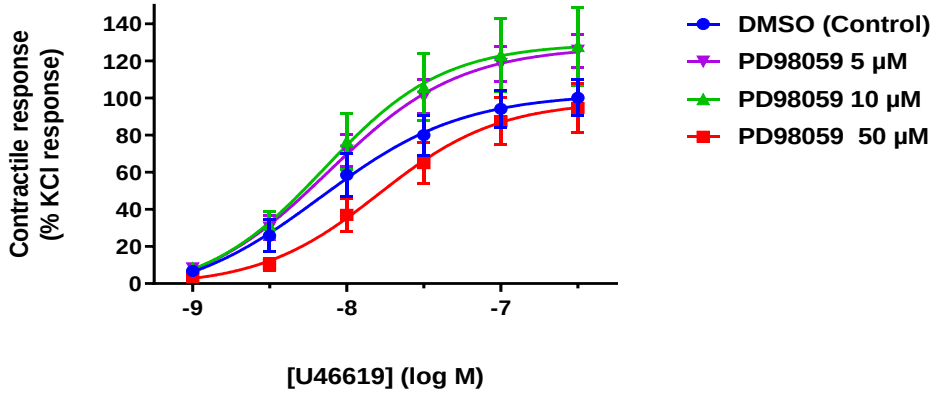

Figure 2.13: Log concentration-response curves for the vasocontraction effects of U46619 with pre-incubation of PD98059 (5, 10, 50 µM). Data are expressed as a percentage of the contraction to 60 mM KCl and are mean ± SEM of 6 experiments. P>0.05 v control, One-way ANOVA followed by Sidak post-hoc test.

Concentrations of PD98059	R_{max} (KCl response, mean ± SEM)	pEC_{50} (Mean ± ESM)
Control	104 ± 9%	8.1 ± 0.1
5 µM	128 ± 9%	8.1 ± 0.1
10 µM	130 ± 21%	8.1 ± 0.1
50 µM	97 ± 13%	8 ± 0.1

Table 2.5: Maximum contraction expressed as a percentage of the response to 60 mM KCl and log EC50 value for U46619 in the absence (control), or presence of PD98059 (5, 10, and 50 µM) in the PCA. Data are expressed as mean ± SEM of 6 experiments. p> 0.05 v control, One-way ANOVA followed by Sidak post-hoc test.

In the absence of calcium and absence of PD98059, U46619 also produced contraction of the PCA, although the maximum response was reduced compared to addition of U46619 in the presence of calcium (Response at maximum concentration = 20 ± 1.3%, (n = 7, P>0.05). In the presence of PD98059, U46619-induced contraction was inhibited significantly at the intermediate concentration (Response at maximum concentration = 17.4 ± 2%, (n = 7, P>0.05). Figure 2.14

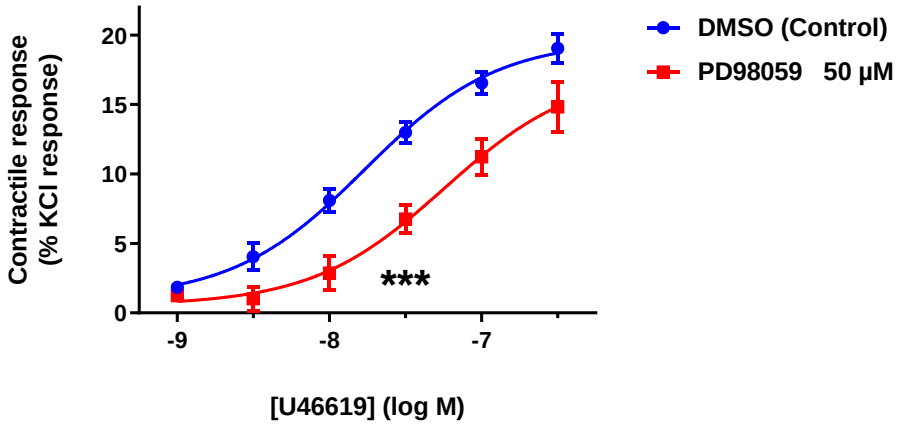

Figure 2.14: Log concentration-response curves for the vasocontraction effects of U46619 with pre-incubation of PD98059 (50 µM) in the absence of calcium. Control is distilled water. Data are expressed as a percentage of the contraction to 60 mM KCl and are mean ± SEM of 7 experiments. ***p<0.001 v control, Student's 2-tailed paired t-test.

2.3.3.1. The effect of PD89059 on the time profile of the contraction to U46619 in PCA:

In order to determine the effect of inhibition of ERK on the time-dependent contraction profile to U46619, tissues were pre-incubated with a single concentration of PD98059 (50 μM) for 60 min, prior to exposure to a single concentration of U46619 (30 nM). In the presence of 50 μM PD89059, there was a significant inhibition of U46619-induced contraction at most time points as shown in figure 2.15.

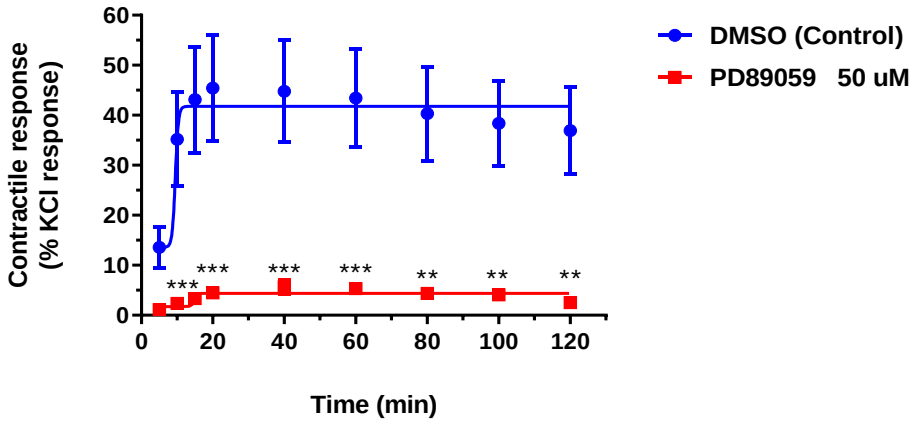

Figure 2.15: Time-response curves for the vasocontraction effects of 30 nM U46619 on PCA pre-incubated with 50 μM PD98059. Control is distilled water. Data are expressed as a percentage of the contraction to 60 mM KCl at different time points and are mean of 6 experiments. **p<0.01 and ***p<0.001 v control, Two-way ANOVA followed by Sidak post-hoc test.

2.3.3.2. The effect of PD89059 on PCA pre-contracted with U46619:

In order to determine the time profile of the relaxant effect of PD98059, the effect of 50 μM PD98059 on tissues pre-contracted with 300 nM of U46619 was determined in coronary artery segments from pig over time. PD98059 caused complete relaxation of pre-contracted PCA through all time points as in figure 2.16 (Mean = -74.2 ±18.7%, mean ± SEM, n=6) comparing to the control (Mean = -7.6 ± 2.2 %, mean ± SEM, n=6).

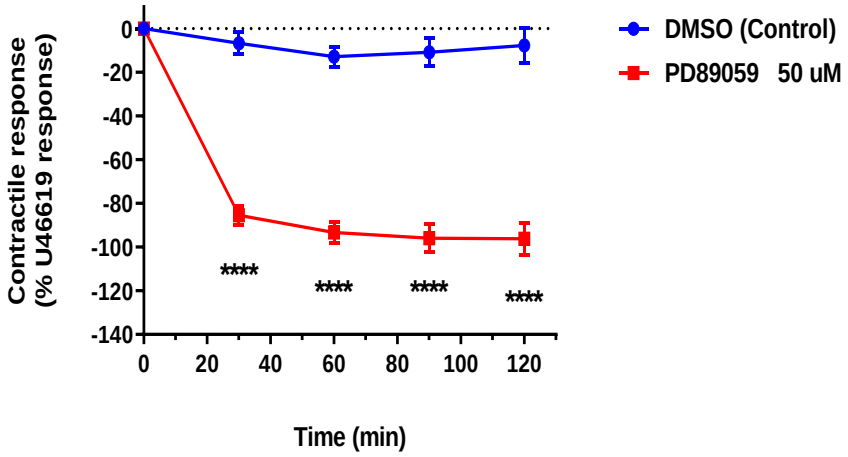

Figure 2.16: Effect of PD98059 (50 μM) on porcine coronary artery pre-contracted with U46619. Control is DMSO. Data are expressed as a percentage of relaxation to 300 nM U46619-induced contraction and are mean of 6 experiments. ****p<0.0001 v control, two-way ANOVA followed by Sidak post-hoc test.

2.3.3.3. The combined effect of simvastatin and PD89059 on U46619-induced contraction in PCA:

We hypothesised that, if simvastatin inhibited ERK activation, inhibition of ERK activation with PD98059 would prevent the inhibitory effect of simvastatin. In order to determine the combined inhibitory effect of simvastatin (10 μM) and PD89059 (50 μM) on concentration-response curves to U46619, tissues were pre-incubated with or without simvastatin (10 μM) for 2 h then with PD89059 (50 μM) for 1 h. The inhibitory effect of simvastatin and PD89059 together was larger than that produced by PD89059 and DMSO (control). (Mean = 15 ± 5%, n=6) comparing to the control (Mean = 41 ± 3.4 %, n=6). Table (2.6) and figure (2.17)

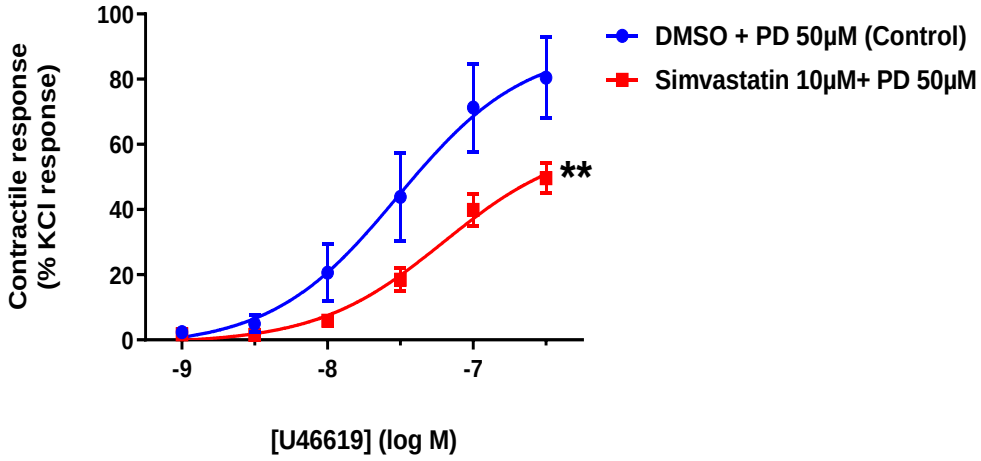

Figure 2.17: Log concentration-response curves for the vasocontraction effects of U46619 with pre-incubation of Simvastatin and PD89059 (50 μM). Control is DMSO+ PD89059. Data are expressed as a percentage of the contraction to 60 mM KCl and are mean ± SEM of 6 experiments. **p<0.01 v control at 300 nM U46619, Student's 2-tailed paired t-test.

	Response at 300 nM U46619 ± SEM
DMSO+ PD89059 (Control)	94 ± 10 %
Simvastatin(10 μM)+ PD89059 (50 μM)	63 ± 4.1 % **

Table 2.6: Response at maximum concentration expressed as a percentage of the response to 60 mM KCl for U46619 in the absence (control, which is DMSO+ PD89059), or presence of simvastatin and PD89059 (50 μM) in PCAs. Data are expressed as mean ± SEM of 6 experiments. **p<0.01 v control at 300 nM U46619, Student's 2-tailed paired t-test.

2.3.3.4. Effect of simvastatin on ERK activation in porcine coronary artery:

ERK activity was determined by measuring changes in phosphorylation of ERK1 and ERK2 at the dual phosphorylation sites of 44KDa and 42KDa. A representative immunoblotting experiment showing the effect of simvastatin incubation and U46619 on ERK activity in isolated PCA rings incubated in tissue baths for 2 h in the presence or absence of 10 μM simvastatin is shown in figure 2.18. Double bands were detected at the predicted molecular weights of 42 and 44kDa with both the total and the phosphorylated ERK antibodies (figure 2.18). In PCA incubated with simvastatin for 2 h, the level of total ERK1 and ERK2 activity did not show significant changes comparing to PCA incubated with U46619 and other incubated with a simvastatin-U46619 combination (figure 2.19 A). Moreover, the level of phosphorylated activity for ERK1 and ERK2 showed no significant differences (figure 2.19 B).

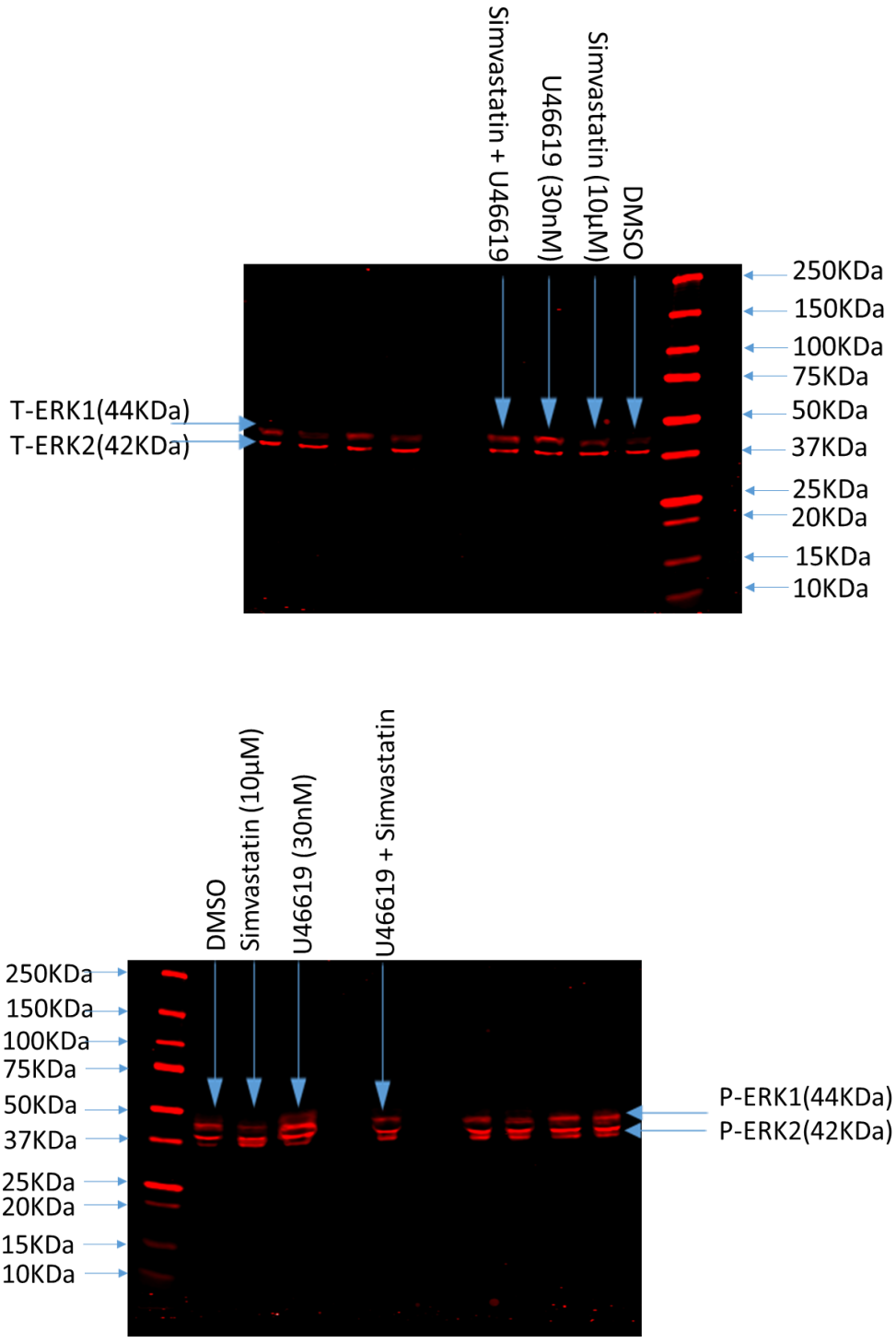

Figure 2.18: Representative Immunoblots assessing the effect of simvastatin on total ERK and phosphorylated ERK in PCA. Prior to freezing and homogenisation, PCA rings were incubated in tissue baths for 2 h in the absence or presence of 10 µM simvastatin.

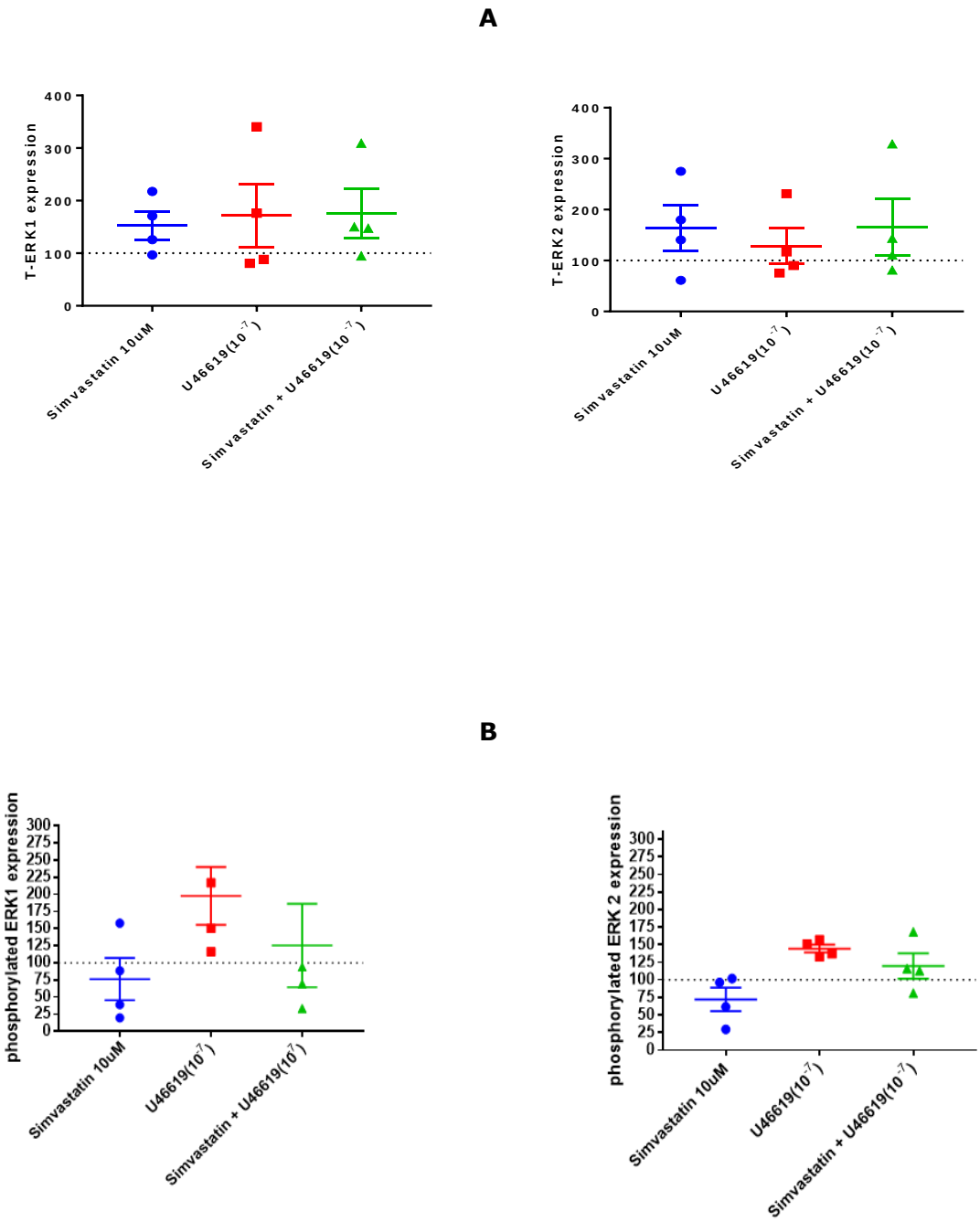

Figure 2.19: A and B are 4-charts show the activity of total and phosphor-ERK from simvastatin, U46619, and simvastatin-U46619 combination treated segments of 3 different tissues. Data are expressed as a percentage of the control (untreated) tissue and are presented as scatterplots, One-way ANOVA followed by Tukey post-hoc test.

2.3.4. The effects of calyculin A (phosphoprotein phosphatase inhibitor) on simvastatin-induced relaxation in PCAs:

Rho kinase inhibits myosin phosphatase and so we hypothesised that, if simvastatin inhibited Rho kinase activation, inhibition of myosin phosphatase would prevent the inhibitory effect of simvastatin. Therefore, tissues were pre-incubated with 100 nM calyculin A, the contracted with U46619 followed by addition of 10 μM simvastatin for 2 h. Calyculin A caused inhibition of the relaxant effect of simvastatin on pre-contracted PCA through most of the 2 h compared to the control (n=8) as shown in figure 2.20.

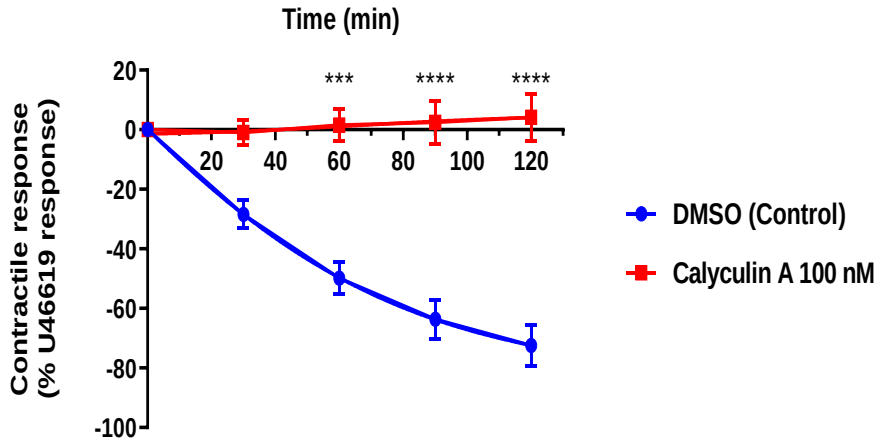

Figure 2.20: Effect of calyculin A (100 nM) on simvastatin relaxation in porcine coronary artery pre-contracted with U46619. Control is vehicle only (0.1% v/v DMSO). Data are expressed as a percentage of relaxation to U46619-induced contraction and are mean of 8 experiments. ***p<0.001, ****p<0.0001 v control, two-way ANOVA followed by Sidak post-hoc test.

2.3.5. Role of mitochondria in Simvastatin response:

2.3.5.1. Effect of antimycin A on the simvastatin response:

Mitochondria can play an important role in the regulation of smooth muscle tone. Therefore, in order to determine whether mitochondria are involved in the simvastatin-induced inhibition of the U46619-induced response, tissues were incubated with 10 μM simvastatin, in the absence or presence of the mitochondrial complex III inhibitor antimycin A (10 μM). Pre-incubation with antimycin A alone inhibited the contractile response at the lower concentrations of U46619 but had no effect on the maximum response obtained, whereas simvastatin inhibited the maximum contraction to U46619. Pre-incubation with antimycin A in the presence of simvastatin did not reverse the inhibitory effect of simvastatin. See table 2.7 and figure 2.21.

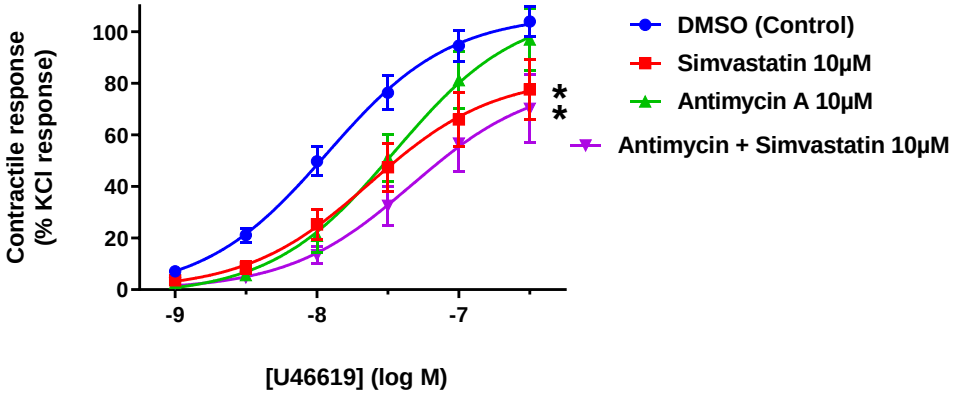

Figure 2.21: Log concentration-response curves for the vasocontractile effects of U46619 with pre-incubation 10 μM antimycin A and/or 10μM simvastatin. Control is vehicle only (0.1% v/v DMSO). Data are expressed as a percentage of the contraction to 60 mM KCl and are mean ± SEM of 7 experiments. *p<0.05 v control, Two-way ANOVA followed by Sidak post-hoc test.

	Response at 300 nM U46619 ± SEM
Control	107 ± 6%
Simvastatin	83 ± 12%*
Antimycin A	110 ± 12%
Simvastatin +Antimycin A	81± 14%*

Table 2.7: Response at maximum concentration expressed as a percentage of the response to 60 mM KCl for U46619 in the absence (control, which is 0.1% v/v DMSO), or presence of 10 μM simvastatin and/or 10 μM antimycin A in PCAs. Data are expressed as mean ± SEM of 7 experiments. *p<0.05 v control, Two-way ANOVA followed by Sidak post-hoc test.

2.3.5.2. Effect of myxothiazol on the simvastatin response:

In order to determine further whether mitochondria are involved in the simvastatin-induced inhibition of the U46619-induced response, tissues were incubated with 10 μM simvastatin, in the absence or presence of another mitochondrial complex III inhibitor, myxothiazol (10 μM). The maximum response observed using the control tissues was 123 ± 8% of the KCl response. Pre-incubation with myxothiazol alone had no significant effect on the contractile response to U46619 in these experiments, whereas simvastatin inhibited the contraction to U46619 (the maximum response observed was 90 ± 5%). Pre-incubation of myxothiazol in the presence of simvastatin did not reverse the inhibitory effect of simvastatin. See table 2.8 and figure 2.22.

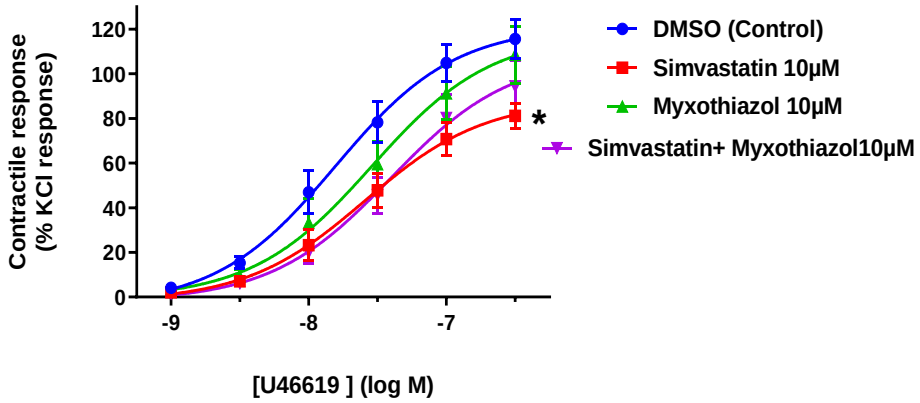

Figure 2.22: Log concentration-response curves for the vasocontractile effects of U46619 with pre-incubation 10 μM myxothiazol and/or 10 μM simvastatin. Control is vehicle only (0.1% v/v DMSO). Data are expressed as a percentage of the contraction to 60mM KCl and are mean ± SEM of 6 experiments. *p<0.05 v control at 300 nM U46619, Two-way ANOVA followed by Sidak post-hoc test.

	Response at 300 nM U46619 ± SEM
Control	123 ± 8%
Simvastatin	90 ± 5%*
Myxothiazol	121 ± 14%
Simvastatin +Myxothiazol	109 ± 12%

Table 2.8: Response at maximum concentration expressed as a percentage of the response to 60 mM KCl for U46619 in the absence (control, which is 0.1% v/v DMSO), or presence of 10 μM simvastatin and/or 10 μM myxothiazol in PCAs. Data are expressed as mean ± SEM of 6 experiments. *p<0.05 v control at 300 nM U46619, Two-way ANOVA followed by Sidak post-hoc test.

2.3.5.3. Effect of rotenone on the simvastatin response:

In order to determine further whether mitochondria are involved in the simvastatin-induced inhibition of the U46619-induced response, tissues were incubated with 10 μM simvastatin, in the absence or presence of the mitochondrial complex I inhibitor, rotenone (10 μM). The maximum response observed of the control tissues was 97 ± 7% of the KCl response. Pre-incubation with rotenone alone had no significant effect on the contractile response to U46619 in this experiment whereas simvastatin inhibited the contraction to U46619 (the maximum response observed was 77± 9%). Pre-incubation of rotenone in the presence of simvastatin did not reverse the inhibitory effect of simvastatin. Table 2.9 and figure 2.23.

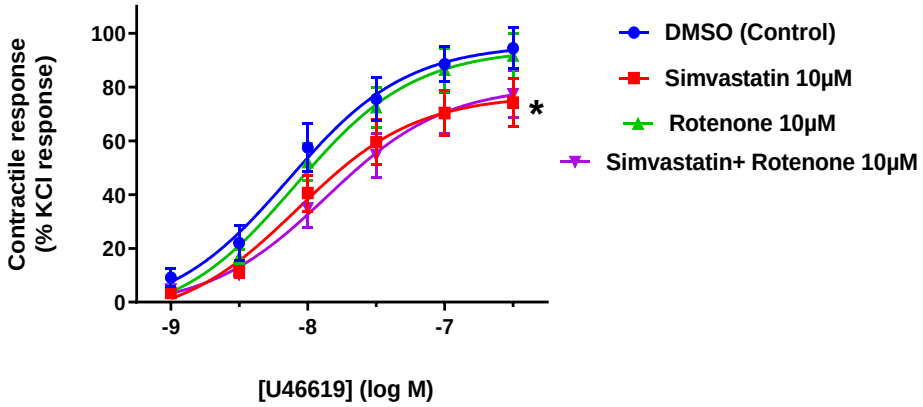

Figure 2.23: Log concentration-response curves for the vasocontractile effects of U46619 with pre-incubation 10 μM rotenone and/or 10μM simvastatin. Control is vehicle only (0.1% v/v DMSO). Data are expressed as a percentage of the contraction to 60mM KCl and are mean ± SEM. of 8 experiments. *p<0.05 v control at 300 nM U46619, Two-way ANOVA followed by Sidak post-hoc test.

	Response at 300 nM U46619 ± SEM
Control	97 ± 7%
Simvastatin	77 ± 9%*
Rotenone	94 ± 8%
Simvastatin + Rotenone	81 ± 8%

Table 2.9: Response at maximum concentration expressed as a percentage of the response to 60 mM KCl for U46619 in the absence (control, which is 0.1% v/v DMSO), or presence of 10 μM simvastatin and 10 μM rotenone in PCAs. Data are expressed as mean ± SEM of 8 experiments. *p<0.05 v control at 300 nM of U46619, Two way ANOVA followed by Sidak post-hoc test.

2.3.5.4. Effect of combination of antimycin A and rotenone on the simvastatin response:

Previous studies had indicated that combinations of mitochondrial complex inhibitors were more effective at preventing the effects of simvastatin. Therefore, the role of antimycin A and rotenone in simvastatin-induced inhibition of the U46619-induced response was determined. Tissues were incubated with 10 μM simvastatin, in the absence or presence of mitochondrial complexes I and III inhibitors, rotenone and antimycin A (10 μM). Pre-incubation with the antimycin A-rotenone combination alone had no significant effect on the contractile response to U46619, whereas simvastatin inhibited the contraction to U46619. Antimycin A-rotenone combination in the presence of simvastatin enhanced the inhibitory effect of simvastatin. See table 2.10 and figure 2.24.

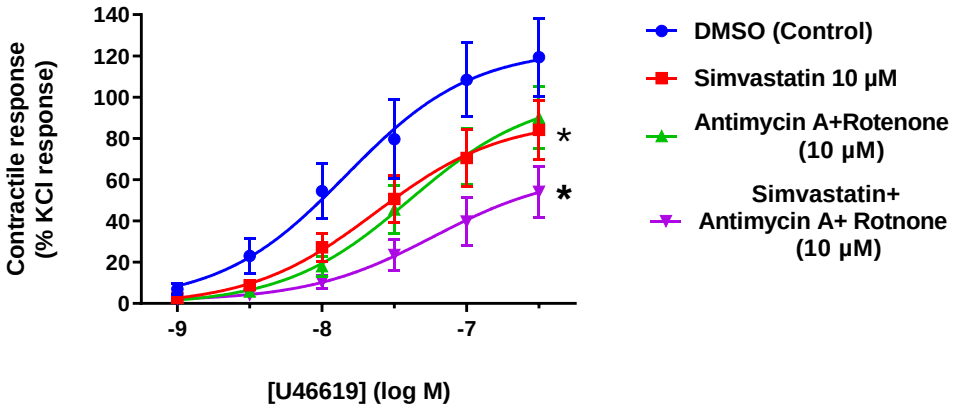

Figure 2.24: Log concentration-response curves for the vasocontractile effects of U46619 with pre-incubation 10 μM (antimycin A and rotenone) and/or 10 μM simvastatin. Control is vehicle only (0.1% v/v DMSO). Data are expressed as a percentage of the contraction to 60 mM KCl and are mean ± SEM of 7 experiments. *p<0.05 v control at 300 nM of U46619, Two-way ANOVA followed by Tukey post-hoc test.

	Response at 300 nM of U46619 ± SEM
Control	119 ± 19%
Simvastatin	84 ± 15%*
Antimycin A-Rotenone	90 ± 15%
Simvastatin + Antimycin A-Rotenone	54 ± 13%*

Table 2.10: Response at maximum concentration expressed as a percentage of the response to 60 mM KCl for U46619 in the absence (control, which is 0.1% v/v DMSO), or presence of 10 μM simvastatin and 10 μM (antimycin A and rotenone) in PCAs. Data are expressed as mean ± SEM of 7 experiments. *p<0.05 v control at 300 nM of U46619, Two-way ANOVA followed by Tukey post-hoc test.

2.3.5.5. Effect of a combination of rotenone-myxothiazol on the simvastatin response:

In order to determine the role of rotenone-myxothiazol combination in simvastatin-induced inhibition of the U46619-induced response, tissues were incubated with 10 μM simvastatin, in the absence or presence of combined mitochondrial complexes inhibitors I and III, rotenone and myxothiazol (10 μM). Pre-incubation with myxothiazol-rotenone combination alone had no significant effect on the contractile response to U46619, whereas simvastatin inhibited the contraction to U46619. Pre-incubation with the myxothiazol-rotenone combination in the presence of simvastatin prevented the inhibitory effect of simvastatin. See table 2.11 and figure 2.25.

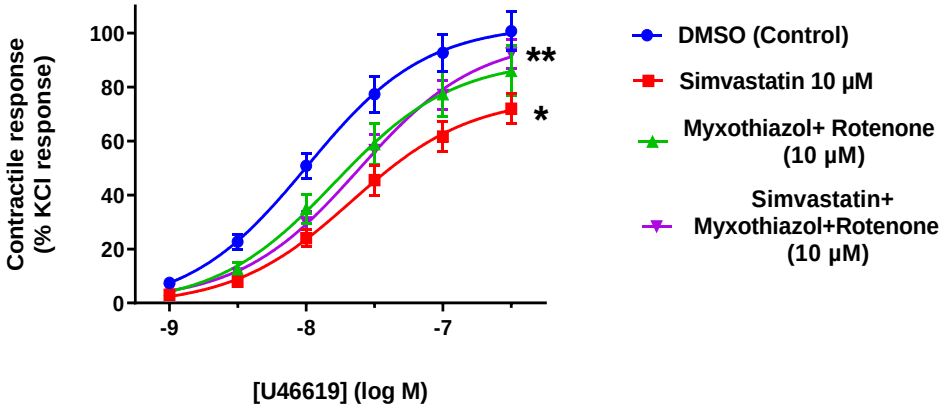

Figure 2.25: Log concentration-response curves for the vasocontractile effects of U46619 with pre-incubation 10 μM (myxothiazol and rotenone) and/or 10 μM simvastatin. Control is vehicle only (0.1% v/v DMSO). Data are expressed as a percentage of the contraction to 60 mM KCl and are mean ± SEM of 9 experiments. *p<0.05 v control, **p<0.01 v simvastatin, Two-way ANOVA followed by Tukey post-hoc test.

	Response at 300 nM of U46619 ± SEM
Control	104 ± 8%
Simvastatin	77 ± 5%*
Myxothiazol-Rotenone	91 ± 9%
Simvastatin + Myxothiazol-Rotenone	100 ± 5%**

Table 2.11: Response at maximum concentration expressed as a percentage of the response to 60 mM KCl for U46619 in the absence (control, which is 0.1% v/v DMSO), or presence of 10 μM simvastatin and 10 μM (myxothiazol and rotenone) in PCAs. Data are expressed as mean ± SEM of 9 experiments. *p<0.05 v control, **p<0.01 v simvastatin at 300nM of U46619, Two-way ANOVA followed by Tukey post-hoc test.

2.3.5.6. Role of AMP kinase in simvastatin response:

Inhibition of mitochondrial function can lead to activation of AMP kinase (Jiang et al. 2013). Therefore, in order to determine whether AMP kinase is involved in the simvastatin-induced inhibition of the U46619-induced response, tissues were incubated with 10 μM simvastatin, in the absence or presence of the AMP kinase inhibitor dorsomorphin (10 μM). Pre-incubation with dorsomorphin alone had no effect on the contractile response to U46619, whereas simvastatin inhibited the contraction to U46619. Pre-incubation with dorsomorphin in the presence of simvastatin did not reverse the inhibitory effect of simvastatin significantly. See table 2.12 and figure 2.26.

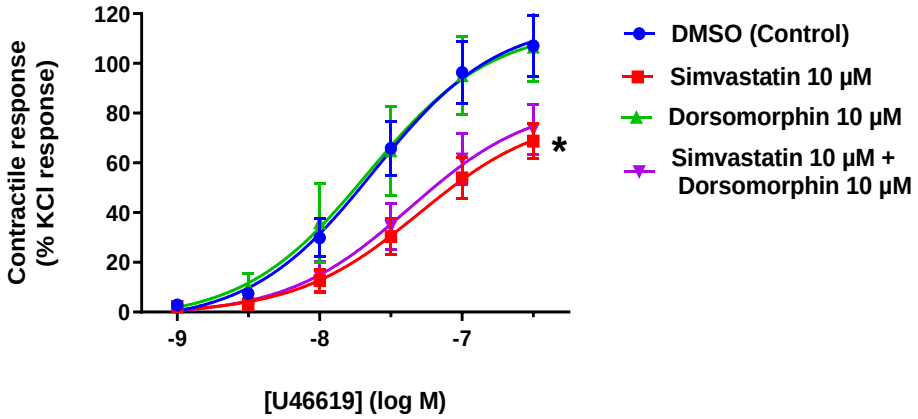

Figure 2.26: Log concentration-response curves for the vasocontractile effects of U46619 with pre-incubation 10 μM dorsomorphin and 10 μM simvastatin. Control is vehicle only (0.1% v/v DMSO). Data are expressed as a percentage of the contraction to 60 mM KCl and are mean ± SEM of 6 experiments. *p<0.05 v control at 300 nM of U46619, Two-way ANOVA followed by Sidak post-hoc test.

	Response at 300 nM of U46619 ± SEM
Control	107± 12%
Simvastatin	69 ± 7%*
Dorsomorphin	107 ± 14%
Simvastatin +Dorsomorphin	73 ± 10%

Table 2.12: Response at maximum concentration expressed as a percentage of the response to 60 mM KCl for U46619 in the absence (control, which is 0.1% v/v DMSO), or presence of 10 μM simvastatin and 10 μM dorsomorphin in PCAs. Data are expressed as mean ± SEM of 6 experiments. *p<0.05 v control at 300 nM of U46619, Two-way ANOVA followed by Sidak post-hoc test.

2.3.5.7. Effect of co-enzyme Q10 on simvastatin response:

If simvastatin inhibits the mitochondrial electron transfer chain at complex I, supplementation with co-enzyme Q10 would be expected to prevent the inhibitory effect of simvastatin. Therefore, tissues were incubated with 10 μM simvastatin, in the absence or presence of co-enzyme Q10 (5 μM). Pre-incubation with co-enzyme Q10 alone had no significant effect on the contractile response to U46619, whereas simvastatin inhibited the contraction to U46619. Pre-incubation with co-enzyme Q10 in the presence of simvastatin had no effect on the inhibitory effect of simvastatin. See table 2.13 and figure 2.27.

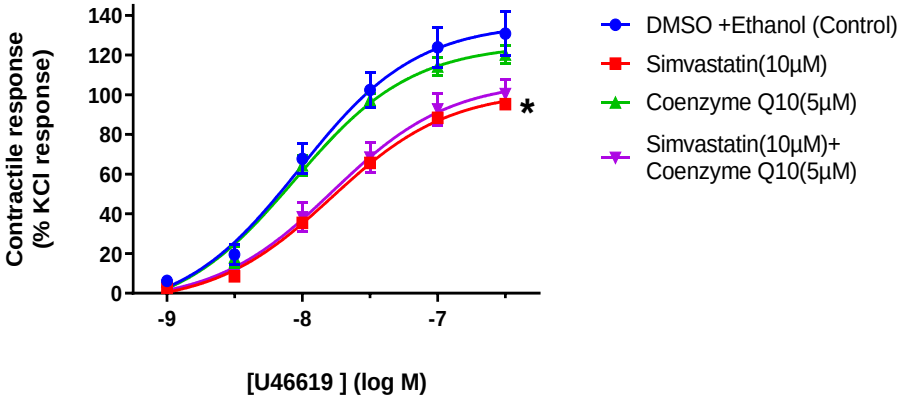

Figure 2.27: Log concentration-response curves for the vasocontraction effects of U46619 with pre-incubation 5 μM co-enzyme Q10 and 10 μM simvastatin. Control is vehicle only (0.1% v/v DMSO+ Ethanol). Data are expressed as a percentage of the contraction to 60 mM KCl and are mean ± SEM of 6 experiments. *p<0.05 v control at 300 nM of U46619. Two-way ANOVA followed by Sidak post-hoc test.

	Response at 300 nM of U46619 ± SEM
Control	137 ± 12%
Simvastatin	103 ± 5%*
Co-enzyme Q10	126 ± 5%
Simvastatin + Co-enzyme Q10	108 ± 8%

Table 2.13: Response at maximum concentration expressed as a percentage of the response to 60 mM KCl for U46619 in the absence (control, which is 0.1% v/v DMSO+ Ethanol), or presence of 10 μM simvastatin and 5 μM co-enzyme Q10 with and without simvastatin in PCAs. Data are expressed as mean ± SEM of 6 experiments. *p<0.05 v control at 300 nM of U46619, Two-way ANOVA followed by Sidak post-hoc test.

2.3.5.8. Effect of mitoquinol on simvastatin response:

Mitoquinol is a mitochondria-targeted version of co-enzyme 10. As the lack of effect of co-enzyme Q10 alone on the simvastatin response could be due to uptake into the cells, the effect of mitoquinol was determined. Tissues were incubated with 10 μM simvastatin, in the absence or presence of mitoquinol (1 μM). Pre-incubation with mitoquinol alone had no significant effect on the contractile response to U46619, whereas simvastatin inhibited the contraction to U46619. Pre-incubation with mitoquinol in the presence of simvastatin, slightly enhanced the inhibitory effect of simvastatin with no further significances. See table 2.14 and figure 2.28.

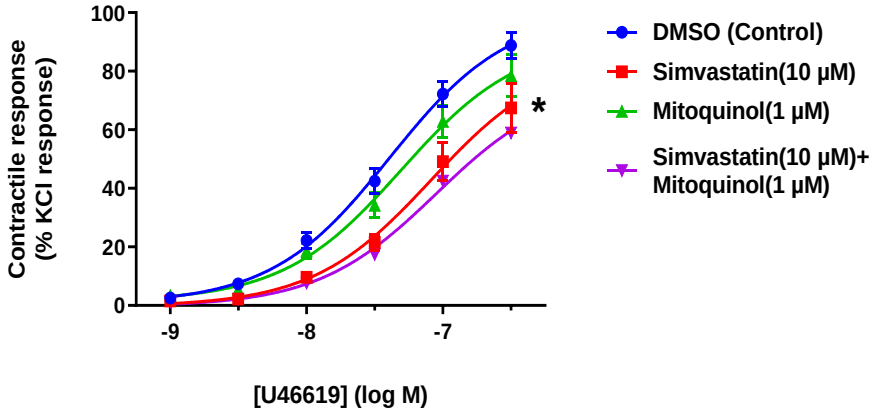

Figure 2.28: Log concentration-response curves for the vasocontraction effects of U46619 with pre-incubation 1 μM mitoquinol and 10 μM simvastatin. Control is vehicle only (0.1% v/v DMSO). Data are expressed as a percentage of the contraction to 60 mM KCl and are mean ± SEM of 6 experiments. *p<0.05 v control at 300 nM of U46619, Two-way ANOVA followed by Sidak post-hoc test.

	Response at 300 nM of U46619 ± SEM
Control	89 ± 5%
Simvastatin	68 ± 8%*
Mitoquinol	79 ± 7%
Simvastatin + Mitoquinol	59 ± 1%*

Table 2.14: Response at maximum concentration expressed as a percentage of the response to 60 mM KCl for U46619 in the absence (control, which is 0.1% v/v DMSO), or presence of 10 μM simvastatin and 1 μM mitoquinol with and without simvastatin in PCAs. Data are expressed as mean ± SEM of 6 experiments. *p<0.05 v control at 300 nM of U46619, Two-way ANOVA followed by Sidak post-hoc test.

2.3.5.9. Effect of FCCP on simvastatin response:

To explore more about the role of mitochondria in the simvastatin response, the effect of a mitochondrial uncoupling agent FCCP was determined. Tissues were incubated with 10 μM simvastatin, in the absence or presence of FCCP (1 μM). The maximum response observed for the control tissues was 99 ± 9% of the KCl response (n= 6). Pre-incubation with FCCP alone or simvastatin inhibited the contraction to U46619. Pre-incubation with FCCP in the presence of simvastatin, enhanced significantly the inhibitory effect of simvastatin. See table 2.15 and figure 2.29.

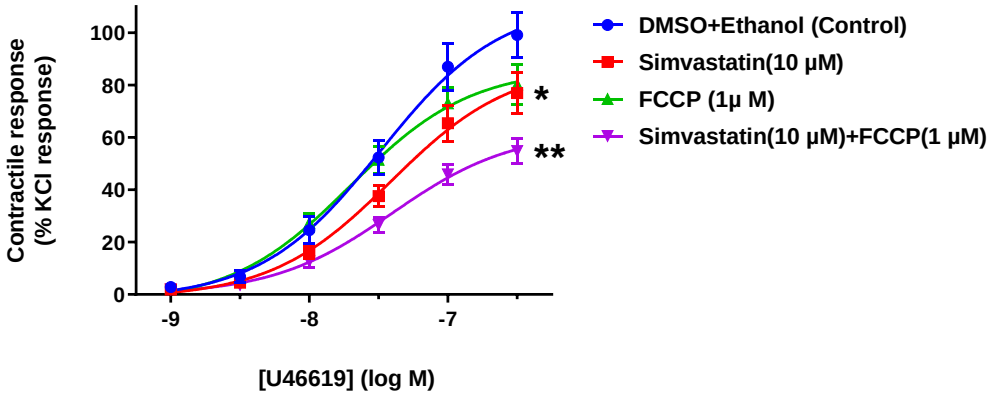

Figure 2.29: Log concentration-response curves for the vasocontraction effects of U46619 with pre-incubation 1 μM FCCP and 10 μM simvastatin. Control is vehicle (0.1% v/v DMSO+ 0.1% v/v ethanol). Data are expressed as a percentage of the contraction to 60 mM KCl and are mean ± SEM of 6 experiments. *p<0.05 and **p<0.01 v control at 300 nM of U46619, Two-way ANOVA followed by Sidak post-hoc test.

	Response at 300 nM of U46619 ± SEM
Control	99 ± 9%
Simvastatin	77 ± 8%*
FCCP	80 ± 8%
Simvastatin + FCCP	55 ± 5%**

Table 2.15: Response at maximum concentration expressed as a percentage of the response to 60 mM KCl for U46619 in the absence (control, which is 0.1% v/v DMSO +0.1% v/v ethanol), or presence of 10 μM simvastatin and 1 μM FCCP with and without simvastatin in PCAs. Data are expressed as mean ± SEM of 6 experiments. *p<0.05 and **p<0.01 v control, Two-way ANOVA followed by Sidak post-hoc test.

2.3.5.10. Effect of removal of extracellular glucose on simvastatin response:

Removal of extracellular glucose will reduce the amount of glucose available for glycolytic ATP production and therefore cellular function should be dependent only on mitochondrial function. Therefore, tissues were incubated with 10 μM simvastatin, in the presence or absence of glucose for 2h (using glucose-free Krebs, GFK). In the presence of glucose, the control tissues reached an R_{max} value of 106 ± 11% of the KCl response with a pEC_{50} value of 8 ± 0.05 (n= 7), while in the absence of glucose, the size of contraction was smaller and the R_{max} of control was 27 ± 7%. In both cases, simvastatin inhibited the contraction to U46619-induced contraction (R_{max}). See table 2.16 and figure 2.30.

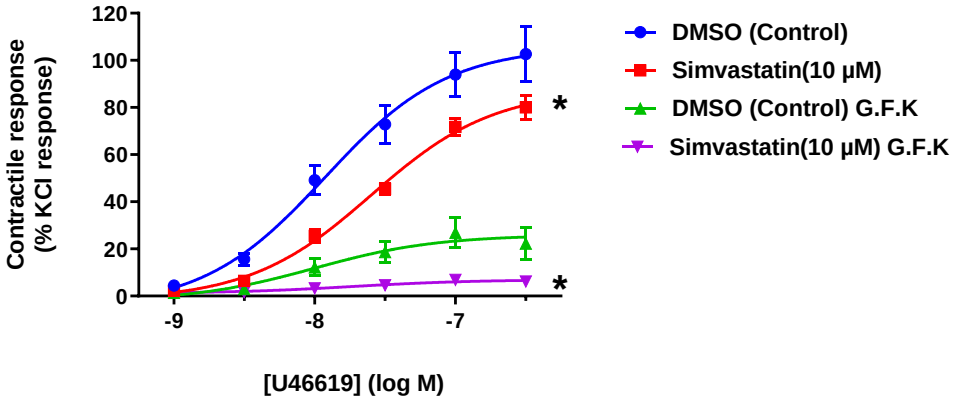

Figure 2.30: Log concentration-response curves for the vasocontraction effects of U46619 with pre-incubation 10 μM simvastatin in the presence or absence of glucose. Control is vehicle only (0.1% v/v DMSO). Data are expressed as a percentage of the contraction to 60 mM KCl and are mean ± SEM of 7 experiments. *p<0.05 v control and control-G.F.K., Student's 2-tailed paired t-test.

	R_{max} (KCl response, mean ± SEM)	**pEC_{50} (Mean ± ESM)**
Control	106 ± 11%	7.9± 0.04
Simvastatin	88 ± 6%*	7.6± 0.07
Control-G.F.K.	27 ± 7%	7.9 ± 0.13
Simvastatin-G.F.K.	7 ± 1.5%*	7.6 ± 0.16

Table 2.16: Maximum contraction (R_{max}) expressed as a percentage of the response to 60 mM KCl and log EC_{50} (pEC_{50}) for U46619 in the absence (control, which is 0.1% v/v DMSO), or presence of 10 μM simvastatin with and without glucose in PCAs. Data are expressed as mean ± SEM of 7 experiments. *p<0.05 v control and control-G.F.K., Student's 2-tailed paired t-test.

2.3.5.11. Effect of Mitochondria-Targeted H2S donor AP39 on simvastatin response:

Mitochondrial H_2S protects the mitochondria from oxidative stress and could help in reducing the impact of reduced complex activity. Therefore, if simvastatin reduces mitochondria complex activity, AP39 might reverse this. As H_2S is a short-lived compound, it was decided to determine its effect on a single concentration of U46619 over time. Therefore, tissues were pre-incubated for 120 min with a single concentration of 10 µM simvastatin and with AP39 (30 µM) for 15 min, prior to exposure to a sub maximum effective concentration of U46619 (30 nM). Pre-incubation with AP39 alone had no significant effect on time-dependent contraction profile to U46619, whereas simvastatin showed a significant inhibition of U46619-induced contraction with most time points. Pre-incubation of AP39 in the presence of simvastatin had no further effect. See figure 2.31.

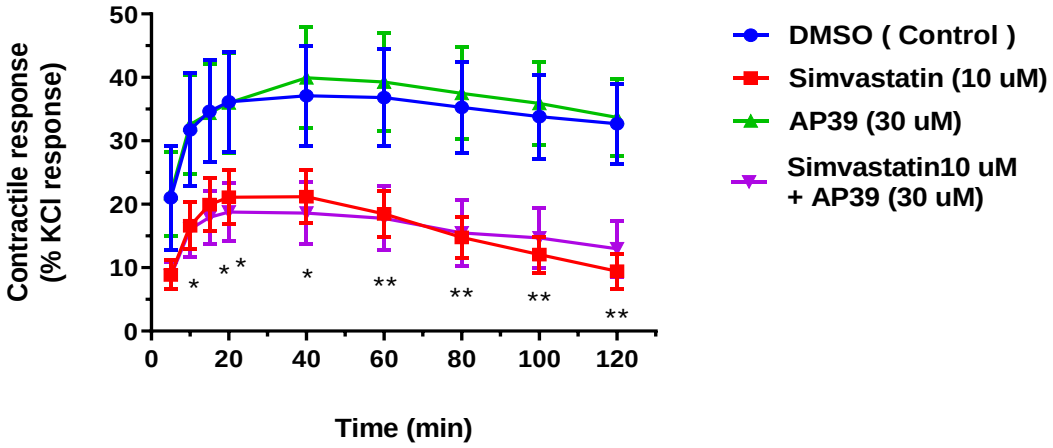

Figure 2.31: Time-response curves for the vasocontraction effects of 30 nM U46619 on PCA pre-incubated with 10 µM simvastatin and AP39 (30 µM). Control is vehicle only (0.1% v/v DMSO). Data are expressed as a percentage of the contraction to 60 mM KCl at different time points and are mean of 6 experiments. *p<0.05 and **p<0.0001 v control, Two-way ANOVA followed by Sidak post-hoc test.

2.3.6. The role of calcium in simvastatin response in PCAs:

In order to determine whether calcium is involved in the simvastatin-induced inhibition of the U46619-induced response, tissues were incubated with and without 10 μM simvastatin in calcium-free buffer. After the incubation period, tissues were exposed to a maximum concentration of U46619 (300 nM). $CaCl_2$ was then added cumulatively (10 μM-3 mM) to induce a contraction. The maximum response observed for the control tissues was 67 ± 7% of the KCl response (n= 9). Pre-incubation with simvastatin inhibited the contraction to $CaCl_2$ (maximum response observed was 52 ± 5%). figure 2.32.

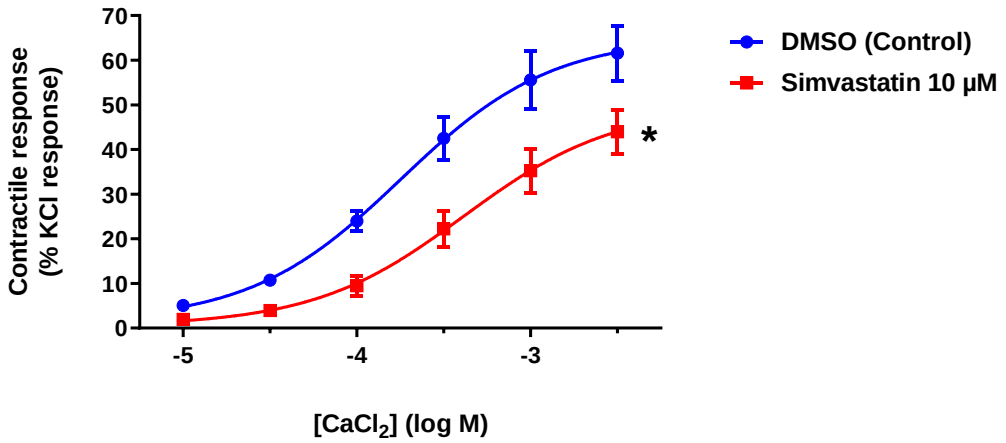

Figure 2.32: Log concentration-response curves for the vasocontraction effects of $CaCl_2$ with pre-incubation of simvastatin (10 μM). Control is vehicle only (0.1% v/v DMSO). Data are expressed as a percentage of the contraction to 60 mM KCl and are mean ± SEM of 9 experiments. *p<0.05 v control, Student's 2-tailed paired t-test.

2.3.6.1. Effect of mitochondrial complex inhibitors antimycin A and rotenone on simvastatin inhibition of calcium-induced contraction:

In order to determine the role of antimycin A and rotenone in simvastatin-induced inhibition of the $CaCl_2$-induced response, tissues were incubated with 10 μM simvastatin, in the absence or presence of combined mitochondrial complexes inhibitors I and III, rotenone and antimycin A (10 μM). The control tissues reached a response of 62 ± 6% of the KCl response at the maximum concentration of calcium (n= 7). Pre-incubation with antimycin A-rotenone combination alone had no significant effect on the contractile response to $CaCl_2$, whereas simvastatin inhibited the contraction to $CaCl_2$. Pre-incubation with antimycin A-rotenone combination in the presence of simvastatin enhanced the inhibitory effect of simvastatin. Table 2.17 and figure 2.33.

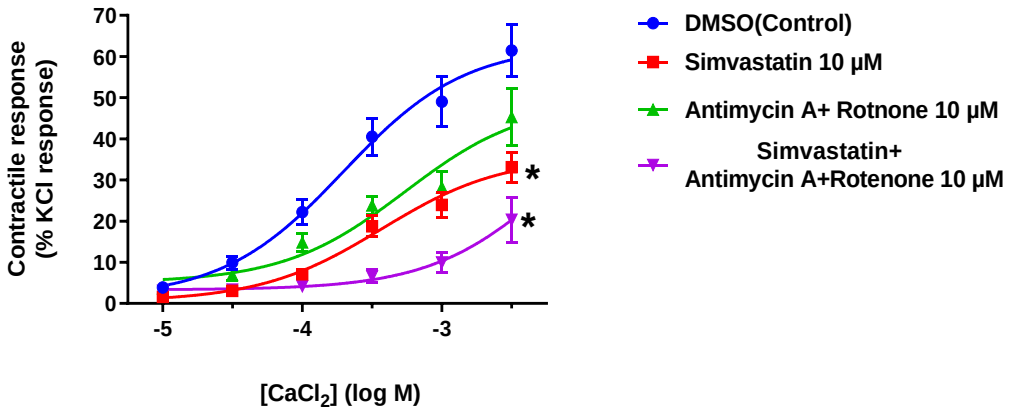

Figure 2.33: Log concentration-response curves for the vasocontraction effects of $CaCl_2$ with pre-incubation 10 μM (antimycin A and rotenone) and 10 μM simvastatin. Control is vehicle only (0.1% v/v DMSO). Data are expressed as a percentage of the contraction to 60 mM KCl and are mean ± SEM of 7 experiments. *p<0.05 v control, Two-way ANOVA followed by Tukey post-hoc test.

	Response at 300 nM of U46619 ± SEM
Control	62 ± 6%
Simvastatin	33 ± 4%*
Antimycin A-Rotenone	45 ± 7%
Simvastatin + Antimycin A-Rotenone	20 ± 6%*

Table 2.17: Response at maximum concentration expressed as a percentage of the response to 60 mM KCl for $CaCl_2$ in the absence (control, which is 0.1% v/v DMSO), or presence of 10 μM simvastatin and 10 μM (antimycin A and rotenone) with and without simvastatin in PCAs. Data are expressed as mean ± SEM of 7 experiments. *p<0.05 v control, Two-way ANOVA followed by Tukey post-hoc test.

2.3.6.2. Effect of mitochondrial complex inhibitors myxothiazol and rotenone on Simvastatin inhibition of calcium-induced contraction:

The combination of myxothiazol and rotenone prevented the inhibitory effect of simvastatin on the U46619-induced contraction (figure 2.21). In order to determine the role of myxothiazol and rotenone in simvastatin-induced inhibition of the $CaCl_2$-induced response, tissues were incubated with 10 μM simvastatin, in the absence or presence of combined mitochondrial complexes I and III inhibitors rotenone and myxothiazol (10 μM). Pre-incubation with the myxothiazol-rotenone combination alone had no effect on the contractile response to $CaCl_2$, whereas simvastatin inhibited the contraction to $CaCl_2$. Pre-incubation with the myxothiazol-rotenone combination in the presence of simvastatin showed no effect on the inhibition seen with simvastatin. See table 2.18 and figure 2.34.

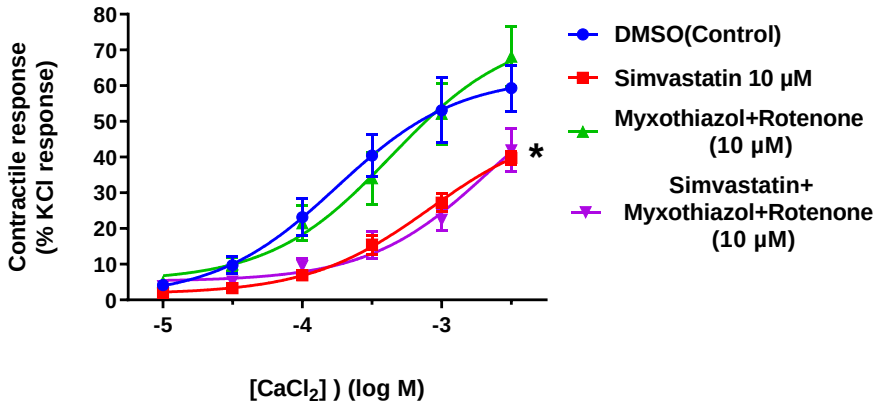

Figure 2.34: Log concentration-response curves for the vasocontraction effects of $CaCl_2$ with pre-incubation 10 μM (myxothiazol and rotenone) and 10 μM simvastatin. Control is vehicle only (0.1% v/v DMSO). Data are expressed as a percentage of the contraction to 60 mM KCl and are mean ± SEM of 9 experiments. *p<0.05 v control, Two-way ANOVA followed by Tukey post-hoc test.

	Response at 300 nM of U46619 ± SEM
Control	59 ± 7%
Simvastatin	40 ± 2%*
Myxothiazol-Rotenone	68 ± 8%
Simvastatin + Myxothiazol-Rotenone	42 ± 6%*

Table 2.18: Response at maximum concentration expressed as a percentage of the response to 60 mM KCl for $CaCl_2$ in the absence (control, which is 0.1% v/v DMSO), or presence of 10 μM simvastatin and 10 μM (myxothiazol and rotenone) with and without simvastatin in PCAs. Data are expressed as mean ± SEM of 6 experiments. *p<0.05 v control, Two-way ANOVA followed by Tukey post-hoc test.

2.3.6.3. Effect of L-type calcium channel blocker on simvastatin response:

In order to determine which calcium channel is involved in the simvastatin-induced inhibition of the U46619-induced response, tissues were incubated with 10 μM simvastatin, in the absence or presence of the L-type calcium channel blocker, nifedipine (5 μM). The control tissues reached a response of 101± 8% of the KCl response at the maximum concentration of U46619 (n= 6). Pre-incubation with nifedipine alone caused a significant inhibition to the U46619 contractile response. Additionally, simvastatin inhibited the contraction to U46619. Pre-incubation with nifedipine in the presence of simvastatin showed no further effect. See table 2.19 and figure 2.35.

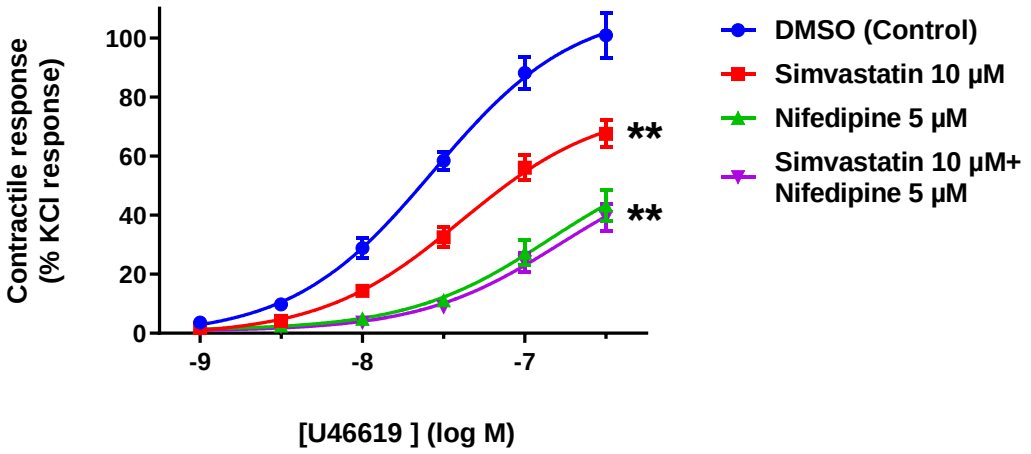

Figure 2.35: Log concentration-response curves for the vasocontraction effects of U46619 with pre-incubation 5 μM nifedipine and 10 μM simvastatin. Control is vehicle only (0.1% v/v DMSO). Data are expressed as a percentage of the contraction to 60 mM KCl and are mean ± SEM of 6 experiments. **p<0.01 v control at 300 nM of U46619, Two-way ANOVA followed by Tukey post-hoc test.

	Response at 300 nM of U46619 ± SEM
Control	101 ± 8%
Simvastatin	68 ± 5%**
Nifedipine	43 ± 5%**
Simvastatin + Nifedipine	39 ± 5%**

Table 2.19: Response at maximum concentration expressed as a percentage of the response to 60 mM KCl for U46619 in the absence (control, which is 0.1% v/v DMSO), or presence of 10 μM simvastatin and 5 μM nifedipine with and without simvastatin in PCAs. Data are expressed as mean ± SEM of 6 experiments. **p<0.01 v control at 300 nM of U46619, Two-way ANOVA followed by Tukey post-hoc test.

2.3.6.4. The effect of simvastatin on L-type calcium channel relaxation to nifedipine:

As there was an apparent effect of simvastatin on $CaCl_2$-induced concentration response curve and to confirm which calcium channel might be involved, tissues were incubated with and without 10 μM simvastatin, then pre-contracted with 30 nM of U46619 followed by adding nifedipine (1 nM-30 μM) to induce relaxation. Nifedipine appeared to produce a biphasic relaxation of the coronary artery. This biphasic effect was more obvious in the presence of simvastatin, which inhibited the relaxation in the first phase between 0.3 and 3 μM. See figure 2.36.

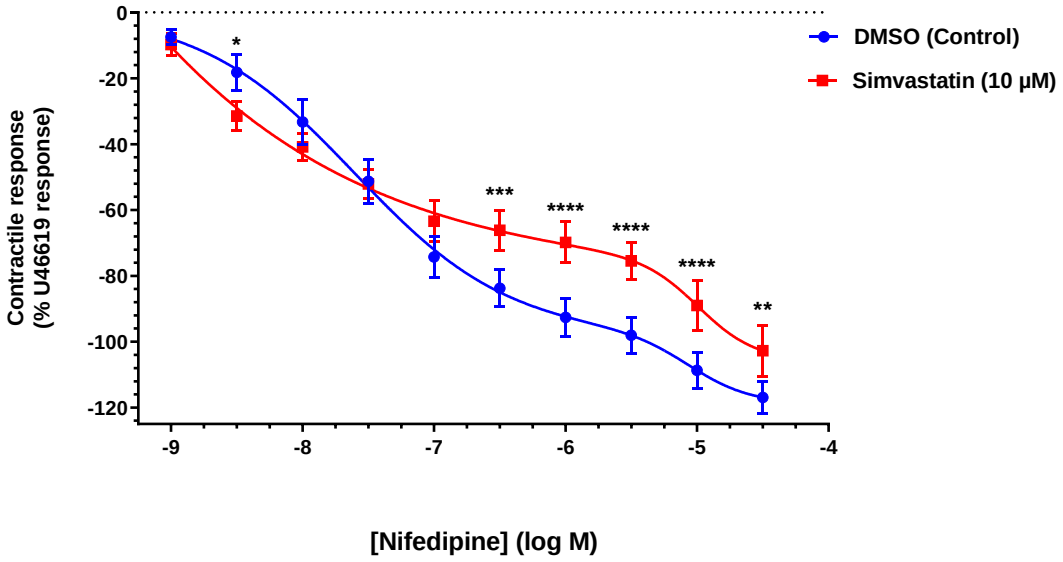

Figure 2.36: Effect of simvastatin (10 μM) on nifedipine-relaxation response curve on PCA pre-contracted with U46619. Control is vehicle only (0.1% v/v DMSO). Data are expressed as a percentage of relaxation to 30 nM U46619-induced contraction and are mean of 6 experiments. *p<0.05, **p<0.01, ***p<0.001 and ****p<0.0001 v control, Two-way ANOVA followed by Sidak post-hoc test.

2.3.6.5. The effect of simvastatin and rotenone-myxothiazol combination on relaxation to nifedipine:

In order to determine if there is a relation between inhibition of mitochondrial function and inhibition of calcium influx, tissues were incubated with 10 μM simvastatin for 2h, with and without 10 μM mitochondrial complex I and III inhibitors (rotenone and myxothiazol), then pre-contracted with 30 nM of U46619 followed by adding nifedipine (1 nM-30 μM) to induce relaxation. Pre-incubation with 10 μM simvastatin with or without the combination (rotenone and myxothiazol) caused no significant effect on the nifedipine-relaxant response curve as shown in figure 2.37. Of note, the biphasic response to nifedipine was not as obvious in these experiments.

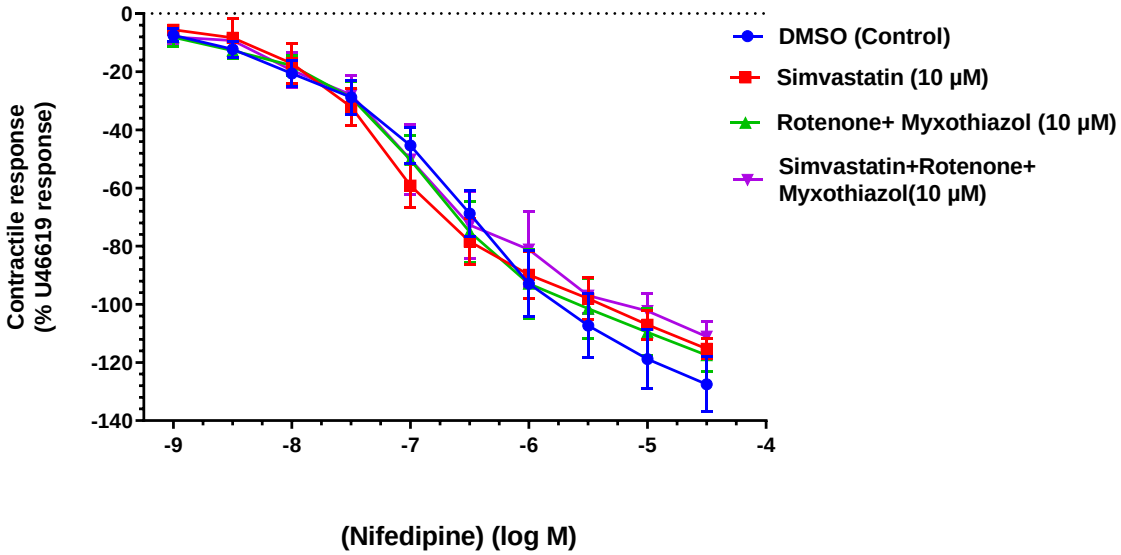

Figure 2.37: Effect of simvastatin (10 μM) and 10 uM rotenone-myxothiazol combination on nifedipine-relaxation response curve on PCA pre-contracted with U46619. Control is vehicle only (0.1% v/v DMSO). Data are expressed as a percentage of relaxation to 30 nM U46619-induced contraction and are mean of 6 experiments. P>0.05 v control, 2-way ANOVA followed by Sidak post-hoc test.

2.3.6.6. The effect of simvastatin on (±)-Bay K 8644 (L-type Ca^{2+} channel activator) induced contraction in porcine coronary arteries:

In order to determine whether simvastatin inhibits the contractile response to L-type Ca^{2+} channel activator, the effect of pre-incubation with simvastatin on (±)-Bay K 8644-induced contractions was determined. The control tissues reached a response of 95± 6% of the KCl response at the maximum concentration of U46619 (n= 6). Pre-incubation with (10 μM) simvastatin caused significant inhibitory effect on the contractile response with response at maximum concentration of 46 ± 6% of the KCl response. See figure 2.38

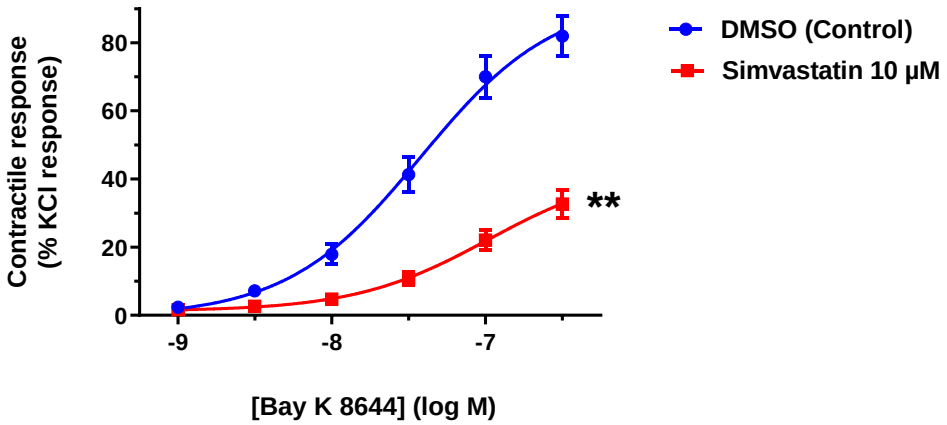

Figure 2.38: Log concentration-response curves for the vasocontraction effects of (±)-Bay K 8644 with pre-incubation of simvastatin (10 μM). Control is vehicle only (0.1% v/v DMSO). Data are expressed as a percentage of the contraction to 60 mM KCl and are mean ± SEM of 6 experiments. **P< 0.01 v control at 300 nM of Bay K 8644, Student's 2-tailed paired t-test.

2.3.6.7. Effect of myxothiazol and rotenone on the Simvastatin inhibition of the Bay K 8644 Response:

In order to determine whether myxothiazol and rotenone prevent the simvastatin-induced inhibition of the (±)-Bay K 8644-induced response, tissues were incubated with 10μM simvastatin, in the absence or presence of a combination of rotenone and myxothiazol (10 μM). The control tissues reached a response of 58± 6% of the KCl response at the maximum concentration of Bay K 8644 (n= 7). Pre-incubation with myxothiazol-rotenone combination alone had no significant effect on the contractile response to (±)-Bay K 8644, whereas simvastatin inhibited the contraction to (±)-Bay K 8644. Pre-incubation of myxothiazol-rotenone combination in the presence of simvastatin partially reversed the inhibitory effect of simvastatin. See table 2.20 and figure 2.39.

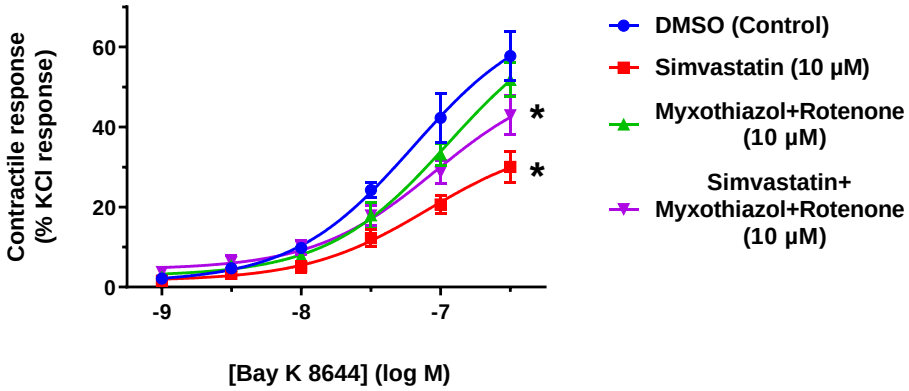

Figure 2.39: Log concentration-response curves for the vasocontraction effects of (±)-Bay K 8644 with pre-incubation 10 μM (myxothiazol and rotenone) and 10 μM simvastatin. Control is vehicle only (0.1% v/v DMSO). Data are expressed as a percentage of the contraction to 60 mM KCl and are mean ± SEM of 7 experiments. *p<0.05 v control at 300 nM of Bay K 8644, Two-way ANOVA followed by Tukey post-hoc test.

	Response at 300 nM Bay K 8644 ± SEM
Control	58 ± 6%
Simvastatin	30 ± 4%*
Myxothiazol-Rotenone	52 ± 4%
Simvastatin + Myxothiazol-Rotenone	43 ± 5%*

Table 2.20: Response at maximum concentration expressed as a percentage of the response to 60 mM KCl for (±)-Bay K 8644 in the absence (control, which is 0.1% v/v DMSO), or presence of 10 μM simvastatin and 10 μM (myxothiazol and rotenone) with and without simvastatin in PCAs. Data are expressed as mean ± SEM of 7 experiments. *p<0.05 v control, Two-way ANOVA followed by Tukey post-hoc test.

2.4. Discussion:

Statins inhibit HMG-CoA reductase, leading to a reduction in the synthesis of mevalonate and hence cholesterol. Many large trials have established that statins are not only safe and well tolerated but also significantly reduce the rate of cardiovascular morbidity and mortality in hypercholesteraemic patients in both primary and secondary prevention (Shepherd et al. 1995; Ford et al. 2007; Ramkumar, Raghunath, and Raghunath 2016). On the other hand, the remarkable benefit achieved with statin treatment in patients with ”normal” cholesterol levels has led to a question about the probable presence of other effects of statins away from their impact on serum cholesterol levels. One of the important pleiotropic effects is the regulation of vascular tone. Pleiotropic effects of statins could occur through prevention of isoprenylation of the small G-proteins Ras, Rho, and Rac, which are upstream of ERK, Rho kinase, and Nox respectively. Moreover, simvastatin/HMG CoA reductase could have an important role in the regulation of the activity of other enzymes such as AMP kinase. Alternatively, studies in our laboratory have demonstrated that statins can have effects on mitochondrial function, which may underlie the effects on vascular tone. Therefore, our aim in this study was to determine the role of Rho kinase, mitochondria and AMP kinase in the regulation of vascular smooth muscle tone by statins.

Based on previous studies, we hypothesized that simvastatin acts to inhibit mitochondrial complexes, leading to inhibition of calcium influx directly or indirectly, possibly through activation of AMP kinase and independent of an effect on Rho kinase or ERK-MAP kinase. Therefore, the effects of known inhibitors of mitochondrial complex I (rotenone) and III (antimycin A and myxothiazol) on the inhibitory effect of simvastatin were determined. In addition, the effect of mitochondrial stimulants (co-enzyme Q10 or mitoquinol), AMP kinase inhibitor and FCCP (potent mitochondrial oxidative phosphorylation uncoupler) were determined. Moreover, the effect of simvastatin and mitochondrial inhibitors on $CaCl_2$ and Bay K 8644-induced contraction were determined as well. The data in this section indicate that simvastatin inhibits U46619-induced contractions in the porcine coronary artery through inhibition of calcium influx, which may be downstream of mitochondrial inhibition. There is no evidence for the involvement of Rho kinase, ERK, or AMP kinase in the inhibitory effect.

Previous studies in the laboratory have demonstrated that simvastatin produces a concentration and time-dependent relaxation of the porcine coronary artery pre-contracted with U46619, with 10 μM simvastatin producing ~100% relaxation after 2 h. Therefore, initial experiments confirmed these data with 10 μM simvastatin causing relaxation of pre-contracted PCA. Subsequently, we determined the effect of a 2 h pre-incubation with simvastatin on concentration-response curves to U46619 in the presence or absence of

Ca^{2+}. In the presence of calcium, pre-incubation with increasing concentrations of simvastatin caused a significant inhibitory effect on the contractile response with 10 μM simvastatin but not with 0.1 μM and 1 μM. Interestingly, previous data indicated that relaxation responses to simvastatin could be observed at concentrations as low as 100 nM. However, in the current study, only 10 μM simvastatin inhibited the U46619-induced contraction when added before the thromboxane receptor agonist. Therefore, we hypothesized that simvastatin may have a greater effect on the maintained contraction to U46619, rather than the initiation of contraction. Initiation of contraction may be due to the influx of calcium whereas maintained contraction may be due to other signaling pathways such as Rho kinase i.e. calcium sensitization signaling (Mizuno et al. 2008; Kizub et al. 2010). In order to test this, we investigated the effect of pre-incubation with simvastatin on the time profile of the contractile response to a single, sub-maximum concentration of U46619. Pre-incubation with simvastatin inhibited the U46619-induced contraction at all-time points, indicating that the initiation of the response is inhibited but actually, the response is still maintained, just at a lower level. This is suggesting that simvastatin possibly inhibited calcium influx rather than by affecting calcium sensitization.

2.4.1. Mechanism of U46619-induced contraction:

Thromboxane A_2 (TXA_2) is a potent contractile agent of smooth muscle cells (FitzGerald, Healy, and Daugherty 1987). Studies revealed that TXA_2 could produce its contractile effect via activation of TP receptors then enhancing an increase in intracellular calcium level via inducing calcium release either from the sarcoplasmic reticulum (SR) and internal stores like mitochondrial calcium or via inducing a calcium entry from extracellular compartment (Ellinsworth et al. 2014; Touchberry et al. 2014). The influx of extracellular calcium involves activation of calcium channels such as receptor-operated calcium channel (ROCC) and store-operated calcium channel (SOCC), which are activated after depletion of calcium from ER(Parekh and Penner 1997; Putney 2001), as well as voltage-gated calcium channels (VGCC), which are activated after membrane depolarization (Berridge 1995; McFadzean and Gibson 2002). In addition to this mechanism, TXA_2 could induce contraction via activation of Rho kinase activity that inhibits phosphatase activity and enhance calcium-activated myosin light chain kinase activity, which is a key point for inducing muscle contraction (Fukata, Amano, and Kaibuchi 2001). On the other hand, there is some evidence about the involvement of extracellular signal-regulated kinases (ERK1/2) pathway in TXA_2-induced contraction in smooth muscle cells via modulation the contractile response (Ishihata, Tasaki, and Katano 2002).

Data in the present study showed that U46619 have the ability to induce a contraction in the presence and absence of calcium but the size of contraction in the absence of calcium was smaller. This means that the U46619 was depending on the influx of calcium from

extracellular compartment to induce contraction as well as on the intracellular calcium that release from internal stores but the latter was to a lesser extent as proposed. This is supported with evidence from the results of present study that showed the ability of simvastatin (chapter 2) and complex III inhibitor myxothiazol (chapter 4) to inhibit the U46619-induced contraction in the presence of calcium only. While in Chapter 3, with antimycin, which is another complex III inhibitor, the study showed that there was an inhibition to U46619-induced contraction in the presence and absence of calcium.

In a study performed on rat pulmonary artery, the researchers found that nifedipine, VGCC blocker, inhibited the contraction induced by the thromboxane analogue U46619. They also found that Rho kinase inhibitors could not inhibit the same contraction (Cogolludo et al. 2003). Another study identified that Rho kinase inhibitors have no ability to inhibit U46619-induced contraction in at pulmonary arteries while diltiazem, which is a VGCC blocker, prevented this contraction and the prevention was greater when combined with a high concentration of 2-APB (2-amino ethoxy diphenyl borate), which is SGCC blocker (Snetkov et al. 2006). In contrast, a study performed on bovine pulmonary arteries detected that contraction induced by U46619 could not be inhibited with VGCC blockers but was inhibited with Rho kinase inhibitors (Alapati et al. 2007). A study performed on rat aorta identified that SB203580 (a p38 MAPK inhibitor) could not inhibit the contraction induced by U46619 but it was inhibited with the calcium channel blocker verapamil. The study demonstrated also that in the absence of calcium, the U46619-induced contraction was strongly attenuated (Tasaki et al. 2003). This indicates that U46619 could elicit a contraction via a calcium-independent pathway. A recent study performed on rat intra-cavernous penile arteries revealed that U46619 signals through both calcium influx via VGCC and/or on calcium sensitization to induce a contraction (Grann et al. 2016). Calcium sensitization means direct inhibition of myosin light chain phosphatase independent of changes in calcium level, which could be regulated via Rho A activation (Somlyo and Somlyo 2000).

Accordingly, it looks that U46619-inducing contraction in smooth muscle cells depends mainly on the influx of calcium, in addition to the calcium release from intracellular stores. In the absence of calcium, U46619 still elicited a contraction but at a lower level depending on the calcium sensitization pathway, which might be regulated via Rho kinase activity. Data from the present study are mostly similar to previous studies in reflecting the dependence on the presence of extracellular calcium to induce contraction, the ability of U46619 to induce smaller contraction in the absence of calcium.

2.4.2. Role of Rho kinase and ERK in the anti-contractile effect of simvastatin:

A study performed by Copley *et al* (Copley, Beltrame, and Wilson 2008) showed that simvastatin at 10 μM reduced the U46619 contraction by 40% in rat caudal artery (RCA). In the presence of H-1152, which is a Rho kinase inhibitor, there was a greater reduction in the RCA contraction by simvastatin and this is similar to what we found in PCA using Y27632 (a selective inhibitor of Rho kinase (Davies et al. 2000)). By using a high concentration of the Rho kinase inhibitor, there should be near complete inhibition of Rho kinase. Therefore, it was hypothesised that if simvastatin inhibited Rho kinase as well, there would not be any additive effect. Therefore, these data bring a suggestion that either simvastatin works via another pathway rather than Rho kinase or it works partly via Rho kinase. The data in the absence of calcium also indicate that Rho kinase is not involved in the effect of simvastatin. Y27632 caused complete inhibition of the calcium-independent contraction caused by U46619, demonstrating that this response is dependent on Rho kinase activity (figure 7). However, simvastatin had no effect on the U46619-induced contraction in the absence of calcium (figure 2). In contrast, inhibition of Rho kinase would lead to activation of myosin phosphatase. As the myosin phosphatase inhibitor (calyculin A) inhibited the simvastatin relaxation, this could indicate that the simvastatin response is dependent on Rho kinase activity. However, calyculin A also inhibited the relaxation responses to antimycin A and myxothiazol (see chapters 2 &3), suggesting a non-specific effect.

In order to confirm a lack of involvement of Rho kinase, we attempted to measure Rho kinase activity by measuring changes in phosphorylation of the Rho kinase substrate myosin phosphatase target subunit 1 (MYPT1) at Thr696, or Thr850. However, neither antibody detected a strong band at the predicted molecular weight of 140kDa, unlike the total MYPT1 antibody.

A group of researchers found that 20mg/kg of simvastatin when given to rats for 16 weeks could provide cardio protection via a series of effects, including a reduction of ROCK activity (Li et al. 2012). In another study performed on bone marrow mesenchymal stem cells, the researchers identified that 1 μM simvastatin could enhance the phosphorylation of MYPT, i.e. ROCK activity, via increasing the cytosolic Rho A and reducing Rho A binding to cell membrane (Tai et al. 2015).

In contrast to this present study, a study performed by (Rattan 2010) found that simvastatin (1 and 10 μM) caused concentration dependent inhibition of the contraction induced by U46619 in the internal anal sphincter, which could be prevented via incubation with the geranylgeranyl transferase substrate geranylgeranyl pyrophosphate, which is involved in isoprenylation of RhoA (Stubbs and Von Zee 2012). In addition, there was a

reduction in the prenylation of RhoA, as well as RhoA/ROCK activity as determined using Western blotting. These data indicate that simvastatin acts through inhibition of posttranslational RhoA prenylation by 3-hydroxy-3-methylglutaryl coenzyme A (HMG-CoA) reductase inhibition but not in the PCA.

It has been found in a number of studies that the elevation in ERK activity is accompanied by an increased contraction of blood vessels, which occurs either as a response to activation of certain G_protein coupled receptors (Dessy et al. 1998; Roberts 2001) or as a response to stretch, which also induces contraction (Oeckler, Kaminski, and Wolin 2003b). Moreover, the same group of researchers as Roberts 2001 found that the contraction of porcine palmar lateral vein and porcine ear artery elicited by α_2-adrenoceptors was dependent on ERK activation and using U46619 increased the contractile effect of α_2-adrenoceptor via enhancing ERK activity (Bhattacharya and Roberts 2003). This is supported by other studies in the porcine palmar lateral vein showing that inhibition of ERK activation caused a reduction in myosin light-chain phosphorylation (Roberts 2001). As statins can inhibit activation of Ras, which is upstream of ERK activity (Will et al. 2014; Stofega et al. 1997), we hypothesised that the inhibitory effect of simvastatin on U46619-induced contraction could be via inhibition of ERK activity. Therefore, we determined the effect of a 1 h pre-incubation with PD98059 a selective inhibitor of MEK, which is upstream of ERK activation (Davies et al. 2000), on concentration-response curves to U46619 in the presence or absence of Ca^{2+}. Pre-incubation with 50 μM PD98059 caused significant inhibitory effect to an intermediate concentration only. The fact that PD98059 did not produce the same inhibitory effect as simvastatin suggests that ERK is not involved in the simvastatin response. To help confirm this we determined the effect of simvastatin on U46619-induced contractions in the presence of 50 μM PD98059. Under these conditions, simvastatin produced a further inhibition of the contraction, suggesting ERK is not involved in the inhibitory effect of simvastatin.

Western blotting was also used to determine changes in ERK activity. ERK is phosphorylated by MEK at threonine 202 and tyrosine 204 and this phosphorylation is required for activity (Stofega et al. 1997; Xu et al. 2016). Therefore, changes in ERK activity can be determined by measuring changes in phosphorylation at these sites. Data from the present study showed that there was no significant change either in phosphorylated- ERK1 or ERK2 indicating no changes in the activity.

The possible interpretation is ERK1/2 pathway might not be downstream of the simvastatin inhibitory effect of the U46619-induced contraction possibly because U46619 induced the contraction via a pathway not involving activation of ERK1/2, as in the present study there

was not much change in phosphorylated-ERK1/2 activity in samples pre-incubated with U46619 and samples pre-incubated with simvastatin then contracted with U46619. This interpretation could be supported by previous studies in which the researchers found that PD98059 (MEK inhibitor) could inhibit MEK1/2 and 5 (i.e. ERK1/2 and 5) and that ERK5 could play a role in U46619-induced contraction and that is why there were no changes in ERK1/2 activity (Kamakura, Moriguchi, and Nishida 1999; Bhattacharya and Roberts 2003).

2.4.3. Role of mitochondria in the anti-contractile effect of simvastatin:

Mitochondria are thought to regulate blood vessel tone via producing ROS, which enhanced calcium sparks and calcium-activated K^+ channel currents leading to vasodilatation of arterial smooth muscle (Xi, Cheranov, and Jaggar 2005). Statins may regulate vascular tone through inhibition of mitochondrial function (Broniarek and Jarmuszkiewicz 2016; Curry et al. 2019). Other studies found that simvastatin and lovastatin (lipid soluble drugs) but not pravastatin (water soluble) have an inhibitory effect on complex I, II, III, IV and complex V of heart and liver mitochondria (Nadanaciva et al. 2007). In a recent study, Almukhtar (2015) found that the relaxant effect of simvastatin on PCA was reduced by inhibition of mitochondrial complexes I and III, which indicates that the relaxation produced by simvastatin is dependent upon the activity of complexes I and III. Therefore, we determined the effect of mitochondrial complex inhibitors on the anti-contractile effect of simvastatin in the PCA. Neither rotenone (complex I inhibitor), myxothiazol nor antimycin A (complex III inhibitors), when added alone, had any effect on the inhibitory effect of simvastatin on U46619-induced contraction. However, the combination of rotenone and myxothiazol prevented the inhibitory effect of simvastatin suggesting that the combined inhibition of complex I and III are required to inhibit the effect of simvastatin. On the other hand, inhibition of complex I with rotenone and complex III with antimycin A enhanced the inhibitory effect of simvastatin on U46619-induced contraction.

These differences in the effects of the combinations of complex inhibitors could be related to the different site of action for both inhibitors of complex III. Antimycin A acts at the Q_i site, which is found in the inner membrane and fronting the mitochondrial matrix, while myxothiazol inhibits the Q_o site, which is oriented toward the intermembrane space (Chen et al. 2003). Q_i represents the reducing site for ubisemiquinone in complex III and blocking with antimycin A could lead to a reduction in persistent sodium currents and the neuronal excitability (Lai et al. 2005). In contrast, Q_o site represents the oxidizing site for ubiquinol and blocking with myxothiazol could lead to enhancement of persistent sodium currents and the neuronal excitability (Lai et al. 2006). In another study the researchers found that using antimycin A to inhibit complex III at Q_i caused an inhibition in the amplitude of voltage-gated Ca^{2+} currents (I_{Ca}) while using myxothiazol to block the same complex but

at Q_o site caused increases in the amplitude of I_{Ca} in rat prefrontal neurons (Wu et al. 2010). In the rat-tail artery, the effect of mitochondrial inhibition with antimycin A was a reduction in the amplitude of cellular calcium waves, which may contribute to inducing vascular relaxation (Swärd et al. 2002). On the other hand, other researchers found that myxothiazol inhibited changes in ROS level and intracellular calcium concentration-induced by hypoxia in pulmonary artery smooth muscle cells (Waypa et al. 2006). Mitochondrial ROS are important for regulating release intracellular Ca^{2+} stores, activation voltage-gated and Ca^{2+}-activated K^+-channels (Sotnikova 1998; Gonzalez-Pacheco et al. 2002). This possibly means that calcium channel activation is downstream of the mitochondria and this is how simvastatin reduces calcium channels. However, it is also possible that the combination of rotenone and myxothiazol opposes the effect of simvastatin directly at the calcium channels, rather than within the mitochondria.

Accordingly, we could say that the inhibition of two different sites for blocking of complex III are giving opposite effects and this could explain the opposite effect towards the inhibitory effect of simvastatin to U46619-induced contraction. As a support, there are several studies, which refer to the relationship between the chemical structure of statins and ability to inhibit mitochondrial function, more precisely inhibition of complex III. One of them revealed that statin lactones, simvastatin being one of the best examples, exert their mitochondrial inhibitory effect mainly via inhibition of the Q_o site of complex III rather than Q_i (Brandt, Schagger, and von Jagow 1988) and (Schirris et al. 2015), hence why myxothiazol prevents the effect of simvastatin. Further studies in the thesis will compare the anti-contractile effects of antimycin A and myxothiazol with simvastatin.

As coenzyme Q10 (CoQ10) is a key component of the mitochondrial electron transport system, in which it is responsible for transfer electron between complexes (Littarru and Tiano 2007) and mitoquinol, the reduced form of CoQ10, a mitochondrial-targeted CoQ10 analogue (Fink et al. 2012), it was hypothesised that supplementation with these compounds might overcome the inhibitory effect of simvastatin if the statin does act through inhibition of complex III. There are several studies that indicate that statins in general and simvastatin, in particular, can cause a reduction in serum level of CoQ10 via inhibiting the mevalonate pathway. This reduction in CoQ10 could disturb the mitochondrial function and lead to inhibition of respiration cycle (Ghirlanda et al. 1993; Deichmann, Lavie, and Andrews 2010). However, pre-incubation of CoQ10 or mitoquinol in the presence of simvastatin for 120 min had no effect on the inhibitory effect of simvastatin. These results may be explained by the inability of CoQ10, in oxidized and reduced form ubiquinol, to compete with the binding site of simvastatin and protect the mitochondria. Anyway, further studies in later chapters will compare the effect of CoQ10 and mitoquinol on the effects of antimycin and myxothiazol

Similar to CoQ10, H_2S may also support the transfer of electrons through the mitochondrial electron transport chain (Szabo, Ransy, Módis, et al. 2014). Intra-mitochondrial H_2S has an important role in maintaining the citric acid cycle and any degradation in H_2S, as in the case of oxidative stress, can lead to a disturbance in mitochondrial function due to loss the protective effect of H_2S (Geng et al. 2004; Doeller et al. 2005; Whiteman et al. 2011; Vandiver and Snyder 2012). In previous studies, researchers found that H_2S could supply the mitochondrial electron transport chain with electrons and enhance the ATP production (Modis et al. 2014; Szabo, Ransy, Modis, et al. 2014). Therefore, if simvastatin is acting through inhibition of the mitochondrial complexes, we hypothesised that treatment with a mitochondrial-targeting hydrogen sulphide donor AP39 would protects the mitochondria and therefore prevent the inhibitory effect of simvastatin. Therefore, tissues were pre-incubated with 10 μM simvastatin for 120 min and with AP39 (30 μM) for 15 min, prior to exposure to a single concentration of U46619 (30 nM). Pre-incubation with AP39 alone had no significant effect on the time-dependent contraction profile to U46619, whereas simvastatin showed significant inhibition at most time points. Pre-incubation of AP39 in the presence of simvastatin had no further effect. This indicates that AP39 cannot prevent the inhibitory effect of simvastatin, which could be because H_2S feeds into the ETC at a different site, e.g. upstream of where simvastatin acts.

In a recent study in isolated cardiac mitochondria from rat (Karwi et al. 2017a), a low concentration of AP39 was shown to supply electrons to the electron transport chain at the co-enzyme Q site and the electrons moved following the direction towards complex III to complex IV without passing complex I and II. This finding supported other previous studies, which demonstrated that inhibition of complex I with rotenone had no effect on oxidation of sulphide while blockage of complex III with antimycin A and complex IV with cyanide inhibited it (Volkel and Grieshaber 1996; Searcy 2001; Goubern et al. 2007; Szabo, Ransy, Modis, et al. 2014). Therefore, it is possible that AP39 had no ability to reverse simvastatin inhibitory effect because, as we hypothesised, simvastatin could inhibit complex III and this inhibited sulphide oxidation then abolished the H_2S protection role in mitochondria. In order to clarify whether mitochondrial H_2S can reverse the inhibition of complex III, the effect of AP39 on the antimycin and myxothiazol responses will be determined in chapters 2 & 3.

To get further clarification about the role of mitochondria, the effect of the mitochondrial uncoupling agent FCCP was determined (Kadenbach 2003). Pre-incubation with FCCP alone or simvastatin both inhibited the contraction to U46619. According to Terada (Terada 1990), the effect of FCCP could be due to inhibition of the transport and coupling of electrons released from the respiratory chain reaction, thus inhibiting the oxidative phosphorylation and ATP synthesis without affecting respiratory chain itself. The possible

consequence of that is the disturbance in calcium homeostasis, which could result in a reduction of intracellular calcium levels and inhibition of contraction. This is supported by several studies, which identified the direct and indirect inhibitory effect of FCCP on store-operated Ca^{2+} entry (SOCE) in a variety of cell types (Hoth, Fanger, and Lewis 1997; Makowska, Zablocki, and Duszynski 2000; Smith et al. 2003). A group of researchers, who worked on rat hepatocytes, found that FCCP have indirect inhibitory effect on store-operated calcium entry when the mitochondria lose buffering capacity and cytosolic calcium increases (To et al. 2010).

Pre-incubation with FCCP in the presence of simvastatin enhanced significantly the inhibitory effect of simvastatin. The additional inhibitory effect by FCCP could support our hypothesis about simvastatin and inducing anti-contractile effect via inhibition of mitochondrial complexes if simvastatin still could inhibit these complexes even after uncoupling the mitochondria from ATP production, which possibly causing more disturbance in calcium levels. Otherwise, what we have is an additional inhibitory effect from FCCP via a different pathway.

To clarify more about the involvement of mitochondria in simvastatin inhibitory effect to U46619-induced contraction in PCA, we tested the removal of extracellular glucose from Krebs'-Henseleit solution. Exogenous glucose is the predominant substrate utilized by vascular smooth muscles to generate ATP through the glycolytic pathway, and this is the main source of ATP required for inducing contraction while glucose entering the pyruvate pathway is mainly utilized in the mitochondrial electron transport chain to generate mitochondrial ATP production (Allen and Hardin 2000). Therefore, we hypothesised that removal of extracellular glucose would increase the requirement for mitochondrial respiration. Therefore, if simvastatin was acting through inhibition of mitochondrial ATP production, a greater effect might be seen in the absence of glucose. Removal of extracellular glucose inhibited the U46619-induced contraction, and this contraction was virtually abolished in the presence of simvastatin (figure 30). The size of the inhibition with simvastatin appeared to be similar in the presence or absence of glucose. However, the large inhibition of the U46619-induced contraction in the absence of glucose limited the contraction and therefore limited the size of the inhibitory response with simvastatin.

Inhibition of mitochondrial function could lead to activation of AMP kinase (Jiang et al. 2013), which could lead to inhibition of smooth muscle contraction (Wang et al. 2011). AMP kinase is thought to cause smooth muscle relaxation through eNOS and NO (Goirand et al. 2007; Mori et al. 2017)or phosphorylating and inactivating myosin light chain kinase (Horman et al. 2008; Lee and Choi 2013). Therefore, we compared the effect of the AMP kinase inhibitor dorsomorphin (Liu et al. 2014) on the inhibitory effects of simvastatin. Pre-

incubation of dorsomorphin in the presence of simvastatin did not reverse or alter the inhibitory effect of simvastatin, indicating that AMP kinase is not involved in the anti-contractile effect of simvastatin in the PCA. The data presented here are in contrast to the study performed on rat mesenteric artery (Rossoni et al. 2011). In this study, it was found that the anti-contractile effect of simvastatin was inhibited by dorsomorphin. The reasons behind this result could be using different tissue and animal, which could exhibit different behaviour. In addition, using a different contractile agent with different concentrations may show different effects.

2.4.4. Role of calcium in the anti-contractile effect of simvastatin:

Previous research has indicated that statins can inhibit calcium influx in vascular smooth muscle (Bergdahl et al. 2003). As discussed above, simvastatin had no effect on the U46619-induced contraction in the absence of extracellular calcium (figure 4). Further studies were carried out to determine the effect of simvastatin on calcium-induced contractions. Pre-incubation with simvastatin inhibited the contraction to $CaCl_2$. This could be due to inhibition of calcium influx, either directly by inhibition of the calcium channels, or indirectly, or it could be due to inhibition of the intracellular signalling pathways downstream of calcium. Similar effects were seen with simvastatin in rat aorta and this was proposed to be due to inhibition of calcium influx (Alvarez de Sotomayor et al. 2001). Other studies suggested that simvastatin could inhibit the release of calcium from intracellular spaces and this induced inhibition of contraction (Ng, Davies, and Wojcikiewicz 1994; Escobales et al. 1996; Tesfamariam, Frohlich, and Gregg 1999). Accordingly, simvastatin could affect calcium influx and intracellular calcium release directly or indirectly.

In order to determine which calcium channels might be involved in the simvastatin-induced inhibition of the U46619-induced response, tissues were incubated with 10 μM simvastatin, in the absence or presence of the calcium channel blocker, nifedipine (5 μM). Pre-incubation with nifedipine alone or simvastatin alone caused a significant inhibition to the U46619 contractile response. On the other hand, there was no further inhibition with simvastatin in the presence of nifedipine. This suggests that simvastatin is unable to block the U46619-induced contraction if calcium channels are already inhibited, indicating that simvastatin either blocks L-type calcium channels or, as indicated above, inhibits the pathway downstream of calcium. These data are supported by the experiments with the L-type calcium channel opener Bay K 8644 in which simvastatin inhibited the contraction. Similarly, simvastatin inhibited the relaxation to nifedipine, although when this experiment was repeated in the presence of rotenone and myxothiazol, there was no inhibition. Nifedipine appeared to produce a biphasic relaxation of the coronary artery. This biphasic effect was more obvious in the presence of simvastatin, which inhibited the relaxation in

the first phase. At high concentrations, nifedipine can block T-type calcium channels (Shcheglovitov et al. 2005), which may explain the biphasic response. The fact that simvastatin appeared to inhibit the first phase suggests that it may be blocking L-type calcium channels.

In a study performed on rat islet beta cells, it was found that simvastatin, but not pravastatin, blocked L-type calcium channels in order to prevent glucose-induced calcium signalling and insulin secretion (Yada et al. 1999; Curry et al. 2019). Other studies have also indicated that simvastatin can alter intracellular calcium homeostasis via disturbing the function of VGCC in vascular smooth muscle (Tesfamariam, Frohlich, and Gregg 1999; Alvarez de Sotomayor et al. 2001; Seto et al. 2007). A more recent study also identified that simvastatin irreversibly inhibited the maintenance phase of contraction induced in rat via interrupt the function of VGCC then inhibition calcium influx (Kang et al. 2014). This group also found that simvastatin inhibits the contraction in response to Bay K 8644 (Kang et al. 2014).

2.4.5. Role of mitochondria in the inhibition of calcium-induced contractions:

The data presented here suggest that simvastatin inhibits contractile responses through effects on both mitochondria and inhibition of calcium-induced contractions. In order to determine whether there is a link between these pathways, the effect of mitochondrial inhibitors on the calcium-induced response was determined. Pre-incubation with an antimycin A-rotenone combination alone had no significant effect on the contractile response to $CaCl_2$, although there was a partial inhibition whereas simvastatin inhibited the contraction to $CaCl_2$ significantly. Pre-incubation with the myxothiazol-rotenone combination alone had no effect on the inhibitory effect of simvastatin on the contraction to increasing concentrations of calcium (figure 34), which was different from the effects seen on the U46619-induced contraction (figure 25). On the other hand, the combination of myxothiazol-rotenone did prevent the inhibitory effect of simvastatin on the Bay K 8644-induced contraction (figure 39). Pre-incubation with the myxothiazol-rotenone combination alone had no significant effect on the contractile response to Bay K 8644, whereas simvastatin inhibited the contraction. These studies indicate that inhibition of complex I and III can prevent the inhibitory effect of simvastatin on the L-type calcium channel induced contractions, suggesting that the effects of simvastatin on the L-type calcium channels could be downstream of inhibition of the mitochondria. The fact that rotenone and myxothiazol did not prevent the inhibitory effect on the calcium-induced contractions is harder to explain. It could be due to the calcium-induced contraction occurring through channels other than the L-type calcium channels.

Pre-incubation of antimycin A-rotenone in combination enhanced the inhibitory effect of simvastatin on the calcium-induced contraction, which is similar to the response seen against the U46619-induced contraction (figure 24). This enhancement of simvastatin inhibitory effect suggests that disturbing mitochondrial function with rotenone and antimycin A had a further inhibitory effect on calcium influx. A previous study clarified that disturbances in calcium homeostasis could result from impairment of mitochondrial ETC (Mohaupt et al. 2009). Another study performed on rat cortical neurons, identified a disturbance in VGCC leading to a reduction in calcium influx after using antimycin A to block complex III (Wu et al. 2010).

A previous study determined that complex III inhibitor antimycin A acts on Q_i site, while myxothiazol, another inhibitor of complex III, acts on the Q_o site (Lai et al. 2005). Thus, inhibition of complex I with rotenone and complex III with myxothiazol possibly impaired mitochondrial respiration without impeding extracellular calcium influx, while blocking Q_i site of complex III with antimycin A and complex I with rotenone could cause more disturbance in mitochondrial respiration, ATP production and possibly inhibit the influx of extracellular calcium via a different pathway.

A study performed on pulmonary artery smooth indicated that blocking of complex I or III using rotenone and myxothiazol respectively inhibited the calcium increases due to hypoxia (Wang et al. 2007). A limitation of this present study is that we did not measure the effect of simvastatin on calcium responses. A previous study in the laboratory demonstrated that simvastatin inhibits calcium influx in freshly isolated smooth muscle cells (Almukhtar Thesis). However, it was not possible to determine whether this could be prevented by the combination of rotenone and myxothiazol.

In summary, the data presented in this chapter demonstrate that simvastatin inhibits the U46619-induced contraction in PCA only in the presence of calcium possibly via mitochondrial inhibition. The combination of mitochondrial inhibitors I and III (rotenone-myxothiazol) reduced this inhibitory effect while the combination of mitochondrial inhibitors I and III (rotenone-antimycin A) enhanced the inhibitory effect of simvastatin. The fact that the rotenone-myxothiazol combination prevented the inhibitory effect of simvastatin on the Bay K8644-induced contraction suggests that the effects of simvastatin on calcium-induced contractions may be due to mitochondrial effects. This suggests that there is a link between inhibition of mitochondrial function, calcium influx and inhibition of smooth muscle contraction by simvastatin in the PCA, as indicated in the pathway in figure 2.40. In order to clarify the role that mitochondria might play in the simvastatin responses in the PCA, it is necessary to compare the effects of simvastatin with known inhibitors of the mitochondrial ETC. Therefore, in the next chapters, the mechanism of the anti-contractile effects of antimycin A and myxothiazol will be determined.

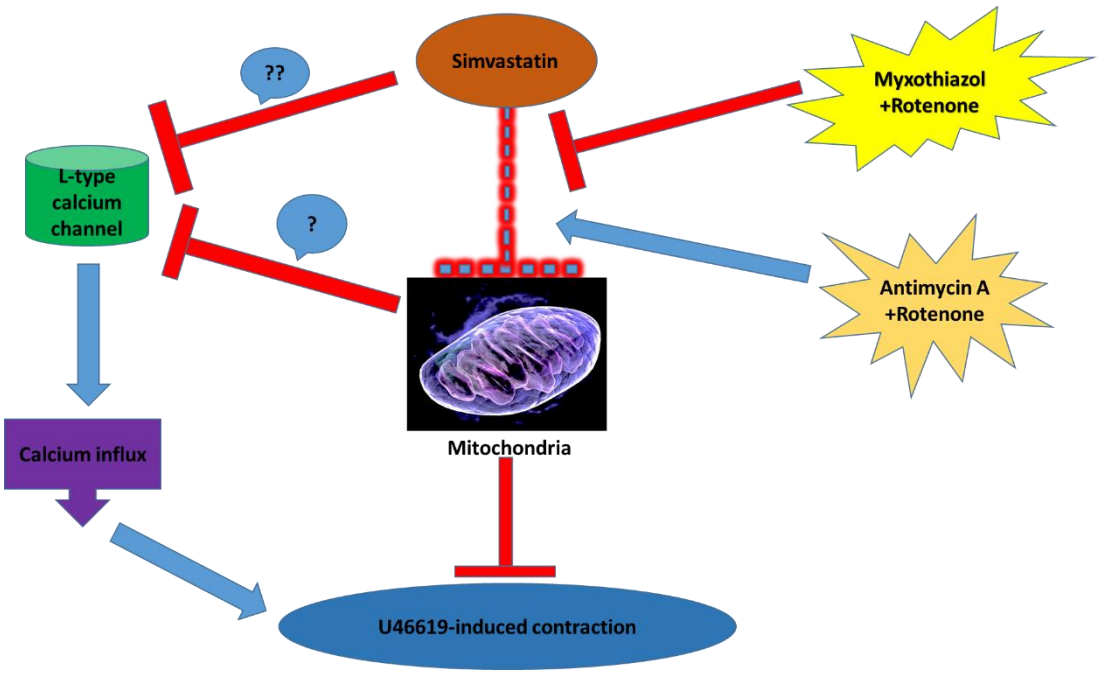

Figure 2.40: Hypothesized schematic diagram effect of 10 μM simvastatin on U46619-induced contraction in PCA. The present study demonstrated the anticontractile effect of simvastatin is through inhibition of calcium influx or inhibition of mitochondria or both of them combined. Blue arrows indicate stimulation whereas red lines indicate inhibition.

Chapter III

The effect of antimycin A on U46619 (thromboxane A_2 receptor agonist) induced contraction in porcine coronary arteries (PCAs)

3.1. Introduction:

Mitochondria are an important organelle in all cells, they have a crucial role in metabolic pathways, including ATP production and supplying energy required for different processes including muscle contraction (Kuznetsov et al. 2009; Scheffler 2001). Thus, mitochondria have a vital role in regulating muscle tone besides other important roles such as Ca^{2+} regulation, cell signaling, cell proliferation and others (Busija et al. 2016). Mitochondria consist of four sections: the outer mitochondrial membrane (OMM), the intermembrane space (IMS), the inner mitochondrial membrane (IMM), and the mitochondrial matrix. The IMM is specialised to facilitate oxidative phosphorylation as it contains a diversity of proteins and mitochondrial complexes in addition to ATP synthase. ATP production depends mainly on the transfer of protons between the mitochondrial complexes according to gradients in the electron transport chain (ETC) (Scheffler 2001). Mitochondria also have a vital role in maintaining calcium homeostasis via calcium uptake into the mitochondria in conjunction with endoplasmic reticulum (ER) (Camello-Almaraz et al. 2006). Mitochondrial calcium is required for a number of processes including protein synthesis and ATP synthesis, activation of oxidative phosphorylation, citric acid cycle dehydrogenases and inducing muscle contraction (Joyal, Hagen, and Aprille 1995; Griffiths and Rutter 2009).

The respiratory chain in IMM consist of five complexes (complex I to complex V) which regulate electron transfer in ETC and aid ATP production (Hatefi 1985). Impairment or damage in mitochondrial complexes could lead to mitochondrial dysfunction that possibly ends with a degenerative cellular process (Cadenas and Davies 2000; Caspersen et al. 2005). On the other hand, mitochondrial complex inhibitors could modulate and modify the function of mitochondria (Camello-Almaraz et al. 2006).

One of these complex inhibitors is antimycin A, which is a compound from *Streptomyces kitazawensis* (Nakayama, Okamoto, and Harada 1956). It is known to act at the Q_i site of cytochrome c reductase that is located in the inner membrane on complex III. Antimycin A prevents the oxidation of ubiquinol in the ETC that blocks the transfer of a mitochondrial electron between cytochrome b and c (Campo, Kinnally, and Tedeschi 1992; Pham, Robinson, and Hedley 2000). See figure 3.1

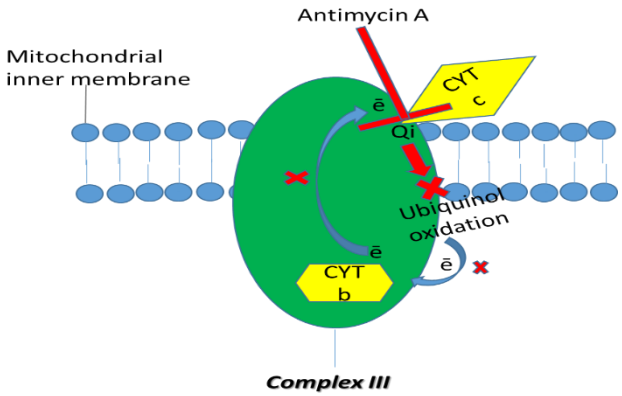

Figure 3.1: schematic diagram of antimycin A inhibitory effect of Qi site of mitochondrial complex III.

Blocking of complex III leads to several consequences, which include a collapse in electron movement, reduction in cellular ATP production and induction of ROS generation (Campo, Kinnally, and Tedeschi 1992; Balaban, Nemoto, and Finkel 2005). Previous studies on rat hippocampal CA1 cells identified that generation of ROS could have downstream effects including inducing a hypoxic response and reducing neuronal excitability via a reduction in sodium currents in the plasma membrane (Lai et al. 2005). In addition, it was found that antimycin A plays an important role in the regulation of guinea pig gallbladder smooth muscle tone via interrupting the normal function of mitochondria, leading to inhibition of spontaneous action potential and Ca^{2+} waves then reducing the contractility (Balemba et al. 2008). Recently, a study in our laboratory indicated that antimycin A caused a relaxation in PCA via inhibition of calcium influx (Almukhtar et al. 2016).

Inhibition of complex I together with complex III could enhance ROS production (Chen et al. 2003), which in turn could disturb mitochondrial function, calcium homeostasis and ATP production (Herrero and Barja 1997; St-Pierre et al. 2002). In contrast and in some pathological conditions, blocking of complex I with rotenone could reduce ROS production such as in ischaemia in the isolated rat heart (Becker et al. 1999).

One potential mechanism by which antimycin A could regulate smooth muscle tone is through activation of AMP-activated protein kinase (AMPK). AMPK is determined as a sensor of energy because when the ATP: AMP ratio decreases, this leads to AMPK activation through the increase in AMP (Suter et al. 2006; Gowans et al. 2013). There are several studies suggesting that increasing AMP Kinase activity could induce relaxation or anti-contractile effects via either activating eNOS pathway(Mori et al. 2017) or via enhancement of phosphorylation of myosin light chain kinase (Horman et al. 2008).

The previous chapter indicated that simvastatin could have an anti-contractile effect through inhibition of the mitochondrial ETC, possibly at complex III. Therefore, in this chapter, we determined the anti-contractile effect of the complex III inhibitor antimycin A, in order to compare the effect of antimycin A with that of simvastatin.

3.2. Material and Methods:

3.2.1. Tissue Preparation:

3.2.2. Isolated organ bath experiments:

Porcine coronary arteries were set up for isolated organ bath experiments as mentioned in chapter II, page 29.

3.2.3. Effect of antimycin A on U46619-induced tone:

In order to determine the effect of antimycin A on U46619-induced tone, tissues were exposed to antimycin A (1-10 μM) or vehicle control (0.1% v/v DMSO) for 2 h. After the incubation period, the thromboxane mimetic U46619 was added in a cumulative manner (1-300 nM). Contractile responses were expressed as a percentage of the response to 60 mM KCl. In some experiments, the Krebs'- Henseleit buffer was replaced with calcium-free Krebs solution in which the calcium was replaced with 2 mM ethylene glycol bis (β amino ethyl ether)-N,N,N,N- tetraacetic acid (EGTA). In other experiments, the Krebs'- Henseleit buffer was replaced with glucose-free Krebs.

3.2.4. Effect of Rho kinase, MEK, phosphatase and L-type calcium channel inhibition on antimycin A response:

After the KCl responses, tissues were exposed to antimycin A (10 μM) in the absence or presence of one of the following compounds: Rho kinase inhibitor Y27632 (10 μM), MEK-ERK inhibitor PD98059 (50 μM), L-type calcium channel blocker nifedipine (5 μM). Control tissues received vehicle only (distilled water for Y27632, 0.1% v/v DMSO for the other compounds). Cumulative concentration-response curves to U46619 were then carried out.

In order to determine the effect of antimycin A on relaxation responses to the phosphoprotein phosphatase inhibitor calyculin A or the L-type calcium channel blocker nifedipine, tissues were incubated with a single concentration of antimycin A (10 μM) for 120 min and then contracted with U46619 to about 40-60% of KCl contraction. This was followed by adding either a single concentration of calyculin A (100 nM) or cumulative concentrations of nifedipine (1 nM-3 μM) to induce relaxation.

3.2.5. Effect of mitochondrial inhibitors (I and III) on antimycin A-induced inhibition of thromboxane contraction:

In order to determine whether the inhibition of the U46619-induced contraction by antimycin A can be prevented by other complex inhibitors, the effects of mitochondrial inhibitors rotenone (complex I inhibitor) and myxothiazol (complex III inhibitor at Qo site), were determined. Tissues were pre-incubated with 10 μM antimycin A, with or without a

combination of rotenone and myxothiazol. Control tissues received vehicle only (0.1% v/v DMSO). Cumulative concentration-response curves to U46619 were then carried out.

3.2.6. Effect of FCCP and AMP kinase inhibitor on the antimycin A-induced inhibition of thromboxane contraction:

In order to determine whether the inhibition of the U46619-induced contraction by antimycin A could be prevented by uncoupling the mitochondria, tissues were pre-incubated with antimycin A (10 μM) in the absence or presence of FCCP (1 μM). Control tissues received vehicle only (0.1% v/v ethanol for FCCP, 0.1% v/v DMSO for antimycin A). Cumulative concentration-response curves to U46619 were then carried out in the presence of extracellular calcium. Contractile responses were expressed as a percentage of the response to 60 mM KCl.

Inhibition of the mitochondrial ETC can lead to activation of AMP kinase (Jiang et al. 2013). Therefore, in order to determine whether increased activity of AMP kinase underlies the inhibitory effect of antimycin A, tissues were pre-incubated with antimycin A in the absence or presence of dorsomorphin (10 μM). Control tissues received vehicle only (0.1% v/v DMSO). Cumulative concentration-response curves to U46619 were then carried out in the presence or absence of extracellular calcium. Contractile responses were expressed as a percentage of the response to 60 mM KCl.

3.2.7. Effect of mitochondrial stimulants on the antimycin A-induced inhibition of thromboxane contraction:

In order to determine if the inhibitory effect of antimycin A could be prevented by supplementation with co-enzyme Q10, tissues were exposed to co-enzyme Q10 (5 μM) or mitoquinol (1 μM), a mitochondria-targeted form of co-enzyme Q10. Control tissues received vehicle only (0.1% v/v ethanol for co-enzyme Q10 and 0.1% v/v DMSO for the rest). Cumulative concentration-response curves to U46619 were then carried out in the presence of extracellular calcium. Contractile responses were expressed as a percentage of the response to 60 mM KCl.

Blocking complex III could increase mitochondrial ROS production, which can be prevented by mitochondrial H_2S. Therefore, the effect of the mitochondria-targeted H_2S donor AP39 (30 μM) on the inhibitory effect of antimycin A was determined. Tissues were exposed to a single concentration of U46619 (30 nM) then tension recorded for up to 120 min. Contractile responses were expressed as a percentage of the response to 60 mM KCl.

3.2.8. Effect of antimycin A on $CaCl_2$ and Bay K 8644-induced contraction:

In order to determine whether the inhibition of the U46619-induced contraction by antimycin A requires the presence of extracellular calcium, tissues were pre-incubated with antimycin A (10 μM) in calcium-free Krebs-Henseleit buffer. Control tissues received vehicle only (0.1% v/v DMSO). After the incubation period, tissues were exposed to a maximum concentration of U46619 (300 nM). $CaCl_2$ was then added cumulatively (10 μM-3 mM) to induce a contraction. Contractile responses were expressed as a percentage of the response to 60 mM KCl.

In other experiments and in order to determine and confirm the involvement of L-type calcium channel in the inhibitory effect of antimycin A, tissues were pre-incubated with antimycin A (10 μM). Control tissues received vehicle only (0.1% v/v DMSO). After the incubation period, the L-type calcium channel opener Bay K 8644 was then added cumulatively (1-300 nM). Contractile responses were expressed as a percentage of the response to 60 mM KCl.

3.2.9. Drugs and Chemicals:

U46619, Y27632, PD98059 and Bay K 8644 were purchased from Tocris Bioscience, UK. antimycin A, myxothiazol, rotenone, dorsomorphin, co-enzyme Q10, FCCP, and nifedipine were purchased from Sigma, UK. Mitoquinol and AP39 were purchased from Cayman Chemical Company, USA. Finally, calyculin A was purchased from Cell Signalling Technology, UK.

Stock solutions of Y27632 were dissolved in distilled water. The stock solution of co-enzyme Q10 was dissolved in ethanol. The stock solutions of U46619 were made to 10mM in ethanol. All further dilutions of the stock solutions were made using distilled water. Furthermore, stock solutions of all remaining chemicals were dissolved in dimethyl sulfoxide (DMSO).

The following modified Krebs-Henseleit buffer solution was used (in mM): NaCl 118, KCl 4.8, $CaCl_2.H_2O$ 1.3, $NaHCO_3$ 25.0, KH_2PO_4 1.2, $MgSO_4.7H_2O$ and glucose 11.1, previously gassed with a mixture of 5% CO_2 and 95% O_2 with pH of approximately 7.5 and used at 37 ^oC. All stocks were kept frozen at -20 ^oC, except for KCl and $CaCl_2$ that were kept at room temperature.

3.2.10. Statistical Analysis:

Data were expressed as mean ± SEM where n = the number of different animals. The concentration-response curves were fitted to a sigmoidal curve with a variable slope using four parameters (Top, bottom, log EC50 and slope) logistic equation using Graph-Pad Prism software. The maximum percentage contraction (R_{max}) and the negative log of concentration required to produce half the response to that ligand (pEC_{50}) were derived from the fitted curves where appropriate. Data were analyzed using 2-tailed, paired (dependent) for one group sample tested twice or unpaired (independent) Student's t-test to compare the means of 2 groups-tested once. Differences between 3 or more groups were assessed using one-way ANOVA or two-way ANOVA in conjunction with the Sidak's post-hoc test or Tukey post-hoc test to assess possible difference at individual concentrations. The P-value <0.05 was considered statistically significant. Statistical analysis was performed by Graph-Pad Prism (Version 7).

3.3. Results:

3.3.1. The effect of antimycin A on U46619 (thromboxane A2 mimetic) induced contraction in porcine coronary arteries (PCAs):

In order to determine whether antimycin A inhibited the contractile response to thromboxane receptor activation, the effect of pre-incubation with antimycin A on U46619-induced contractions was determined in the presence of calcium (fig.3.2) and in the absence of calcium (fig.3.3). In the presence of calcium, the R_{max} response of control tissues was 96 ± 5% of the KCl response with pEC_{50} of 7.65± 0.04 (n= 12). Pre-incubation with increasing concentrations of antimycin A caused a significant inhibitory effect on the contractile response with 10 µM antimycin A mainly at 30 µM. See figure 3.2 and table 3.1.

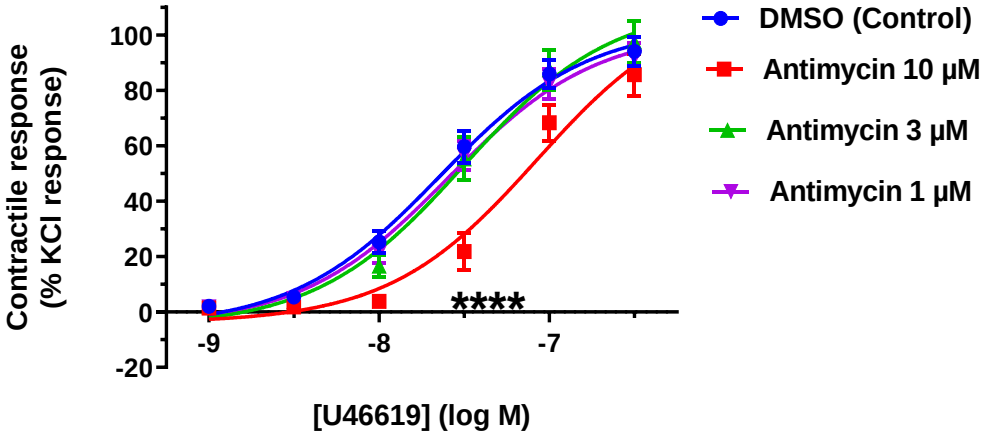

Figure 3.2: Log concentration-response curves for the vasocontractile effects of U46619 with pre-incubation of antimycin A (1, 3 and 10 µM). Control is vehicle only (0.1% v/v DMSO). Data are expressed as a percentage of the contraction to 60 mM KCl and are mean ± SEM of 12 experiments. ****p-value< 0.0001 v control at 30 nM of U46619, One-way ANOVA followed by Tukey post-hoc test.

	R_{max} (% KCl response, mean ± SEM)	pEC50 (mean ± SEM)
Control	96 ± 5	7.65 ± 0.04
1 µM Antimycin A	94 ± 5	7.60 ± 0.06
3 µM Antimycin A	98 ± 7	7.55 ± 0.05
10 µM Antimycin A	86 ± 7	7.27 ± 0.05****

Table 3.1: Response at maximum concentration expressed as a percentage of the response to 60 mM KCl and log EC_{50} (pEC_{50}) for U46619 in the absence (control, which is 0.1% v/v DMSO), or presence of antimycin A (1, 3, and 10µM) in PCAs. Data are expressed as mean ± SEM of 12 experiments. ****p-value< 0.0001 v control at 30 nM of U46619, One-way ANOVA followed by Tukey post-hoc test.

In the absence of calcium, the size of contraction to U46619 was smaller than that in the presence of calcium. Pre-incubation with 10 µM antimycin A showed smaller inhibitory effect between 30 and 100 nM of U46619 induced contraction of the PCA (Response at maximum concentration 300 nM U46619 = 12.5 ± 2.7%, mean ± SEM, n=6) compared to the control (Response at maximum concentration 300 nM U46619 = 14.6 ± 3%, mean ± SEM, n=6). See figure 3.3.

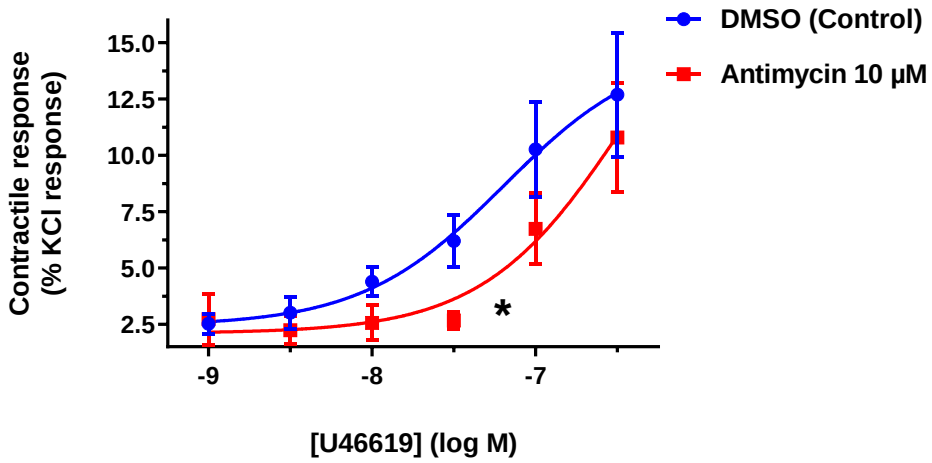

Figure 3.3: Log concentration-response curves for the vasocontraction effects of U46619 with pre-incubation of antimycin A (10 µM) in the absence of calcium. Control is vehicle only (0.1% v/v DMSO). Data are expressed as a percentage of the contraction to 60 mM KCl and are mean ± SEM of 6 experiments. *p-value< 0.05 v control, Student's 2-tailed paired t-test.

3.3.2. Effect of rotenone (complex I inhibitor) on antimycin A response:

In order to determine whether the effect of antimycin A could be prevented with a complex I inhibitor, tissues were incubated with 10 μM antimycin A, in the absence or presence of mitochondrial complex inhibitor I rotenone (10 μM). Response at maximum concentration of U46619 in the control tissues was 115 ± 7.6% of the KCl response (n= 6). Pre-incubation with rotenone alone had no significant effect on the contractile response to U46619, whereas antimycin A inhibited the contraction to U46619 at 30-100 nM. Pre-incubation of rotenone in the presence of antimycin A had no more effect on the inhibitory effect of antimycin A. See table 3.2 and figure 3.4.

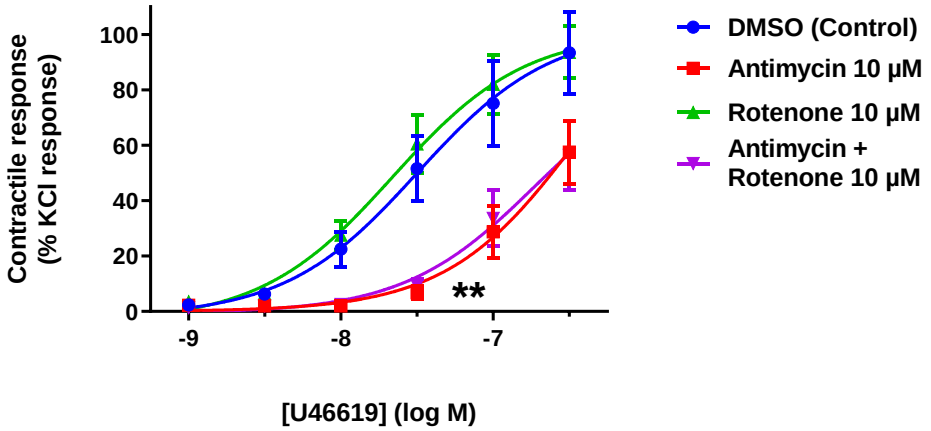

Figure 3.4: Log concentration-response curves for the vasocontractile effects of U46619 with pre-incubation 10 μM rotenone and 10 μM antimycin A. Control is vehicle only (0.1% v/v DMSO). Data are expressed as a percentage of the contraction to 60 mM KCl and are mean ± SEM of 6 experiments. **p<0.01 v control at 30-100 nM of U46619, Two-way ANOVA followed by Tukey post-hoc test.

	Response at 300 nM U46619 ± SEM
Control	115 ±7.6%
Antimycin A	75 ± 3.4%
Rotenone	101 ± 7.1%
Antimycin A + Rotenone	68 ± 18%

Table 3.2: Response at maximum concentration expressed as a percentage of the response to 60 mM KCl for U46619 in the absence (control, which is 0.1% v/v DMSO), or presence of 10 μM antimycin A and 10 μM rotenone with and without antimycin A in PCAs. Data are expressed as mean ± SEM of 6 experiments. Two-way ANOVA followed by Tukey post-hoc test.

3.3.3. Effect of the rotenone-myxothiazol combination on antimycin A response:

In order to determine whether inhibition of complex I and complex III at Qi site could prevent the inhibitory effect of antimycin A, tissues were incubated with 10μM antimycin A, in the absence or presence of the mitochondrial complex I and III inhibitors rotenone and myxothiazol (10 μM). The control tissues reached a R_{max} of 94± 11% of the KCl response with pEC_{50} value of 8.0 ± 0.1 (n= 6). Pre-incubation with myxothiazol-rotenone combination alone had no significant effect on the contractile response to U46619, whereas antimycin A inhibited the contraction to U46619 at 10nM. Pre-incubation of myxothiazol-rotenone combination in the presence of antimycin A had no significant effect on the inhibitory effect of antimycin A. See table 3.3 and figure 3.5.

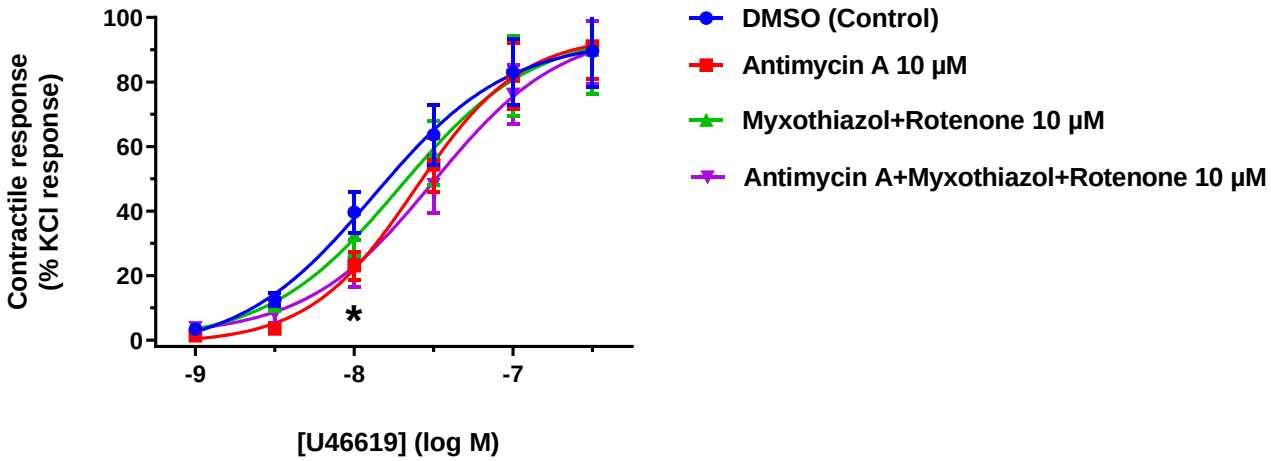

Figure 3.5: Log concentration-response curves for the vasocontractile effects of U46619 with pre-incubation 10 μM (myxothiazol and rotenone) and 10 μM antimycin A. Control is vehicle only (0.1% v/v DMSO). Data are expressed as a percentage of the contraction to 60 mM KCl and are mean ± SEM of 6 experiments. *p<0.05 v control at 10 nM of U46619, Two-way ANOVA followed by Tukey post-hoc test.

	R_{max} (% KCl response, mean ± SEM)	**pEC50 (mean ± SEM)**
Control	94 ± 11%	7.8 ± 0.06
Antimycin A	101 ± 11%	7.6± 0.03*
Myxothiazol-Rotenone	97 ± 14%	7.7 ± 0.04
Antimycin A + Myxothiazol-Rotenone	100 ± 11%	7.5± 0.09

Table 3.3: Maximum contraction (Rmax) expressed as a percentage of the response to 60 mM KCl and log EC_{50} (pEC_{50}) for U46619 in the absence (control, which is 0.1% v/v DMSO), or presence of 10 μM antimycin A and 10 μM (myxothiazol and rotenone) with and without antimycin A in PCAs. Data are expressed as mean ± SEM of 6 experiments. *p<0.05 v control at 10 nM of U46619, Two-way ANOVA followed by Tukey post-hoc test.

3.3.4. Effect of AMP kinase inhibitor on antimycin A response:

In order to determine whether AMP kinase is involved in the anti-contractile effect of antimycin A, the effect of 10 μM dorsomorphin with or without 10 μM antimycin A on U46619-induced contractions in PCA was determined in the presence (Fig.5) and absence of calcium (Fig.6). In the presence of calcium, the control tissues reached a response at maximum concentration of U46619 used of 83.9± 7.24% of the KCl response (n= 6). Pre-incubation with 10 μM dorsomorphin had no effect on the contractile response to U46619 while pre-incubation with antimycin A inhibited the U46619 contraction. Pre-incubation with dorsomorphin attenuated the inhibitory effect of antimycin A on the contractile response of U46619. See figure 3.6 and table 3.4

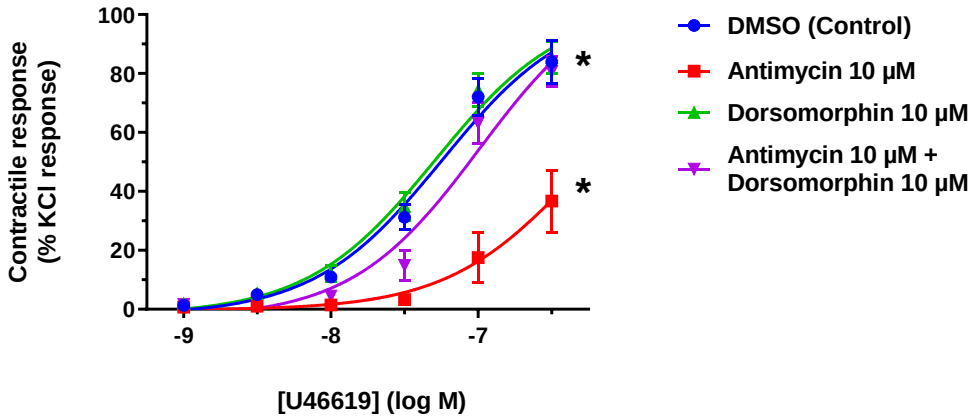

Figure 3.6: Log concentration-response curves for the vasocontractile effects of U46619 with pre-incubation 10 μM dorsomorphin and 10 μM antimycin A in the presence of calcium. Control is vehicle only (0.1% v/v DMSO). Data are expressed as a percentage of contraction to 60 mM KCl and are mean ± SEM of 6 experiments. *p-value < 0.05 v control at 300 nM of U46619, Two-way ANOVA followed by Tukey post-hoc test.

	Response at 300 nM U46619 ± SEM
Control	83.9 ± 7.24%
Antimycin A	36.7 ± 10.5%*
Dorsomorphin	85.36 ± 5.4%
Dorsomorphin+ Antimycin A	80.6 ± 5.1%*

Table 3.4: Response at maximum concentration expressed as a percentage of the response to 60 mM KCl for U46619 in the absence (control, which is 0.1% v/v DMSO), or presence of 10 μM antimycin A and 10 μM dorsomorphin with and without antimycin A in PCAs. Data are expressed as mean ± SEM of 6 experiments performed in the presence of calcium. *p-value < 0.05 v control at 300 nM of U46619, Two-way ANOVA followed by Tukey post-hoc test.

In contrast, in the absence of calcium, dorsomorphin enhanced the inhibitory effect of antimycin A on the U46619-induced contraction, reducing the response at maximum concentration from 10.5 ± 0.72% to 7.3± 0.46% (as shown in table 3.5 and figure 3.7).

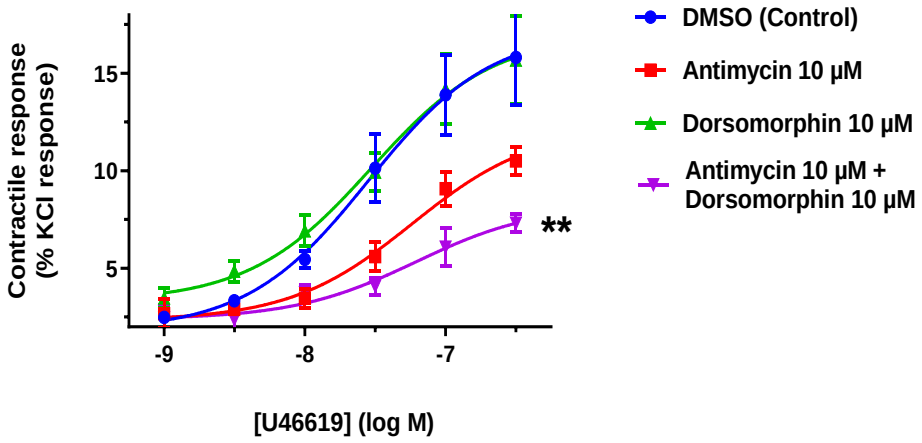

Figure 3.7: Log concentration-response curves for the vasocontractile effects of U46619 with pre-incubation 10 µM dorsomorphin and 10 µM antimycin A in absence of calcium. Control is vehicle only (0.1% v/v DMSO). Data are expressed as a percentage of the contraction to 60 mM KCl and are mean ± SEM of 6 experiments. **p-value < 0.01 v control at 300 nM of U46619, Two-way ANOVA followed by Tukey post-hoc test.

	Response at 300 nM U46619 ± SEM
Control	15.8 ± 2.44%
Antimycin A	10.5 ± 0.72%
Dorsomorphin	15.7 ± 2.24%
Dorsomorphin+ Antimycin A	7.3 ± 0.46%**

Table 3.5: Response at maximum concentration expressed as a percentage of the response to 60 mM KCl for U46619 in the absence (control, which is 0.1% v/v DMSO), or presence of 10 µM antimycin A and 10 µM dorsomorphin with and without antimycin A in PCAs. Data are expressed as mean ± SEM of 6 experiments performed in absence of calcium. **p<0.01 v control at 300 nM of U46619, Two-way ANOVA followed by Tukey post-hoc test.

3.3.5. Effect of co-enzyme Q10 on antimycin A response:

In order to determine whether supplementation with coenzyme Q10 could prevent the antimycin A-induced inhibition of the U46619-induced response, tissues were incubated with 10 μM antimycin A, in the absence or presence of coenzyme Q10 (5 μM). Response at maximum concentration of U46619 in the control tissues was 108 ± 6% of the KCl response (n= 6). Pre-incubation with coenzyme Q10 alone had no significant effect on the contractile response to U46619, whereas antimycin A inhibited the contraction to U46619. Pre-incubation of coenzyme Q10 in the presence of antimycin A attenuated the inhibitory effect of antimycin A. See table 3.6 and figure 3.8.

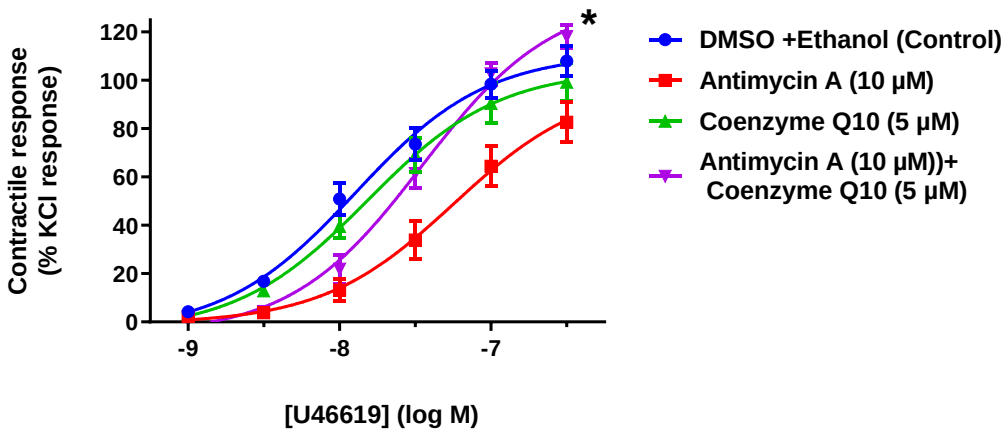

Figure 3.8: Log concentration-response curves for the vasocontraction effects of U46619 with pre-incubation 5 μM coenzyme Q10 and 10 μM antimycin A. Control is vehicle only (0.1% v/v DMSO+ Ethanol). Data are expressed as a percentage of the contraction to 60 mM KCl and are mean ± SEM of 6 experiments. *p<0.05 v coenzyme, Two-way ANOVA followed by Tukey post-hoc test.

	Response at 300 nM U46619 ± S.E.M
Control	108 ± 6%
Antimycin A	83 ± 8%
Coenzyme Q10	99 ± 8%
Antimycin A + Coenzyme Q10	118 ± 5%*

Table 3.6: Response at maximum concentration expressed as a percentage of the response to 60 mM KCl for U46619 in the absence (control, which is 0.1% v/v DMSO+ Ethanol), or presence of 10 μM antimycin A and 5 μM co-enzyme Q10 with and without antimycin A in PCAs. Data are expressed as mean ± SEM of 6 experiments. *p<0.05 v coenzyme, Two-way ANOVA followed by Tukey post-hoc test.

3.3.6. Effect of mitoquinol on antimycin A response:

In order to determine whether mitoquinol prevented the antimycin A-induced inhibition of the U46619-induced response, tissues were incubated with 10 μM antimycin A, in the absence or presence of mitoquinol (1 μM). The control tissues reached a Rmax of 93 ± 6% of the KCl response with pEC_{50} of 8 ± 0.1 (n= 6). Pre-incubation with mitoquinol alone had no significant effect on the contractile response to U46619, whereas antimycin A inhibited the contraction to U46619. Pre-incubation of mitoquinol in the presence of antimycin A moderately attenuated the inhibitory effect of antimycin A. See table 3.7 and figure 3.9.

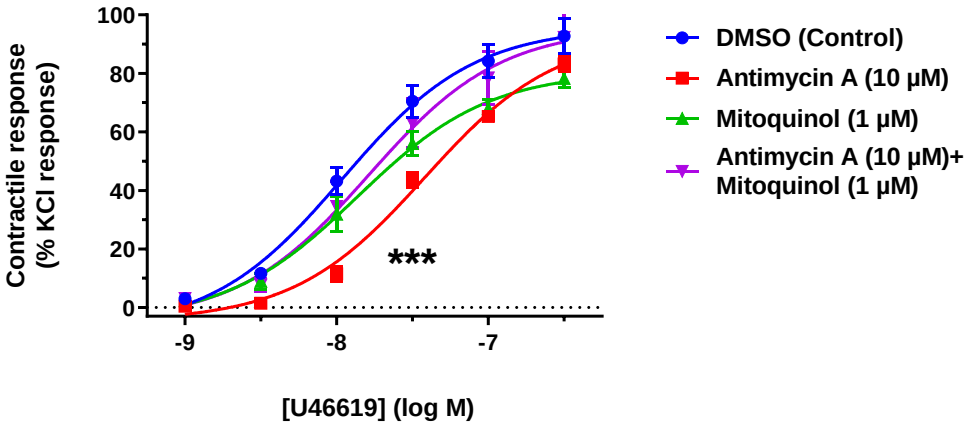

Figure 3.9: Log concentration-response curves for the vasocontractile effects of U46619 with pre-incubation 1 μM mitoquinol and 10 μM antimycin A. Control is vehicle only (0.1% v/v DMSO). Data are expressed as a percentage of the contraction to 60 mM KCl and are mean ± SEM of 6 experiments. ***p<0.001 v control at 30 nM of U46619, Two-way ANOVA followed by Tukey post-hoc test.

	R_{max} (% KCl response, mean ± SEM)	**pEC50 (mean ± SEM)**
Control	93 ± 6%	8 ± 0.1
Antimycin A	83 ± 3%	7 ± 0.1***
Mitoquinol	78 ± 3%	8 ± 0.1
Antimycin A + Mitoquinol	92 ± 8%	8 ± 0.2

Table 3.7: Maximum contraction (Rmax) expressed as a percentage of the response to 60 mM KCl and log EC_{50} (pEC_{50}) for U46619 in the absence (control, which is 0.1% v/v DMSO), or presence of 10 μM antimycin A and 1 μM mitoquinol with and without antimycin A in PCAs. Data are expressed as mean ± SEM of 6 experiments. ***p<0.001 v control at 30 nM of U46619, Two-way ANOVA followed by Tukey post-hoc test.

3.3.7. Effect of FCCP on antimycin A response:

In order to determine whether uncoupling the mitochondria prevented the antimycin A-induced inhibition of the U46619-induced response, tissues were incubated with 10 μM antimycin A, in the absence or presence of FCCP (1 μM). The response at maximum concentration of U46619 in the control tissues was 90 ± 6% of the KCl response (n= 6). Pre-incubation with FCCP alone had no significant inhibitory effect on the contractile response to U46619, whereas antimycin A inhibited the contraction to U46619. Pre-incubation of FCCP in the presence of antimycin A, attenuated the inhibitory effect of antimycin A. In fact, in the presence of antimycin A and FCCP, the contraction to U46619 appeared to be enhanced compared to control. See table 3.8 and figure 3.10.

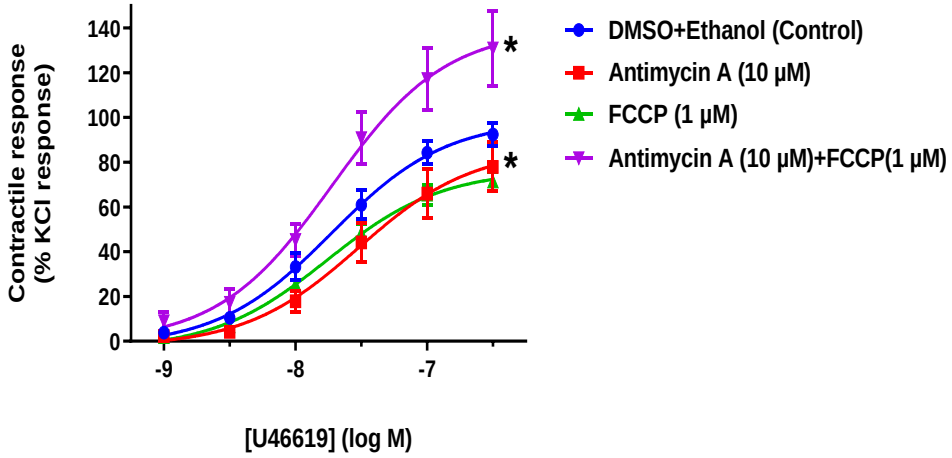

Figure 3.10: Log concentration-response curves for the vasocontractile effects of U46619 with pre-incubation 1 μM FCCP and 10 μM antimycin A. Control is vehicle only (0.1% v/v DMSO +ethanol). Data are expressed as a percentage of the contraction to 60 mM KCl and are mean ± SEM of 6 experiments. *p<0.05 v control at 300 nM of U46619, Two-way ANOVA followed by Tukey post-hoc test.

	Response at 300 nM U46619 ± S.E.M
Control	90 ± 6%
Antimycin A	69 ± 8%*
FCCP	73 ± 5%
Antimycin A + FCCP	125 ± 20%*

Table 3.8: Response at maximum concentration expressed as a percentage of the response to 60 mM KCl for U46619 in the absence (control, which is 0.1% v/v DMSO +ethanol), or presence of 10 μM antimycin A and 1 μM FCCP with and without antimycin A in PCAs. Data are expressed as mean ± SEM of 6 experiments. *p<0.05 v control at 300 nM of U46619, Two-way ANOVA followed by Tukey post-hoc test.

3.3.8. Effect of removal of extracellular glucose on antimycin A response:

Removal of extracellular glucose increases the cell's reliance on mitochondrial oxidative phosphorylation and, therefore, mitochondrial function. Therefore, under these conditions, inhibition of mitochondrial complexes should lead to a greater effect. To test this, tissues were incubated with 10 μM antimycin A, in the presence or absence of glucose (using glucose-free Krebs). In the presence of glucose, the response at maximum concentration of U46619 in the control tissues was 116 ± 13% of the KCl response (n= 6). Pre-incubation with antimycin A caused inhibition to U46619-induced contraction at 30 nM of U46619. In the absence of glucose, the size of contraction was smaller, the response at maximum concentration of U46619 in the control tissues was 28 ± 8% and Antimycin A still inhibited the contraction to U46619-induced contraction under these conditions. See table 3.9 and figure 3.11.

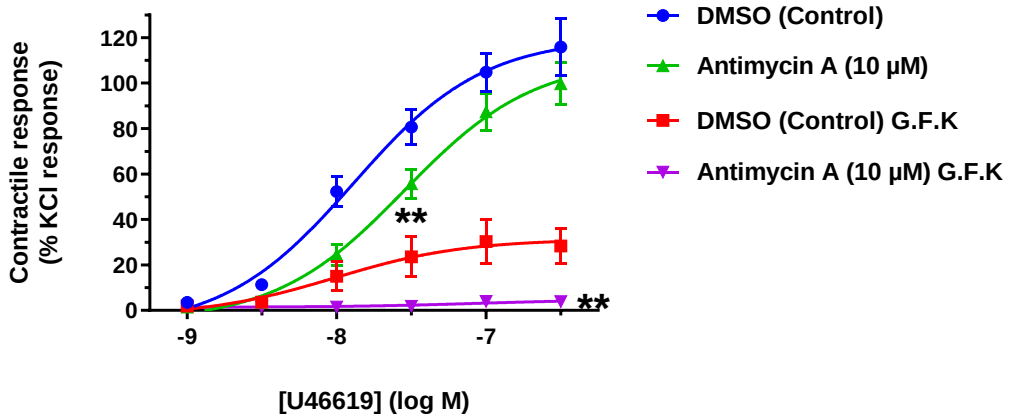

Figure 3.11: Log concentration-response curves for the vasocontractile effects of U46619 with pre-incubation 10 μM antimycin A in the presence and absence of glucose. Control is vehicle only (0.1% v/v DMSO). Data are expressed as a percentage of the contraction to 60 mM KCl and are mean ± SEM of 6 experiments. **p<0.01 v his control, Student's 2-tailed paired t-test.

	Response at 300 nM U46619 ± S.E.M
Control	116 ± 13%
Antimycin A	100 ± 9%
Control-G.F.K.	28 ± 8%
Antimycin A-G.F.K.	4 ± 2%**

Table 3.9: Response at maximum concentration expressed as a percentage of the response to 60 mM KCl for U46619 in the absence (control, which is 0.1% v/v DMSO), or presence of 10 μM antimycin A with and without glucose in PCAs. Data are expressed as mean ± SEM of 6 experiments. **p<0.01 v his control, Student's 2- tailed paired t-test.

3.3.9. Effect of H_2S donor AP39 on antimycin A response:

Mitochondrial (H_2S) can protect cells from increases in mitochondrial ROS production. In order to determine whether mitochondrial H_2S could prevent the antimycin A effect, tissues were pre-incubated for 120 min with a single concentration of 10 μM antimycin A and with AP39 (30 μM) for 15 min, prior to exposure to a single sub maximum concentration of U46619 (30 nM). 15 min for the pre-incubation with AP39 was chosen as H_2S is a short-lived compound and is based on other observations of AP39 in the laboratory. Pre-incubation with AP39 alone had no significant effect on time-dependent contraction profile to U46619, whereas antimycin A showed significant inhibition of U46619-induced contraction with most time points. Pre-incubation of AP39 in the presence of antimycin A showed a partial reduction in antimycin A inhibitory effect, see figure 3.12.

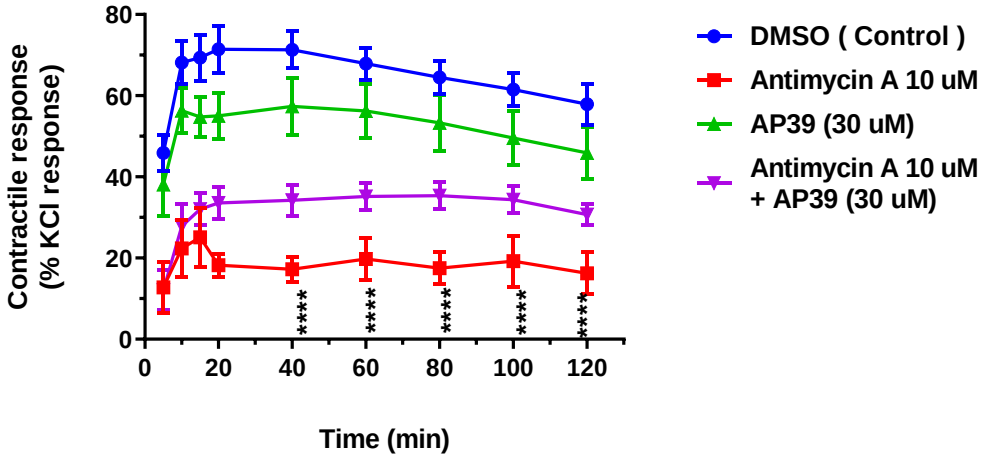

Figure 3.12: Time-response curves for the vasocontraction effects of 30 nM U46619 on PCA pre-incubated with 10 μM antimycin A and AP39 (30 μM). Control is vehicle only (0.1% v/v DMSO). Data are expressed as a percentage of the contraction to 60 mM KCl at different time points and are mean of 6 experiments. ****p<0.0001 v control at most of the time points, 2-way ANOVA followed by Tukey post-hoc test.

3.3.10. Effect of Y27632 (Rho Kinase Inhibitor) on antimycin A response:

In order to determine the combined inhibitory effect of antimycin A (10 μM) and Y27632 (10 μM) on concentration-response curves to U46619, tissues were pre-incubated with and without antimycin A (10 μM) for 2 h and with Y27632 (10 μM) for 1 h. The inhibitory effect of antimycin A and Y27632 together was larger than that produced by Y27632 alone. See table 3.10 and figure 3.13.

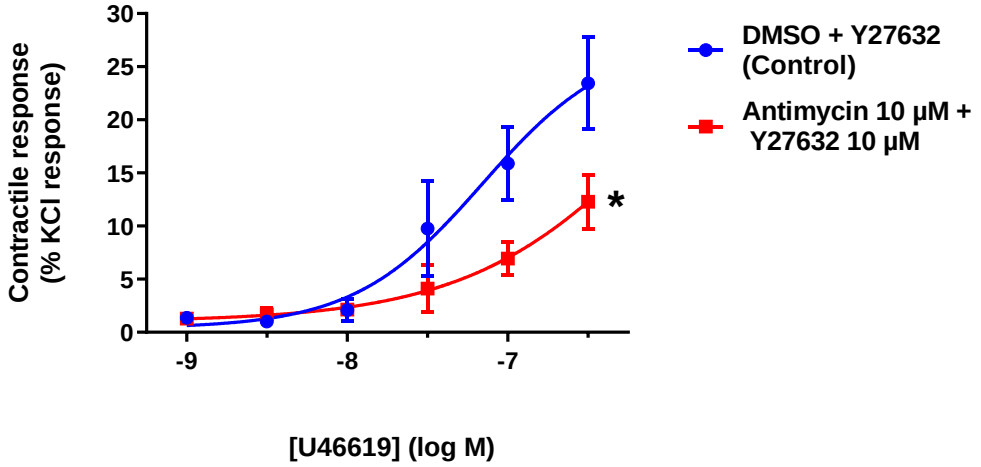

Figure 3.13: Log concentration-response curves for the vasocontractile effects of U46619 with pre-incubation of antimycin A and Y27632 (10 μM). Control is 0.1% v/v DMSO+Y27632. Data are expressed as a percentage of the contraction to 60 mM KCl and are mean ± S.E.M. of 6 experiments. *p<0.05 v control at 300 nM of U46619, Student's 2-tailed paired t-test.

	Response at 300 nM of U46619± SEM
DMSO+Y27632 (Control)	24± 4 %
Antimycin A+Y27632 (10 μM)	15 ± 2 % *

Table 10: Response at maximum concentration expressed as a percentage of the response to 60 mM KCl and for U46619 in the absence (control, which is 0.1% v/v DMSO+Y27632), or presence of antimycin A and Y27632 (10 μM) in PCAs. Data are expressed as mean ± SEM of 6 experiments. *p<0.05 v control at 300 nM of U46619, Student's 2-tailed paired t-test.

3.3.11. Effect of PD98059 (MEK Inhibitor) on antimycin A response:

In order to determine the combining inhibitory effect of antimycin A (10 μM) and PD98059 (50 μM) on concentration-response curves to U46619, tissues were pre-incubated with and without antinycin A (10 μM) for 2 h and with PD98059 (50 μM) for 1. The inhibitory effect of antimycin A and PD98059 together was larger than that produced by PD98059 and DMSO (control). Table (3.11) and figure (3.14)

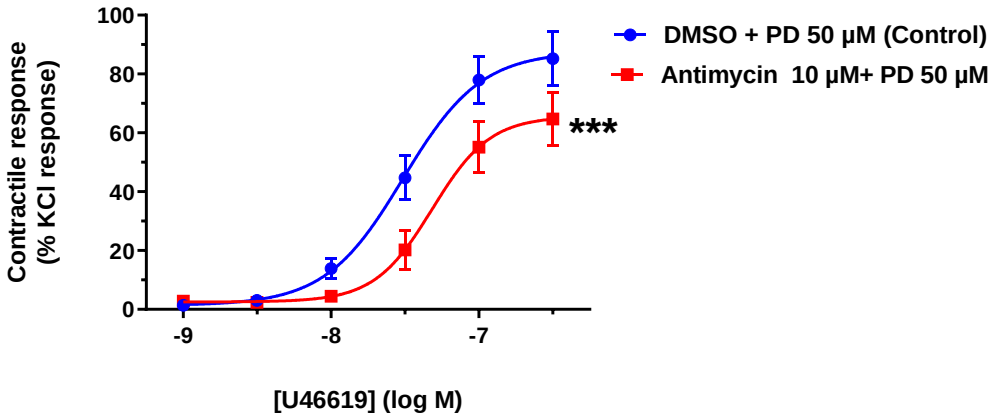

Figure 3.14: Log concentration-response curves for the vasocontractile effects of U46619 with pre-incubation of antimycin A (10 μM) and PD98059 (50 μM). Control is 0.1% v/v DMSO+ PD98059. Data are expressed as a percentage of the contraction to 60 mM KCl and are mean ± SEM of 6 experiments. ***p<0.001 v control at 300 nM of U46619, Student's 2-tailed paired t-test.

	R_{max}± S.E.M	**pEC_{50}± S.E.M**
DMSO+ PD98059 (Control)	87.3 ± 9.3%	7.5 ± 0.03
Antimycin A+ PD98059 (10 μM)	65.7 ± 9 % ***	7.2 ± 0.03***

Table 3.11: Maximum contraction (R_{max}) expressed as a percentage of the response to 60 mM KCl and log EC_{50} (pEC_{50}) for U46619 in the absence (control, which is 0.1% v/v DMSO+ PD98059), or presence of antimycin A (10 μM) and PD98059 (50 μM) in PCAs. Data are expressed as mean ± SEM of 6 experiments. ***p<0.001 v control at 300 nM of U46619, Student's 2-tailed paired t-test.

3.3.12. Effect of calyculin A (Phosphatase inhibitor) on antimycin A response:

Rho kinase inhibits myosin phosphatase. Therefore, we hypothesized that, if 10 μM antimycin A inhibited Rho kinase activation, inhibition of myosin phosphatase would prevent the inhibitory effect of antimycin A. Therefore, the effect of pre-incubation with 100 nM calyculin A on relaxation responses to antimycin A (10 μM) was determined. Calyculin A caused inhibition of the relaxant effect of antimycin A on pre-contracted PCA through almost all of the 2 h compared to the control (n=8) as shown in figure 3.15.

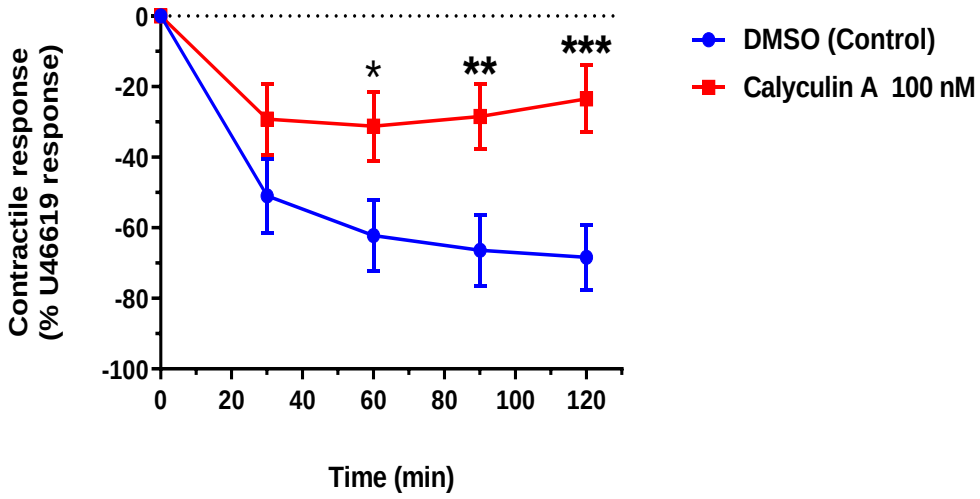

Figure 3.15: Effect of calyculin A (100 nM) on antimycin A (10 μM) relaxation in porcine coronary artery pre-contracted with U46619. Control is vehicle only (0.1% v/v DMSO). Data are expressed as a percentage of relaxation to U46619-induced contraction and are mean of 8 experiments. *p<0.05 v control, **p<0.01 v control, ***p<0.001 v control 2-way ANOVA followed by Sidak post-hoc test.

3.3.13. The effects of antimycin A on calcium-induced contractions in PCAs:

In order to determine whether antimycin A inhibits calcium-influx to inhibit the U46619-induced contraction, tissues were incubated with or without 10 μM antimycin A in calcium-free buffer. After the incubation period, tissues were exposed to a maximum concentration of U46619 (300 nM). $CaCl_2$ was then added cumulatively (10 μM-3 mM) to induce a contraction. The control tissues reached a R_{max} of 61 ± 10% of the KCl response with pEC_{50} of 3.9± 0.04 (n= 9). Pre-incubation with antimycin A inhibited the contraction to $CaCl_2$ at the pEC_{50} (3.5 ± 0.1%) as shown in figure 3.16.

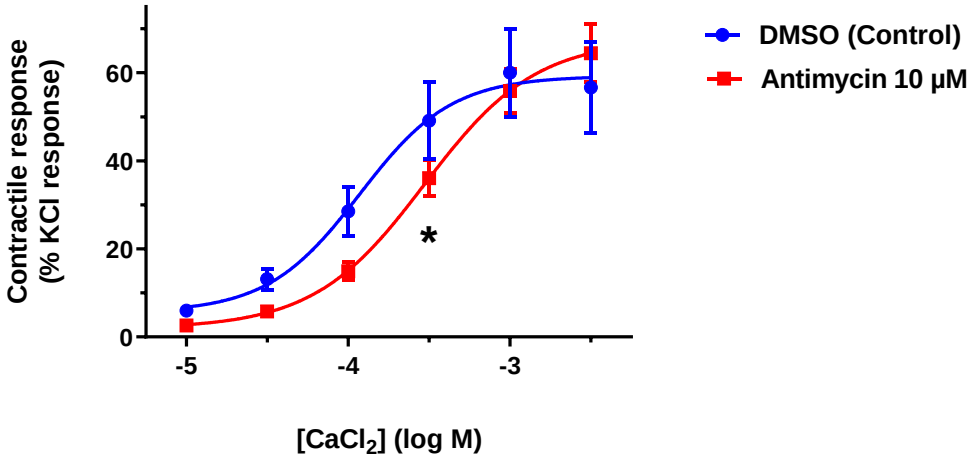

Figure 3.16: Log concentration-response curves for the vasocontractile effects of $CaCl_2$ with pre-incubation of antimycin A (10 μM). Control is vehicle only (0.1% v/v DMSO). Data are expressed as a percentage of the contraction to 60 mM KCl and are mean ± SEM of 9 experiments. *p<0.05 v control, Student's 2-tailed paired t-test.

3.3.14. Effect of L-type calcium channel blocker on antimycin A response:

In order to determine which calcium channel is involved in the antimycin A-induced inhibition of the U46619-induced response, tissues were incubated with 10 μM antimycin A, in the absence or presence of calcium channel blocker, nifedipine (5 μM). The control tissues reached a contraction at 300 nM of U46619 used of 55 ± 11% of the KCl response (n= 6). Pre-incubation with nifedipine alone caused inhibition to the contractile response. Pre-incubation of nifedipine in the presence of antimycin A caused no further effect. Table 3.12 and figure 3.17.

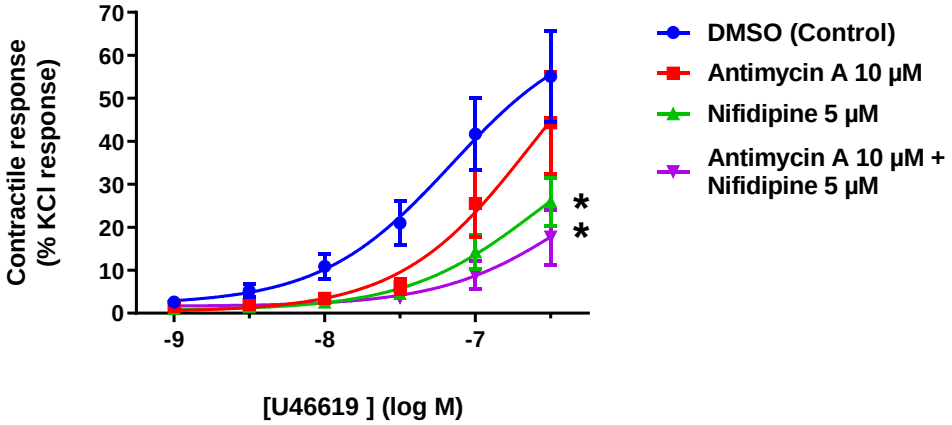

Figure 3.17: Log concentration-response curves for the vasocontractile effects of U46619 with pre-incubation 5 μM nifedipine and 10 μM antimycin A. Control is vehicle only (0.1% v/v DMSO). Data are expressed as a percentage of the contraction to 60 mM KCl and are mean ± SEM of 6 experiments. *p<0.05 v control at 300 nM of U46619, Two-way ANOVA followed by Tukey post-hoc test.

	Response at 300 nM of U46619 ± SEM
Control	55 ± 11%
Antimycin A	44 ± 12%
Nifedipine	26 ± 6%
Antimycin A + Nifedipine	18 ± 6%*

Table 3.12: Response at maximum concentration expressed as a percentage of the response to 60 mM KCl for U46619 in the absence (control, which is 0.1% v/v DMSO), or presence of 10 μM antimycin A and 10 μM nifedipine with and without antimycin A in PCAs. Data are expressed as mean ± SEM of 6 experiments. *p<0.05 v control at 300nM of U46619, Two-way ANOVA followed by Tukey post-hoc test.

3.3.15. The effect of antimycin A on relaxation response to nifedipine:

As there was an apparent effect of antimycin A on $CaCl_2$-induced concentration-response curve and to confirm which calcium channel is involved, tissues were incubated with or without 10 μM antimycin A, then pre-contracted with 30 nM of U46619 and followed by adding nifedipine (1-30 μM) to induce a relaxation. Nifedipine appeared to produce a biphasic relaxation response. Pre-incubation with 10 μM antimycin A had no effect on the nifedipine-induced relaxation as shown in figure 3.18.

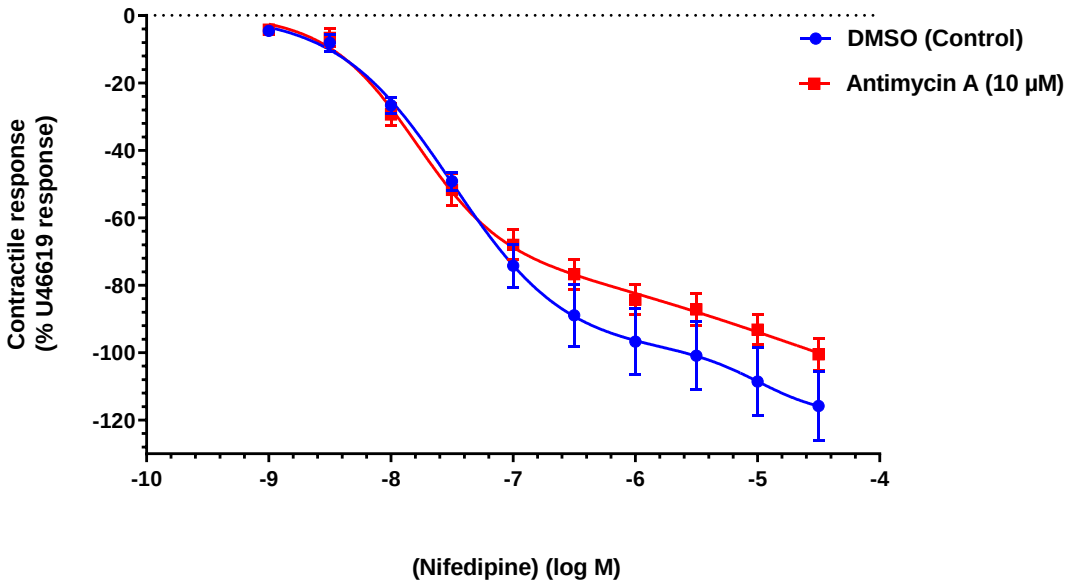

Figure 3.18: Effect of antimycin A (10 μM) on nifedipine-relaxation response curve on PCA pre-contracted with U46619. Control is vehicle only (0.1% v/v DMSO). Data are expressed as a percentage of relaxation to 30 nM U46619-induced contraction and are mean of 6 experiments. P-value >0.05 v control, 2-way ANOVA followed by Sidak post-hoc test.

3.3.16. The effect of antimycin A on (±)-Bay K 8644 (L-type Ca^{2+} channel activator) induced contraction in porcine coronary arteries:

In order to determine whether antimycin A inhibits the contractile response to an L-type Ca^{2+} channel activator to explore more about the role of calcium channels, the effect of pre-incubation with antimycin A on (±)-Bay K 8644-induced contractions was determined. At the maximum concentration used, control tissues reached a contraction of 77 ± 5% of the KCl response (n= 6). Pre-incubation with (10 μM) antimycin A caused a significant inhibitory effect on the contractile response with maximum contraction 38 ± 3% of the KCl response. See figure 3.19.

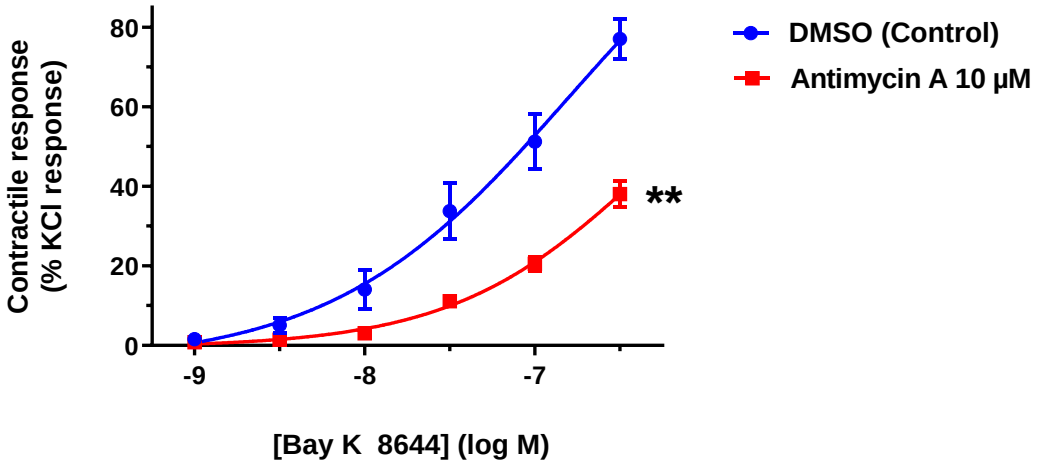

Figure 3.19: Log concentration-response curves for the vasocontractile effects of (±)-BAY K 8644 with pre-incubation of antimycin A (10 μM). Control is vehicle only (0.1% v/v DMSO). Data are expressed as a percentage of the contraction to 60 mM KCl and are mean ± SEM of 6 experiments. **P-value< 0.01 v control at 300 nM of Bay K 8644, Student's 2-tailed paired t-test.

3.4. Discussion:

The aim of this study was to determine the effect of antimycin A on U46619-induced contraction then determine the role of Rho Kinase, ERK, AMP Kinase, calcium, and mitochondria in the regulation of vascular smooth muscle tone.

3.4.1. Role of extracellular calcium in the antimycin A response:

As previous studies and our present study indicated that simvastatin might be acting through inhibition of mitochondrial function, we tested the effects of antimycin A, a known complex III inhibitor (Xia et al. 2013) on U46619-induced contraction and investigated the possible pathway for exerting its effect, as a comparison with simvastatin. Pre-incubation with increasing concentrations of antimycin A (1, 3, and 10 μM) in the presence and absence of calcium showed significant inhibition of contraction with 10 μM antimycin A. Although, the size of contraction to U46619 was smaller in the absence of calcium, antimycin A still inhibited the contraction. This suggests it does not interfere with calcium influx. This effect of antimycin A is different from that seen with simvastatin in the previous chapter in which the inhibitory effect of simvastatin was not seen in the absence of calcium.

A previous study performed on the smooth muscle of guinea-pig taenia coli and rabbit aorta showed that antimycin A had a significant inhibitory effect on K^+-induced contraction in guinea-pig taenia and noradrenaline-induced contraction in rabbit aorta. The study suggested that antimycin A exerts its action via causing a disturbance in mitochondrial function that leads to inhibition of K^+-induced intracellular Ca^{2+} increase, possibly from mitochondrial stores (Nakagawa et al. 1985). The data suggest that antimycin A might be inhibiting the calcium-induced contraction. Another study, this time in guinea pig gallbladder smooth muscle, also suggested that antimycin A altered smooth muscle contractility through alteration of calcium handling by the mitochondria (Balemba et al. 2008).

Although these data suggest that antimycin A does not lead to inhibition of calcium influx, pre-incubation with antimycin A inhibited the contraction to calcium in the PCA, in the presence of U46619. Previous studies identified that ROS, especially H_2O_2, cause a reduction in voltage-gated Ca^{2+}currents (I_{Ca}) in rat prefrontal neurons (Wu et al. 2010). As antimycin A inhibits the Qi site on complex III, where ubisemiquinon is reduced, this caused a disruption in the ETC followed by several consequences including production of ROS (Junemann, Heathcote, and Rich 1998). In another study performed on isolated heart mitochondria from guinea pigs, the researchers found that inhibition of complex III with antimycin A in the presence of an excess of $CaCl_2$ enhanced the production of ROS, mainly H_2O_2 (Lindsay et al. 2015). Therefore, inhibition of complex III with antimycin A can lead to inhibition of calcium influx, which would explain the effects on the calcium-induced

contraction. Thus to clarify more about calcium role and which calcium channel could be involved, we examined the effect of nifedipine, an L- type VGCC blocker, with antimycin A on U46619-induced contraction. The combination of antimycin A with nifedipine had no further inhibitory effect compared to nifedipine alone, which would suggest that antimycin A is acting to inhibit L-type VGCC. This is supported by the experiments showing that pre-incubation with antimycin A caused a significant inhibition of the Bay K 8644 (L-type VGCC activator)-induced contraction in PCA. On the other hand, antimycin A had no significant effect on the nifedipine-induced relaxation. It is possible that, whatever the mechanism by which antimycin A inhibits the calcium influx through L-type VGCC, it cannot compete with nifedipine. This suggests that antimycin A may not be acting directly at the dihydropyridine binding site on the L-type VGCC or nifedipine can't be displaced.

These findings are supported by a previous study performed on rat ventricular cardiac myocytes, which identified that carbon monoxide enhanced the production of ROS at complex III due to making a leak in mitochondrial ETC. These ROS, in turn, caused a modulation in cardiac L-type VGCC leading to inhibition of calcium influx (Scragg et al. 2008). Since complex III is one the main ETC sites for ROS production, inhibition of complex III with antimycin A will generate ROS (Turrens 2003; Park et al. 2007). These data could be clarified that this is the possible pathway for the ability of antimycin A to inhibit calcium influx and involvement of L- type VGCC in its inhibitory effect.

Ca^{2+} influx into a cell is reliant on various channels and exchangers (Mehta and Shaha 2004). This is suggesting that antimycin A probably induced its inhibitory effect via another mechanism or pathway beside inhibition of calcium influx from L-type VGCC and another channel may be involved. Previous studies identified that ATP could enhance calcium influx via non-selective cation calcium channel to induce contraction in VSMCs (Benham 1992). Researchers found that in rat basilar artery, ATP induced contraction after enhancing calcium release and increasing calcium influx via non L-type VGCC (Zhang et al. 1995). Another group of researchers found in their study on rat aorta that ATP increased cytosolic calcium via enhancement calcium influx and to a lesser extent calcium release to induce contraction (Kitajima, Ozaki, and Karaki 1993).

3.4.2. Effect of complex I and III inhibition:

In our investigations of the anti-contractile effect of simvastatin, we determined the effect of complex I and complex III inhibitors. Therefore, as a comparison, we determined the effect of a complex I inhibitor (rotenone) and complex III inhibitor (myxothiazol) (Li et al. 2003) on the antimycin A response. Pre-incubation with rotenone alone had no significant effect on the contractile response to U46619, whereas antimycin A inhibited the contraction to U46619 at EC_{50}. Pre-incubation of rotenone in the presence of antimycin A had no effect on the inhibitory effect of antimycin A. There are several studies that refer to complexes I and III as the main site for ROS (Turrens and Boveris 1980; Li et al. 2003; Lai et al. 2005) and simultaneous inhibition of both complexes could enhance ROS production that could induce smooth muscle relaxation(St-Pierre et al. 2002). On the other hand, the researchers found in a separate study performed using rat hearts that inhibition of mitochondrial complex I with rotenone in ischaemia, could reduce ROS rather than induce ROS production (Lesnefsky et al. 2006). Accordingly, this possibly means that blocking complex III increases ROS production, but inhibition of complex I might prevent this increase in ROS, as there would be no electrons to transfer.

The relation between ROS and smooth muscle tone is a bit complicated or not obvious. For example, in a study performed on cerebral arteries, the study showed that Ca^{2+} sparks could be activated in smooth muscle cells due to mitochondrial ROS generation and this leads to arterial dilatation as the Ca^{2+} sparks triggered large-conductance Ca^{2+}-activated K^+ channels (Xi, Cheranov, and Jaggar 2005). In contrast, another study performed on pulmonary arterial smooth muscle cells, the researchers found that ROS produced from mitochondria could induce cytosolic calcium increase and smooth muscle contraction in hypoxia (Waypa et al. 2002). This indicates that ROS play an important role in the regulation of smooth muscle tone in which the nature of smooth muscle cells and the amount of ROS could have an effect on the result.

Researchers have identified that complex III has two different blocking sites; Q_i, is commonly blocked with antimycin A, the second site Q_o, is commonly blocked with myxothiazol (Chen et al. 2003). Therefore, the effect of combining inhibition of complex I and III with rotenone and myxothiazol on the inhibitory effect of antimycin A was determined. The present study showed that rotenone-myxothiazol combination had no significant effect on the inhibitory response of antimycin A. This suggests that blocking complex I and the Q_o site of complex III is unable to overcome the inhibitory effect of antimycin A. These results are different from those seen with simvastatin in which the combination of myxothiazol and rotenone prevented the anti-contractile effect of simvastatin (chapter 2). This is further evidence to suggest that antimycin A acts in a different way from simvastatin.

To clarify the signalling pathway for the inhibitory effect of antimycin A on U46619-induced contractions, we determined if supplementation with co-enzyme Q10 or adding mitoquinol can prevent the inhibitory effect. Pre-incubation with co-enzyme Q10 or mitoquinol in the presence of antimycin A attenuated the inhibitory effect of antimycin A. This indicates that inhibition of complex III at Q_i site can be overcome by adding co-enzyme Q10 (Campo, Kinnally, and Tedeschi 1992; Pham, Robinson, and Hedley 2000). Adding co-enzyme Q10 (oxidized form) or mitoquinol (reduced form) filled the gaps, returned the balance to the electron transport chain to keep the electrons moving (Siciliano et al. 2007) and therefore prevented the inhibitory effect of antimycin A. Another study performed on mice identified that CoQ10 supplementation could prevent mitochondrial deterioration and improve mitochondrial function (Ben-Meir et al. 2015).

Following that, we tested whether uncoupling the mitochondria could prevent the antimycin A-induced inhibition of the U46619-induced response. Data from the present study showed that pre-incubation with FCCP attenuated the inhibitory effect of antimycin A. This supports the idea that the inhibitory effect of antimycin A on the U46619-induced contraction is mediated through its effects on the mitochondria. Interestingly, the U46619-induced contraction in the presence of both antimycin A and FCCP was enhanced.

U46619 induce contraction in smooth muscle cells via activating TP receptors that induce an increase in cytosolic calcium level via either enhancing the calcium release from stores or enhancing calcium entry through calcium channels on the cell membrane (Berridge 1995; Parekh and Penner 1997). Cytosolic calcium homeostasis is controlled by a calcium uniporter that is driven by mitochondrial membrane potential and cytosolic calcium concentration (Brookes et al. 2004). Uncoupling of mitochondria with FCCP means separation of the ETC from the phosphorylation process, which caused an inhibition in ATP production and change in membrane potential (Terada 1990). A study performed on pulmonary artery smooth muscle cells identified that FCCP could induce changes in mitochondrial membrane potential and inhibit mitochondrial calcium uptake during release from the sarcoplasmic reticulum (Drummond and Tuft 1999a). On the other hand, mitochondrial inhibitors could deteriorate the respiration process and impair membrane potential, which lead to enhance mitochondrial calcium release and then cytosolic calcium increase (Duchen 1999). This suggests that FCCP and antimycin A in combination could lead to a greater increase in intracellular calcium concentration, besides that induced by U46619 alone, and this possibly the reason for seeing the enhancement in U46619 contraction.

Removal of extracellular glucose increases the cell's reliance on mitochondrial oxidative phosphorylation and, therefore, mitochondrial function. Therefore, under these conditions, inhibition of mitochondrial complexes should have greater impact. Therefore, we tested

the inhibition of mitochondrial complex III with antimycin A in the presence and absence of glucose. Antimycin A caused inhibition of the U46619-induced contraction in both the presence and absence of glucose. The size of the U46619-induced contraction was smaller and the antimycin A inhibitory effect was greater in the absence of glucose. Glucose is a vital constituent in any cell, it plays an important role in muscle contraction and regulation of tone (Richter and Hargreaves 2013). After glycolysis, it supplies body cells with ATP as a direct source of energy and supplies the mitochondria with pyruvate as a key for initiating both Krebs cycle and ETC (respiration process) which in turn provides the oxidative phosphorylation process with sources of energy production (Vaishnavi et al. 2010). Therefore, glucose removal disturbs the respiration process, oxidative phosphorylation and leads to a reduction in ATP production, hence reduced contraction. These could be the reasons for observing a higher significant inhibitory effect of antimycin A and small size of contraction in the absence of glucose.

Inhibition of mitochondrial complex III with antimycin A can lead to enhanced production of ROS (Turrens 1997), and the consequences for that could be inhibition of calcium influx and therefore inhibition of contraction. AP39, which is a mitochondrial H_2S donor, can protect cells from increases in mitochondrial ROS production (Gerő et al. 2016). Therefore, we tested whether AP39 could prevent the inhibitory effect of antimycin A on the U46619-induced contraction. Pre-incubation of AP39 in the presence of antimycin A showed a partial reduction in the antimycin A inhibitory effect. This provides further support for the effect of antimycin A on the mitochondria.

3.4.3. Role of AMP kinase in the antimycin A response:

One potential mechanism by which mitochondria could regulate smooth muscle tone is through activation of AMPK. AMPK is considered a sensor of energy because when the ATP: AMP ratio decreases, this leads to AMPK activation (Suter et al. 2006; Gowans et al. 2013). Therefore, the effect of dorsomorphin, an AMPK inhibitor, on the antimycin A response was determined in the presence and absence of calcium. Dorsomorphin attenuated the inhibitory effect of antimycin A in the presence of calcium, while in absence of calcium it enhanced the antimycin A inhibitory effect. These data suggest that antimycin A when inhibiting complex III, disturbs the ETC ending with a reduction in ATP production because there is no more proton gradient (Kim et al. 1999). This reduction in ATP/AMP ratio leads to an increase in AMPK activity (Hardie, Carling, and Carlson 1998), which in turn could induce a relaxation or anti-contractile effect via either activating eNOS pathway(Mori et al. 2017) or via enhanced a phosphorylation of myosin light chain kinase (Horman et al. 2008). Another study performed on H4IIE cells showed that antimycin A at 50-200 nM could induce AMPK activity (Hawley et al. 2002).

In addition, the presence of extracellular calcium means more calcium influx and this increases in calcium concentration induced more elevation in AMPK activity (Kahn et al. 2005). A recent study performed on arteries isolated from hamster and mouse revealed that activation of AMP Kinase caused a reduction of intracellular calcium concentration via stimulation BK_{Ca} channels activity that lead to dilation of vascular smooth muscle cells (Schneider et al. 2015). On the other hand, ROS produced from sources such as mitochondria, xanthine oxidase and NO synthase could play an important role as a signal mediator in non-pathological conditions. It has been found in some previous studies that exogenous ROS could stimulate AMPK activity (Choi et al. 2001; Nagata et al. 2004). In addition, a study performed on rat thoracic aortas identified that stimulation of thromboxane receptors by U46619 significantly induced the production of ROS such as H_2O_2, which in turn caused concentration-dependent increases in AMPK activity, as evidenced by increased phosphorylation of AMPK-Thr172 (Zhang et al. 2008). Therefore, what is happening in the present result is that the AMPK activation by antimycin inhibits calcium influx; therefore inhibiting AMPK prevents this effect.

In the absence of calcium, surprisingly, there was an enhancement of antimycin A inhibitory effect in the presence of dorsomorphin. This unanticipated result could be due to the absence of calcium itself as a key for initiating smooth muscle contraction (Cool et al. 2006). In a study performed on rat aortic VSMCs, the researchers found that blocking the calcium channels with nifedipine and preventing calcium influx enhanced AMPK activity (Sung and Choi 2012). Thus, if antimycin A acts through AMPK to inhibit calcium influx, it would be expected that the inhibitory effect of dorsomorphin would not be seen in the absence of calcium or would still see some inhibitory effect, but the effect may be reduced. This is indeed the case, although the further inhibitory effect of dorsomorphin was unexpected.

3.4.4. Role of Rho kinase and ERK-MAP kinase in antimycin A response:

In the previous chapter, we determined the effect of Rho kinase and ERK-MAP kinase pathways in the simvastatin response. Therefore, as a comparison, we determined whether these pathways play a role in the antimycin A response. Several studies revealed that ROS produced as by-products of metabolism or due to blocking of mitochondrial complexes (Taverne et al. 2013) could enhance Rho A activity, which plays an important role in regulation smooth muscle tone (Heo et al. 2006). In these studies performed in the REF-52 fibroblasts-Rat cell line, the researchers found that inhibition of complex III with antimycin A enhanced the production of superoxide and other ROS and these, in turn, increased Rho A activity via a pathway concerning critical cysteine residues present in a redox-sensitive motif (Aghajanian et al. 2009; Heo et al. 2006). Therefore, we tested whether inhibition of the Rho kinase pathway with Y27632 could prevent the antimycin A

inhibitory effect. The data showed that the inhibitory effect of antimycin A and Y27632 together was larger than that produced by Y27632 alone. This possibly indicates that antimycin A does not rely on the Rho kinase pathway to induce its inhibitory effect but it has a different inhibitory mechanism as the effect of Y27632 and antimycin A were additive.

Rho kinase inhibits myosin phosphatase to induce smooth muscle contraction (Nagumo et al. 2000; Kimura et al. 1996). Therefore, if we hypothesized that antimycin A inhibited Rho kinase activation, then inhibition of myosin phosphatase with calyculin A would prevent the inhibitory effect of antimycin A. Pre-incubation with calyculin A caused inhibition of the relaxant effect of antimycin A, indicating that phosphoprotein phosphatase activity is required for the antimycin A response. However, the data with Y26732 would rule out an effect on Rho kinase. This does not mean that myosin phosphatase is not involved, but it may involve other pathways rather than Rho kinase activity.

ROS produced by antimycin A as a consequence of blocking complex III and inducing a collapse in ETC, could enhance ERK phosphorylation and increase ERK activity (Guyton et al. 1996; Rygiel et al. 2008). Although, this would cause contraction rather than relaxation, this still indicates that mitochondria could regulate ERK activity. Therefore, we determined the effect of combining antimycin A and PD98059, a known inhibitor of MEK, on concentration-response curves to U46619. The inhibitory effect of antimycin A and PD98059 together was larger than that produced by PD98059 alone. This suggests that antimycin A does not rely on the ERK pathway because using of a MEK inhibitor did not prevent the inhibitory effect of antimycin A and rather than that, it caused more inhibition to U46619-induced contraction. As with the Rho kinase inhibitor, the assumption is that PD98059 caused maximum inhibition of ERK activation at the concentration used. Previous studies in the laboratory have used these inhibitors and these concentrations to cause complete inhibition of ERK and Rho kinase activation (Roberts, 2001; Roberts 2004). Furthermore, Davies et al. demonstrated that these compounds produce near complete inhibition of these kinases in enzyme assays (Davies et al., 2000).

In summary, the main finding in this chapter was identifying that the complex III inhibitor antimycin A inhibited contractile responses in the porcine coronary artery. The data suggest that the anti-contractile effects are mediated through inhibition of calcium influx through L-type VGCC as well as inhibition of calcium-independent contractions. The effects of the AMPK inhibitor dorsomorphin indicates that antimycin A activates AMPK, which could lead to the opening of calcium channels. Neither inhibition of complex I with rotenone alone nor the rotenone-myxothiazol combination had an effect on antimycin A inhibitory effect. On the other hand, addition of co-enzyme Q10 or mitoquinol attenuated the inhibitory effect of antimycin A. In addition, uncoupling the mitochondria with FCCP also attenuated the inhibitory effect of antimycin.

The results from this study are different from those obtained with simvastatin in the previous chapter, suggesting that antimycin A and simvastatin act in different ways. This could be evidence that simvastatin does not act through inhibition of complex III Q_i in the mitochondria, or that antimycin A is acting on a different site of complex III. Therefore, in the next chapter, the effect of the complex III Q_o inhibitor myxothiazol on the U46619-induced contraction will be determined.

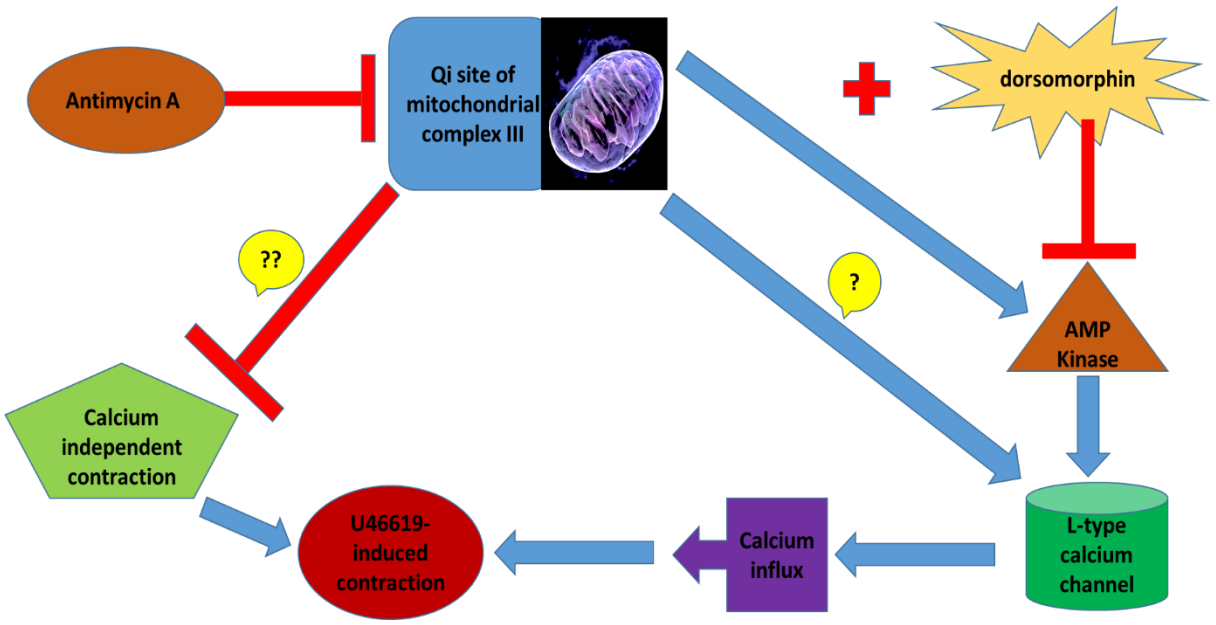

Figure 3.20: Hypothesized schematic diagram of effect of antimycin A effect on U46619-induced contraction in PCA. The present study demonstrated that antimycin A inhibited calcium-independent contraction via an unknown pathway. In addition, antimycin A inhibited calcium-dependent contraction via inhibiting calcium influx via AMPK or via another pathway.

Chapter IV

The effects of myxothiazol on U46619 (thromboxane A2 mimetic) induced contraction in porcine coronary arteries (PCAs)

4.1. Introduction:

The regulation of smooth muscle contraction and relaxation depend on several factors and could involve multiple pathways. The presence of intracellular free calcium and ATP to initiate and supply the contraction with motivating force are examples of the main factors (Barnes 1998). Each contractile agent has a specific mechanism or pathway to induce its effect (Brozovich et al. 2016). The data in chapter 3 indicates that inhibition of complex III inhibited U46619-induced contractions through activation of AMPK and inhibition of calcium influx.

Complex III has two inhibitory sites; Q_i, which is located in the inner membrane and the Q_o, which is oriented toward the intermembrane space (Chen et al. 2003). Blocking of the Q_o site with myxothiazol has many consequences including impairment of respiration process, enhancing superoxide production (ROS), reducing ATP production (Gao, Laude, and Cai 2008; Muller et al. 2003), losing the regulation of calcium homeostasis, and modulation of channels and protein activity (Makowska, Zablocki, and Duszynski 2000). The amount of ROS produced with myxothiazol is much lower than that produced with antimycin A. Blocking of the Q_i site with antimycin A enhances the accumulation of semiquinone at the proximal and distal sites of the Q_o site, which reduces O_2^- radical to produce superoxide. While with myxothiazol, blocking of the Q_o site allows the formation but not oxidation of semiquinone and just at the distal site (Muller et al. 2003). This means that in the presence of myxothiazol there is only the distal site of Q_o available for ROS production while in the presence of antimycin A there are two sites, the proximal and distal sites.

Blocking of complex III with myxothiazol could enhance or reduce ROS production and to date there is controversy about that. A study performed on mouse pulmonary artery smooth muscle cells showed that mitochondrial ROS generated from complex III enhanced intracellular calcium concentration and are involved in the underlying mechanism of hypoxia-induced vasoconstriction. Myxothiazol inhibited this vasoconstriction, indicating that opposes the formation of ROS from complex III (Yadav et al. 2013). Another study revealed that exposure of liver hepatocytes and isolated mitochondria to myxothiazol is associated with increased ROS production (Young, Cunningham, and Bailey 2002). Other studies identified that blocking of the Q_o site of complex III with myxothiazol could enhance ROS production at complex I (Hansford, Hogue, and Mildaziene 1997) and complex II (Quinlan et al. 2012). In a study performed on rat heart and brain mitochondria, the researchers found that myxothiazol could enhance ROS generation depending on the succinate/fumarate ratio. This might be one of the factors that explain different effects of complex inhibitor (myxothiazol) on ROS production each time, in addition to the difference in tissue or cell line used (Starkov and Fiskum 2001).

There are multiple signalling pathways by which myxothiazol could regulate the smooth muscle tone and one of these is AMPK activity. One consequence of blocking complex III with myxothiazol is inhibition of respiration thus reducing ATP production. This reduction in the ATP: AMP ratio could enhance AMPK activity (Gowans et al. 2013). In addition, enhancement of ROS production by myxothiazol effect could increase MAP kinase activity especially ERK1/2 and ERK5 (Wall et al. 2006). Moreover, mitochondrial ROS could regulate smooth muscle tone via inhibitory and modulatory effect on the channels and exchangers such as inhibition of L-Type calcium channel activity (Makowska, Zablocki, and Duszynski 2000).

The previous chapters indicated that simvastatin could have an anti-contractile effect through inhibition of the mitochondrial ETC, possibly at complex III. Antimycin A (blocker of Q_i site) also had an anti-contractile effect, although the mechanism appears to be different from the effect of simvastatin. Therefore, in this chapter, we determined the anti-contractile effect of myxothiazol (blocker of Q_o site), in order to compare the effect of myxothiazol with that of simvastatin and antimycin A.

4.2. Material and Methods:

4.2.1. Tissue Preparation:

4.2.2. Isolated organ bath experiments:

Tissue preparation and isolated organ bath experiments are the same as mentioned in chapter II, page 29.

4.2.3. Effect of myxothiazol on U46619-induced tone:

In order to determine the effect of myxothiazol on U46619-induced tone, tissues were exposed to myxothiazol (10 µM) or vehicle control (0.1% v/v DMSO) for 2 h. After the incubation period, the thromboxane mimetic U46619 was added in a cumulative manner (1-300n M). Contractile responses were expressed as percentage of the response to 60 mM KCl. In some experiments, the Krebs'- Henseleit buffer was replaced with calcium-free Krebs solution in which the calcium was replaced with 2 mM ethylene glycol bis (β amino ethyl ether)-N,N,N,N- tetra acetic acid (EGTA). In other experiments, the Krebs'- Henseleit buffer was replaced with glucose-free Krebs.

4.2.4. Effect of Rho kinase, MEK, phosphatase and L-type calcium channel inhibition on myxothiazol -induced inhibition of thromboxane contraction:

After the KCl responses, tissues were exposed to myxothiazol (10 µM) in the absence or presence of one of the following compounds: Rho kinase inhibitor Y27632 (10 µM), MEK-ERK inhibitor PD98059 (50 µM), L-type calcium channel blocker nifedipine (5 µM). Control tissues received vehicle only (distilled water for Y27632, 0.1% v/v DMSO for the other compounds). Cumulative concentration-response curves to U46619 were then carried out.

In order to determine the effect of myxothiazol on relaxation responses to the phosphoprotein phosphatase inhibitor calyculin or the L-type calcium channel blocker nifedipine, tissues were incubated with a single concentration of myxothiazol (10 µM) for 120 min and then contracted with U46619 to about 40-60% of KCl contraction. This was followed by adding either a single concentration of calyculin (100 nM) or cumulative concentrations of nifedipine (1 nM-3 µM) to induce relaxation.

4.2.5. Effect of FCCP and AMP Kinase inhibitor on the myxothiazol-induced inhibition of thromboxane contraction:

In order to determine whether the inhibition of the U46619-induced contraction by myxothiazol could be prevented by uncoupling the mitochondria, tissues were pre-incubated with myxothiazol (10 µM) in the absence or presence of FCCP (1 µM). Control tissues received vehicle only (0.1% v/v ethanol for FCCP, 0.1% v/v DMSO for myxothiazol). Cumulative concentration-response curves to U46619 were then carried out in the

presence of extracellular calcium. Contractile responses were expressed as a percentage of the response to 60 mM KCl.

Inhibition of the mitochondrial ETC can lead to activation of AMPK. Therefore, in order to determine whether increased activity of AMPK underlies the inhibitory effect of myxothiazol, tissues were pre-incubated with myxothiazol in the absence or presence of dorsomorphin (10 μM). Control tissues received vehicle only (0.1% v/v DMSO). Cumulative concentration-response curves to U46619 were then carried out in the presence of extracellular calcium. Contractile responses were expressed as a percentage of the response to 60 mM KCl.

4.2.6. Effect of mitochondrial stimulants on the myxothiazol-induced inhibition of thromboxane contraction:

In order to determine if the inhibitory effect of myxothiazol could be prevented by supplementation with coenzyme Q10, tissues were exposed to co-enzyme Q10 (5 μM) or mitoquinol (1 μM), a mitochondria-targeted form of co-enzyme Q10. Control tissues received vehicle only (0.1% v/v ethanol for co-enzyme Q10 and 0.1% v/v DMSO for the rest). Cumulative concentration-response curves to U46619 were then carried out in the presence of extracellular calcium. Contractile responses were expressed as a percentage of the response to 60 mM KCl.

Blocking complex III could increase mitochondrial ROS production, which can be prevented by mitochondrial H_2S. Therefore, the effect of the mitochondria-targeted H_2S donor AP39 on the inhibitory effect of myxothiazol was determined. Tissues were exposed to a single concentration of U46619 (30 nM) then tension recorded for up to 120 min. Contractile responses were expressed as a percentage of the response to 60 mM KCl.

4.2.7. Effect of myxothiazol on $CaCl_2$ and Bay K 8644-induced contraction:

In order to determine whether the inhibition of the U46619-induced contraction by myxothiazol requires the presence of extracellular calcium, tissues were pre-incubated with myxothiazol (10 μM) in calcium-free Krebs-Henseleit buffer. Control tissues received vehicle only (0.1% v/v DMSO). After the incubation period, tissues were exposed to a maximum concentration of U46619 (300 nM). $CaCl_2$ was then added cumulatively (10 μM-3 mM) to induce a contraction. Contractile responses were expressed as a percentage of the response to 60 mM KCl. In other experiments and in order to determine and confirm the involvement of L-type VGCC in the inhibitory effect of myxothiazol, tissues were pre-incubated with myxothiazol (10 μM). Control tissues received vehicle only (0.1% v/v DMSO). After the incubation period, the L-type VGCC opener Bay K 8644 was then added cumulatively (1-300 nM). Contractile responses were expressed as a percentage of the response to 60 mM KCl.

4.2.8. Drugs and Chemicals:

U46619, Y27632, PD98059 and Bay K 8644 were purchased from Tocris Bioscience, UK. Antimycin A, myxothiazol, rotenone, dorsomorphin, co-enzyme Q10, FCCP, and nifedipine were purchased from Sigma, UK. Mitoquinol and AP39 were purchased from Cayman Chemical Company, USA. Finally, calyculin A was purchased from Cell Signalling Technology, UK.

Stock solutions of Y27632 were dissolved in distilled water. The stock solution of co-enzyme Q10 was dissolved in ethanol. The stock solutions of U46619 were made to 10mM in ethanol. All further dilutions of the stock solutions were made using distilled water. Furthermore, stock solutions of all remaining chemicals were dissolved in dimethyl sulfoxide (DMSO).

The following modified Krebs-Henseleit buffer solution was used (in mM): NaCl 118, KCl 4.8, $CaCl_2.H_2O$ 1.3, $NaHCO_3$ 25.0, KH_2PO_4 1.2, $MgSO_4.7H_2O$ and glucose 11.1, previously gassed with a mixture of 5% CO_2 and 95% O_2 with pH of approximately 7.5 and used at 37 ^oC. All stocks were kept frozen at -20 ^oC, except for KCl and $CaCl_2$ which were kept at room temperature.

4.2.9. Statistical Analysis:

Data were expressed as mean ± SEM where n = the number of different animals. The concentration-response curves were fitted to a sigmoidal curve with a variable slope using four parameters (Top, bottom, log EC50 and slope) logistic equation using Graph-Pad Prism software. The maximum percentage contraction (R_{max}) and the negative log of concentration required to produce half the response to that ligand (pEC_{50}) were derived from the fitted curves where appropriate. Data were analyzed using 2-tailed, paired (dependent) for one group sample tested twice or unpaired (independent) Student's t-test to compare the means of 2 groups-tested once. Differences between 3 or more groups were assessed using one-way ANOVA or two-way ANOVA in conjunction with the Sidak's post-hoc test or Tukey post-hoc test to assess possible difference at individual concentrations. The P-value <0.05 was considered statistically significant. Statistical analysis was performed by Graph-Pad Prism (Version 7).

4.3. Results:

4.3.1. The effects of myxothiazol on U46619 (thromboxane A2 mimetic) induced contraction in porcine coronary arteries (PCAs):

In order to determine whether myxothiazol inhibited the contractile response to thromboxane receptor activation, the effect of pre-incubation with myxothiazol on U46619-induced contractions was determined in the presence of calcium (Fig4.1) and in the absence of calcium (Fig4.2). In the presence of calcium, control tissues reached an Rmax of 127 ± 12% KCl response with a pEC_{50} value of 7.7± 0.05 (n= 6). Pre-incubation with 10 μM myxothiazol caused a significant inhibitory effect on the contractile response with R_{max} of 79 ± 12% KCl response and pEC_{50} value of 7.3 ± 0.06 (n= 6).

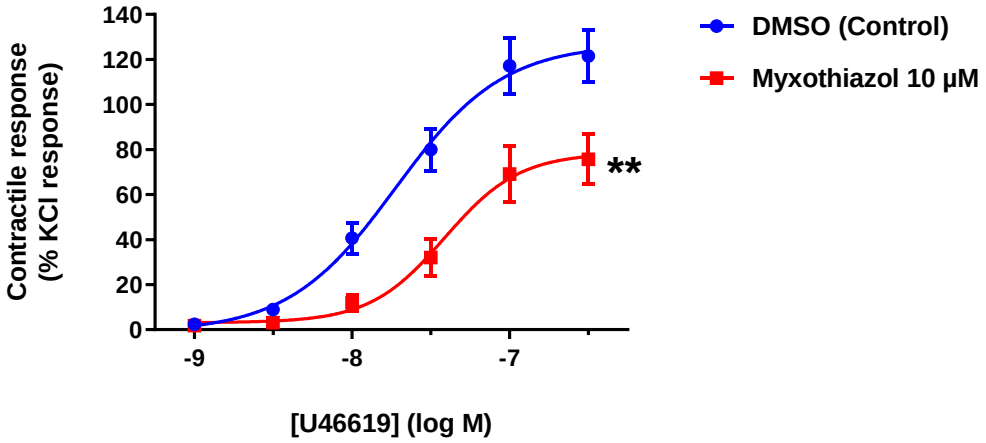

Figure 4.1: Log concentration-response curves for the vasocontraction effects of U46619 with pre-incubation of myxothiazol (10 μM). Control is vehicle only (0.1% v/v DMSO). Data are expressed as a percentage of the contraction to 60 mM KCl and are mean ± SEM of 6 experiments. **p-value< 0.01 v control, Student's 2-tailed paired t-test.

On the other hand, in the absence of calcium, the size of contraction to U46619 was smaller than that in the presence of calcium. Pre-incubation with 10 μM myxothiazol showed no inhibitory effect of U46619 induced contraction (Response at maximum concentration= 12 ± 1%, estimated pEC_{50} = 7.55± 0.2, mean ± SEM, n=6) compared to the control (Response at maximum concentration= 14 ± 2%, estimated pEC_{50} = 7.59 ± 0.1, mean ± SEM, n=6). See figure 4.2.

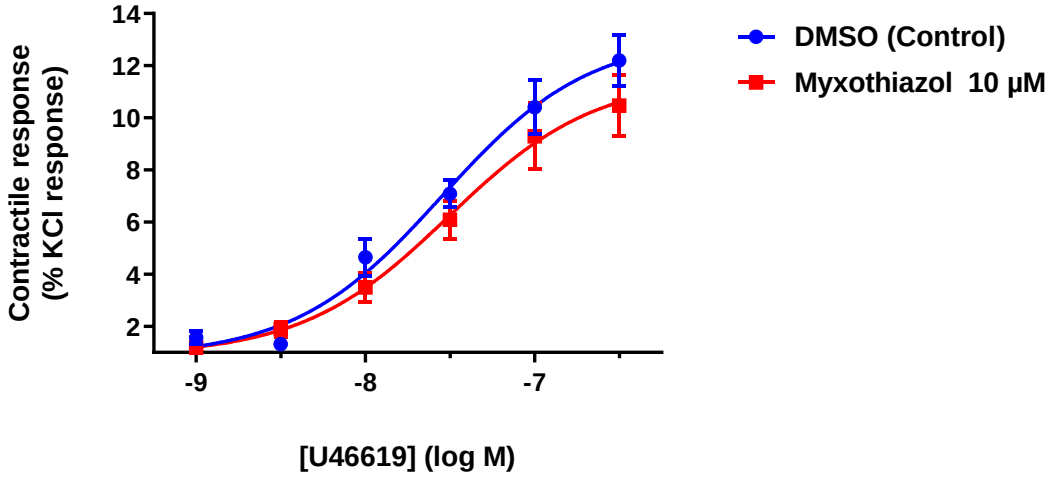

Figure 4.2: Log concentration-response curves for the vasocontraction effects of U46619 with pre-incubation of myxothiazol (10 μM) in the absence of calcium. Control is vehicle only (0.1% v/v DMSO). Data are expressed as a percentage of the contraction to 60 mM KCl and are mean ± SEM of 6 experiments. P-value> 0.05 v control, Student's 2-tailed paired t-test.

4.3.2. Role of AMPK in myxothiazol response:

As inhibition of AMPK prevented the inhibitory effect of antimycin A, we determined whether AMPK is also involved in the anti-contractile effect of myxothiazol. Tissues were exposed to 10 μM myxothaizol in the absence or presence of 10 μM dorsomorphin. Cumulative concentration response curves to U46619 were then carried out (Fig4.3). The control tissues reached a response at maximum concentration to 80± 5% of the KCl response (n= 6). Pre-incubation with 10 μM dorsomorphin had no significant effect on the contractile response to U46619 while pre-incubation with myxothiazol inhibited the U46619 contraction. Pre-incubation of dorsomorphin did not reverse the inhibitory effect of myxothaizol significantly in the presence of myxothiazol. See table 4.1 and figure 4.3.

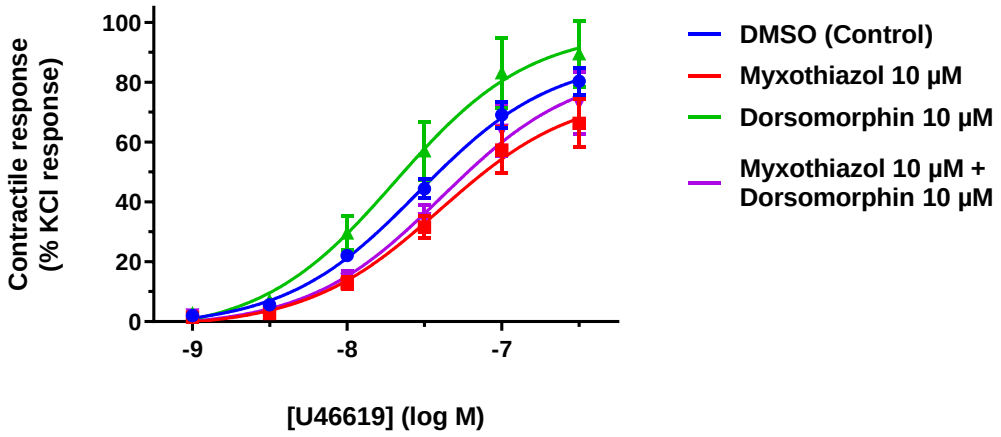

Figure 4.3: Log concentration-response curves for the vasocontraction effects of U46619 with pre-incubation 10 μM dorsomorphin and 10 μM myxothiazol. Control is vehicle only (0.1% v/v DMSO). Data are expressed as a percentage of contraction to 60 mM KCl and are mean ± SEM of 6 experiments. p> 0.05 v control, Two-way ANOVA followed by Tukey post-hoc test.

	Response at 300 nM of U46619 ± SEM
Control	80 ± 5%
myxothiazol	66 ± 8%
Dorsomorphin	90 ± 11%
Dorsomorphin+ myxothiazol	73 ± 11%

Table 4.1: Response at maximum concentration expressed as a percentage of the response to 60 mM KCl for U46619 in the absence (control, which is 0.1% v/v DMSO), or presence of 10 μM myxothiazol and 10 μM dorsomorphin with and without myxothiazol in PCAs. Data are expressed as mean ± SEM of 6 experiments. p>0.05 v control, Two-way ANOVA followed by Tukey post-hoc test.

4.3.3. Effect of Co-enzyme Q10 on myxothiazol response:

In order to determine whether supplementation with co-enzyme Q10 prevents the myxothiazol-induced inhibition of the U46619-induced response, tissues were incubated with 10 μM myxothiazol, in the absence or presence of co-enzyme Q10 (5 μM). The control tissues reached an Rmax of 117 ± 9% of the KCl response with pEC_{50} of 7.9 ± 0.07 (n= 6). Pre-incubation with co-enzyme Q10 alone had no significant effect on the contractile response to U46619, whereas myxothiazol inhibited the contraction to U46619. Pre-incubation of co-enzyme Q10 did not prevent the inhibitory effect of myxothiazol in the presence of myxothiazol. See table 4.2 and figure 4.4.

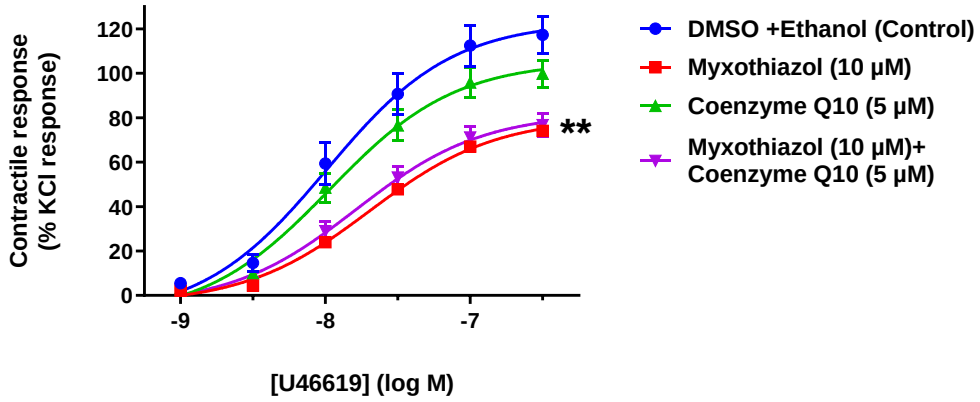

Figure 4.4: Log concentration-response curves for the vasocontraction effects of U46619 with pre-incubation 5 μM co-enzyme Q10 and 10 μM myxothiazol. Control is vehicle only (0.1% v/v DMSO+ Ethanol). Data are expressed as a percentage of the contraction to 60 mM KCl and are mean ± SEM of 6 experiments. **p<0.01 v control, Two-way ANOVA followed by Tukey post-hoc test.

	R_{max} (% KCl response, mean ± SEM)	**pEC50 (mean ± SEM)**
Control	117 ± 9%	7.9 ± 0.07
myxothiazol	74 ± 6%**	7.6 ± 0.04
Co-enzyme Q10	100 ± 6%	7.9 ± 0.07
myxothiazol + Co-enzyme Q10	77 ± 5%	7.7 ± 0.06

Table 4.2: Maximum contraction (R_{max}) expressed as a percentage of the response to 60 mM KCl and log EC_{50} (pEC_{50}) for U46619 in the absence (control, which is 0.1% v/v DMSO+ 0.1% v/v Ethanol), or presence of 10 μM myxothiazol and 5 μM co-enzyme Q10 with and without myxothiazol in PCAs. Data are expressed as mean ± SEM of 6 experiments. **p<0.01 v control, Two-way ANOVA followed by Tukey post-hoc test.

4.3.4. Effect of mitoquinol on myxothiazol response:

In order to determine the effect of mitoquinol on myxothaizol-induced inhibition of the U46619-induced response, tissues were incubated with 10 μM myxothiazol, in the absence or presence of mitoquinol (1 μM). The control tissues reached a response at the maximum concentration used of 107 ± 15% of the KCl response (n= 6). Pre-incubation with mitoquinol alone had no significant effect on the contractile response to U46619, whereas myxothiazol inhibited the contraction to U46619. Pre-incubation of mitoquinol in the presence of myxothiazol, caused no effect to the inhibitory effect of myxothiazol. See table 4.3 and figure 4.5.

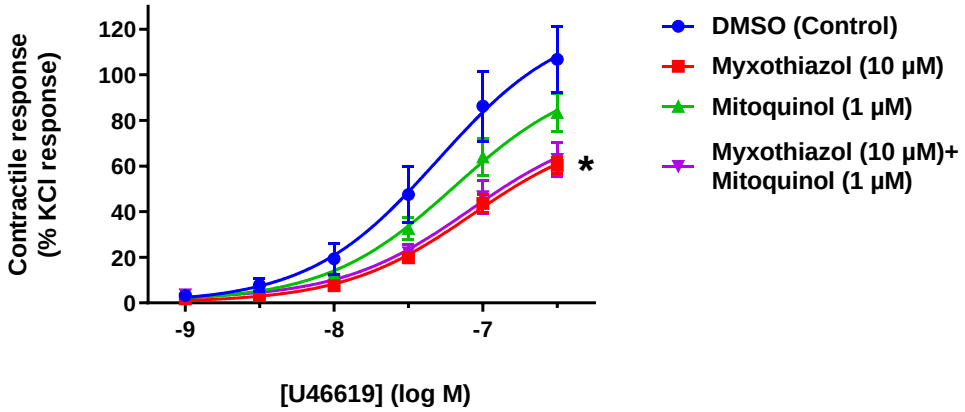

Figure 4.5: Log concentration-response curves for the vasocontraction effects of U46619 with pre-incubation 1 μM mitoquinol and 10 μM myxothiazol. Control is vehicle only (0.1% v/v DMSO). Data are expressed as a percentage of the contraction to 60 mM KCl and are mean ± SEM of 6 experiments. *p<0.05 v control at 300 nM U46619. Two-way ANOVA followed by Tukey post-hoc test.

	Response at 300 nM U46619± SEM
Control	107 ± 15%
myxothiazol	60 ± 4%*
Mitoquinol	83 ± 8%
myxothiazol + Mitoquinol	63 ± 7%*

Table 4.3: Response at maximum concentration expressed as a percentage of the response to 60 mM KCl for U46619 in the absence (control, which is 0.1% v/v DMSO), or presence of 10 μM myxothiazol and 1 μM mitoquinol with and without myxothiazol in PCAs. Data are expressed as mean ± SEM of 6 experiments. *p<0.05 v control at 300 nM U46619, Two-way ANOVA followed by Tukey post-hoc test.

4.3.5. Effect of FCCP on myxothiazol response:

In order to determine whether uncoupling the mitochondria prevents the inhibitory effect of myxothiazol, tissues were incubated with 10 μM myxothiazol, in the absence or presence of FCCP (1 μM). The control tissues reached a response at the maximum concentration used of 86 ± 6% of the KCl response (n= 6). Pre-incubation with FCCP alone had no significant inhibitory effect on the contractile response to U46619, whereas myxothiazol inhibited the contraction to U46619. Pre-incubation of FCCP in the presence of myxothiazol, prevented the inhibitory effect of myxothiazol. See table 4.4 and figure 4.6.

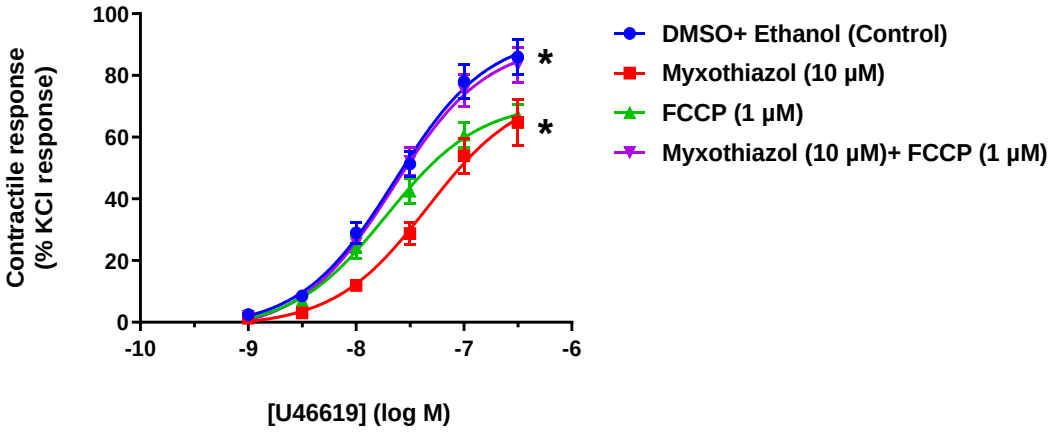

Figure 4.6: Log concentration-response curves for the vasocontraction effects of U46619 with pre-incubation 1 μM FCCP and 10 μM myxothiazol. Control is vehicle only (0.1% v/v DMSO). Data are expressed as a percentage of the contraction to 60 mM KCl and are mean ± SEM of 6 experiments. *p<0.05 v control, *p<0.05 v Myxothiazol+FCCP at 300 nM of U46619, Two-way ANOVA followed by Tukey post-hoc test.

	Response at 300 nM U46619 ± SEM
Control	86 ± 6%
Myxothiazol	65 ± 8%*
FCCP	67 ± 4%
Myxothiazol + FCCP	83 ± 6%*

Table 4.4: Response at maximum concentration expressed as a percentage of the response to 60 mM KCl for U46619 in the absence (control, which is 0.1% v/v DMSO), or presence of 10 μM myxothiazol and 1 μM FCCP with and without myxothiazol in PCAs. Data are expressed as mean ± SEM of 6 experiments. *p<0.05 v control, *p<0.05 v Myxothiazol+FCCP at 300 nM of U46619, Two-way ANOVA followed by Tukey post-hoc test.

4.3.6. Effect of removal of extracellular glucose on myxothiazol response:

In order to determine whether removal of glucose alters the myxothiazol-induced inhibition of the U46619-induced response, tissues were incubated with 10 μM myxothiazol, in the presence or absence of glucose (using glucose-free Krebs). In the presence of glucose, the control tissues reached an R_{max} of 109 ± 9% of the KCl response with pEC_{50} of 7.6 ± 0.06 (n= 6). Pre-incubation with myxothiazol caused inhibition to U46619-induced contraction. In the absence of glucose, the size of contraction was smaller and the R_{max} of control was 65 ± 17%. Myxothiazol caused a large inhibition of the contraction to U46619 in the absence of glucose. See table 4.5 and figure 4.7.

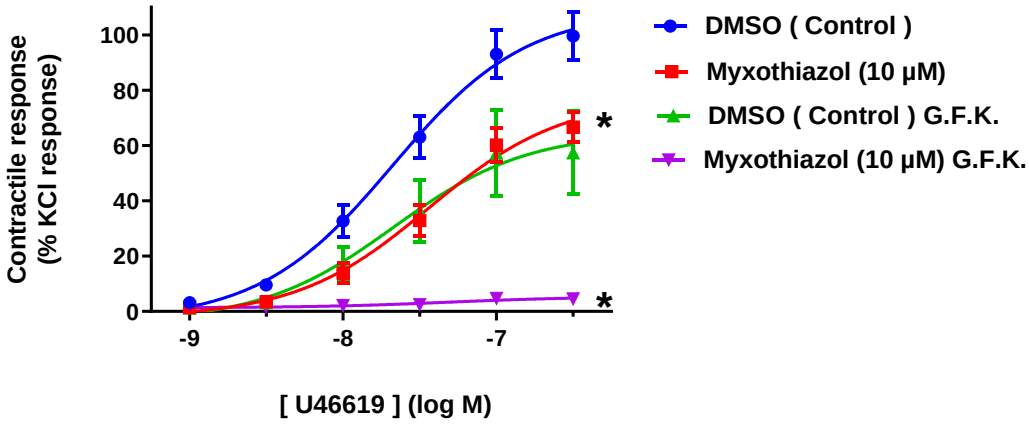

Figure 4.7: Log concentration-response curves for the vasocontraction effects of U46619 with pre-incubation 10 μM myxothiazol in the presence and absence of glucose (G.F.K.). Control is vehicle only (0.1% v/v DMSO). Data are expressed as a percentage of the contraction to 60 mM KCl and are mean ± SEM of 6 experiments. *p<0.05 v his control, Student's 2 tailed paired t-test. .

	R_{max} (% KCl response, mean ± SEM)	**pEC50 (mean ± SEM)**
Control	109 ± 9%	7.6 ± 0.06
Myxothiazol	78 ± 5%*	7.4 ± 0.07
Control-G.F.K.	65 ± 17%	7.5 ± 0.08
Myxothiazol-G.F.K.	6 ± 2%*	7.3 ± 0.13

Table 4.5: Maximum contraction (R_{max}) expressed as a percentage of the response to 60 mM KCl and log EC_{50} (pEC_{50}) for U46619 in the absence (control, which is 0.1% v/v DMSO), or presence of 10 μM myxothiazol with and without glucose in PCAs. Data are expressed as mean ± SEM of 6 experiments. *p<0.05 v his control, Student's 2 tailed paired t-test.

4.3.7. Effect of the mitochondrial H_2S donor AP39 on myxothiazol response:

The inhibitory effect of myxothiazol on the U46619-induced contraction could be due to increases in mitochondrial ROS production. In order to determine whether mitochondrial hydrogen sulphide (H_2S) can prevent the myxothiazol-induced inhibition, tissues were pre-incubated for 120 min with a single concentration of 10 μM myxothiazol and with AP39 (30 μM) for 15 min, prior to exposure to a single sub maximum concentration of U46619 (30 nM). Pre-incubation with AP39 alone had no significant effect on time-dependent contraction profile to U46619, whereas myxothiazol showed a significant inhibition of U46619-induced contraction. Pre-incubation of AP39 did not prevent the inhibitory effect of myxothiazol in the presence of myxothiazol. See figure 4.8.

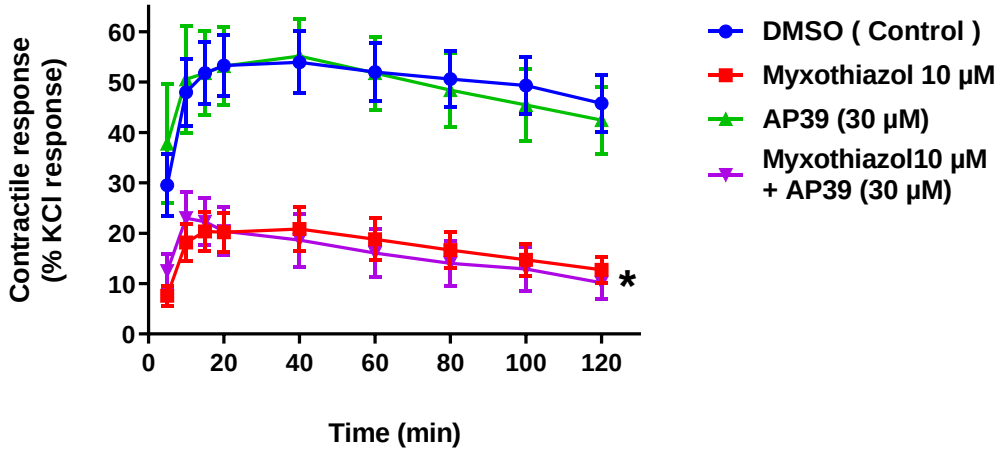

Figure 4.8: Time-response curves for the vasocontraction effects of 30 nM U46619 on PCA pre-incubated with 10 μM myxothiazol and AP39 (30 μM). Control is vehicle only (0.1% v/v DMSO). Data are expressed as a percentage of the contraction to 60 mM KCl at different time points and are mean of 6 experiments. *p<0.05 v control, 2-way ANOVA followed by Tukey post-hoc test.

4.3.8. Effect of Y27632 (Rho Kinase Inhibitor) on myxothiazol response:

In order to determine the combined inhibitory effect of myxothiazol (10 μM) and Y27632 (10 μM) on concentration-response curves to U46619, tissues were pre-incubated with orwithout myxothiazol (10 μM) for 2 h and with Y27632 (10 μM) for 1 h. The inhibitory effect of myxothiazol and Y27632 combined was larger than that produced by Y27632 and DMSO (control). See table 4.6 and figure 4.9.

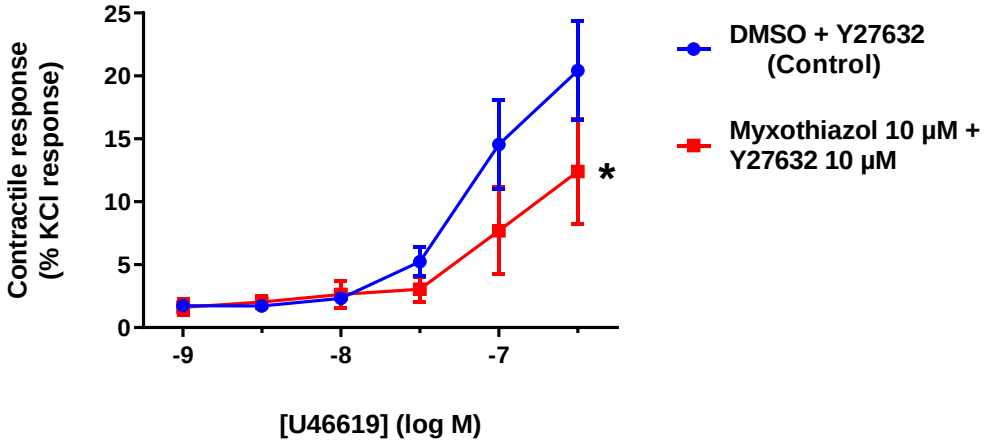

Figure 4.9: Log concentration-response curves for the vasocontraction effects of U46619 with pre-incubation of myxothiazol and Y27632 (10 μM). Control is DMSO+Y27632. Data are expressed as a percentage of the contraction to 60 mM KCl and are mean ± SEM of 6 experiments. *p<0.05 v control at 300 nM of U46619, Student's 2-tailed paired t-test.

	Response at 300 nM U46619 ± SEM
DMSO+Y27632 (Control)	20.4 ± 3.9 %
Myxothiazol+Y27632 (10 μM)	12.4 ± 4.1 % *

Table 4.6: Response at maximum concentration expressed as a percentage of the response to 60 mM KCl for U46619 in the absence (control, which is DMSO+Y27632), or presence of myxothiazol and Y27632 (10 μM) in PCAs. Data are expressed as mean ± SEM of 6 experiments. *p<0.05 v control at 300 nM of U46619, Student's 2-tailed paired t-test.

4.3.9. Effect of PD98059 (MEK Inhibitor) on myxothiazol response:

In order to determine the combined inhibitory effect of myxothiazol (10 μM) and PD98059 (50 μM) on concentration-response curves to U46619, tissues were pre-incubated with and without myxothiazol (10 μM) for 2 h and with PD98059 (50 μM) for 1 h. The inhibitory effect of myxothiazol and PD98059 together was larger than that produced by PD98059 and DMSO (control). See table 4.7 and figure 4.10.

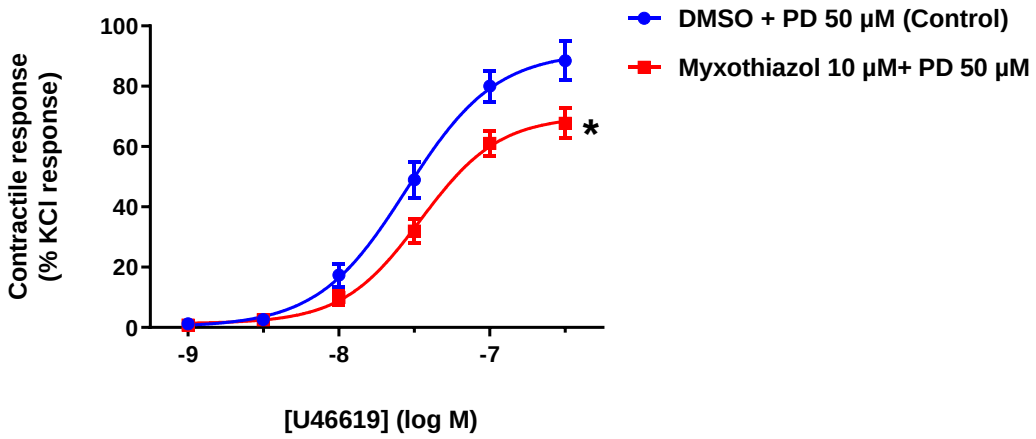

Figure 4.10: Log concentration-response curves for the vasocontraction effects of U46619 with pre-incubation of myxothiazol (10 μM) and PD98059 (50 μM). Control is DMSO+ PD98059. Data are expressed as a percentage of the contraction to 60 mM KCl and are mean ± SEM of 6 experiments. *p<0.05 v control, Student's 2 tailed paired t-test.

	R_{max} (% KCl response, mean ± SEM)	**pEC50 (mean ± SEM)**
DMSO+ PD98059 (Control)	88.4 ± 6.4%	7.5 ± 0.07
Myxothiazol (10 μM)+ PD98059 (50 μM)	67.7 ± 4.9 % *	7.3 ± 0.08

Table 4.7: Maximum contraction (R_{max}) expressed as a percentage of the response to 60 mM KCl and log EC_{50} (pEC_{50}) for U46619 in the absence (control, which is DMSO+ PD98059), or presence of myxothiazol (10 μM) and PD98059 (50 μM) in PCAs. Data are expressed as mean ± SEM of 6 experiments. *p<0.05 v control, Student's 2 tailed paired t-test.

4.3.10. Effect of calyculin A (phosphoprotein phosphatase inhibitor) on myxothiazol response:

Rho kinase inhibits myosin phosphatase. Therefore, we hypothesised that, if myxothiazol inhibited Rho kinase activation, inhibition of myosin phosphatase would prevent the inhibitory effect of myxothiazol. Therefore, the effect of pre-incubation with 100 nM calyculin A on myxothiazol relaxations was determined. Myxothiazol caused a time-dependent relaxation of the U46619-induced contraction. Calyculin A caused inhibition of the relaxant effect of myxothiazol on pre-contracted PCA through almost of the 2 h comparing to the control (n=8). See figure 4.11.

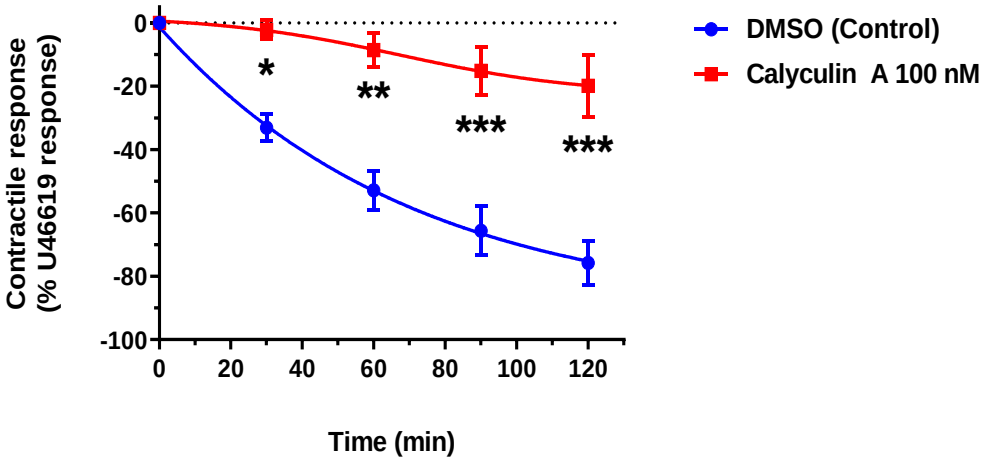

Figure 4.11: Effect of calyculin A (100 nM) on myxothiazol relaxation in porcine coronary artery pre-contracted with U46619. Control is vehicle only (0.1% v/v DMSO). Data are expressed as a percentage of relaxation to U46619-induced contraction and are mean of 8 experiments. *p<0.05 v control, **p<0.01 v control, ***p<0.001 v control, Tow-way ANOVA followed by Sidak post-hoc test.

4.3.11. The role of calcium in myxothiazol response in PCAs:

In order to determine whether extracellular calcium is involved in the myxothiazol-induced inhibition of the U46619-induced response, tissues were incubated with or without 10 μM myxothiazol in calcium-free buffer. After the incubation period, tissues were exposed to a maximum concentration of U46619 (300 nM). $CaCl_2$ was then added cumulatively (10 μM-3 mM) to induce a contraction. Response at maximum concentration for control tissues reached to 58 ± 10% of the KCl response (n= 9). Pre-incubation with myxothiazol inhibited the contraction of $CaCl_2$ with response at maximum concentration 39 ± 9%. See figure 4.12.

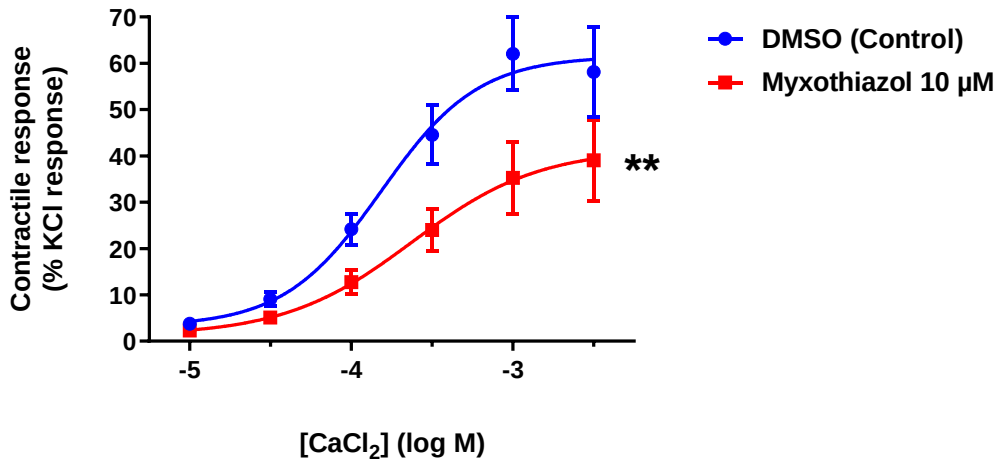

Figure 4.12: Log concentration-response curves for the vasocontraction effects of $CaCl_2$ with pre-incubation of myxothiazol (10 μM). Control is vehicle only (0.1% v/v DMSO). Data are expressed as a percentage of the contraction to 60 mM KCl and are mean ± SEM of 6 experiments. **p<0.01 v control at 3mM $CaCl_2$, Student's 2 tailed paired t-test.

4.3.12. Effect of L-type VGCC blocker on myxothiazol response:

In order to determine which calcium channel is involved in the myxothiazol-induced inhibition of the U46619-induced response, tissues were incubated with 10 μM myxothiazol, in the absence or presence of the L-type VGCC blocker, nifedipine (5 μM). The response at the maximum concentration for the control tissues reached to 105 ± 15% of the KCl response (n= 6). Pre-incubation with nifedipine caused significant inhibitory effect on the U46619-induced contraction. There was no difference in the size of the inhibition with the combination of nifedipine and myxothiazol, compared to nifedipine alone. See table 4.8 and figure 4.13.

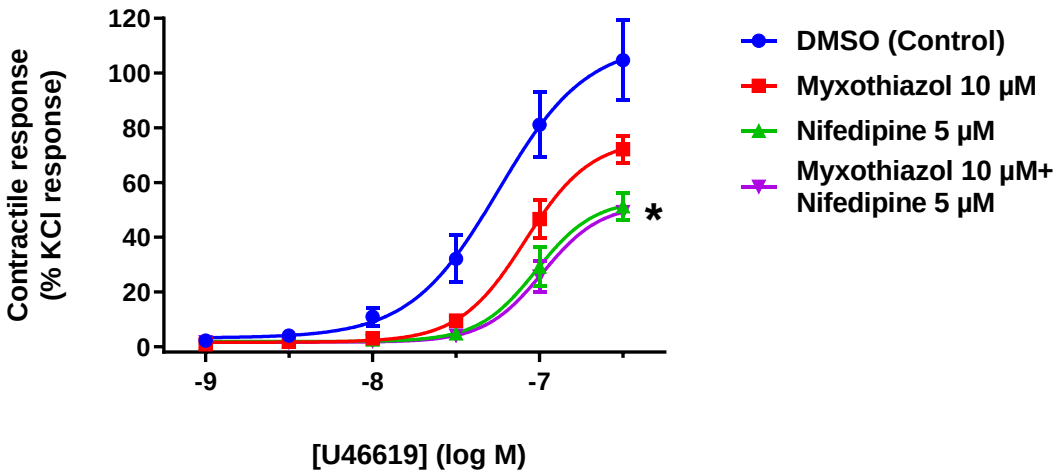

Figure 4.13: Log concentration-response curves for the vasocontraction effects of U46619 with pre-incubation 5 μM nifedipine and 10 μM myxothiazol. Control is vehicle only (0.1% v/v DMSO). Data are expressed as a percentage of the contraction to 60 mM KCl and are mean ± SEM of 6 experiments. *p<0.05 v control at 300 nM of U46619, Two-way ANOVA followed by Tukey post-hoc test.

	Response at 300 nM U46619 ± SEM
Control	105 ± 15%
Myxothiazol	72 ± 5%
Nifedipine	51 ± 5%*
Myxothiazol + Nifedipine	49 ± 2%*

Table 4.8: Response at maximum concentration ± expressed as a percentage of the response to 60 mM KCl for U46619 in the absence (control, which is 0.1% v/v DMSO), or presence of 10 μM myxothiazol and 10 μM nifedipine with and without myxothiazol in PCAs. Data are expressed as mean ± SEM of 6 experiments. *p<0.05 v control at 300 nM of U46619, Two-way ANOVA followed by Tukey post-hoc test.

4.3.13. Effect of L-type VGCC blocker on myxothiazol-rotenone combination response:

In order to determine the effect of myxothiazol-rotenone combination on U46619-induced contraction and to clarify which calcium channel could involve in myxothiazol-rotenone response, tissues were incubated with a combination 10 μM myxothiazol-rotenone, in the absence or presence of VGCC blocker, nifedipine (5 μM). Response at maximum concentration of the control tissue reached to 77 ± 6% of the KCl response (n= 6). Pre-incubation with nifedipine alone caused significant inhibitory effect to U46619-induced contraction, while the myxothiazol-rotenone combination caused no significant inhibition. Pre-incubation with nifedipine in the presence of myxothiazol-rotenone combination caused no further effect compared to nifedipine alone. See table 4.9 and figure 4.14.

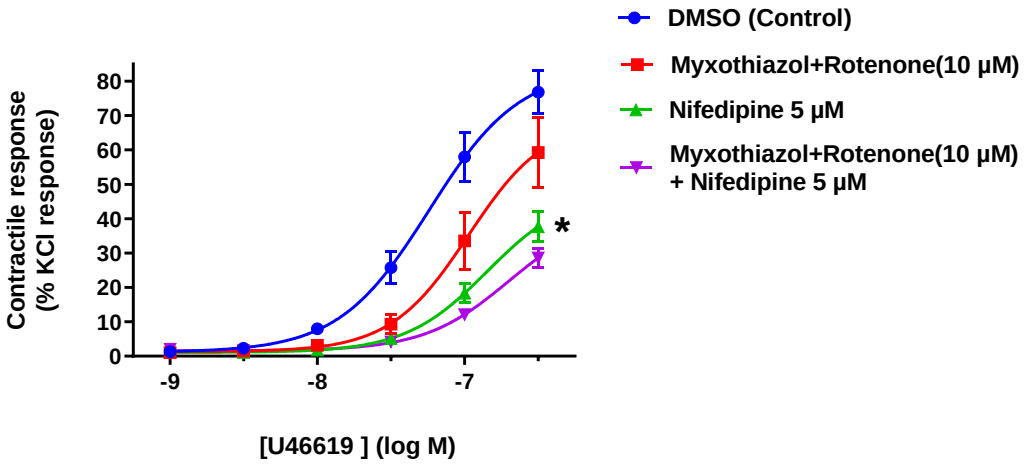

Figure 4.14: Log concentration-response curves for the vasocontraction effects of U46619 with pre-incubation 5 μM nifedipine and 10 μM myxothiazol. Control is vehicle only (0.1% v/v DMSO). Data are expressed as a percentage of the contraction to 60 mM KCl and are mean ± SEM of 6 experiments. *p<0.05 v control at 300 nM of U46619, Two-way ANOVA followed by Tukey post-hoc test.

	Response at 300 nM U46619 ± SEM
Control	77 ± 6%
Myxothiazol-Rotenone	59 ± 10%
Nifedipine	38 ± 4%*
Myxothiazol-Rotenone + Nifedipine	29 ± 3%

Table 4.9: Response at maximum concentration expressed as a percentage of the response to 60 mM KCl for U46619 in the absence (control, which is 0.1% v/v DMSO), or presence of 10 μM myxothiazol and 10 μM nifedipine with and without myxothiazol in PCAs. Data are expressed as mean ± SEM of 6 experiments. *p<0.05 v control, Two-way ANOVA followed by Tukey post-hoc test.

4.3.14. The effect of myxothiazol on relaxation to nifedipine:

As there was an apparent effect of myxothiazol on the $CaCl_2$-induced concentration response curve and to confirm which calcium channel could be involved, tissues were incubated with or without 10 μM myxothiazol then pre-contracted with 30 nM of U46619 and followed by adding nifedipine (1 nM-30 μM) to induce relaxation. Pre-incubation with 10 μM myxothiazol caused a slight inhibition of the relaxant effect of nifedipine. See figure 4.15.

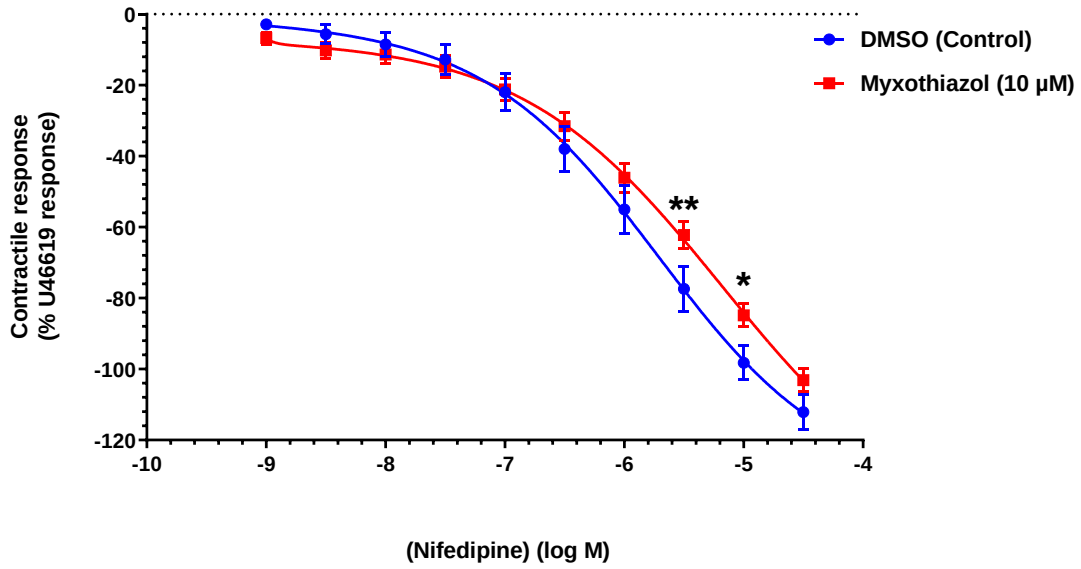

Figure 4.15: Effect of myxothiazol (10 μM) on nifedipine-relaxation response curve on PCA pre-contracted with U46619. Control is vehicle only (0.1% v/v DMSO). Data are expressed as a percentage of relaxation to 30 nM U46619-induced contraction and are mean of 6 experiments. Non-significant indicates P>0.05, *P< 0.05 and **P< 0.01 v control, 2-way ANOVA followed by Sidak post-hoc test.

4.3.15. The effect of myxothiazol on (±)-Bay K 8644 (L-type VGCC activator) induced contraction in porcine coronary arteries:

In order to determine whether myxothiazol inhibited the contractile response to L-type VGCC activator to explore more about the role of calcium, the effect of pre-incubation with myxothiazol on (±)-Bay K 8644-induced contractions was determined. Control tissues reached a response at maximum concentration used of 69 ± 12% of the KCl response (n= 6). Pre-incubation with (10 μM) myxothiazol caused a significant inhibitory effect on the contractile response with a response at maximum concentration of 30 ± 10% of the KCl response. See figure 4.16.

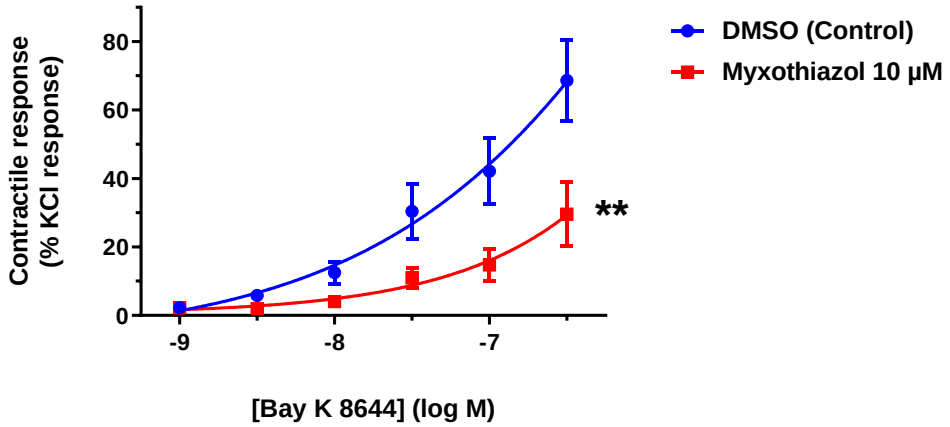

Figure 4.16: Log concentration-response curves for the vasocontraction effects of (±) BAY K 8644 with pre-incubation of myxothiazol (10 μM). Control is vehicle only (0.1% v/v DMSO). Data are expressed as a percentage of the contraction to 60 mM KCl and are mean ± SEM of 6 experiments. **P-value< 0.01 v control at 300 nM of Bay K 8644, Student's paired t-test.

4.4. Discussion:

The aim of the experiments in this chapter was to determine the effect of myxothiazol (mitochondrial complex III inhibitor) on U46619-induced contraction then to determine the mechanism underlying the anti-contractile effect. The data indicate that myxothiazol caused inhibition of calcium-induced contractions.

4.4.1. Role of extracellular calcium in the myxothiazol response:

The data in this present study has identified the possibility of simvastatin acting through inhibition of mitochondrial complexes but not through inhibition of complex III at site Q_i. Therefore, we tested the effects of myxothiazol, a known complex III inhibitor at the Q_o site (Chen et al. 2003) on the U46619-induced contractions and determined the possible pathway for its effect, as a comparison with simvastatin. In the presence of calcium, pre-incubation with 10 μM myxothiazol caused a significant inhibitory effect on the contractile response while in the absence of calcium, myxothiazol showed no inhibitory effect of U46619 induced contraction. These data suggest that myxothiazol induces its inhibitory effect via inhibition the influx of extracellular calcium, as calcium has a key role in the initiation of contraction. In the absence of extracellular calcium, U46619-induces contraction via calcium-independent contractions, such as activation of Rho kinase. A study performed on Jurkat cells showed that blocking of complex III with myxothiazol caused inhibition of respiration process, a collapse in mitochondrial membrane potential and inhibition of the activation of plasma membrane calcium channels, which prevented calcium influx. Furthermore, the study identified that when the same cells were suspended in calcium-free medium, myxothiazol showed no effect on the intracellular calcium concentration (Makowska, Zablocki, and Duszynski 2000). Taken together, these data suggest that blocking complex III at the Q_o site with myxothiazol could induce its anti-contractile effect via inhibition of calcium influx. To confirm this result and to clarify more about the role of calcium, the effect of myxothiazol on $CaCl_2$-induced contraction was determined in the presence of U46619. Pre-incubation with myxothiazol inhibited the contraction to $CaCl_2$, which confirmed the role of extracellular calcium. The influx of calcium through L-type VGCC is the main entry site for calcium induce a contraction in smooth muscle cells (Ghosh et al. 2017). In order to determine whether myxothiazol prevents influx through L-type VGCC, experiments were carried out showing that pre-incubation with myxothiazol caused a significant inhibition of the Bay K 8644 induced contraction in PCA.

To clarify further that myxothiazol is acting through L-type VGCC, the calcium channels were blocked with nifedipine in the absence or presence of myxothiazol. As expected, nifedipine inhibited the U46619-induced contraction. The combination of myxothiazol and

nifedipine had no further effect on the U46619-induced contraction compared to nifedipine alone, indicating that, when L-type calcium channels are blocked, myxothiazol has no effect. Therefore, myxothiazol is likely to be acting through inhibition of L-type calcium channels. In order to determine whether myxothiazol could be binding to the dihydropyridine binding site on L-type calcium channels, concentration-response curves to nifedipine were carried out in the absence or presence of myxothiazol. Although there was a slight inhibition of the relaxant effect of nifedipine, this was not enough to suggest that myxothiazol might be competing with nifedipine for binding.

Previous studies identified that complex I and complex III are the major sites for producing mitochondrial ROS due to incomplete reduction of oxygen molecules (Duchen 1999); blocking of complex I with rotenone and complex III with myxothiazol enhance the production of ROS (Raha et al. 2000; Young, Cunningham, and Bailey 2002; Muller et al. 2003; Li et al. 2003). A review of literatuer showed that ROS could play an important role as a mediator to regulate SMC tone as in pulmonary artery vasoconstriction and cerebral artery vasodilation (Clempus and Griendling 2006). A reduction in ROS production could inhibit redox-sensitive K^+ channels, which regulate pulmonary artery smooth muscle tone. This, in turn, enhances the influx of calcium via L-type VGCC and induces smooth muscle contraction (Moudgil, Michelakis, and Archer 2005). In a study performed on the cerebral artery, it was found that mitochondrial ROS caused a sequential activation of ryanodine-sensitive calcium channels in sarcoplasmic reticulum, activating large conductance calcium-activated potassium channels (BKCa) on the plasma membrane and then inducing smooth muscle vasodilation (Xi, Cheranov, and Jaggar 2005).

These data and supporting evidence indicate that myxothiazol inhibits or modulate the activity of L-type calcium channel, probably through its effects on complex III.

4.4.2. Role of mitochondria in the myxothiazol response:

To clarify the signalling pathway for the inhibitory effect of myxothiazol on U46619-induced contractions, we determined whether supplementation with co-enzyme Q10 or adding mitoquinol could prevent the inhibitory effect. Pre-incubation of co-enzyme Q10 or mitoquinol did not prevent the inhibitory effect of myxothiazol. Although co-enzyme Q10 or mitoquinol (reduced form of coenzyme Q10) have an important role in regulation and maintaining of oxidative phosphorylation processes and ATP production (Lenaz, Daves, and Kfolkers 1968; Ogasahara et al. 1989), there is no evidence that they can prevent the anti-contractile effect of myxothiazol. The usual function of co-enzyme Q10 (reduced and oxidized forms) is to transfer electrons coming from NADH (complex I) and $FADH_2$ (complex II) to cytochrom *b* in the complex III then to the final electron acceptor which is cytochrome *c* (Dallner and Sindelar 2000; Moudgil, Michelakis, and Archer 2005). One possible

explanation is that the concentrations of co-enzyme Q10 and mitoquinol used were not sufficient to reverse the inhibitory effect on the mitochondria. However, the same concentrations prevented the effects of antimycin A (chapter 3).

Another possible explanation is that co-enzyme Q10 and mitoquinol were prevented from binding to Q_o, as the site was completely blocked with myxothiazol. Thus, this prevented the transfer of electron to the Rieske iron sulfur center at cytochrome b, which is required for oxidizing ubiquinol to the ubisemiquinone radical. Another study performed on heart mitochondria from aogMclk1 KO mice showed that co-enzyme Q10 defeciency caused a reduction in ROS production when assessed in the presence of rotenone (complex I inhibitor) and antimycin A (complex III inhibitor) but not with myxothiazol (Wang, Oxer, and Hekimi 2015). This indicates that co-enzyme Q10 can reverse the effects on inhibition of the Qi site, but not in the case of blocking the Q_o site.

To further confirm that myxothiazol's anti-contractile effect is mediated through the mitochondria, tissues were pre-incubated with FCCP to uncouple the mitochondria. FCCP prevented the inhibitory effect of myxothiazol. This supports the idea that the inhibitory effect of myxothiazol on the U46619-induced contraction is mediated through its effects on the mitochondria.

Similarly, removal of extracellular glucose increases the cell's reliance on mitochondrial oxidative phosphorylation and, therefore, mitochondrial function. Thus, inhibition of mitochondrial complexes should lead to a greater effect. Therefore, we tested the inhibition of mitochondrial complex III with myxothiazol in the presence and absence of glucose. Myxothiazol caused inhibition of the U46619-induced contraction in the presence and absence of glucose. The size of contraction was smaller and the myxothiazol inhibitory effect was greater in the absence of glucose. Glucose is an energetic constituent in any cell, it participates and regulates many cell s activity including muscle contraction and regulation of tone (Richter and Hargreaves 2013). As glucose in the body undergoes glycolysis it produces ATP as direct source of energy to the cells. For mitochondria, it provides other products which are needed for the respiration process, such as NADH, which feeds into complex I and FADH2, which provid electrons to complex II. Both are energy-rich molecules as each contains a pair of electrons having a high motive force. Complex I and II both are parts of electron transport chain that provide phosphorylation process with required electrons and sources for producing mitochondrial ATP (Brown, Lakin-Thomas, and Brand 1990; Vaishnavi et al. 2010). On the other hand, ATP is a vital requirment in smooth muscle contraction since it provides the required energy for sliding myosin and actin filaments over each other to initiate the contraction (Aguilar and Mitchell 2010). Accordingly, glucose removal disturbed the respiration process, oxidative phosphorylation and reduced ATP production, hence reduced contraction. These could be the reasons for

observing a higher inhibitory effect of myxothiazol and small size of contraction in absence of glucose.

Blocking of the Q_o site of mitochondrial complex III with myxothiazol can lead to enhanced production of ROS (Muller et al. 2003) and the consequences for that could be inhibition of calcium influx and therefore inhibition of smooth muscle contraction (Makowska, Zablocki, and Duszynski 2000). AP39, which is a mitochondrial H_2S donor, can protect cells from increases in mitochondrial ROS production (Gerő et al. 2016). Therefore, we tested whether AP39 could prevent the inhibitory effect of myxothiazol on the U46619-induced contraction. Pre-incubation of AP39 in the presence of myxothiazol showed no effect on the myxothiazol inhibitory effect. This indicates that H_2S can not reverse the myxothiazol effect and this could be due to feeding of electrons at different site on electron transport chain. In a study performed on isolated mitochondria from human colon adenocarcinoma cell lines, the researchers identified that H_2S feeds the mitochondrial respiratory chain with electrons between complex I and III and co-enzyme Q10 is the intermediate and the acceptor of these electrons to transfer them to complex III then to complex IV, until the oxidative-phosphorlation process is completed succefully (Goubern et al. 2007). As mentioned before in this chapter, co-enzyme Q10 failed to antagonize the myxothiazol inhibitory effect. Therefore, it is possible that increasing mitochondrial H_2S with AP39 cannot reverse the inhibition of Q_o with myxothiazol. The effects of AP39 on inhibition of mitochondrial complexes is untested. Therefore, the next chapter will determine the effects of AP39 on the changes in mitochondrial membrane potential in the presence of mitochondrial complex inhibitors.

4.4.3. Role of AMP kinase in the myxothiazol response:

Mitochondrial activation of AMPK is another mechanism by which the mitochondria could regulate smooth muscle tone. AMPK is considered a regulator of cellular energy homeostasis. When the ATP: AMP ratio decreases, this leads to activation of AMPK (Suter et al. 2006; Gowans et al. 2013). In the previous chapter, inhibition of AMPK prevented the anti-contractile effects of antimycin A. Therefore, the effect of dorsomorphin, an AMPK inhibitor, on the myxothiazol response was determined. Dorsomorphin could not attenuate the inhibitory effect of myxothiazol indicating that, unlike antimycin A, AMPK is not involved in the myxothiazol response. Interestingly, dorsomorphin alone enhanced the contraction induced by U46619. A study performed on vascular smooth muscle cells (VSMCs) showed that activation of the TP receptor with U46619 enhanced the ROS production, which in turn enhanced AMPK activity (Zhang et al. 2008). Therefore, it is possible that activation of AMPK after TP receptor activation limits the contractile response. On inhibiting AMPK, the contraction is thus enhanced. It is beyond the scope of this thesis to investigate this further. The lack of effect of inhibition of AMPK is similar to that seen with simvastatin

(chapter 2), but different from that seen with antimycin A, which supports our hypothesis that simvastatin and myxothiazol could have the same pathway.

4.4.4. Role of Rho kinase and ERK-MAP kinase in myxothiazol response:

In the previous chapters, we determined the effect of Rho kinase and ERK-MAP kinase pathways in the simvastatin and antimycin A response. Therefore, as a comparison, we determined whether these pathways play a role in the myxothiazol response. Previous studies have shown that blocking of mitochondrial complexes enhances the production of ROS (Chen et al. 2003), which could enhance Rho-A activity that plays a vital role in regulation of smooth muscle tone (Fukata, Amano, and Kaibuchi 2001). A study performed on rat pulmonary artery showed that U46619 enhanced ROS production in the cytosol and using myxothiazol could not prevent this production. ROS in turn enhanced the translocation of Rho A from cytosol to the cell membrane (MacKay et al. 2017), which is a required step for activating Rho kinase (Mori and Tsushima 2004). Studies clarified that activated Rho kinase could induce smooth muscle contraction via activating Ca^{2+} sensitization and inhibiting myosin light chain phosphatase (Somlyo and Somlyo 2003; Dimopoulos et al. 2007). Therefore, we tested whether inhibition of the Rho kinase pathway with Y27632 could prevent myxothiazol inhibitory effect. The data showed that the inhibitory effect of myxothiazol and Y27632 together was larger than that produced by Y27632 alone. This possibly indicates that myxothiazol does not rely on Rho kinase pathway to induce its inhibitory effect but it has a different inhibitory mechanism as the effect of Y27632 and myxothiazol were additive.

To induce smooth muscle contraction via activation of Rho kinase involves inhibition of myosin phosphatase (Kitazawa et al. 2003). Thus, if we hypothesized that if myxothiazol inhibited Rho kinase activation, then inhibition of myosin phosphatase with calyculin A would prevent the inhibitory effect of myxothiazol. Pre-incubation with calyculin A caused inhibition of the relaxant effect of myxothiazol, indicating that phosphatase activity is required for the myxothiazol response. However, the data with Y26732 would rule out an effect on Rho kinase. This does not mean that myosin phosphatase is not involved, but it may involve other pathways rather than Rho kinase activity. In other words, the calyculin A inhibitory effect looks to be non-specific as the present study showed the same results with simvastatin (chapter 2) and antimycin A (chapter 3).

ERK1/2 are MAP kinases that play an important role in cell signalling, intracellular processes and targeting the mitochondria. Studies showed that MAP kinases could directly interact with the mitochondria outer membrane then translocate to inside (Kharbanda et al. 2000; Ballard-Croft et al. 2005). Other studies showed that MAP kinases could indirectly regulate some mitochondrial function such as cell survival and death, proliferation and

smooth muscle tone via their effect on Ca^{2+} and ROS signalling (Bogoyevitch et al. 2000; Wall et al. 2006). A study performed on trout hepatocytes showed that activation of ERK1/2 was involved in copper-induced ROS generation, mitochondrial ATP production and intracellular Ca^{2+} for modulating activity (Nawaz et al. 2006). Recent study revealed that there is a crosslink between mitochondrial ROS and non-mitochondrial ROS production and activation of ERK1/2, although, the mechanism is not clear (Javadov, Jang, and Agostini 2014). Mitochondrial complex III is one of the sites that is responsible for producing ROS and blocking of Q_o site of this complex with myxothiazol enhance ROS production, which could inhibit respiration process and reduced ATP production. Accordingly, we determined the effect of combining myxothiazol and PD98059, a known inhibitor of MEK, on concentration-response curves to U46619. Myxothiazol still inhibited the U46619-induced contraction in the presence of PD98059 indicating that myxothiazol is likely to be acting through a pathway that does not involve ERK. As with the Rho kinase inhibitor, the assumption is that PD98059 caused maximum inhibition of ERK activation at the used concentration.

In summary, the main finding in this chapter was identifying that the complex III inhibitor myxothiazol inhibits contractile responses in the porcine coronary artery and only in the presence of calcium. The data suggest that the anti-contractile effects are mediated through inhibition of calcium influx through L-type calcium channels. The effects of the AMP kinase inhibitor dorsomorphin indicates that, unlike antimycin A, myxothiazol does not activate AMP kinase. Neither inhibition of Rho kinase nor inhibition of ERK activity had an effect on the myxothiazol inhibitory effect. Similarly, addition of co-enzyme Q10 or mitoquinol did not attenuate the inhibitory effect of myxothiazol. On the other hand, uncoupling the mitochondria through addition FCCP attenuated the inhibitory effect of myxothiazol. These data suggest that inhibition of complex III at the Qo site leads to inhibition of calcium influx through L-type calcium channels.

Some of the results from this study are different from those obtained in the presence of antimycin A in the previous chapter (chapter3) but they are similar to simvastatin, suggesting that myxothiazol and simvastatin might act in a similar way. This could be evidence that simvastatin acts through inhibition of complex III Q_o in the mitochondria. Therefore, in the next chapter, the effect of simvastatin on isolated mitochondria will be compared with, rotenone, antimycin A, myxothiazol, co-enzyme Q10 and mitoquinol.

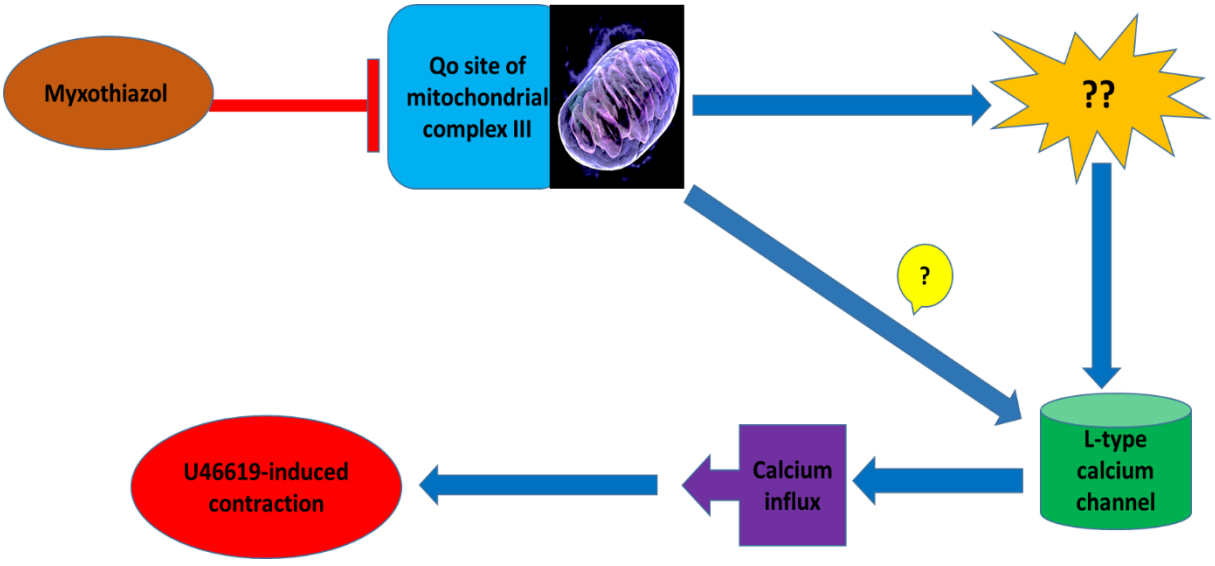

Figure 4.17: Hypothesized schematic diagram of effect of myxothiazol on U46619-induced contraction in PCA. The present study demonstrated that myxothiazol inhibited calcium-dependent contraction via inhibiting calcium influx either via inhibiting L-type calcium channel directly or via another pathway.

Chapter V

Effect of simvastatin, mitochondrial complex inhibitors and mitochondrial stimulants on isolated mitochondria

5.1. Introduction:

Mitochondria are the site of energy production that is used by different cellular process inside the body of human and animals (Piomboni et al. 2012). Mitochondria have many other jobs such as calcium uptake and maintenance of calcium homeostasis, regulation muscle tone, regulation of cell proliferation and death (Lee and Peng 2008). There is evidence that impairment of mitochondrial function is associated with serious diseases/disorders (Vafai and Mootha 2012). An example is the epilepsy associated with mitochondrial dysfunction in neurological tissue (Zsurka and Kunz 2010) as well as neurodegenerative disorders and ageing in which mitochondrial dysfunction is implicated (Ekstrand et al. 2007). In addition, it has been found that diabetes mellitus type 2 is associated with mitochondrial dysfunction in skeletal muscle and liver (Szendroedi et al. 2007). Furthermore, mitochondrial dysfunction has been associated with cardiac diseases such as heart failure, atherosclerosis, ischaemia and hypertension (Siasos et al. 2018). Therefore, it is important to study mitochondrial function directly to understand the molecular changes in cellular metabolism that lead to many diseases or disorders. Using isolated mitochondria rather than intact tissue or cells could be more insightful as isolation of intact mitochondria offers the ability to analyse either whole organelle or protein fraction levels more deeply and precisely (Lampl et al. 2015).

Oxidative phosphorylation is an important mitochondrial process responsible for ATP production (Covian and Balaban 2012). The mitochondrial membrane potential (Ψ_M), which represents a proton motive force that is regulated by complexes I, III and IV, is an important component in the oxidative phosphorylation process. This proton gradient is required for aerobic energy production and is essential for various processes inside and outside the mitochondria (Gerencser et al. 2012). Several studies have determined that release of ROS, which are produced by mitochondrial complexes and play an important role in the regulation of vascular tone, could be doubled in well-polarized Ψ_M (Michelakis et al. 2002; Starkov and Fiskum 2003).

Previous studies identified that there are many cationic dyes used to measure changes in mitochondrial membrane potential ($\Delta\Psi_M$) and one of them is rhodamine 123 (Rh123) (Chen 1988; Smith 1990; Dykens and Stout 2001). These dyes have an ability to distribute electrophoretically into the mitochondrial matrix and across the inner membrane. Their charge and solubility in aqueous space of matrix and lipid space of inner mitochondrial membrane enable these dyes to accumulate in mitochondria (Rottenberg 1984; Jackson and Nicholls 1986). Rh123 dye could be used to measure $\Delta\Psi_M$ either by microscope stain (Johnson, Walsh, and Chen 1980) or by cytofluorometry (Johnson et al. 1981) and this requires observing the increase in fluorescence due to its electrophoretic accumulation in mitochondria (Ronot et al. 1986).

Active and passive movement of protons across the inner mitochondrial membrane during oxidative phosphorylation process usually produce changes in Ψ_M that appear as a decrease or increase in Rh123 fluorescence due to quenching of dye from the mitochondria (Hafner, Brown, and Brand 1990). Adding a mitochondrial complex inhibitor blocks electron movement through the electron transport chain which leads to a decrease in mitochondrial membrane potential, which appears as an elevation in Rh123 fluorescence (Baracca et al. 2003). These changes in Ψ_M frequently help to identify the effect of compounds and in understanding the physiological and pathological processes inside the mitochondrial (Fontaine et al. 1997).

The data presented in the previous chapters of the present study demonstrated that simvastatin inhibits the U46619-induced contraction in PCA only in the presence of calcium and possibly via mitochondrial inhibition. The data from the previous chapters also indicate that co-enzyme Q10 and AP39 have different effects on the responses to the known complex III inhibitors antimycin A and myxothiazol. Therefore, the aims of these experiments were to determine if simvastatin has the direct effect of simvastatin on isolated mitochondria, in comparison with the complex III inhibitors, and to determine the effect of co-enzyme Q10 and AP39 on these responses.

5.2. Materials and method:

5.2.1. Tissue preparation:

Isolated mitochondria from rat liver were used to characterize the effects of simvastatin and mitochondrial complexes inhibitors on mitochondrial membrane potential. Rat livers were obtained from male Wistar rats (~250g), killed according to Schedule 1. A coarse dissection was conducted to isolate the liver. Liver tissue was washed with isolation buffer, composed of (mannitol 210mM, sucrose 70mM, EDTA 1mM, Tris 50mM, pH 7.4), to remove excess blood and then the tissue was weighed.

To isolate the mitochondria, ~ 13 g of tissue was chopped with scissors and homogenised in 130 ml of ice-cold isolation buffer using manual glass homogenizer. The homogenate was then centrifuged at 1000 g for 20 min to remove nuclei and un-homogenised material. The supernatant was then re-centrifuged at 5000 g for 15 min. The resulting supernatant layer was discarded and the pellet re-suspended. This was re-centrifuged at 10,000 g for 15 min. The resultant pellets (mitochondria) were then re-suspended in a minimum volume of isolation buffer and kept ice cold.

Isolated mitochondria were added to respiration buffer (potassium chloride 100 mM, mannitol 75 mM, sucrose 25mM, Tris 10 mM, EDTA 0.1 mM, potassium dihydrogen phosphate 10 mM, magnesium sulphate 1 mM, pH 7.1) at 37◦C in a clean dry cuvette. Glutamate 1 M, malate 250 mM, and bovine serum albumin 2.5 mg/ml were added to provide respiratory substrates for the mitochondria. After that, Rh123 (0.2 µM) was added to the mixture. The cuvette was then placed in the fluorimeter and stirred continuously using a magnetic stirrer bar.
A Hitachi F-2500 fluorescence spectrophotometer was used to measure the changes in fluorescence of Rh123 at an excitation wavelength of 503 nm and emission 527 nm. After about 60 seconds of adding the Rh123 and observing a steady reading, isolated mitochondria were added causing a rapid drop in the fluorescence reading due to sequestering of the fluorescent dye (Rh123) by functioning mitochondria.

5.2.2. Effect of simvastatin or mitochondrial inhibitors on rat liver isolated mitochondria:

In order to determine whether simvastatin could alter the mitochondrial membrane potential, rat liver isolated mitochondria were placed in a cuvette at 37 °C in a fluorimeter as above. Fluorescence signals were allowed to stabilise before compounds were added; simvastatin, rotenone (complex I inhibitor), antimycin A (complex III inhibitor at Q_i site) or myxothiazol (complex III inhibitor at Q_o site) all at 10 µM, or 0.01% v/v DMSO as a vehicle control. In some experiments the active form of simvastatin, simvastatin hydroxy

acid sodium salt, was added. Fluorescence was then measured for around 20 min. At the end of the experiments 1 µM FCCP was added to uncouple mitochondrial respiration and provide the maximum release of Rh123. The fluorescence obtained with test compounds was expressed as a percentage of the total response after addition of 1 µM FCCP.
In the case of mitochondrial stimulants, 1 µM mitoquinol, 5 µM co-enzyme Q10, 0.3 and 10 µM AP39 were added then the fluorescence measured for about 20 min. The experiments were terminated by adding 1 µM FCCP to uncouple mitochondrial respiration.

5.2.3. Effect of mitochondrial inhibitors or mitochondrial stimulants on simvastatin, antimycin A or myxothiazol response in rat liver isolated mitochondria:

In order to determine the effect of mitochondrial inhibitors or stimulants on the changes in Rh123 fluorescence in response to simvastatin, antimycin A or myxothiazol, the isolated mitochondria were exposed to one of these compounds: rotenone (complex I inhibitor), antimycin A (complex III inhibitor at Q_i site) or myxothiazol (complex III inhibitor at Q_o site) 10 µM each. In case of mitochondrial stimulants, 1 µM mitoquinol, 5 µM co-enzyme Q10, 0.3 or 10 µM AP39 were added. Fluorescence was then measured for about 20 min, prior to addition of simvastatin, antimycin A or myxothiazol, as appropriate. FCCP was added at the end of the experiment, as above.

5.2.4. Drugs and Chemicals:

Simvastatin was purchased from Tocris Bioscience, Bristol, UK. Simvastatin hydroxy acid sodium salt was purchased from Santa Cruz Biotechnology, Dallas, USA. Antimycin A, myxothiazol, rotenone, coenzyme Q10 rhodamine 123 and FCCP were purchased from Sigma Aldrich, Poole, UK. Mitoquinol and AP39 were purchased from Cayman Chemical Company, Michigan, USA.
Stock solutions of rhodamine 123 were dissolved in distilled water. A stock solution of co-enzyme Q10 and FCCP were dissolved in ethanol. Stock solutions of all remaining chemicals were dissolved in dimethyl sulfoxide (DMSO). All further dilutions of the stock solutions were made using dimethyl sulfoxide (DMSO) and respiration buffer. All stocks were kept frozen at -20 ^{o}C.
Mitochondrial isolation buffer: mannitol 210 mM, sucrose 70mM, EDTA 1mM, Tris 50mM (pH 7.4). Mitochondrial respiration buffer (potassium chloride 100 mM, mannitol 75 mM, sucrose 25mM, Tris 10 mM, EDTA 0.1 mM, potassium dihydrogen phosphate 10 mM, magnesium sulphate 1 mM pH 7.1) at 37 ^{o}C.

5.2.5. Statistical Analysis:

Data were expressed as a percentage of the maximum change in fluorescence obtained by the addition of FCCP at the end of the experiment. Data were presented as mean ± SEM where n = the number of different animals. Data were analyzed using 2-tailed, paired or unpaired Student's t-test to compare differences between 2 groups, as appropriate. Differences between 3 or more groups were assessed using one-way ANOVA in conjunction with the Tukey post-hoc test. The P-value <0.05 was considered statistically significant. Statistical analysis was performed by Graph-Pad Prism (Version 7).

5.3. Results:

5.3.1. The effect of simvastatin on mitochondria isolated from liver of rat:

In order to determine whether simvastatin has a direct effect on mitochondrial membrane potential, the effect of 10 µM simvastatin on the isolated mitochondria was determined. Simvastatin had no effect on membrane potential compared to the vehicle control in the isolated mitochondria loaded with Rh123. See figure 5.1 and 5.2.

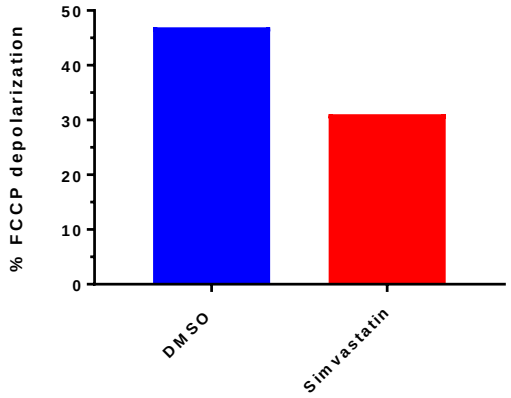

Figure 5.1: Cumulative fluorescence data for isolated mitochondria from liver of rat loaded with Rh123 in the presence of simvastatin (10 µM) or vehicle control (0.1% v/v DMSO). Data are expressed as a percentage of the response to 1 µM FCCP in the same isolated mitochondria and are mean ± SEM from n=3.

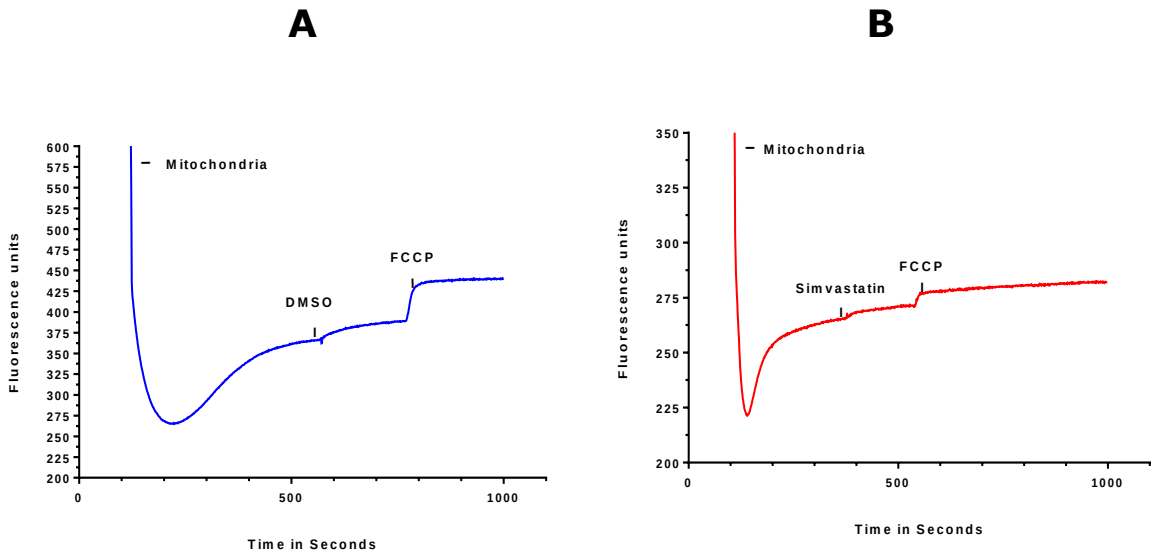

Figure 5.2: Typical trace showing the effect of **A-** 0.1% v/v DMSO and **B-** 10 µM simvastatin on Rh123 fluorescence in isolated mitochondria from liver of rat. FCCP 1 µM was added as a positive control to get the maximum fluorescence and the DMSO as a solvent control.

5.3.2. The effect of simvastatin on mitochondria isolated from liver of rat:

As DMSO produced a large response on its own, experiments were carried out by diluting compounds in respiration buffer in order to reduce the concentration of DMSO added. In these experiments, the fluorescence response to DMSO was reduced to ~6% of the FCCP response (figure 5.3). However, the response to simvastatin was lower than that seen with vehicle (figure 5.3 & 5.4).

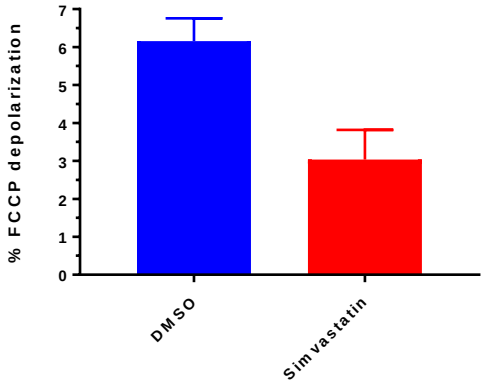

Figure 5.3: Fluorescence data from isolated mitochondria from rat livers loaded with Rh123 in the presence of simvastatin (10 µM) or vehicle control (0.01% v/v DMSO). Data are expressed as a percentage of the maximum fluorescence obtained after addition of 1 µM FCCP in the same isolated mitochondria and are mean ± SEM from n=3.

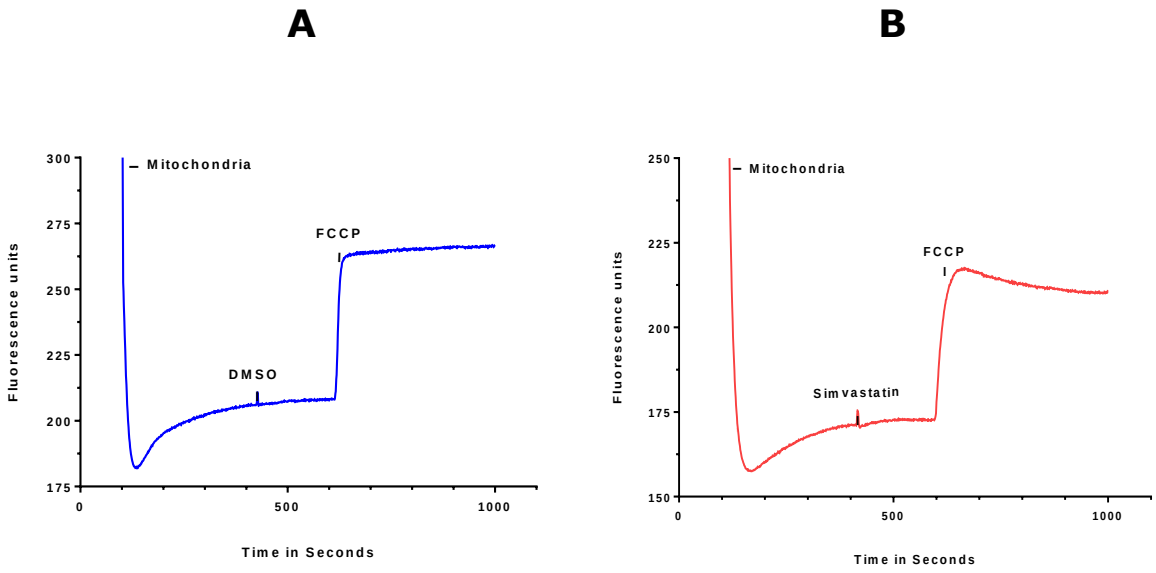

Figure 5.4: Typical trace showing the effect of **A-** 0.01% v/v DMSO and **B-** 10 µM simvastatin on Rh123 fluorescence in isolated mitochondria from rat livers. FCCP 1 µM was added as a positive control to get the maximum fluorescence.

5.3.3. The effect of rotenone (mitochondrial complex I inhibitor) on simvastatin response in rat liver isolated mitochondria:

In order to determine whether adding of 10 μM rotenone could have an effect on the simvastatin response, the isolated mitochondria were exposed to 10 μM simvastatin in the absence or presence of rotenone (10 μM), complex I inhibitor. The effect of simvastatin and rotenone on mitochondrial membrane potential were determined. Although rotenone produced a response on its own (figure 5.6), simvastatin failed to produce a response either on its own or in the presence of rotenone (figure 5.5 & 5.6). Neither simvastatin alone nor rotenone alone had a significant effect on membrane potential compared to control. In addition, there were no significant changes in simvastatin effect in the presence of rotenone. See figure 5.5 and 5.6.

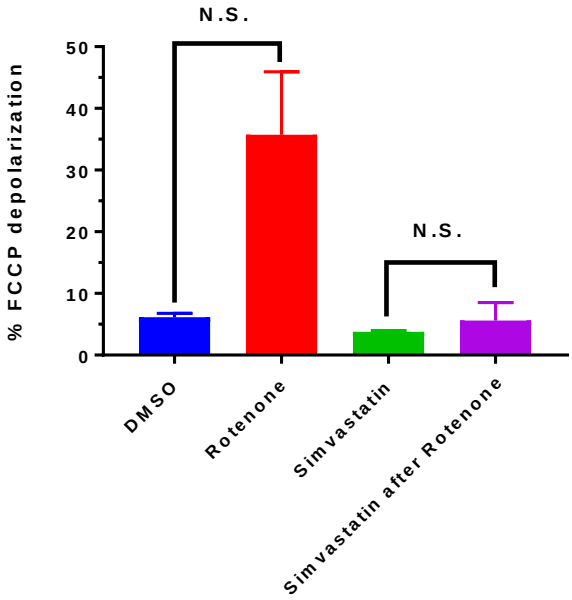

Figure 5.5: Fluorescence data from isolated mitochondria from liver of rat loaded with Rh123 in the presence of simvastatin (10 μM) and rotenone (10 μM) or vehicle control (0.01% v/v DMSO). Data are expressed as a percentage of the maximum fluorescence obtained after addition of 1 μM FCCP in the same isolated mitochondria and are mean ± SEM from n=3. One-way ANOVA followed by Tukey post-hoc test.

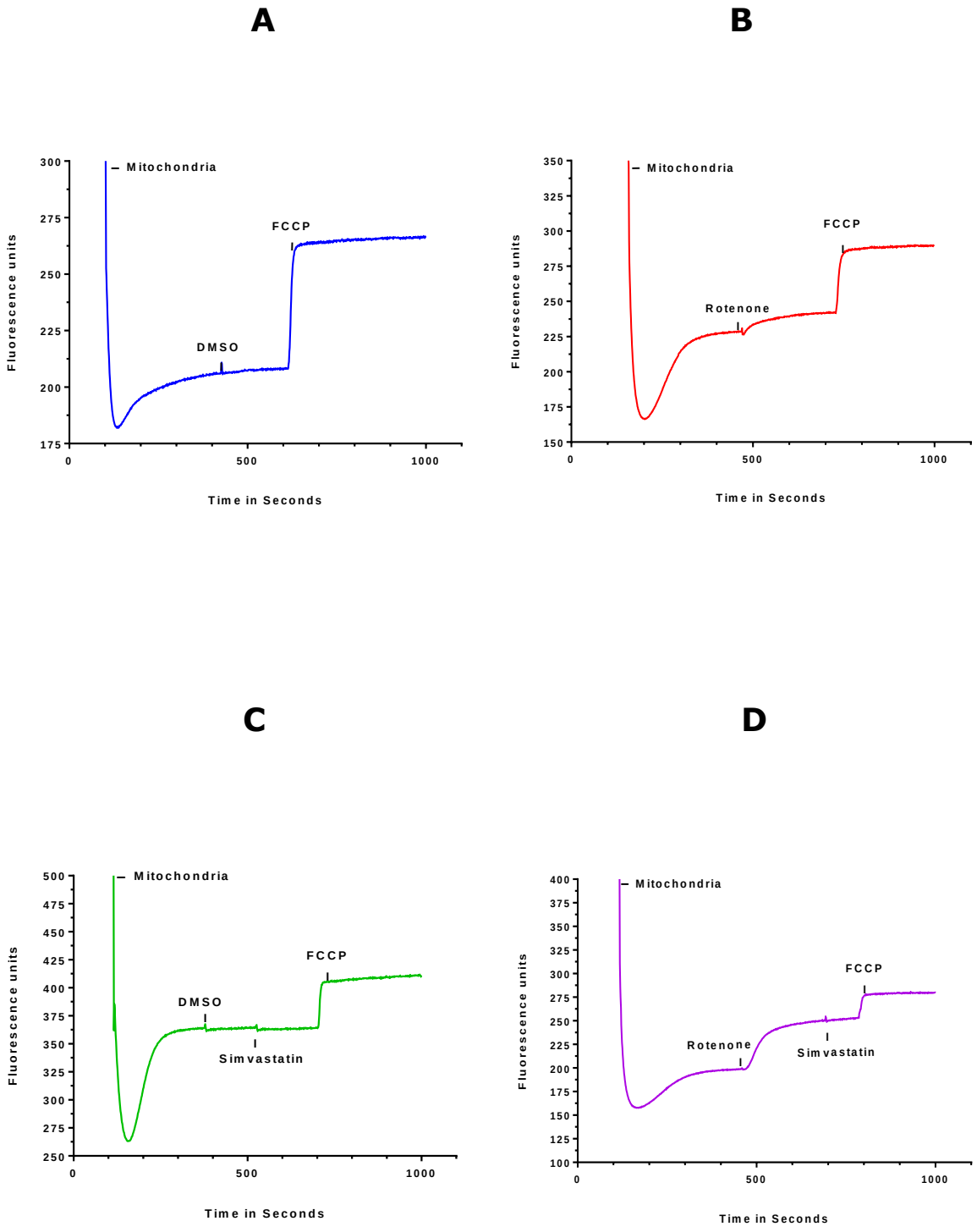

Figure 5.6: Typical traces showing the effect of **A-** 0.01% v/v DMSO, **B-** rotenone (10 μM), **C**- simvastatin (10 μM) and **D**- simvastatin after rotenone (10 μM each) on Rh123 fluorescence in isolated mitochondria from rat liver. FCCP 1 μM was added as a positive control to get the maximum fluorescence.

5.3.4. The effect of antimycin A (mitochondrial complex III inhibitor at Q_i site) on simvastatin response in rat liver isolated mitochondria:

In order to determine whether addition of 10 μM antimycin A could have an effect on the simvastatin response, the isolated mitochondria were exposed to 10 μM simvastatin in the absence or presence of mitochondrial complex inhibitor III antimycin A (10 μM). The effect of simvastatin and antimycin A on mitochondrial membrane potential were determined. Antimycin A alone caused a significant increase in total fluorescence in the isolated mitochondria loaded with Rh123 (fluorescence = 82± 6%) compared to the control (fluorescence = 6± 0.6%). Simvastatin had no significant effect on membrane potential while adding of simvastatin after antimycin A caused a reduction in total fluorescence (fluorescence = 1± 1%) compared to the simvastatin alone (fluorescence = 4± 0.2%). See figure 5.7 and 5.8.

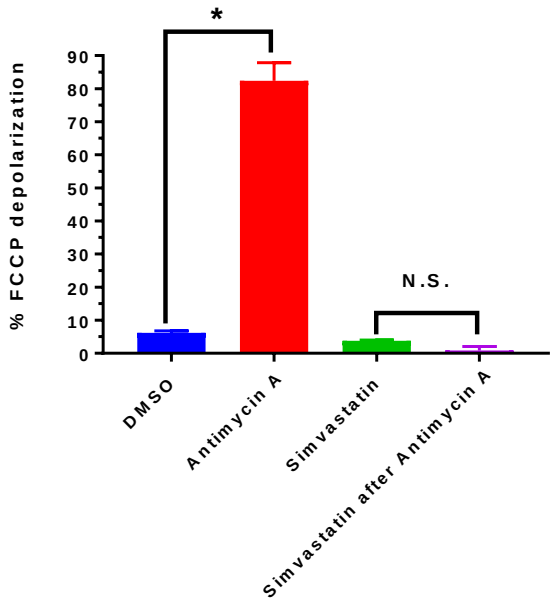

Figure 5.7: Fluorescence data from isolated mitochondria from liver of rat loaded with Rh123 in the presence of simvastatin (10 μM) and antimycin A (10 μM) or vehicle control (0.01% v/v DMSO). Data are expressed as a percentage of the maximum fluorescence obtained after addition of 1 μM FCCP in the same isolated mitochondria and are mean ± SEM from n=3, *p<0.05, One-way ANOVA followed by Tukey post-hoc test.

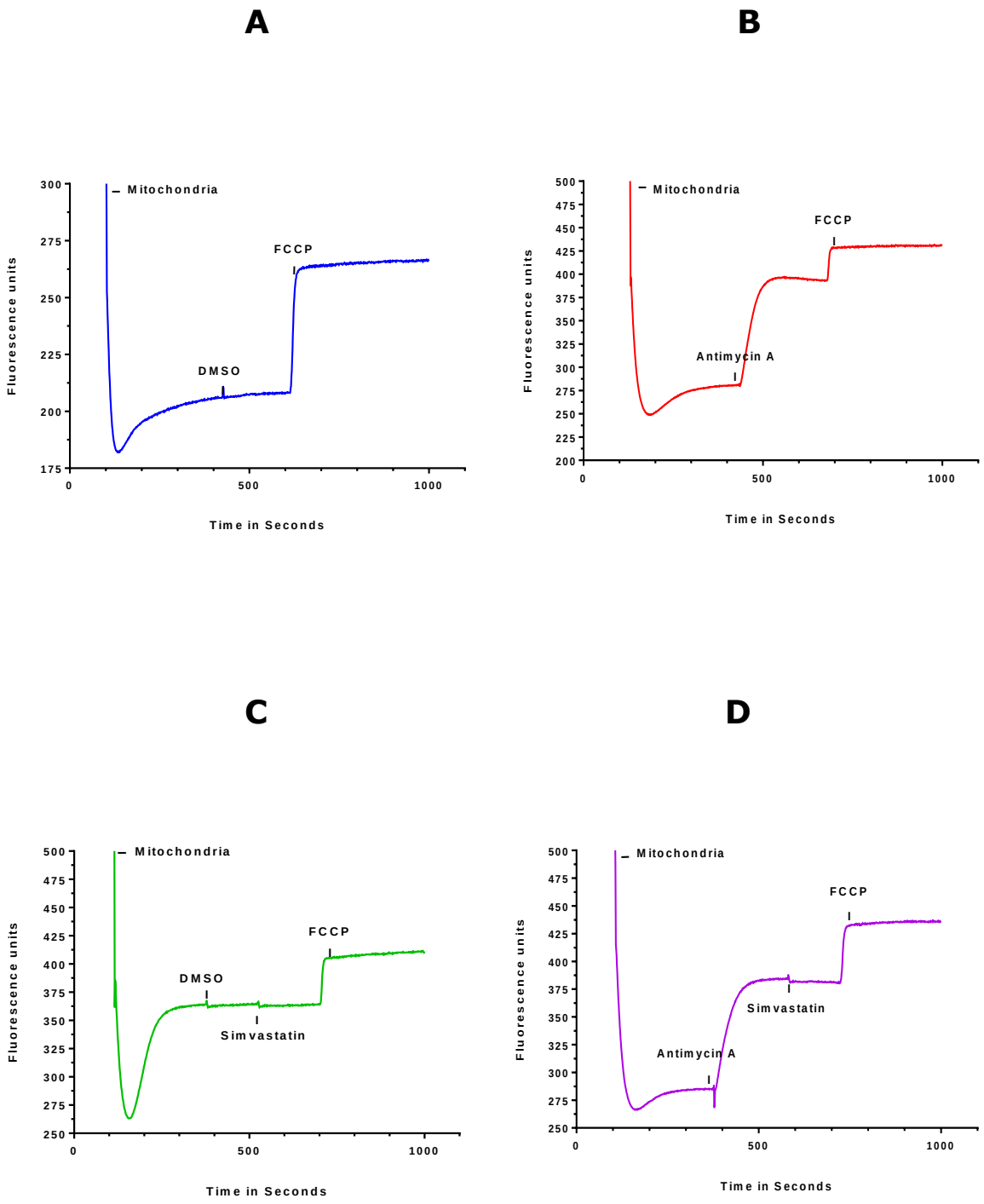

Figure 5.8: Typical traces showing the effect of **A-** 0.01% v/v DMSO, **B-** antimycin A (10 µM), **C**- simvastatin (10 µM) and **D**- simvastatin after antimycin A (10 µM each) on Rh123 fluorescence in isolated mitochondria from rat's liver. FCCP 1 µM was added as a positive control to get the maximum fluorescence.

5.3.5. The effect of myxothiazol (mitochondrial complex III inhibitor at Q_o site) on simvastatin response in rat liver isolated mitochondria:

In order to determine whether adding 10 μM myxothiazol could have an effect on the simvastatin response, the isolated mitoc DONE--Stevehondria were exposed to 10 μM simvastatin in the absence or presence of myxothiazol (10 μM). The effect of simvastatin and myxothiazol on mitochondrial membrane potential were determined. Myxothiazol alone caused a significant increase in total fluorescence in the isolated mitochondria loaded with Rh123 (fluorescence = 84± 6%) compared to the control (fluorescence = 6± 0.6%). Simvastatin had no significant effect on membrane potential and there was no further effect after adding simvastatin after myxothiazol. See figure 5.9 and 5.10.

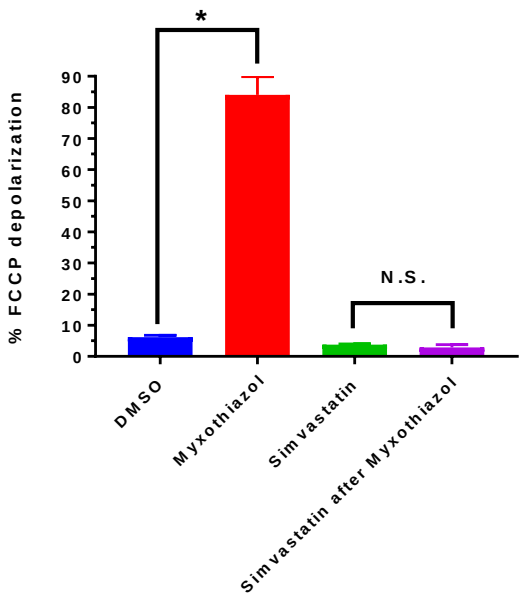

Figure 5.9: Fluorescence data from isolated mitochondria from liver of rat loaded with Rh123 in the presence of simvastatin (10 μM) and myxothiazol (10 μM) or vehicle control (0.01% v/v DMSO). Data are expressed as a percentage of the maximum fluorescence obtained after addition of 1 μM FCCP in the same isolated mitochondria and are mean ± SEM from n=3, *p<0.05, One-way ANOVA followed by Tukey post-hoc test.

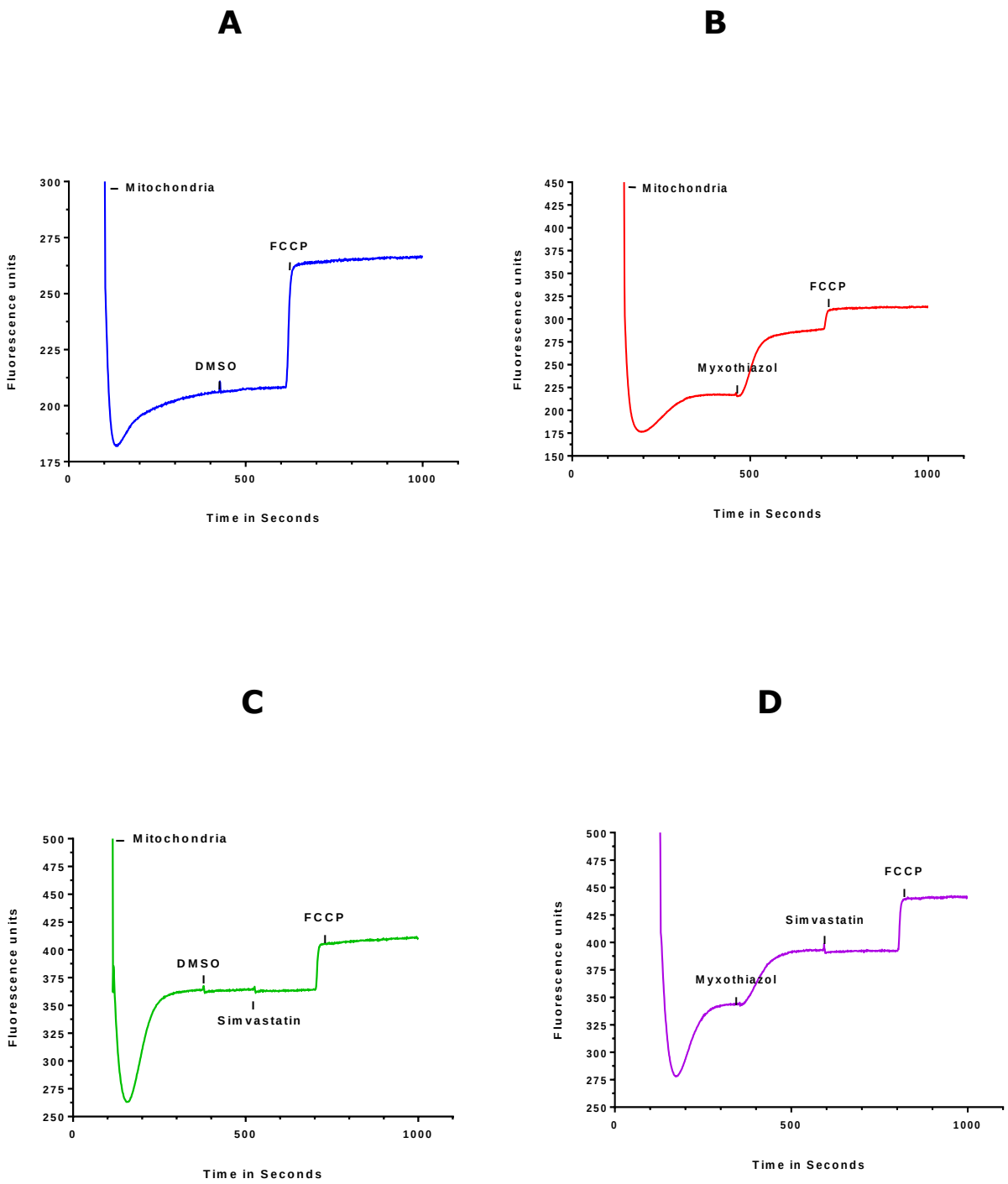

Figure 5.10: Typical traces showing the effect of **A-** 0.01% v/v DMSO, **B-** myxothiazol (10 µM), **C**- simvastatin (10 µM) and **D**- simvastatin after myxothiazol (10 µM each) on Rh123 fluorescence in isolated mitochondria from rat liver. FCCP 1 µM was added as a positive control to get the maximum fluorescence.

5.3.6. The effect of co-enzyme Q10 on simvastatin response in rat liver isolated mitochondria:

In order to determine whether supplementation with co-enzyme Q10 could have an effect on the simvastatin response, the isolated mitochondria were exposed to 10 μM simvastatin in the absence or presence of co-enzyme Q10 (5 μM). The effect of simvastatin and co-enzyme Q10 on mitochondrial membrane potential were determined. Although co-enzyme Q10 produced a change in fluorescence, this was no different from the 0.1% v/v ethanol used as a vehicle control. In addition, co–enzyme Q10 had no significant effect on simvastatin response. See figure 5.11 and 5.12.

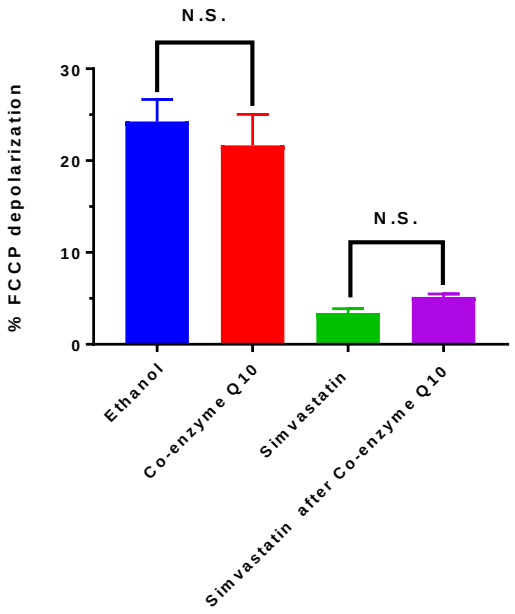

Figure 5.11: Fluorescence data from isolated mitochondria from liver of rat loaded with Rh123 in the presence of simvastatin (10 μM) and co-enzyme Q10 (5 μM) or vehicle control (0.1% v/v ethanol). Data are expressed as a percentage of the maximum fluorescence obtained after addition of 1 μM FCCP in the same isolated mitochondria and are mean ± SEM from n=3. One-way ANOVA followed by Tukey post-hoc test.

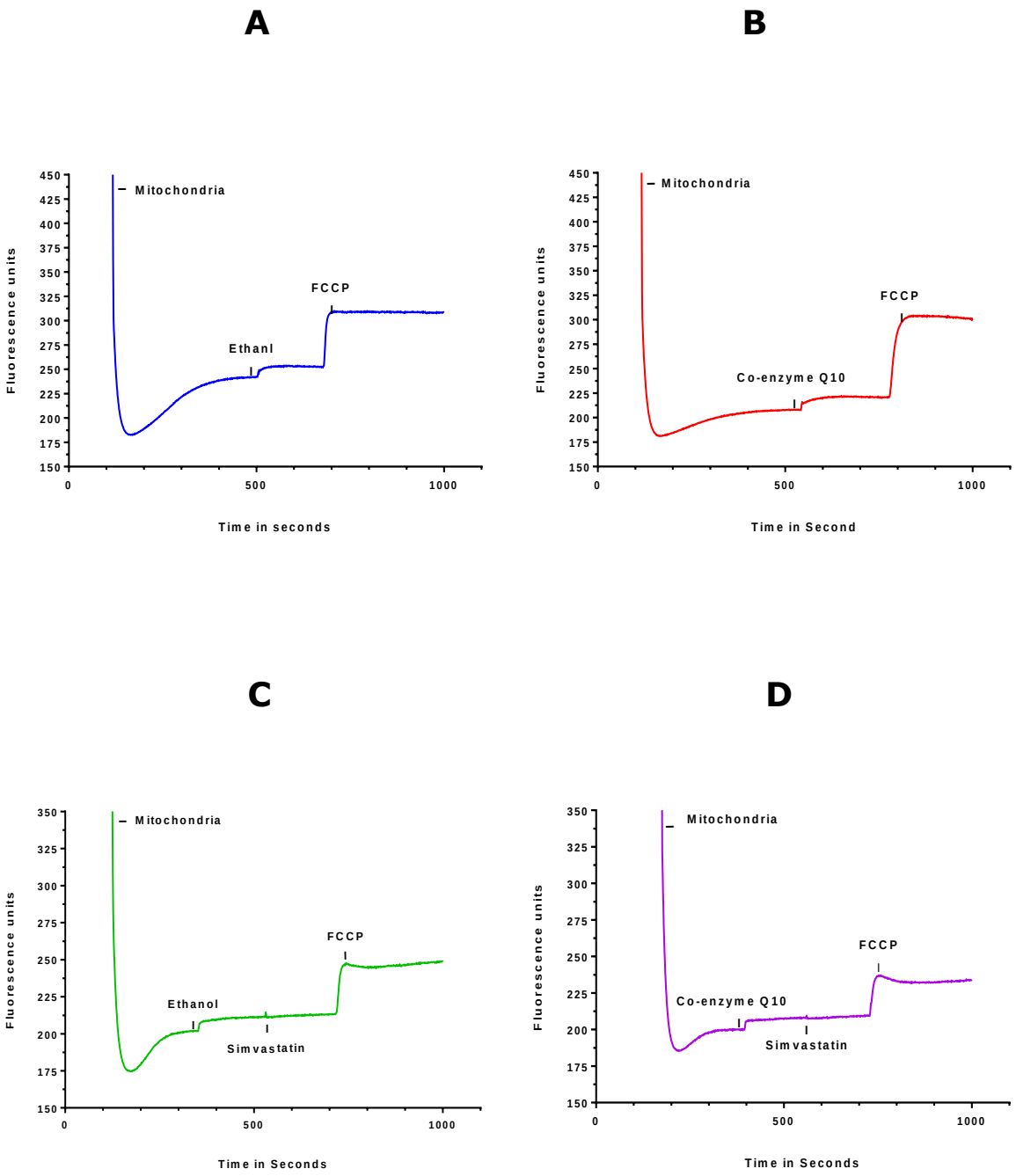

Figure 5.12: Typical traces showing the effect of **A-** 0.1% v/v ethanol, **B-** co-enzyme Q10 (5 µM), **C**- simvastatin (10 µM) and **D**- simvastatin after co-enzyme Q10 (5 µM each) on Rh123 fluorescence in isolated mitochondria from rat liver. FCCP 1 µM was added as a positive control to get the maximum fluorescence.

5.3.7. The effect of co-enzyme Q10 on rotenone (mitochondrial complex I inhibitor) response in rat liver isolated mitochondria:

In order to determine whether supplementation with co-enzyme Q10 could have an effect on the rotenone response, the isolated mitochondria were exposed to 10 µM rotenone in the absence or presence of co-enzyme Q10 (5 µM). The effect of rotenone and co-enzyme Q10 on mitochondrial membrane potential were determined. Co-enzyme Q10 had no effect on the membrane potential compared to the vehicle control (0.1% v/v ethanol). In addition, rotenone had no effect on its own compared to the ethanol control. Similarly, co–enzyme Q10 had no significant effect on rotenone response. See figure 5.13 and 5.14.

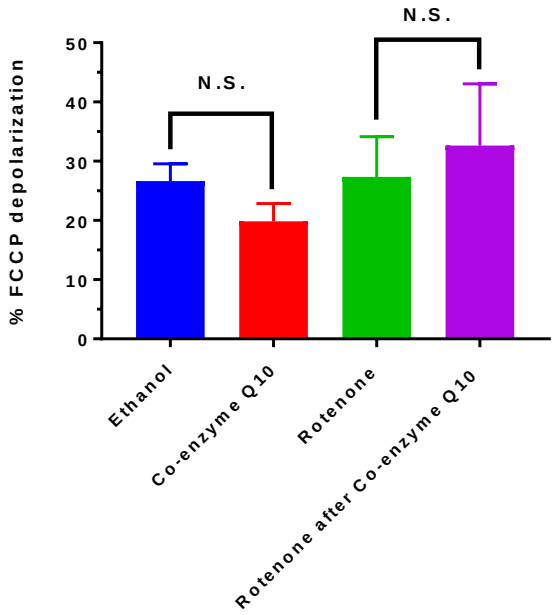

Figure 5.13: Fluorescence data from isolated mitochondria from liver of rat loaded with Rh123 in the presence of rotenone (10 µM) and co-enzyme Q10 (5 µM) or vehicle control (0.1% v/v ethanol). Data are expressed as a percentage of the maximum fluorescence obtained after addition of 1 µM FCCP in the same isolated mitochondria and are mean ± SEM from n=3. One-way ANOVA followed by Tukey post-hoc test.

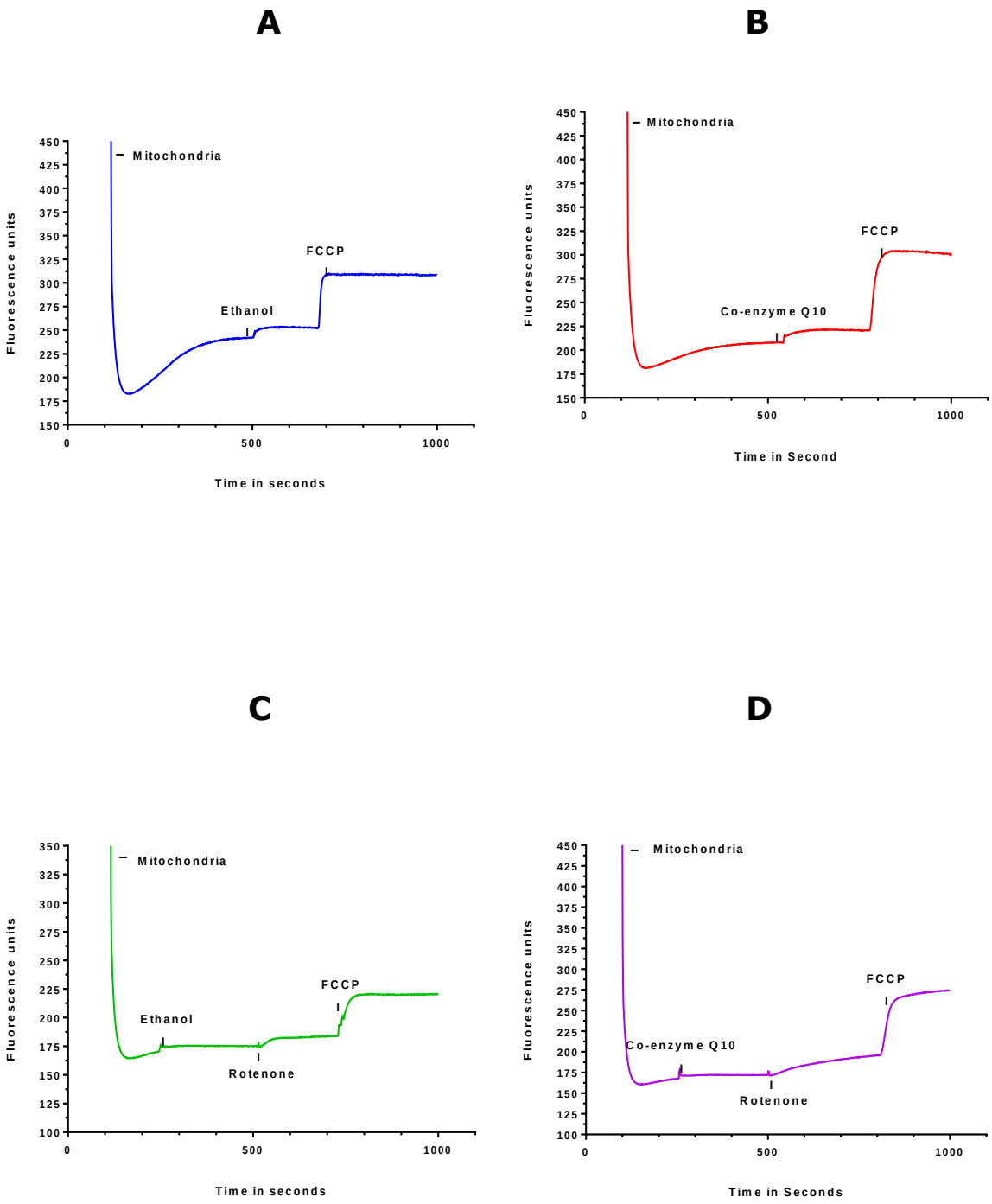

Figure 5.14: Typical traces showing the effect of **A-** 0.1% v/v ethanol, **B-** co-enzyme Q10 (5 µM), **C**- rotenone (10 µM) and **D**- rotenone after co-enzyme Q10 (10 µM each) on Rh123 fluorescence in isolated mitochondria from rat liver. FCCP 1 µM was added as a positive control to get the maximum fluorescence.

5.3.8. The effect of co-enzyme Q10 on antimycin A (mitochondrial complex III inhibitor) response in rat liver isolated mitochondria:

In order to determine whether supplementation with co-enzyme Q10 could prevent the antimycin A response, the isolated mitochondria were exposed to 10 µM antimycin A in the absence or presence of co-enzyme Q10 (5 µM). The effect of antimycin A and co-enzyme Q10 on mitochondrial membrane potential were determined. Co-enzyme Q10 had no effect on the membrane potential compared to its vehicle control (0.1% v/v ethanol). In addition, co–enzyme Q10 had no significant effect on the antimycin A response. See figure 5.15 and 5.16.

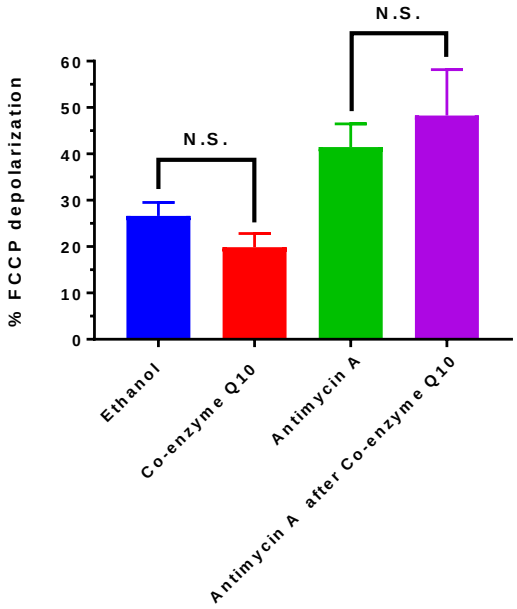

Figure 5.15: Fluorescence data from isolated mitochondria from liver of rat loaded with Rh123 in the presence of antimycin A (10 µM) and co-enzyme Q10 (5 µM) or vehicle control (0.1% v/v ethanol). Data are expressed as a percentage of the maximum fluorescence obtained after addition of 1 µM FCCP in the same isolated mitochondria and are mean ± SEM from n=3. One-way ANOVA followed by Tukey post-hoc test.

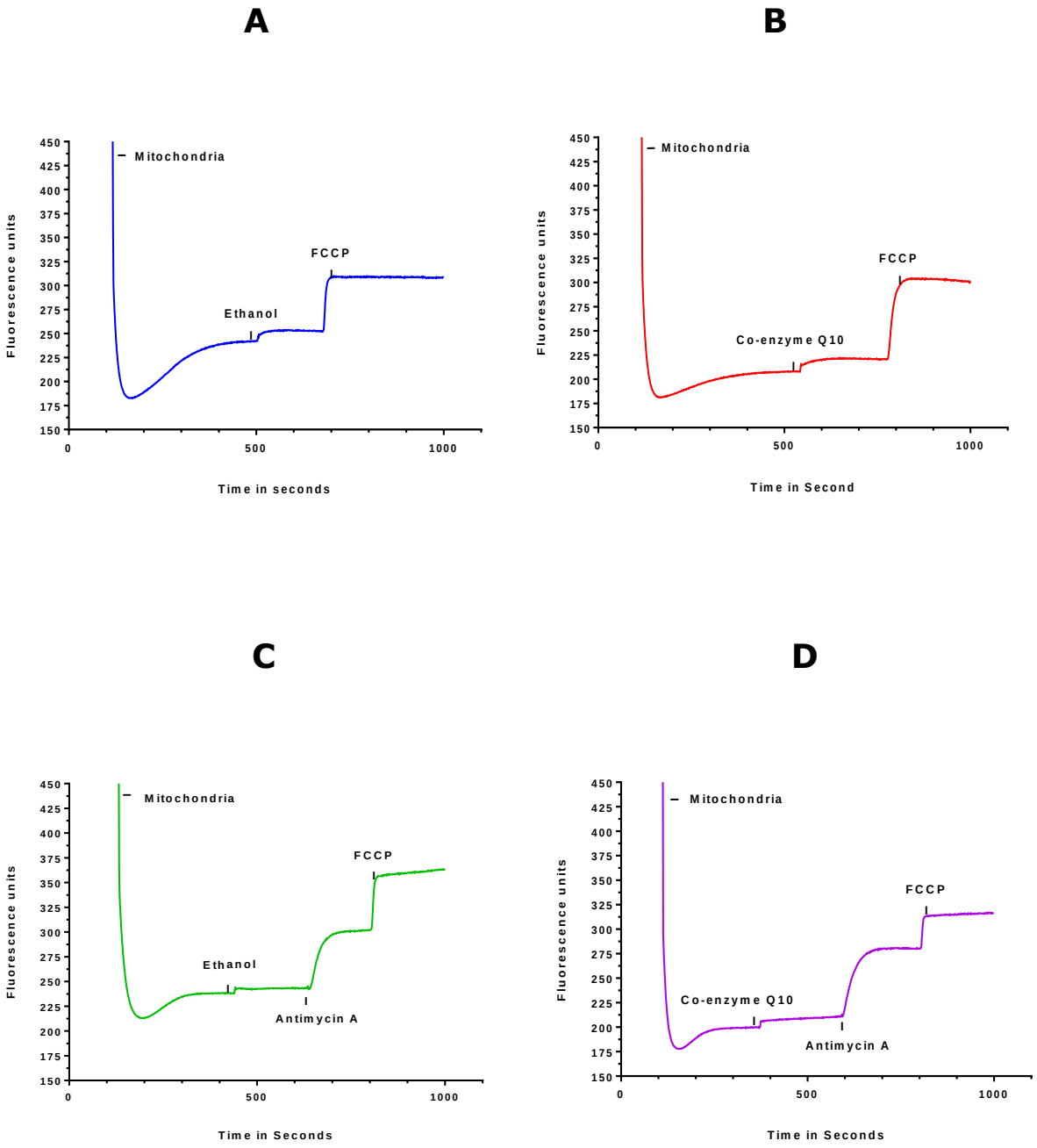

Figure 5.16: Typical traces showing the effect of **A-** 0.1% v/v ethanol, **B-** co-enzyme Q10 (5 µM), **C**- antimycin A (10 µM) and **D**- antimycin A after co-enzyme Q10 (10 µM each) on Rh123 fluorescence in isolated mitochondria from rat liver. FCCP 1µM was added as a positive control to get the maximum fluorescence.

5.3.9. The effect of co-enzyme Q10 on myxothiazol (mitochondrial complex III inhibitor at Q_o site) response in rat liver isolated mitochondria:

In order to determine whether supplementation with co-enzyme Q10 could prevent the myxothiazol response, the isolated mitochondria were exposed to 10 µM myxothiazol in the absence or presence of co-enzyme Q10 (5 µM). The effect of myxothiazol and co-enzyme Q10 on mitochondrial membrane potential were determined. Co-enzyme Q10 had no effect on the membrane potential compared to its vehicle control (0.1% v/v ethanol). In addition, co–enzyme Q10 had no significant effect on the myxothiazol response. See figure 5.17 and 5.18.

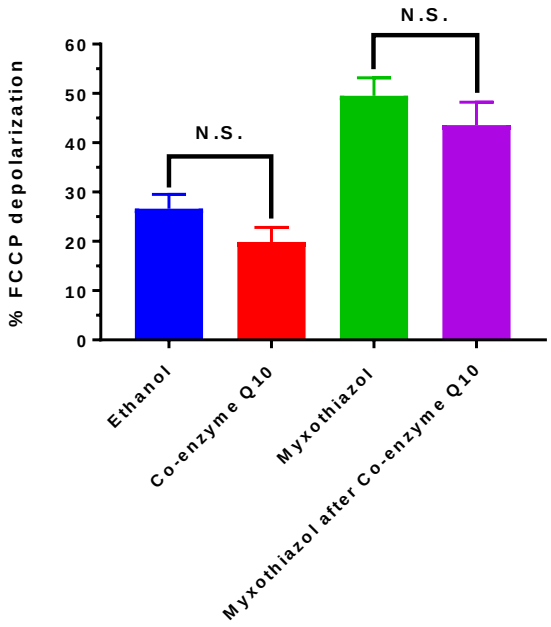

Figure 5.17: Fluorescence data from isolated mitochondria from liver of rat loaded with Rh123 in the presence of myxothiazol (10 µM) and co-enzyme Q10(5 µM), or vehicle control (0.1% v/v ethanol). Data are expressed as a percentage of the maximum fluorescence obtained after addition of 1 µM FCCP in the same isolated mitochondria and are mean ± SEM from n=3. One-way ANOVA followed by Tukey post-hoc test.

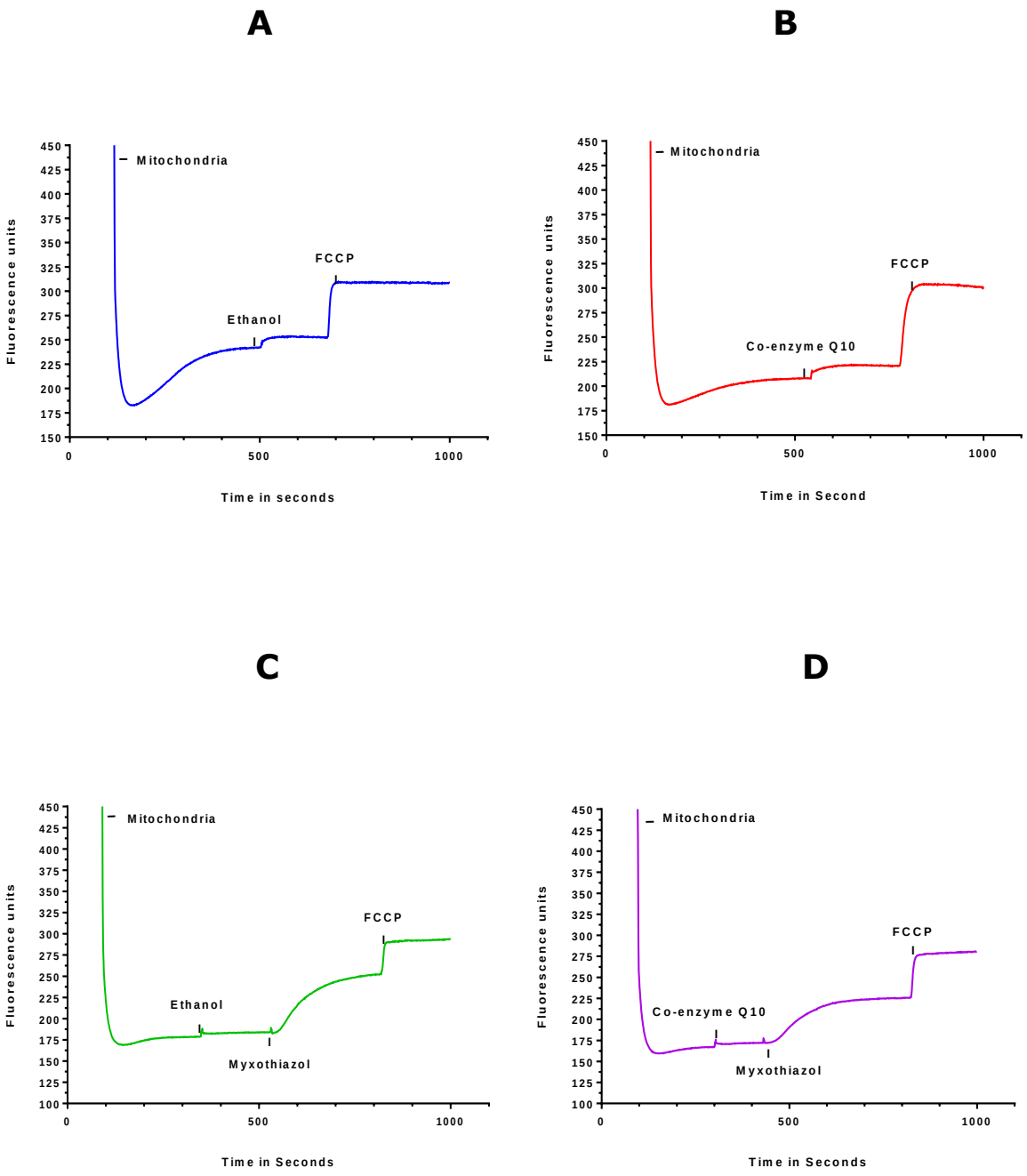

Figure 5.18: Typical traces showing the effect of **A-** 0.1% v/v ethanol, **B-** co-enzyme Q10 (5 µM), **C**- myxothiazol (10 µM) and **D** myxothiazol after co-enzyme Q10 (10 µM each) on Rh123 fluorescence in isolated mitochondria from rat liver. FCCP 1 µM was added as a positive control to get the maximum fluorescence.

5.3.10. The effect of mitoquinol on simvastatin response in isolated mitochondria from rat liver:

In order to determine whether adding of mitoquinol could have an effect on simvastatin response, the isolated mitochondria were exposed to 10 μM simvastatin in the absence or presence of mitoquinol (1 μM). Mitoquinol alone caused an increase in total fluorescence in the isolated mitochondria loaded with Rh123 (fluorescence = 38± 8%) compared to the control (fluorescence = 8± 2%). Simvastatin had no significant effect on membrane potential and adding of mitoquinol before simvastatin showed no significant changes in simvastatin response. See figure 5.19 and 5.20.

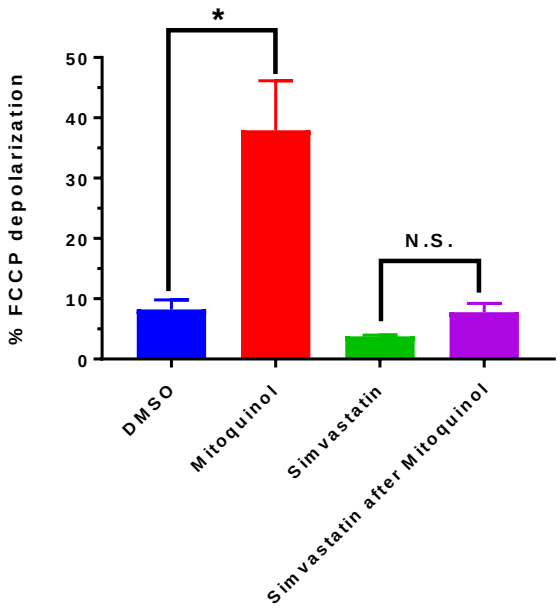

Figure 5.19: Fluorescence data from isolated mitochondria from liver of rat loaded with Rh123 in the presence of simvastatin (10 μM) and mitoquinol (1 μM) or vehicle control (0.01% v/v DMSO). Data are expressed as a percentage of the maximum fluorescence obtained after addition of 1 μM FCCP in the same isolated mitochondria and are mean ± SEM from n=3. *p<0.05, One-way ANOVA followed by Tukey post-hoc test.

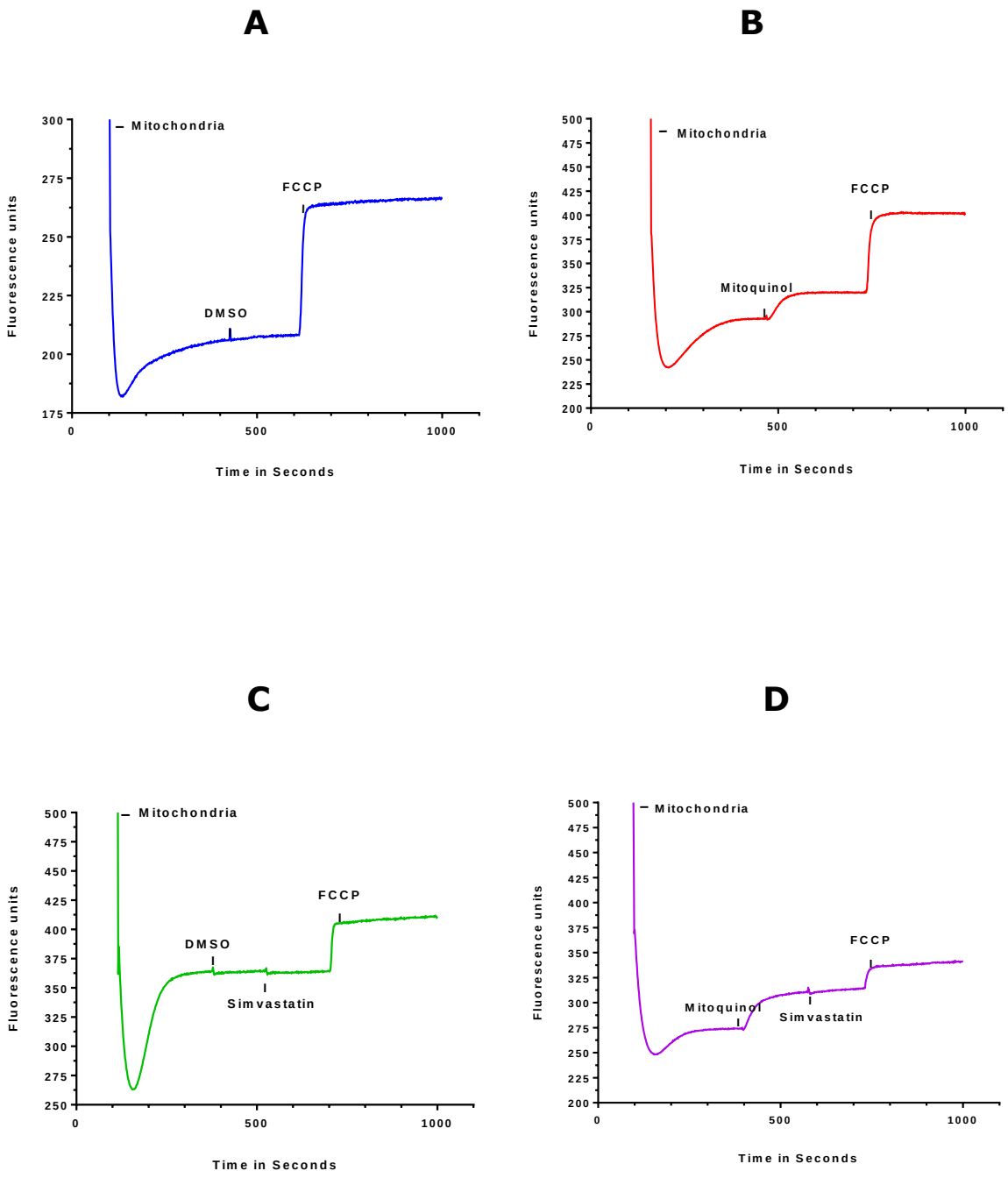

Figure 5.20: Typical traces showing the effect of **A-** 0.01% v/v DMSO, **B-** mitoquinol (1 μM), **C**- simvastatin (10 μM) and **D**- simvastatin (10 μM) after mitoquinol (1 μM) on Rh123 fluorescence in isolated mitochondria from rat liver. FCCP 1 μM was added as a positive control to get the maximum fluorescence.

5.3.11. The effect of mitoquinol on rotenone (mitochondrial complex I inhibitor) response in isolated mitochondria from rat liver:

In order to determine whether adding of mitoquinol could have an effect on rotenone response, the isolated mitochondria were exposed to 10 µM rotenone in the absence or presence of mitoquinol (1 µM). Mitoquinol alone and rotenone alone both caused an increase in total fluorescence in the isolated mitochondria loaded with Rh123 (fluorescence = 35± 7%, 39± 5% respectively) compared to the vehicle control (fluorescence = 8± 1%). On the other hand, adding mitoquinol before rotenone caused a non-significant reduction in the rotenone response (absorbance= 23± 8%). See figure 5.21 and 5.22.

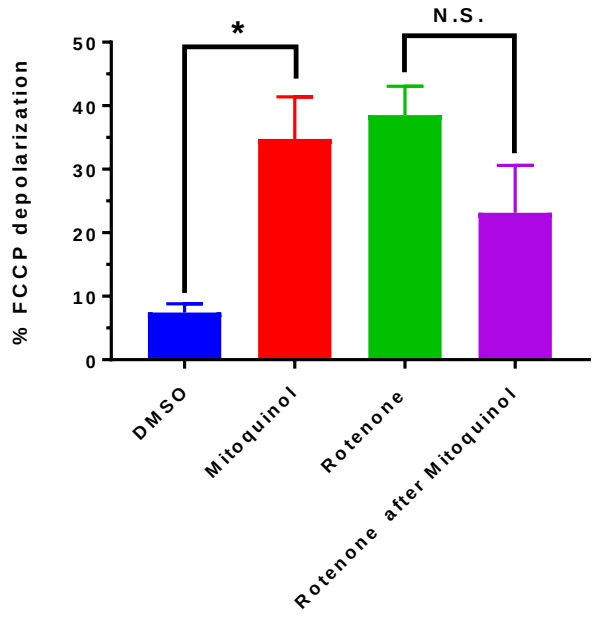

Figure 5.21: Fluorescence data from isolated mitochondria from liver of rat loaded with Rh123 in the presence of rotenone (10 µM) and mitoquinol (1 µM) or vehicle control (0.01% v/v DMSO). Data are expressed as a percentage of the maximum fluorescence obtained after addition of 1 µM FCCP in the same isolated mitochondria and are mean ± SEM from n=3. *p<0.05, One-way ANOVA followed by Tukey post-hoc test.

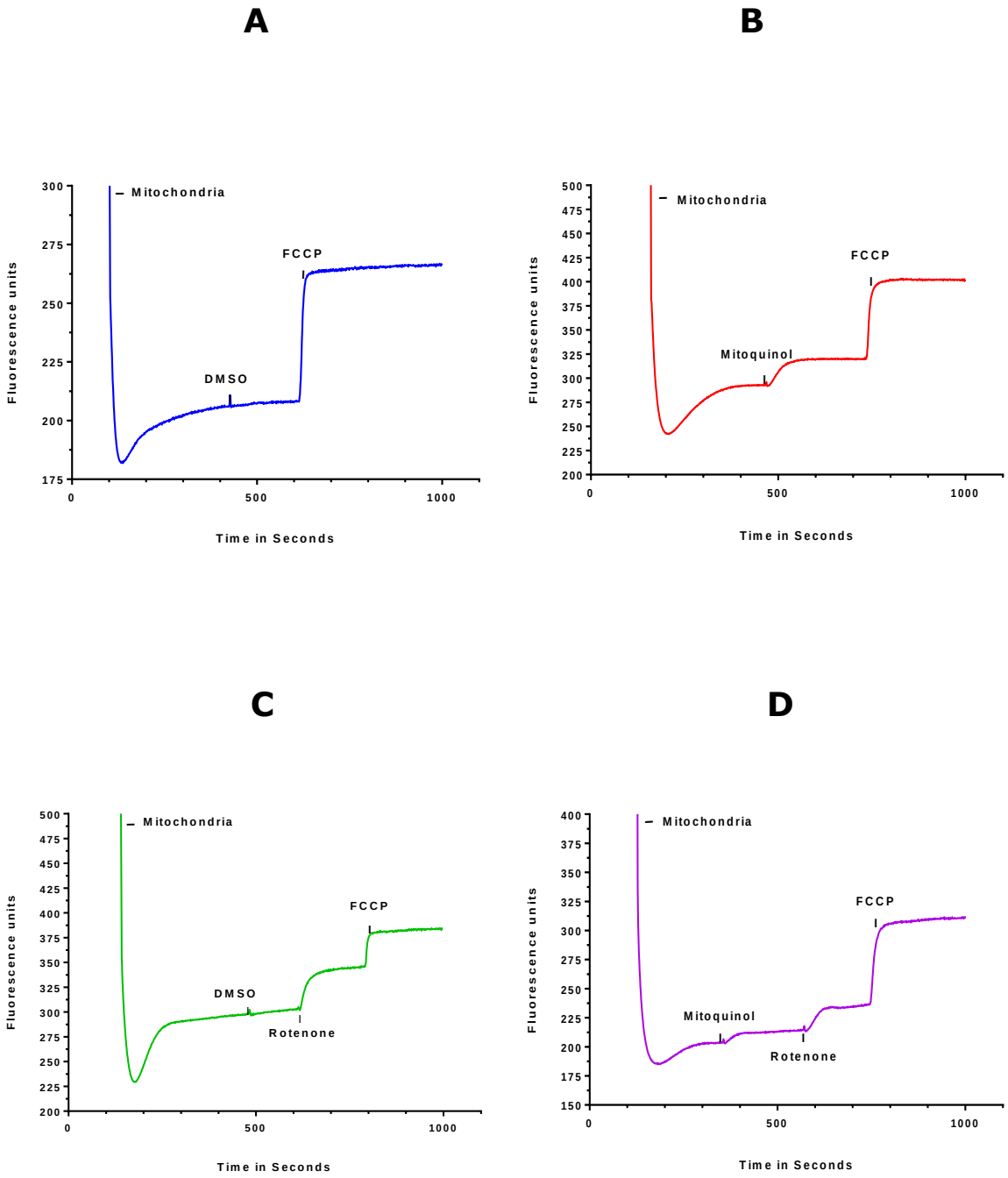

Figure 5.22: Typical traces showing the effect of **A-** 0.01% v/v DMSO, **B-** mitoquinol (1 µM), **C**- rotenone (10 µM) and **D**- rotenone (10 µM) after mitoquinol (1 µM) on Rh123 fluorescence in isolated mitochondria from rat liver. FCCP 1 µM was added as a positive control to get the maximum fluorescence.

5.3.12. The effect of mitoquinol on antimycin A (mitochondrial complex III inhibitor at Q_i site) response in isolated mitochondria from rat liver:

In order to determine whether adding mitoquinol could have an effect on the antimycin A response, the isolated mitochondria were exposed to 10 µM antimycin A in the absence or presence of mitoquinol (1 µM). Mitoquinol alone and antimycin A alone both caused an increase in total fluorescence in the isolated mitochondria loaded with Rh123 (fluorescence = 35± 7% and fluorescence = 42± 10% respectively) compared to the vehicle control (absorbance= 8± 1%). On the other hand, adding mitoquinol before antimycin A enhanced the antimycin A response but not significantly (absorbance= 67± 6%). See figure 5.23 and 5.24.

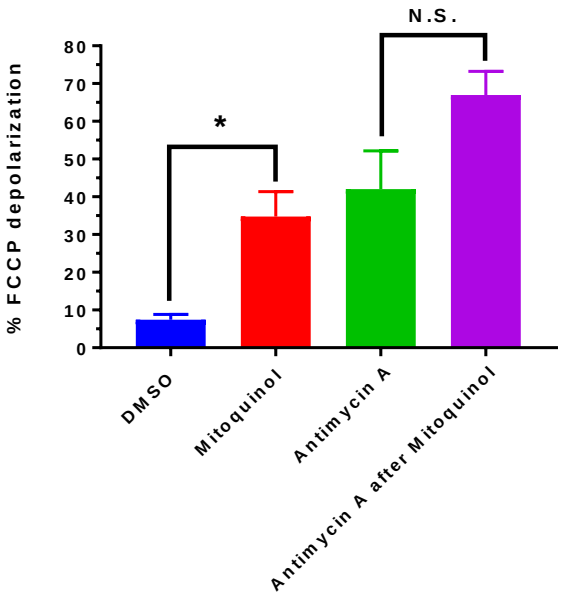

Figure 5.23: Fluorescence data from isolated mitochondria from liver of rat loaded with Rh123 in the presence of antimycin A (10 µM) and mitoquinol (1 µM) or vehicle control (0.01% v/v DMSO). Data are expressed as a percentage of the maximum fluorescence obtained after addition of 1 µM FCCP in the same isolated mitochondria and are mean ± SEM from n=3. *p<0.05, One-way ANOVA followed by Tukey post-hoc test.

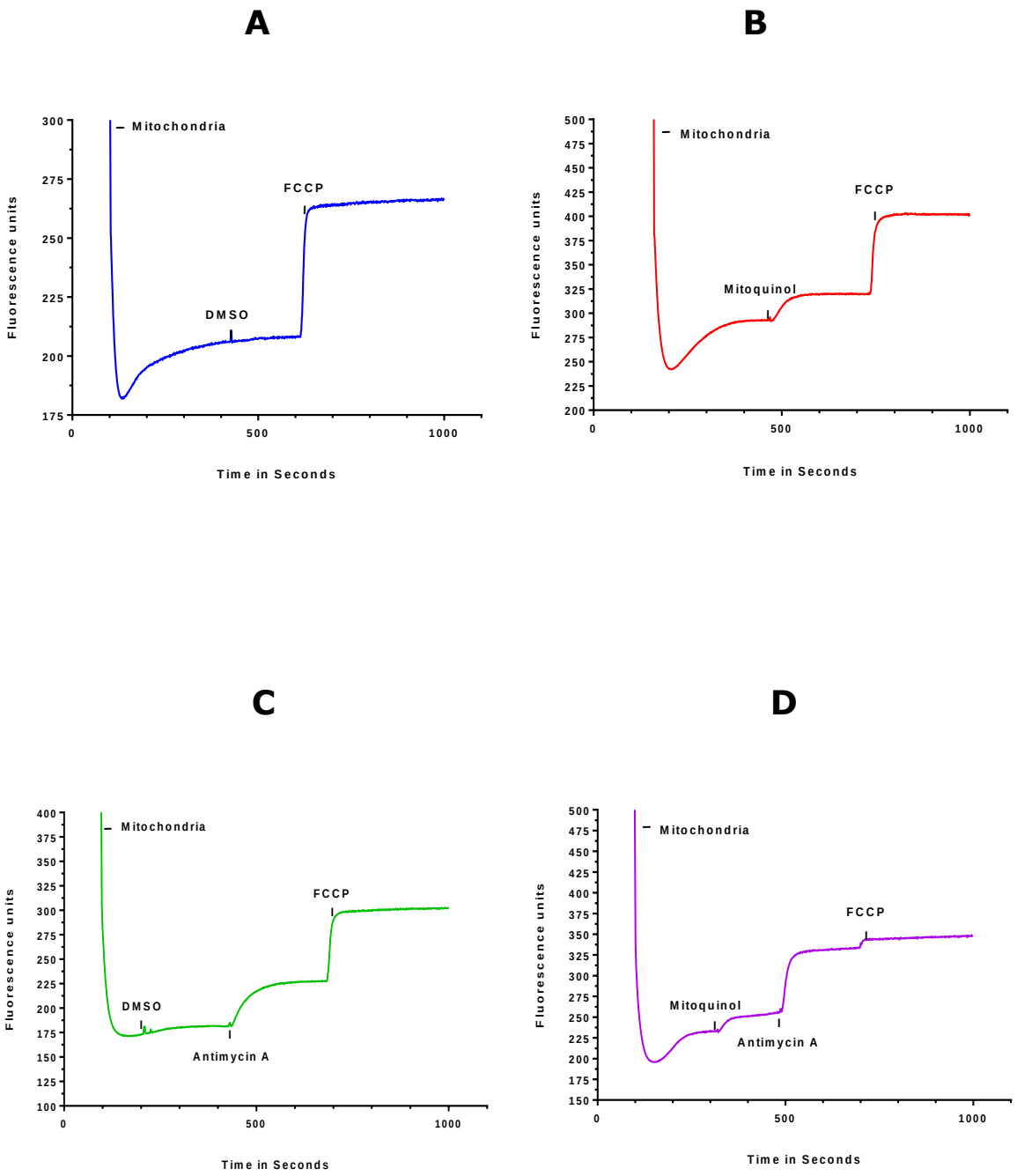

Figure 5.24: Typical traces showing the effect of **A-** 0.01% v/v DMSO, **B-** mitoquinol (1 µM), **C**- antimycin A (10 µM) and **D**- antimycin A (10 µM) after mitoquinol (1 µM) on Rh123 fluorescence in isolated mitochondria from rat liver. FCCP 1 µM was added as a positive control to get the maximum fluorescence.

5.3.13. The effect of mitoquinol on myxothiazol (mitochondrial complex III inhibitor at Q_o site) response in isolated mitochondria from rat liver:

In order to determine whether adding mitoquinol could have an effect on myxothiazol response, the isolated mitochondria were exposed to 10 μM myxothiazol in the absence or presence of mitoquinol (1 μM). Mitoquinol alone caused an increase in total fluorescence in the isolated mitochondria loaded with Rh123 (absorbance= 35± 7%) compared to the vehicle control (absorbance= 8± 1%). Myxothiazol alone caused an increase in total fluorescence (absorbance= 44± 4%) compared to the vehicle control. However, this was unaltered in the presence of mitoquinol. See figure 5.25 and 5.26.

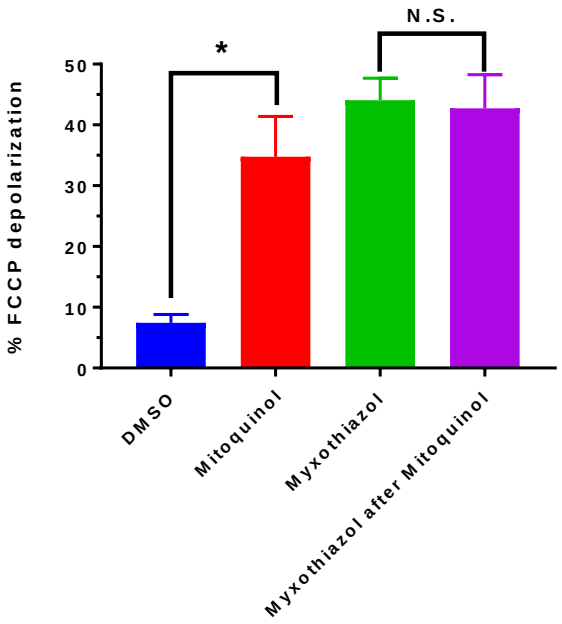

Figure 5.25: Fluorescence data from isolated mitochondria from liver of rat loaded with Rh123 in the presence of myxothiazol (10 μM) and mitoquinol (1 μM) or vehicle control (0.01% v/v DMSO). Data are expressed as a percentage of the maximum fluorescence obtained after addition of 1 μM FCCP in the same isolated mitochondria and are mean ± SEM from n=3. *p<0.05, One-way ANOVA followed by Tukey post-hoc test.

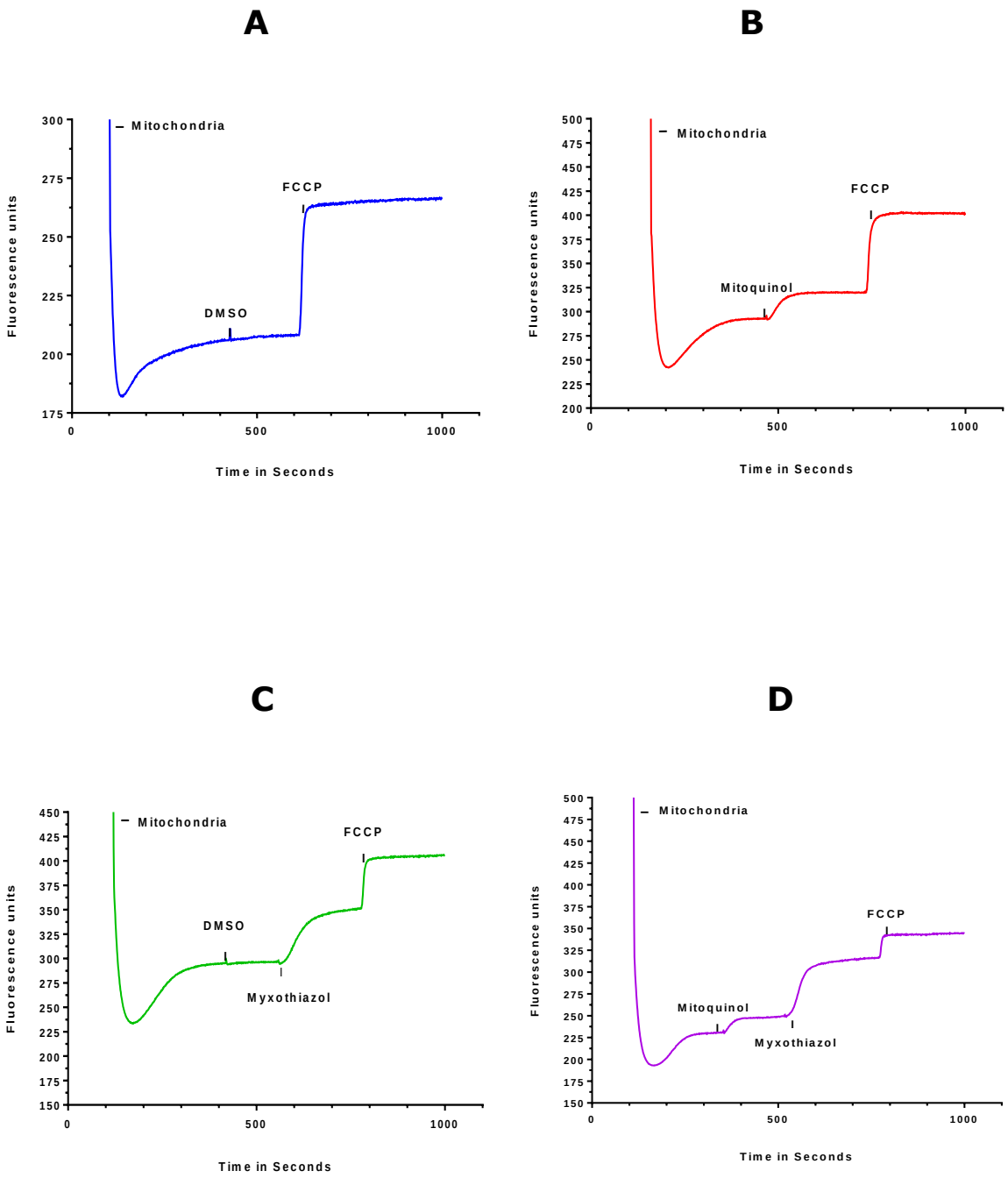

Figure 5.26: Typical traces showing the effect of **A-** 0.01% v/v DMSO, **B-** mitoquinol (1 μM), **C**- myxothiazol (10 μM) and **D**- myxothiazol (10 μM) after mitoquinol (1 μM) on Rh123 fluorescence in isolated mitochondria from rat liver. FCCP 1 μM was added as a positive control to get the maximum fluorescence.

5.3.14. The effect of AP39 (mitochondrial H_2S donor) on simvastatin response in isolated mitochondria from rat liver:

Mitochondrial H_2S can protect cells from increases in mitochondrial ROS production. In order to determine whether mitochondrial H_2S could have an effect on the simvastatin effect, the isolated mitochondria were exposed to 10 μM simvastatin in the absence or presence of AP39 (0.3 μM or 10 μM). The 0.3 μM AP39 alone had no effect on mitochondrial membrane potential compared to the control. In these experiments, although there was an apparent increase in total fluorescence in the isolated mitochondria with simvastatin compared to the vehicle control, this was not significant. Similarly, 0.3 μM AP39 appeared to reduce the simvastatin response but failed to achieve statistical significance. See figure 5.27 and 5.28.

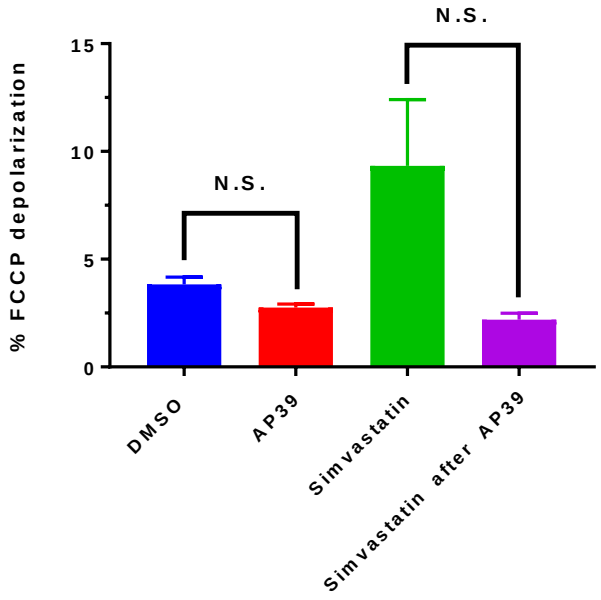

Figure 5.27: Cumulative fluorescence data from isolated mitochondria from liver of rat loaded with Rh123 in the presence of simvastatin (10 μM) and AP39 (0.3 μM) or vehicle control (0.01% v/v DMSO). Data are expressed as a percentage of the maximum fluorescence obtained after addition of 1 μM FCCP in the same isolated mitochondria and are mean ± SEM from n=3. One-way ANOVA followed by Tukey post-hoc test.

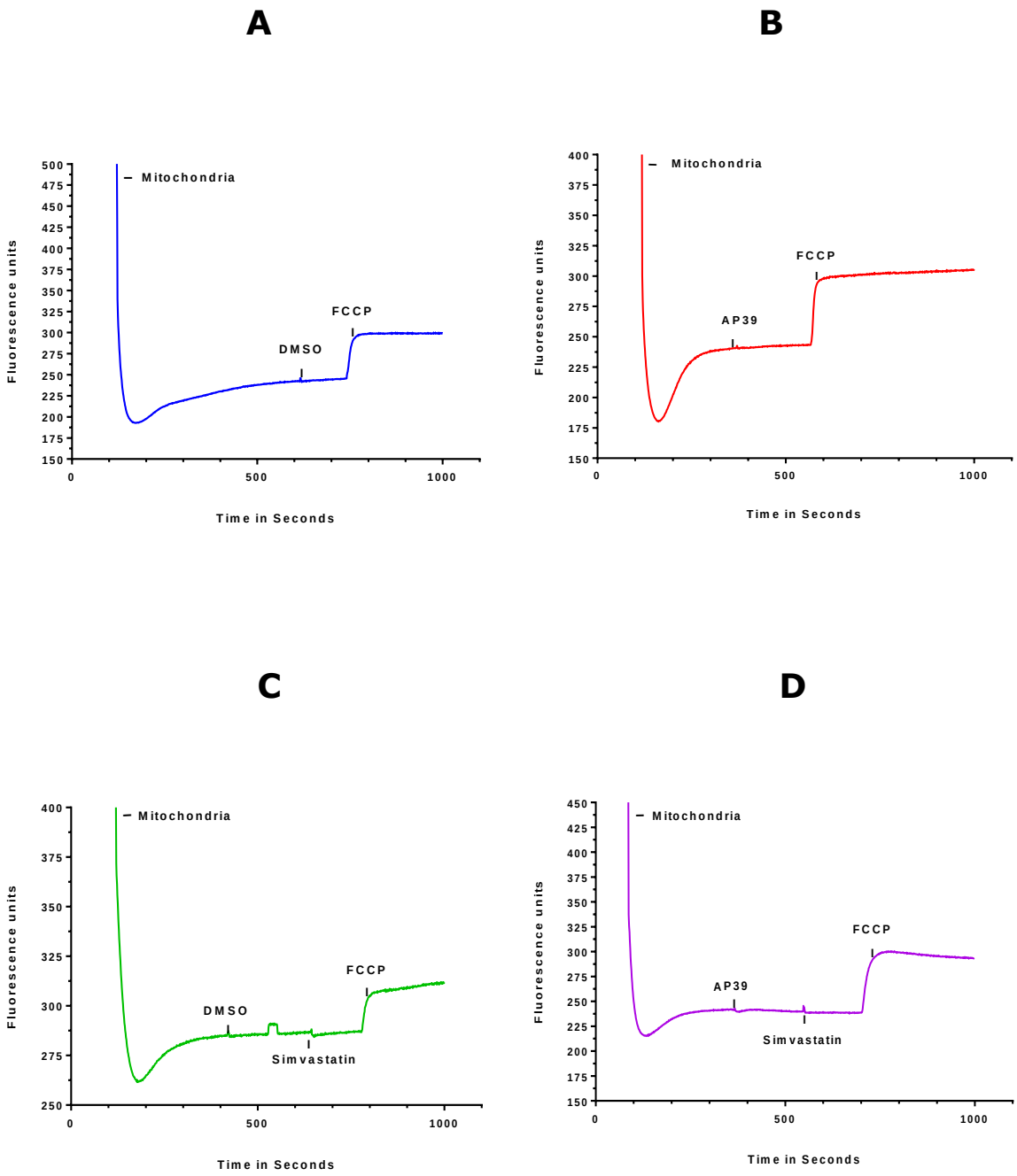

Figure 5.28: Typical traces showing the effect of **A-** 0.01% v/v DMSO, **B-** AP39 (0.3 μM), **C**- simvastatin (10 μM) and **D**- simvastatin (10 μM) after AP39 (0.3 μM) on Rh123 fluorescence in isolated mitochondria from rat liver. FCCP 1 μM was added as a positive control to get the maximum fluorescence.

In case of 10 μM AP39 alone, there was an increase in total fluorescence in the isolated mitochondria loaded with Rh123 (absorbance= 74± 2%) compared to the vehicle control (absorbance= 3± 1%). Simvastatin had no effect on mitochondrial membrane potential in the presence or absence of 10 μM AP39. See figure 5.29 and 5.30.

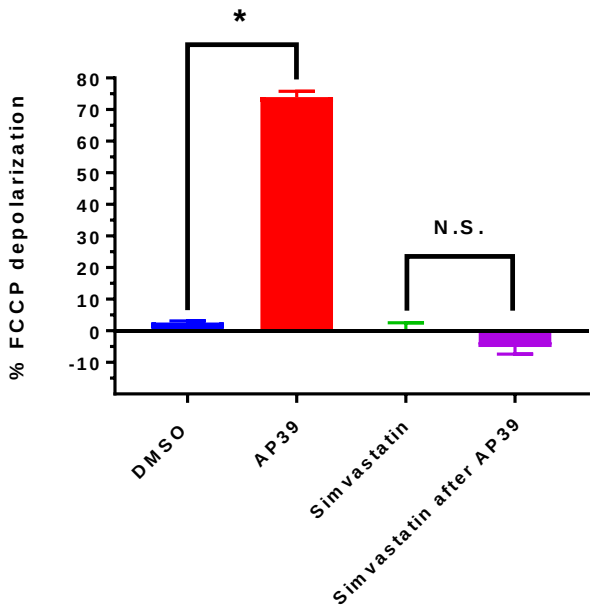

Figure 5.29: Fluorescence data from isolated mitochondria from liver of rat loaded with Rh123 in the presence of simvastatin (10 μM) and AP39 (10 μM) or vehicle control (0.01% v/v DMSO). Data are expressed as a percentage of the maximum fluorescence obtained after addition of 1 μM FCCP in the same isolated mitochondria and are mean ± SEM from n=3. *p<0.05, One-way ANOVA followed by Tukey post-hoc test.

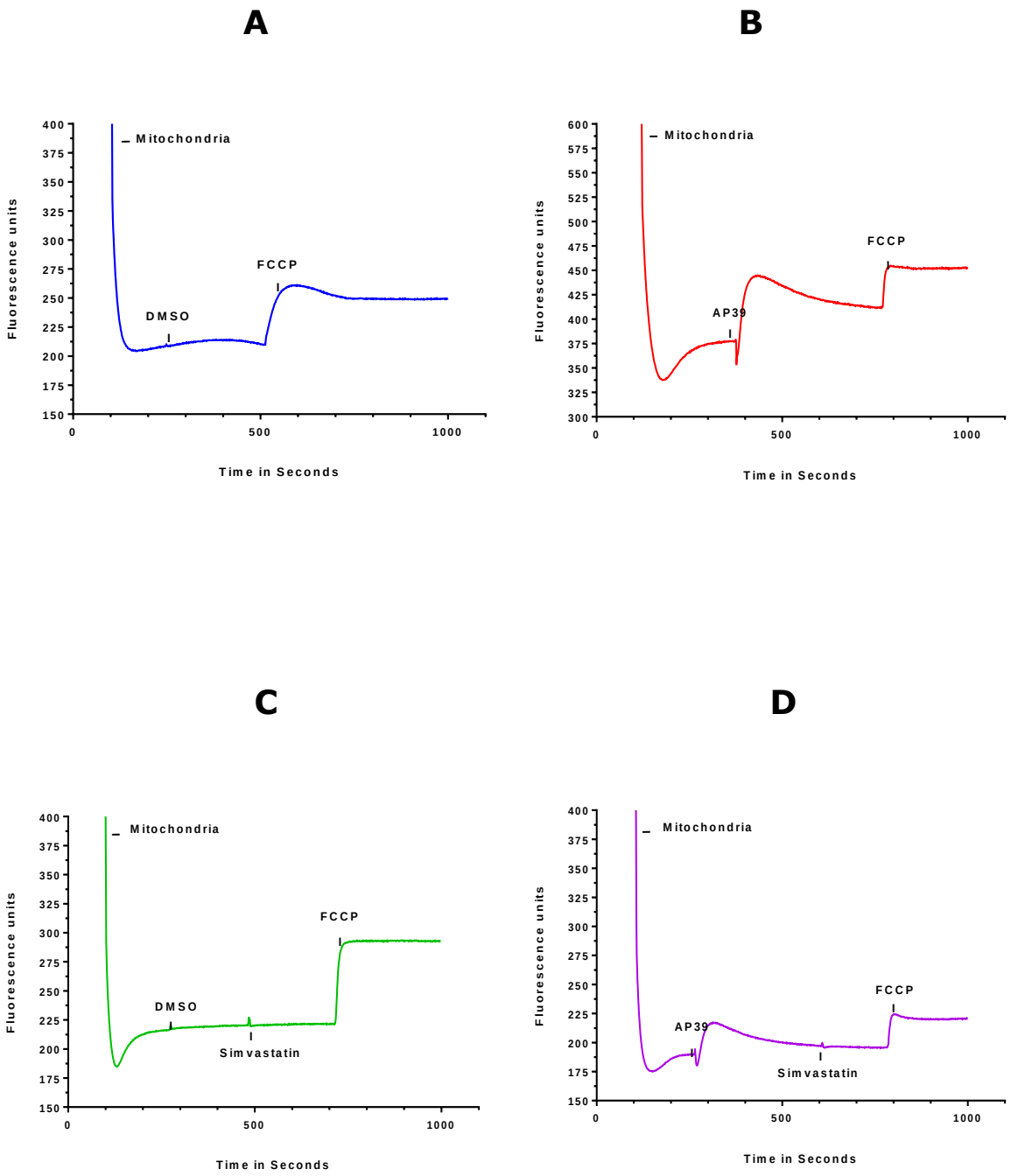

Figure 5.30: Typical traces showing the effect of **A-** 0.01% v/v DMSO, **B-** AP39 (10 μM), **C**- simvastatin (10 μM) and **D**- simvastatin (10 μM) after AP39 (10 μM) on Rh123 fluorescence in isolated mitochondria from rat liver. FCCP 1 μM was added as a positive control to get the maximum fluorescence.

5.3.15. The effect of AP39 (mitochondrial H_2S donor) on antimycin A (mitochondrial complex III inhibitor at Q_i site) response in isolated mitochondria from liver rat:

In order to determine whether mitochondrial H_2S could prevent the antimycin A effect, therefore, the isolated mitochondria were exposed to 10 μM antimycin A in the absence or presence of AP39 (0.3 μM or 10 μM). The 0.3 μM of AP39 alone had no effect on mitochondrial membrane potential comparing to the vehicle control. On the other hand, AP39 had no significant effect on the antimycin A response. See figure 5.31 and 5.32.

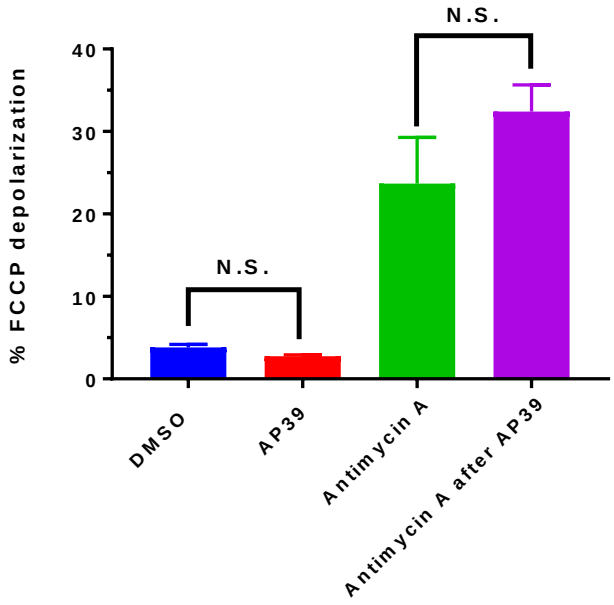

Figure 5.31: Cumulative fluorescence data from isolated mitochondria from liver of rat loaded with Rh123 in the presence of antimycin A (10 μM) and AP39 (0.3 μM) or vehicle control (0.01% v/v DMSO). Data are expressed as a percentage of the maximum fluorescence obtained after addition of 1 μM FCCP in the same isolated mitochondria and are mean ± SEM from n=3. One-way ANOVA followed by Tukey post-hoc test.

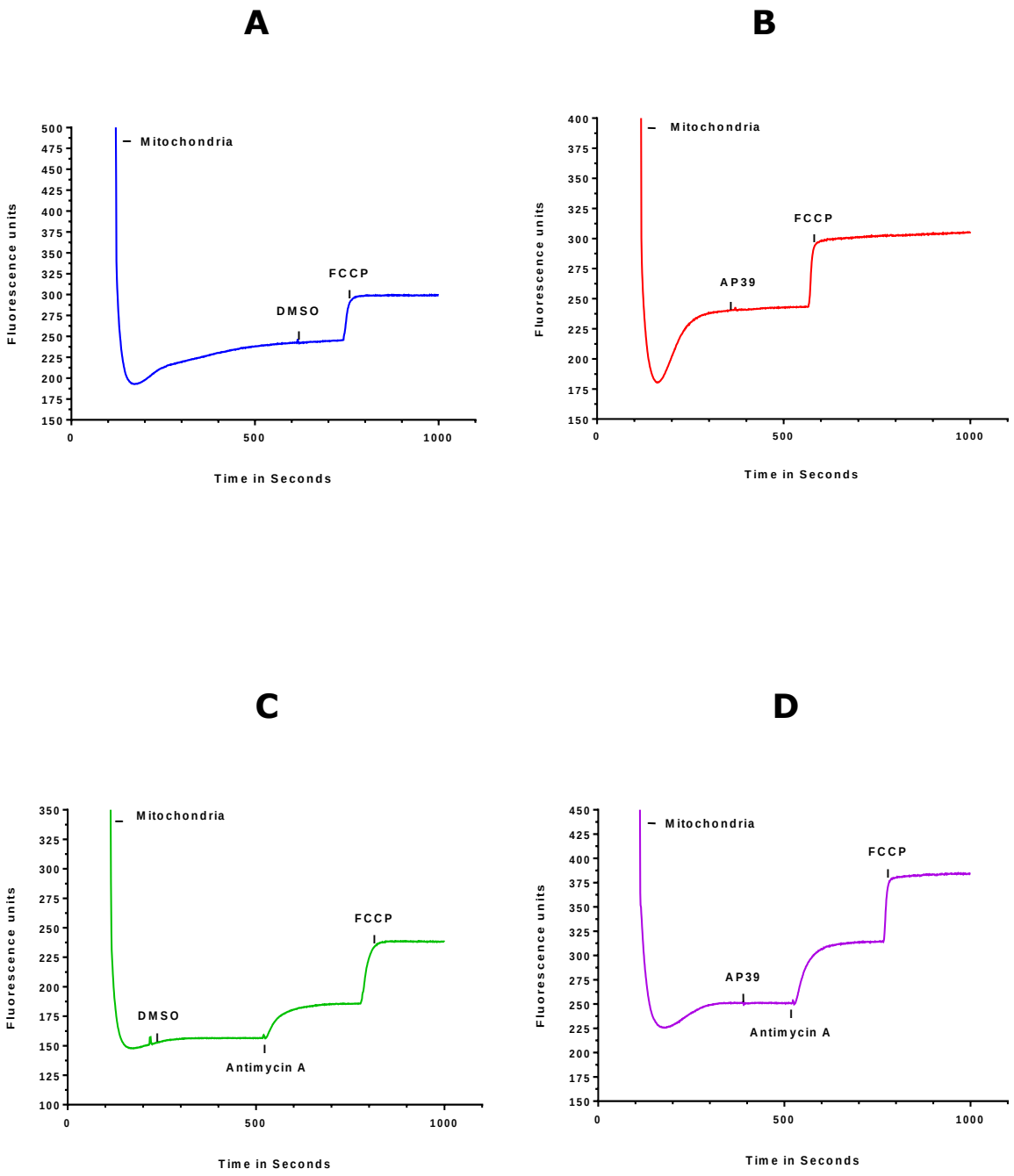

Figure 5.32: Typical traces showing the effect of **A-** 0.01% v/v DMSO, **B-** AP39 (0.3 μM), **C**- antimycin A (10 μM) and **D**- antimycin A (10 μM) after AP39 (0.3 μM) on Rh123 fluorescence in isolated mitochondria from rat liver. FCCP 1 μM was added as a positive control to get the maximum fluorescence.

In case of 10 μM AP39 alone, there was an increase in total fluorescence in the isolated mitochondria loaded with Rh123 (absorbance= 74± 2%) compared to the vehicle control (absorbance= 3± 1%). 10 μM AP39 had no significant effect on the antimycin A response. See figure 5.33 and 5.34.

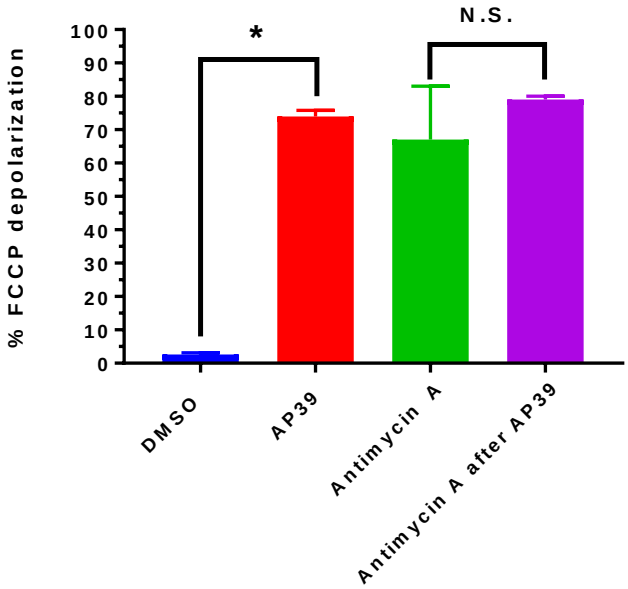

Figure 5.33: Fluorescence data from isolated mitochondria from liver of rat loaded with Rh123 in the presence of antimycin A (10 μM) and AP39 (10 μM) or vehicle control (0.01% v/v DMSO). Data are expressed as a percentage of the maximum fluorescence obtained after addition of 1 μM FCCP in the same isolated mitochondria and are mean ± SEM from n=3. *p<0.05, One-way ANOVA followed by Tukey post-hoc test.

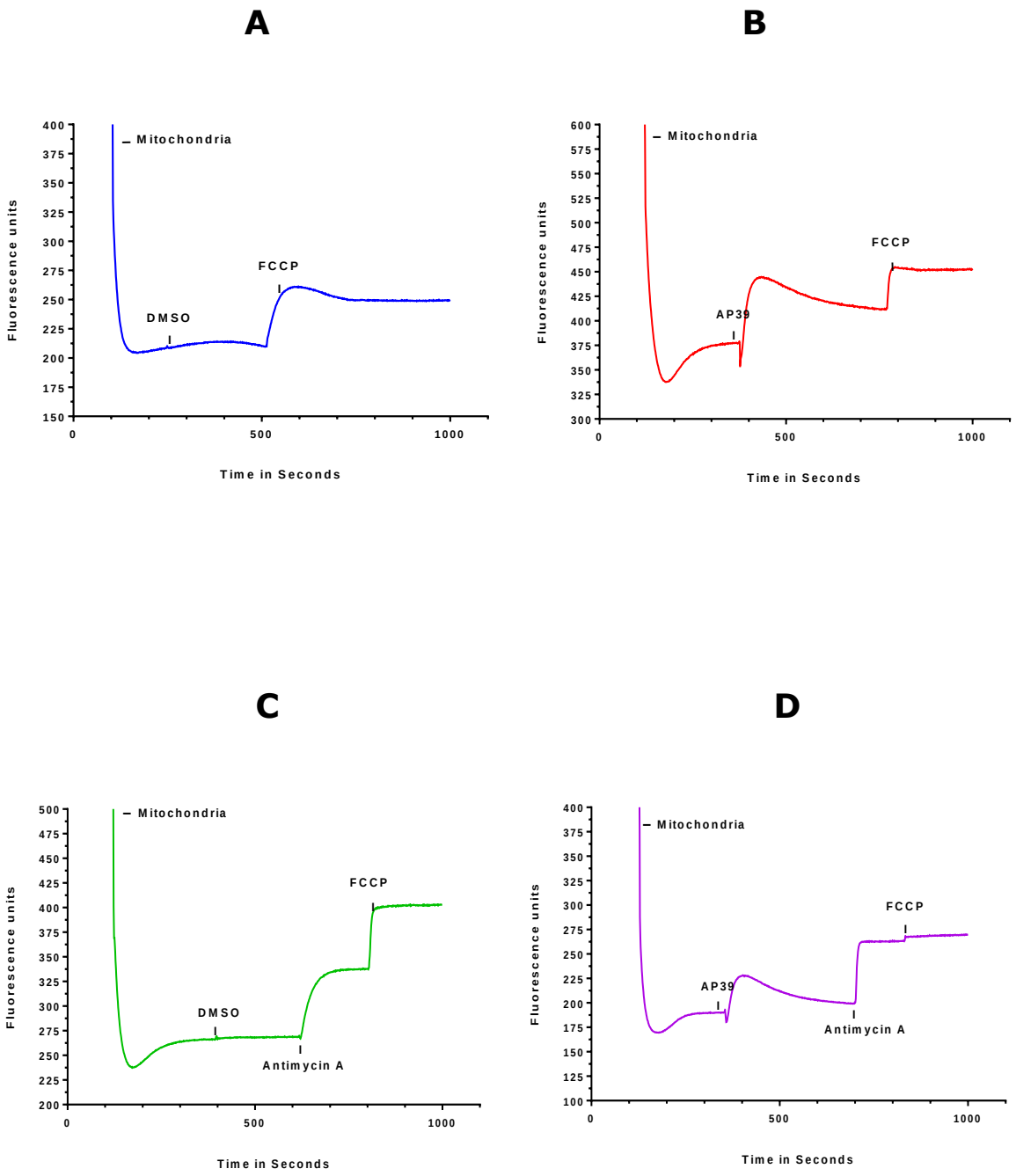

Figure 5.34: Typical traces showing the effect of **A-** 0.01% v/v DMSO, **B-** AP39 (10 μM), **C**- antimycin A (10 μM) and **D**- antimycin A (10 μM) after AP39 (10 μM) on Rh123 fluorescence in isolated mitochondria from rat liver. FCCP 1 μM was added as a positive control to get the maximum fluorescence.

5.3.16. The effect of AP39 (mitochondrial H_2S donor) on myxothiazol (mitochondrial complex III inhibitor at Q_o site) response in isolated mitochondria from rat liver:

In order to determine whether mitochondrial H_2S could prevent myxothiazol effect, therefore, the isolated mitochondria were exposed to 10 µM myxothiazol in the absence or presence of AP39 (0.3 µM). AP39 alone had no effect on mitochondrial membrane potential compared to the vehicle control or on the myxothiazol response. See figure 5.35 and 5.36.

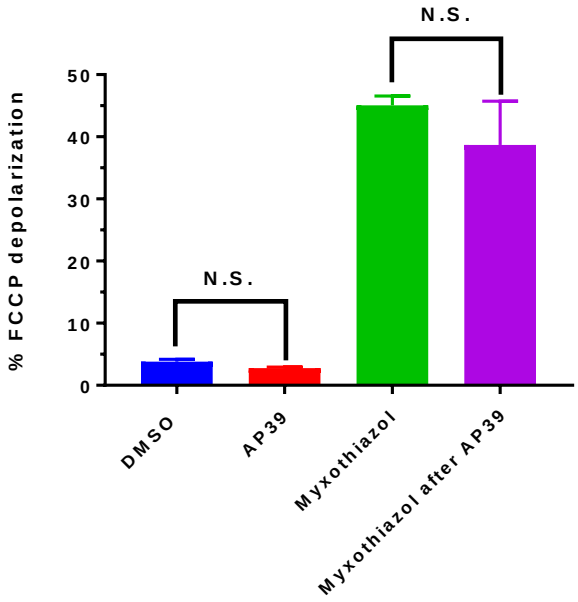

Figure 5.35: Fluorescence data from isolated mitochondria from liver of rat loaded with Rh123 in the presence of myxothiazol (10 µM) and AP39 (0.3 µM) or vehicle control (0.01% v/v DMSO). Data are expressed as a percentage of the maximum fluorescence obtained after addition of 1 µM FCCP in the same isolated mitochondria and are mean ± SEM from n=3. One-way ANOVA followed by Tukey post-hoc test.

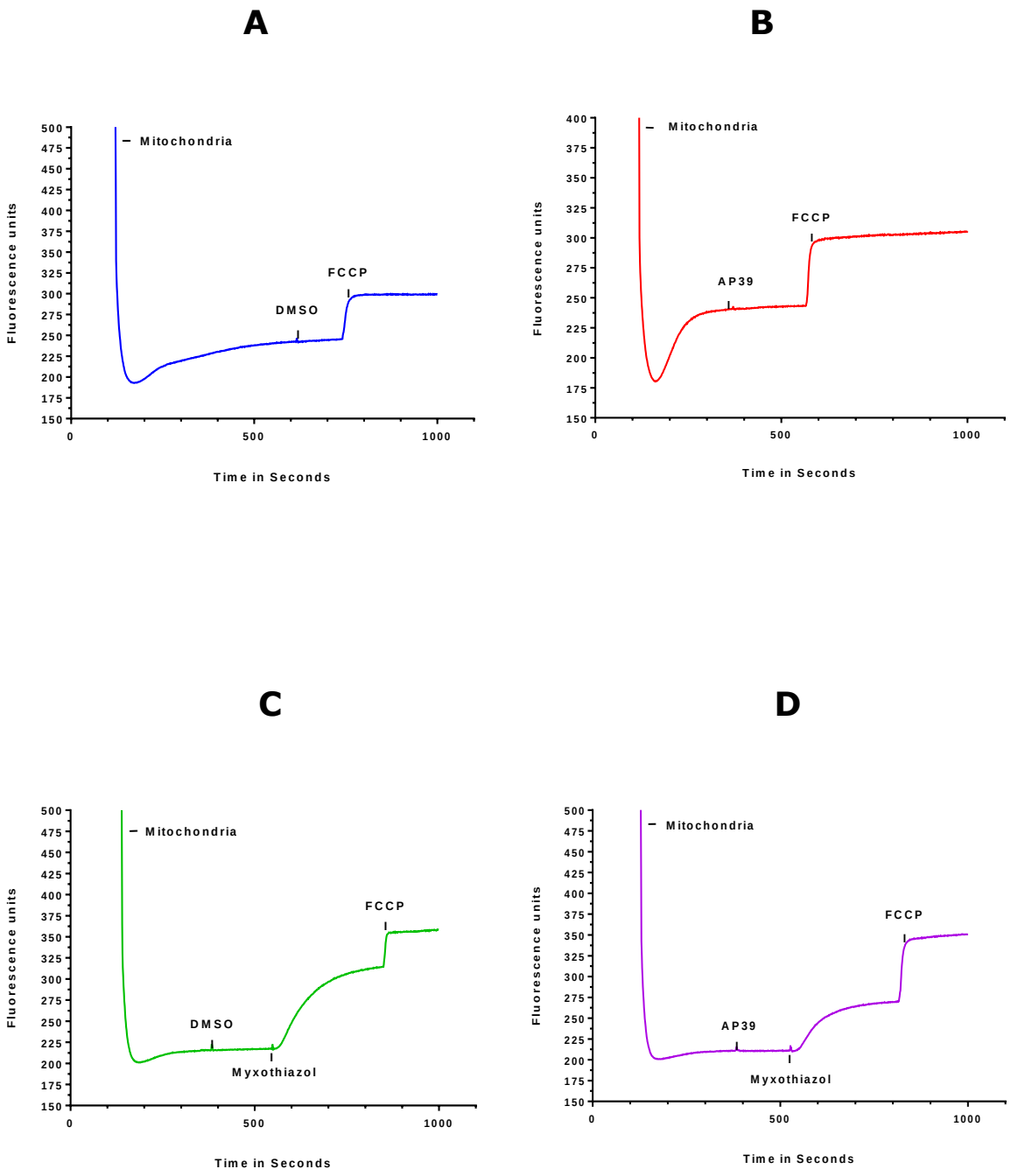

Figure 5.36: Typical traces showing the effect of **A-** 0.01% v/v DMSO, **B-** AP39 (0.3 μM), **C**- myxothiazol (10 μM) and **D**- myxothiazol (10 μM) after AP39 (0.3 μM) on Rh123 fluorescence in isolated mitochondria from rat liver. FCCP 1 μM was added as a positive control to get the maximum fluorescence.

5.3.17. The effect of lactone form of simvastatin (pro-drug) and hydroxy acid form of simvastatin (pharmacologically active) on mitochondria isolated from liver of rat:

In order to determine whether the active form of simvastatin has a different effect on mitochondrial membrane potential compared to the lactone form of simvastatin, the effect of 10 µM simvastatin and 10 µM of the active metabolite of simvastatin on the isolated mitochondria were determined. Simvastatin and the active form of simvastatin had no significant effect on membrane potential compared to the vehicle control in the isolated mitochondria loaded with Rh123. See figure 5.37 and 5.38.

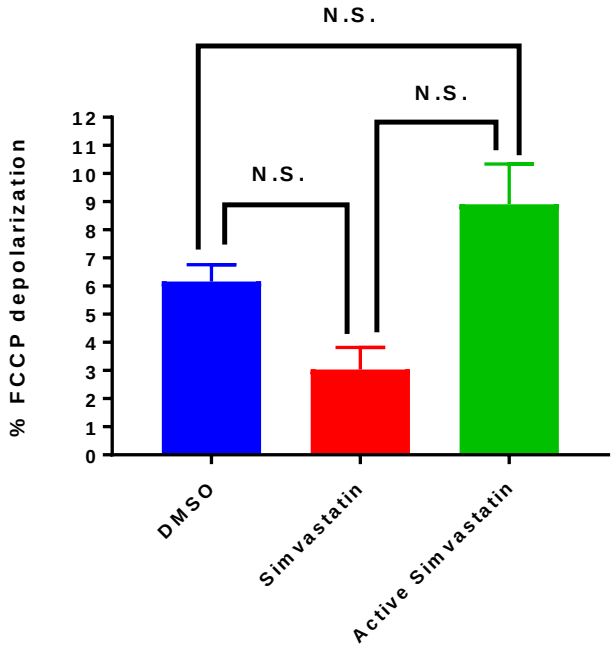

Figure 5.37: Fluorescence data from isolated mitochondria from rat's liver loaded with Rh123 in the presence of simvastatin (10 µM), active simvastatin (10 µM) or vehicle control (0.01% v/v DMSO). Data are expressed as a percentage of the maximum fluorescence obtained after addition of 1 µM FCCP in the same isolated mitochondria and are mean ± SEM from n=3. One-way ANOVA followed by Tukey post-hoc test.

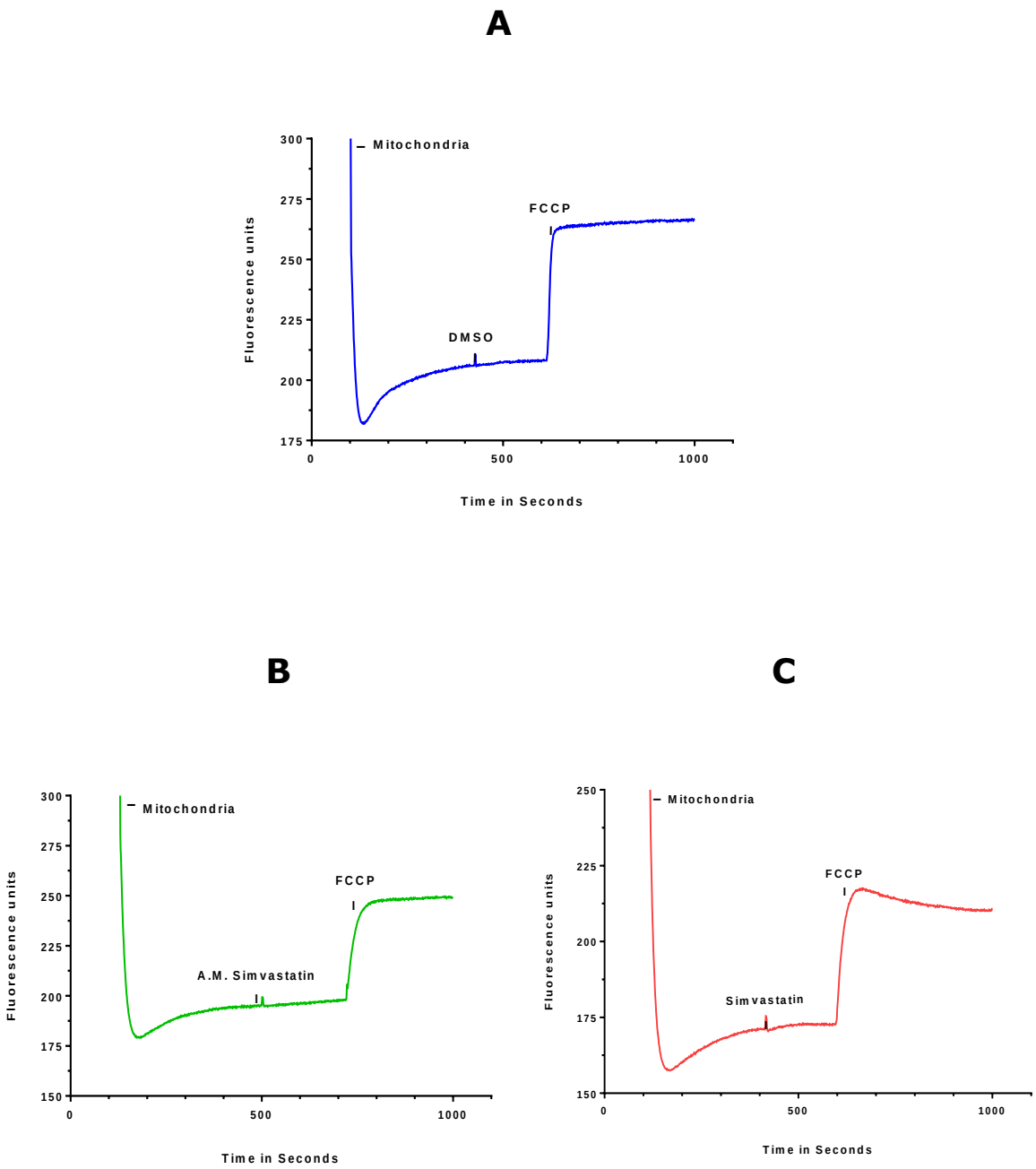

Figure 5.38: Typical trace showing the effect of **A-** 0.01% v/v DMSO, **B-** simvastatin (10 µM) and **C-** active metabolite simvastatin (10 µM) on Rh123 fluorescence in isolated mitochondria from rat liver. FCCP 1 µM was added as a positive control to get the maximum fluorescence.

5.4. Discussion:

Statins inhibit HMG-CoA reductase, leading to a reduction in synthesis of mevalonate and hence cholesterol. Many large trials have established that statins are significantly declined the rate of cardiovascular morbidity and mortality (Shepherd et al. 1995; Ford et al. 2007; Ramkumar, Raghunath, and Raghunath 2016). On the other hand, the Heart Protection study demonstrated that statins benefit patients with ”normal” cholesterol levels (Pedersen 2010). The overall beneficial effects of statins not only come from the reduction of cholesterol, but also come from cholesterol-independent effects known as pleiotropic effects (Barone, Di Domenico, and Butterfield 2014). One of the important pleiotropic effects is the regulation of vascular tone.

The data presented in the previous chapters demonstrated that simvastatin inhibited the U46619-induced contraction in PCA only in the presence of calcium and possibly via mitochondrial inhibition at complex III. Inhibition of complex III with antimycin A or myxothiazol also inhibits the U46619-induced contraction. However, there were differences in the mechanism by which these inhibitors produced their effect, with myxothiazol showing similarities with the effect of simvastatin. Indeed, CoQ10 and mitoquinol only prevented the effect of antimycin A; they had no effect on either the simvastatin or the myxothiazol response. Therefore, the aim of this chapter was to determine the effect of simvastatin and the mitochondrial complex inhibitors on mitochondrial membrane potential and then to determine whether CoQ10, mitoquinol or the H_2S donor AP39 could prevent these effects.

Although a previous study in our laboratory showed that simvastatin has an effect on mitochondrial membrane potential in intact blood vessels and smooth muscle cells via using similar method and technique used in the present study (Almukhtar et al. 2016). The data in this present study showed that simvastatin could not increase the Rh123 fluorescence beyond that seen with the vehicle control. Initial studies used simvastatin in 0.1% DMSO. However, this concentration of DMSO produced a relatively large change in fluorescence on its own, which we thought might be preventing the effects of simvastatin. We, therefore, reduced the DMSO concentration. Although the effect of vehicle control was lower, simvastatin still failed to produce a change in fluorescence beyond that seen with the vehicle control. This suggests that simvastatin has no direct effect on the mitochondria, or, at least, not in a way that changes rhodamine fluorescence.

A previous study in our laboratory showed that simvastatin caused a change in mitochondrial membrane potential in the intact porcine coronary artery at 10 μM (Almukhtar et al. 2016). Similarly, a study in skeletal muscle myocytes showed that simvastatin altered mitochondrial membrane potential with an EC_{50} of around 2 μM (Sirvent

et al. 2005). Studies on isolated mitochondria have used far higher concentrations than those used in this study.

For example, in a study performed on isolated mitochondria from rat, the researchers found that simvastatin has a direct effect on mitochondria in a concentration-dependent manner (10-80 μM) via inducing changes in mitochondrial transition permeability (Velho et al. 2006). A previous study showed that 20 μM statin has a direct effect on mitochondrial electron transport chain and caused an impairment in mitochondria functions such as maintenance of calcium homeostasis and antioxidant effect (De Pinieux et al. 1996). Studies have suggested that statins effect on mitochondria is more likely to depend on statin concentrations. At lower micromolar concentrations and in a neonatal rat cardiac myocytes, the statins induced a protective mitochondrial effect via an antioxidant mechanism involving inhibition of Rac1 (Takemoto et al. 2001). At concentrations higher than 10 μM, statins could produce a damaging effect to the mitochondria as in a study performed on human rhabdomyosarcoma cells in which 30 μM simvastatin enhanced the mitochondrial pathway of apoptosis (Werner, Sacher, and Hohenegger 2004).

As the effects of simvastatin on mitochondrial membrane depolarization at low micromolar concentrations were seen in intact cells or tissues, we hypothesized that the ability of simvastatin to depolarize mitochondria depends primarily on the conversion of simvastatin to an active metabolite and, therefore, requires intact cells. This would explain why simvastatin had no effect on isolated mitochondria but has been seen to have an effect in intact tissues. Consequently, we used 10 μM of an active form of simvastatin. However, again, we did not see significant changes in mitochondrial membrane potential, although, there was a larger increase in Rh123 fluorescence compared to the lactone form of simvastatin (10 μM). It is possible that the active form cannot be taken up into the isolated mitochondria. The inactive pro-drug may need to be converted into the active form, but the incubation time was not long enough for this to occur (Kearney et al. 1993). Studies showed that simvastatin can be converted from the lactone form (pharmacologically inactive) to the hydroxy acid form (active) in an alkaline medium within 24 h while in acidic medium, the rate of conversion is too slow and it needs more time. Therefore, any change in the pH could change the acid-base balance and the chemical reactions required for simvastatin interconversion (Prueksaritanont et al. 2001; Prueksaritanont et al. 2005). In addition, the solubility is important for penetration of mitochondrial membrane and inducing an effect. The lactone form simvastatin is more lipophilic while the hydroxy acid form of simvastatin is more hydrophilic (Beretta et al. 2011). This suggests that preparing conditions nearer to the physiological conditions could enable simvastatin for better penetration with enough concentration to induce the change in mitochondrial membrane

potential. Longer incubation with the active form may have led to a response in the mitochondria. Indeed, in the intact blood vessels, a 2 h incubation was carried in order to observe anti-contractile effects (chapter 2).

In order to see if inhibition of the mitochondrial ETC could uncover a response to simvastatin, mitochondria were exposed to 10 μM rotenone (complex I inhibitor), 10 μM antimycin A (complex III inhibitor at Q_i site) or 10 μM myxothiazol (complex III inhibitor at Q_o site). Unlike simvastatin, both antimycin A and myxothiazol increased Rh 123 fluorescence, indicating that inhibition of complex III can lead to a change in the mitochondrial membrane potential. The changes in the proton movement across the inner membrane space and the respiratory chain were followed by using Rh123 fluorescence dye, which represents the changes in mitochondrial membrane potential as increase or decrease in Rh123 fluorescence (Emaus, Grunwald, and Lemasters 1986). Adding a mitochondrial complex inhibitor blocks electron movement through the electron transport chain which leads to a decrease in mitochondrial membrane potential, which appears as an elevation in Rh123 fluorescence (Baracca et al. 2003). The fact that myxothiazol and antimycin A caused a change in Rh123 fluorescence, whereas simvastatin did not, suggests that simvastatin does not act through complex III.

In the tissue bath studies, co-enzyme Q10 (CoQ_{10}), which is a vital component of the mitochondrial electron transport system (Littarru and Tiano 2007) and mitoquinol, the reduced form of CoQ_{10} (Fink et al. 2012) both prevented the anti-contractile effect of antimycin A, but not myxothiazol or simvastatin. We hypothesised that this could be because these compounds are able to prevent the effects of antimycin A on the electron transport chain and hence on the mitochondrial membrane potential. CoQ_{10} at 5μM had no effect on mitochondrial membrane potential. However, supplementation of isolated mitochondria with CoQ_{10} could not prevent the reduction in mitochondrial membrane potential caused by antimycin A and myxothiazol. This could indicate that the effect of CoQ_{10} on the antimycin A anti-contractile effect is not due to a reversal of the effect of antimycin A on the electron transport chain. In a study performed on isolated mitochondria from pig brain, the study showed that high concentration of co-enzyme Q10 (12.5-100 μM) could improve mitochondrial respiration rate which mostly linked at complex I. This probably means that there is support of electron transfer between complex I and complex III, possibly through integration of co-enzyme Q10 into the inner mitochondrial membrane (Fisar et al. 2016).

Mitoquinol (a reduced form of coenzyme Q10), in contrast, increased Rh123 fluorescence on its own. The antimycin A effect on mitochondrial membrane potential was non-significantly enhanced in the presence of mitoquinol whereas the myxothiazol effect was unaltered. A study performed on rat liver mitochondria and on mitochondria within cells

showed that mitoquinol in a concentration more than 25 μM resulted in a loss of the mitochondrial membrane potential, and the oxidizing of mitoquinol to mitoquinone in mitochondria was inhibited by the complex III inhibitor myxothiazol (Kelso et al. 2002). This probably could explain the inability of 1 μM mitoquinol to alter the myxothiazol effect. In contrast, there was non-significant prevention of the effect of rotenone on mitochondrial action potential by mitoquinol. This possibly indicates that mitoquinol could displace rotenone from its binding site even partially, as the reduction in Rh123 fluorescence was not too much, and then improve the forward movement of electron. On the other hand, mitoquinol enhances the movement of electrons in the opposite direction at complex III where the Q cycle and CoQ_{10} are predominate. In contrast to the data presented here, a previous study performed on isolated mitochondria from endothelial cells identified that 1 μM mitoquinol could prevent the 5 μM rotenone effect and inhibit ROS production at complex I while at complex III, mitoquinol had a little enhancement effect on ROS production depending on substrate provided for mitochondria fuel (O'Malley et al. 2006) and concentration of the complex inhibitor used (Fink et al. 2009).

Similar to CoQ10, H_2S may also support the transfer of electrons through the mitochondrial electron transport chain (Szabo, Ransy, Módis, et al. 2014). AP39, an H_2S donor, at 0.3 μM showed no effect on mitochondrial membrane potential while 10 μM AP39 caused a significant elevation in Rh 123 fluorescence. This suggests that at this high concentration it has a direct effect on the mitochondrial membrane potential but towards disruption of mitochondrial function. Therefore, we used the lower concentration of AP39 to ensure that it does not have an inhibitory effect on the mitochondrial ETC.

Although simvastatin had no effect on the mitochondrial membrane potential beyond that seen with DMSO, there was a non-significant reduction in this response in the presence of AP39 at both concentrations. This suggests that the effect of DMSO on the mitochondrial membrane potential could be prevented by the release of H_2S in the mitochondria. Similarly, there was a non-significant reduction in the myxothiazol response and a non-significant enhancement in antimycin A response in the presence of AP39. The lack of effect of AP39 could be due to the high concentration produced an effect on the isolated mitochondria on its own, whereas the low concentration was not high enough to prevent the effects of the complex inhibitors. Alternatively, the limited number of repeats may not have been enough to see a significant effect.

A study performed on chicken liver mitochondria showed that inhibition of complex I with 5 μM rotenone had no effect on >5 μM sulfide oxidation and mitochondrial respiration while inhibition of complex III with 10 μM antimycin A impeded it (Yong and Searcy 2001). Another study performed on bovine heart mitochondria revealed that AP39 could reduce elevated mitochondrial membrane potential due to hyperglycaemia and improve

mitochondrial respiration at complex III (Gero et al. 2016). Moreover, a study performed on cardio-myocyte mitochondria isolated from mouse showed that AP39 could feed the mitochondrial ETC with electrons but without affecting mitochondrial respiration rate. In addition, the study clarified that AP39 supplied the ETC with electrons at the level of coenzyme Q where sulfide quinone reductase activity is involved, thus, the electrons moved toward complex III and IV without passing complex I and II (Karwi et al. 2017b). The study also identified that AP39 at low concentration (1 μM) could reduce mitochondrial ROS production but this effect was decreased with increasing AP39 concentration (Goubern et al. 2007; Szabo, Ransy, Modis, et al. 2014).

Finally, an alternative explanation for the effects of CoQ10, mitoquinol, and AP39 on the anti-contractile effect of antimycin A, as seen in the previous chapter, is that these compounds have antioxidant effects, which prevents the anti-contractile response, but does not prevent the effects of antimycin A on the mitochondrial membrane potential. In other words, inhibition of complex III by antimycin A leads to the production of ROS, which are then "mopped up" by these antioxidants. Alternatively, other measurements of mitochondrial function, such as respiration rate, may be a better indication of mitochondrial function under these conditions, compared to changes in mitochondrial membrane potential.

In summary, the data presented in this chapter demonstrated that simvastatin had no direct effect on the isolated mitochondria, in contrast to previous studies in intact cells or tissues. Antimycin A and myxothiazol (complex III inhibitors) both changed the Rh123 fluorescence, indicating that they decreased the mitochondrial membrane potential, and confirming their effect on the mitochondria. Adding mitoquinol alone also reduced the mitochondrial membrane potential, as did a high concentration of AP39 (H_2S donor). Figure 5.39 shows a schematic diagram summarising the results from this chapter.

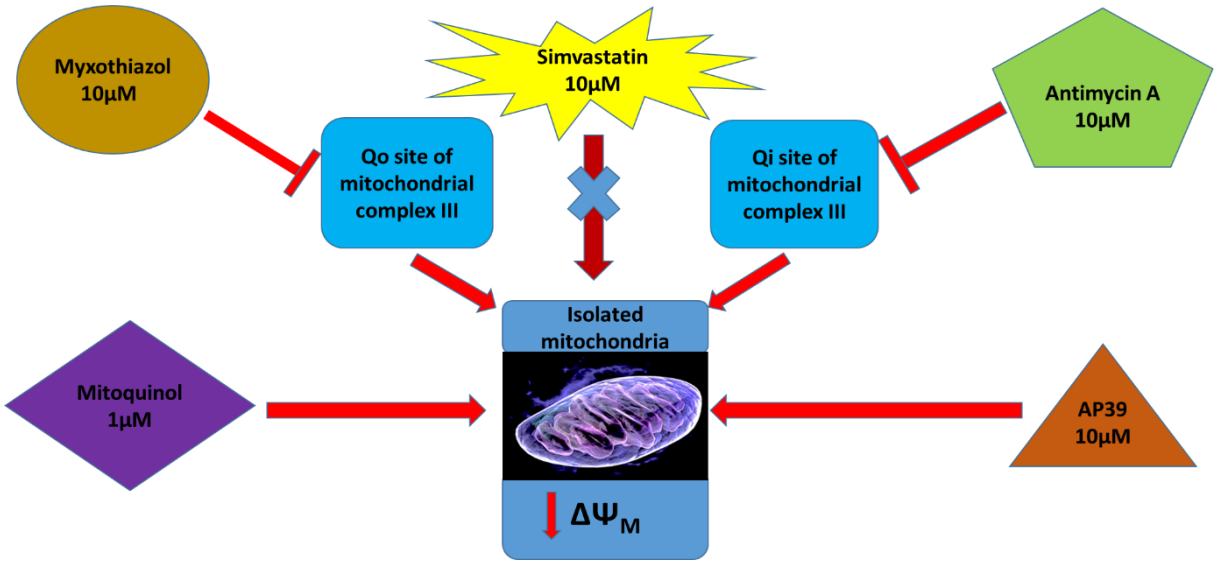

Figure 5.39: Hypothesized schematic diagram of effect of simvastatin, antimycin A, myxothiazol, AP39 and mitoquinol on isolated mitochondria. The present study demonstrated that simvastatin had no direct effect while antimycin A, myxothiazol, AP39 and mitoquinol reduced mitochondrial membrane potential.

Chapter VI

General discussion

6.1. General discussion:

The main findings of this study were as follows; in the second chapter, the study showed that simvastatin inhibits the U46619-induced contraction in PCA only in the presence of calcium possibly via mitochondrial inhibition. The combination of inhibitors of mitochondrial complexes I and III (rotenone-myxothiazol) reduced this inhibitory effect. This was consistent with the finding of others who suggested that statins may regulate vascular tone through inhibition of mitochondrial function (Bełtowski and Jamroz-Wiśniewska 2012; Broniarek and Jarmuszkiewicz 2016; Almukhtar et al. 2016). The data presented in chapter two also indicated that simvastatin inhibited calcium influx. One aim of this study was to determine if the inhibition of calcium influx is related to the effect of simvastatin on the mitochondria. The combination of rotenone-myxothiazol prevented the inhibitory effect of simvastatin on the Bay K 8644-induced contraction suggesting that the effects of simvastatin on calcium-induced contractions may be due to mitochondrial effects. This possibly means that calcium channel activation is downstream of the mitochondria and this is how simvastatin reduces calcium channels activity. Alternatively, the combination of rotenone and myxothiazol could oppose the effect of simvastatin directly at the calcium channels, rather than within the mitochondria. This suggests that there is a link between inhibition of mitochondrial function, calcium influx and inhibition of smooth muscle contraction by simvastatin in PCA. In order to clarify the role that mitochondria might play in the simvastatin responses in the PCA, we tested the effect of complex III inhibitors (antimycin A and myxothiazol) on the U46619-induced contraction in PCA then compared with simvastatin effect in the second and third chapters.

With antimycin A, we found that it inhibits the contractile responses in PCA and the anti-contractile effects are mediated through inhibition of calcium influx through L-type calcium channels as well as inhibition of calcium-independent contractions. Unlike simvastatin, the rotenone-myxothiazol combination had no effect on the antimycin A inhibitory effect, suggesting differences between the mechanism of action of simvastatin and antimycin A. On the other hand, the inhibitory effect of myxothiazol on the U46619-induced contraction showed similarities with simvastatin. Both simvastatin and myxothiazol inhibited the contractile responses in PCA only in the presence of calcium and the data suggest that the anti-contractile effects of both are mediated through inhibition of calcium influx through L-type VGCC, which was similar to previous finding (Makowska, Zablocki, and Duszynski 2000).

Further experiments demonstrated differences between simvastatin and antimycin A, but similarities between simvastatin and myxothiazol. Addition of co-enzyme Q10 or mitoquinol attenuated the inhibitory effect of antimycin A but had no effect on either the myxothiazol and simvastatin response. In addition, the AMPK inhibitor dorsomorphin inhibited the anti-

contractile effect of antimycin A, but had not effect on simvastatin or myxothiazol. Furthermore, adding the mitochondrial H_2S donor AP39 had no effect on the simvastatin or myxothiazol response while with antimycin A there was partial prevention. These data from the functional studies indicate a similarity in action between simvastatin and myxothiazol, which suggests that simvastatin might be acting through inhibition of the complex III Q_o site in the mitochondria. This finding is consistent with the previous findings of others (Brandt, Schagger, and von Jagow 1988) and (Schirris et al. 2015) who revealed that statin lactones, in which simvastatin is one of the best examples for widely used statin lactones medication, exert their mitochondrial inhibitory effect mainly via inhibition at the Q_o site of complex III rather than Q_i .

The present study also identified the role of calcium inhibition in the simvastatin inhibitory effect and brought more evidence to confirm the similarity between simvastatin and myxothiazol. The study showed that simvastatin, myxothiazol, and antimycin A inhibited $CaCl_2$-induced contraction and Bay K 4668-induced contraction. The combination of antimycin A and rotenone enhanced the simvastatin inhibitory effect on the calcium-induced contraction, whereas the myxothiazol-rotenone combination had no further effect above that of simvastatin. In addition, the nifedipine-induced relaxation was partially inhibited at the higher concentrations by simvastatin and myxothiazol but not antimycin A. These data suggest that inhibition of complex III at the Q_o site leads to inhibition of calcium influx through L-type calcium channels.

In order to confirm the inhibitory effects of the compounds on mitochondrial function, experiments performed on mitochondria isolated from rat liver. However, we found that simvastatin had no direct effect on the isolated mitochondria, in contrast to previous studies in intact tissues or cells (Almukhtar et al. 2016). Antimycin A and myxothiazol (complex III inhibitors) both changed Rh123 fluorescence, indicating that they decreased the mitochondrial membrane potential. The fact that myxothiazol and antimycin A caused a change in Rh123 fluorescence, whereas simvastatin did not, suggesting that simvastatin does not act through complex III. Adding mitoquinol reduced the mitochondrial membrane potential and enhanced the effect of antimycin A. In contrast, the rotenone effect on mitochondrial membrane potential was prevented by adding mitoquinol, which possibly indicates that mitoquinol acts as mitochondrial protector at complex I rather than complex III. Similarly, the mitochondria-targeted H_2S donor AP39 had no effect on the change in mitochondrial membrane potential induced by the complex inhibitors. The lack of effect of AP39 could be due to the fact that at a high concentration produced an effect on the isolated mitochondria on its own, whereas the low concentration was insufficient to prevent the effects of the complex inhibitors.

As a conclusion, the data from the functional studies support the hypothesis that simvastatin produces anti-contractile effects through inhibition of the Q_o site at mitochondrial complex III. The data also support the hypothesis that inhibition of complex III at the Q_o site leads to inhibition of calcium influx through L-type calcium channels, although how this occurs is yet unknown. These data are supported by comparisons with mitochondrial complex inhibitors and do not necessarily indicate a direct inhibition of complex III, but could indicate an indirect mechanism. Indeed, the experiments on isolated mitochondria do not support a direct effect on the mitochondria, although we cannot rule out that any inhibition of mitochondrial function is due to a metabolite. The finding of this study come to support previous studies, which identified the effect of simvastatin on calcium influx and on mitochondria. In addition, this study brought more clarification and evidence about the anti-contractile effect of simvastatin that could underlie the pleiotropic effects of statins. The data also support the role of mitochondria in the regulation of vascular tone and indicate the targeting the mitochondria at different complexes of the ETC produce different signalling effects.

6.2. Limitations:

One of the limitations in this present study was the use of rat liver mitochondria rather than mitochondria obtained from pigs, as a comparison with the functional studies. We found it was difficult to get stable and active isolated mitochondria from pigs heart. Another major limitation is the attempt to link effects on the mitochondria using functional studies. A limitation with tools for disrupting or preserving mitochondrial function meant that comparisons had to be made with known mitochondrial complex inhibitors. Although similarities were observed between the effects of simvastatin and myxothiazol, these could be incidental.

Another major limitation is that the present study demonstrated the acute effect of simvastatin on mitochondria and calcium influx but does the chronic or long term incubation have a similar effect? Because long-term use could lead to accumulation in mitochondria, this possibly means that we could obtain an effect on mitochondria and calcium channel activity at lower concentrations than used acutely. A study performed on groups of people treated with 40 mg simvastatin /day and other statins as well showed that the mean concentration of statins in human serum is between 1-15 nM and for simvastatin is between 2.2–4.3 nM (Keskitalo et al. 2009), while the lowest effective concentration in experimental cells studies to produce significant pleiotropic effect is 1-10 μM with minimum incubation for 30 min (Bu et al. 2010). Thus, the concentration used in the present study (10 μM) is higher than that in human serum. However if statins accumulate in the mitochondria, the acute effects seen with a high concentration of simvastatin in this study may be replicated with chronic exposure to low concentrations.

Another limitation of the project is that only simvastatin was tested. However, previous studies in the laboratory have demonstrated that the anti-contractile effects of statins are related to lipophilicity in that simvastatin had greater effect than lovastatin, whereas pravastatin had no effect (Almukhtar et al. 2015).

6.3. Suggestions:

Regarding the effect of simvastatin on isolated mitochondria, more experiments are needed using different concentrations of simvastatin (Abdoli, Azarmi, and Eghbal 2015) with longer incubation times, as these factors could play a role (Gerencser et al. 2012). In addition, by using cultured cell lines, such as smooth muscle cells, we could explore the effect of longer-term incubation with statins on mitochondrial function. Other indications of mitochondrial function such as ATP synthesis (Brookes et al. 2004), generation of ROS (Zorov, Juhaszova, and Sollott 2014), mitochondrial calcium sequestration (McCarron, Olson, and Chalmers 2012), and respiration rate (Dohlmann et al. 2019) would give further information about the effect of statins. Further experiments could look at measuring uptake of statins into mitochondria to determine if they do accumulate over time.

Regarding the inhibitory effect on calcium influx, measurement or detection of the amount of intracellular Ca^{2+} using for example Flow Cytometry, fluorescence microscopy, using Ca^{2+} sensitive dye such as Fura-2 in cells might be required (Chalmers et al. 2007; Ali et al. 2016). This will allow us to link the effects of mitochondrial inhibition to calcium influx more easily. In the present study, attempts to measure changes in intracellular calcium with fura-2AM in intact blood vessels were unsuccessful. However, a limitation in the use of cultured cells, though, is the fact that they dedifferentiate into a proliferative phenotype and lose VGCC expression.

The data presented in this thesis indicate that inhibition of complex III leads to inhibition of calcium influx. It is important to determine the mechanism by which this occurs as this is a potential mechanism by which statins and other drugs could alter vascular tone (Curry et al. 2019). There are many potential mechanisms. For example, ROS could prevent calcium influx via inhibition of calcium channels (Green and Peers 2002; Görlach et al. 2015). In addition, the mitochondrial uptake of calcium could have a direct or indirect effect on the calcium channel activity and this could shape the calcium signalling (Hajnoczky et al. 2006). Preventing mitochondrial calcium uptake will enhance the negative feedback mechanism of IP_3R and inhibit calcium release due to increase local calcium in cytoplasm (Williams et al. 2013; McCarron, Olson, and Chalmers 2012). By permeabilizing the cells and adding exogenous calcium, mitochondrial Ca^{2+} could be measured using the fluorescent Ca^{2+} indicator Fluo-4, AM and confocal microscopy (McKenzie, Lim, and Duchen 2017).

Simvastatin might accumulate in mitochondria with time but unfortunately, there are not enough studies about that; the low concentration might have the same effect as the acute exposure to the higher concentration on mitochondria, calcium influx and consequently smooth muscle contraction. In order to determine whether longer incubation with lower

concentrations of statins could produce the same effect as acute exposure, the effect of lower simvastatin concentrations with longer time incubation such as overnight or longer would be required.

As mitochondrial function decreases with age, the effects of mitochondrial inhibitors may be enhanced in older animals i.e. they may be more sensitive (Conley, Jubrias, and Esselman 2000; Short et al. 2005). As statins are more likely to be prescribed to older patients, the effects of statins on mitochondria, and hence vascular tone, may be enhanced in these patients (Mendes, Robles, and Mathur 2014). Therefore, it would be beneficial to determine the effect of simvastatin in blood vessels from different age groups of animals. Similarly, the effects of statins on mitochondrial function and vascular tone may be different in patients with hypercholesterolaemia (Hernandez-Mijares et al. 2016). Little is known about the effects of hypercholesterolaemia on mitochondrial function. The effect of hypercholesterolemia on myocardium is thought to be due to inducing a deterioration in mitochondrial function, leading to an enhancement in ROS production and mitochondrial matrix overload with Ca^{2+} (Baines 2010; Halestrap 2009). If mitochondrial function is impaired, the effect of statins on the mitochondrial pathway and vascular tone may be enhanced. Addition of age may impair mitochondrial function further, thereby further enhancing the effect of the statins.

References:

Abdoli, N., Y. Azarmi, and M. A. Eghbal. 2015. 'Mitigation of statins-induced cytotoxicity and mitochondrial dysfunction by L-carnitine in freshly-isolated rat hepatocytes', *Res Pharm Sci*, 10: 143-51.

Abdoli, N., R. Heidari, Y. Azarmi, and M. A. Eghbal. 2013. 'Mechanisms of the statins cytotoxicity in freshly isolated rat hepatocytes', *J Biochem Mol Toxicol*, 27: 287-94.

Acosta, M. J., L. Vazquez Fonseca, M. A. Desbats, C. Cerqua, R. Zordan, E. Trevisson, and L. Salviati. 2016. 'Coenzyme Q biosynthesis in health and disease', *Biochim Biophys Acta*, 1857: 1079-85.

Aghajanian, A., E. S. Wittchen, S. L. Campbell, and K. Burridge. 2009. 'Direct activation of RhoA by reactive oxygen species requires a redox-sensitive motif', *PLoS One*, 4: e8045.

Aguilar, H. N., and B. F. Mitchell. 2010. 'Physiological pathways and molecular mechanisms regulating uterine contractility', *Hum Reprod Update*, 16: 725-44.

Alapati, V. R., C. McKenzie, A. Blair, D. Kenny, A. MacDonald, and A. M. Shaw. 2007. 'Mechanisms of U46619- and 5-HT-induced contraction of bovine pulmonary arteries: role of chloride ions', *Br J Pharmacol*, 151: 1224-34.

Ali, N., R. Begum, M. S. Faisal, A. Khan, M. Nabi, G. Shehzadi, S. Ullah, and W. Ali. 2016. 'Current statins show calcium channel blocking activity through voltage gated channels', *BMC Pharmacol Toxicol*, 17: 43.

Allen, T. J., and C. D. Hardin. 2000. 'Influence of glycogen storage on vascular smooth muscle metabolism', *Am J Physiol Heart Circ Physiol*, 278: H1993-2002.

Almukhtar, H., M. J. Garle, P. A. Smith, and R. E. Roberts. 2016. 'Effect of simvastatin on vascular tone in porcine coronary artery: Potential role of the mitochondria', *Toxicol Appl Pharmacol*, 305: 176-85.

Altieri, D. C. 2001. 'Statins' benefits begin to sprout', *J Clin Invest*, 108: 365-6.

Alvarez de Sotomayor, M., C. Perez-Guerrero, M. D. Herrera, and E. Marhuenda. 2001. 'Effect of simvastatin on vascular smooth muscle responsiveness: involvement of Ca(2+) homeostasis', *Eur J Pharmacol*, 415: 217-24.

An, J., F. Shi, S. Liu, J. Ma, and Q. Ma. 2017. 'Preoperative statins as modifiers of cardiac and inflammatory outcomes following coronary artery bypass graft surgery: a meta-analysis', *Interact Cardiovasc Thorac Surg*, 25: 958-65.

Andrews, T. C., C. M. Ballantyne, J. A. Hsia, and J. H. Kramer. 2001. 'Achieving and maintaining National Cholesterol Education Program low-density lipoprotein cholesterol goals with five statins', *Am J Med*, 111: 185-91.

Asaria, P., P. Elliott, M. Douglass, Z. Obermeyer, M. Soljak, A. Majeed, and M. Ezzati. 2017. 'Acute myocardial infarction hospital admissions and deaths in England: a national follow-back and follow-forward record-linkage study', *Lancet Public Health*, 2: e191-e201.

Bailey, S. R., S. Mitra, S. Flavahan, and N. A. Flavahan. 2005. 'Reactive oxygen species from smooth muscle mitochondria initiate cold-induced constriction of cutaneous arteries', *Am J Physiol Heart Circ Physiol*, 289: H243-50.

Baines, C. P. 2010. 'The cardiac mitochondrion: nexus of stress', *Annu Rev Physiol*, 72: 61-80.

Balaban, R. S., S. Nemoto, and T. Finkel. 2005. 'Mitochondria, oxidants, and aging', *Cell*, 120: 483-95.

Balemba, O. B., A. C. Bartoo, M. T. Nelson, and G. M. Mawe. 2008. 'Role of mitochondria in spontaneous rhythmic activity and intracellular calcium waves in the guinea pig gallbladder smooth muscle', *Am J Physiol Gastrointest Liver Physiol*, 294: G467-76.

Ballard-Croft, C., G. Kristo, Y. Yoshimura, E. Reid, B. J. Keith, R. M. Mentzer, Jr., and R. D. Lasley. 2005. 'Acute adenosine preconditioning is mediated by p38 MAPK activation in discrete subcellular compartments', *Am J Physiol Heart Circ Physiol*, 288: H1359-66.

Baracca, A., G. Sgarbi, G. Solaini, and G. Lenaz. 2003. 'Rhodamine 123 as a probe of mitochondrial membrane potential: evaluation of proton flux through F(0) during ATP synthesis', *Biochim Biophys Acta*, 1606: 137-46.

Barlow, R. S., A. M. El-Mowafy, and R. E. White. 2000. 'H(2)O(2) opens BK(Ca) channels via the PLA(2)-arachidonic acid signaling cascade in coronary artery smooth muscle', *Am J Physiol Heart Circ Physiol*, 279: H475-83.

Barnes, P. J. 1998. 'Pharmacology of airway smooth muscle', *Am J Respir Crit Care Med*, 158: S123-32.

Barone, E., F. Di Domenico, and D. A. Butterfield. 2014. 'Statins more than cholesterol lowering agents in Alzheimer disease: their pleiotropic functions as potential therapeutic targets', *Biochem Pharmacol*, 88: 605-16.

Bayguinov, O., L. Dwyer, H. Kim, A. Marklew, K. M. Sanders, and S. D. Koh. 2011. 'Contribution of Rho-kinase to membrane excitability of murine colonic smooth muscle', *Br J Pharmacol*, 163: 638-48.

Becker, L. B., T. L. vanden Hoek, Z. H. Shao, C. Q. Li, and P. T. Schumacker. 1999. 'Generation of superoxide in cardiomyocytes during ischemia before reperfusion', *Am J Physiol*, 277: H2240-6.

Bellosta, S., F. Bernini, N. Ferri, P. Quarato, M. Canavesi, L. Arnaboldi, R. Fumagalli, R. Paoletti, and A. Corsini. 1998. 'Direct vascular effects of HMG-CoA reductase inhibitors', *Atherosclerosis*, 137 Suppl: S101-9.

Bellosta, S., and A. Corsini. 2018. 'Statin drug interactions and related adverse reactions: an update', *Expert Opin Drug Saf*, 17: 25-37.

Bełtowski, J., and A. Jamroz-Wiśniewska. 2012. 'Modulation of h(2)s metabolism by statins: a new aspect of cardiovascular pharmacology', *Antioxid Redox Signal*, 17: 81-94.

Ben-Meir, A., E. Burstein, A. Borrego-Alvarez, J. Chong, E. Wong, T. Yavorska, T. Naranian, M. Chi, Y. Wang, Y. Bentov, J. Alexis, J. Meriano, H. K. Sung, D. L. Gasser, K. H. Moley, S. Hekimi, R. F. Casper, and A. Jurisicova. 2015. 'Coenzyme Q10 restores oocyte mitochondrial function and fertility during reproductive aging', *Aging Cell*, 14: 887-95.

Benham, C. D. 1992. 'ATP-gated cation channels in vascular smooth muscle cells', *Jpn J Pharmacol*, 58 Suppl 2: 179p-84p.

Beretta, S., C. Pastori, G. Sala, F. Piazza, C. Ferrarese, A. Cattalini, M. de Curtis, and L. Librizzi. 2011. 'Acute lipophilicity-dependent effect of intravascular simvastatin in the early phase of focal cerebral ischemia', *Neuropharmacology*, 60: 878-85.

Bergdahl, A., E. Persson, P. Hellstrand, and K. Sward. 2003. 'Lovastatin induces relaxation and inhibits L-type Ca(2+) current in the rat basilar artery', *Pharmacol Toxicol*, 93: 128-34.

Berridge, M. J. 1995. 'Capacitative calcium entry', *Biochem J*, 312 (Pt 1): 1-11.

Berridge, M. J., P. Lipp, and M. D. Bootman. 2000. 'The versatility and universality of calcium signalling', *Nat Rev Mol Cell Biol*, 1: 11-21.

Bhattacharya, B., and R. E. Roberts. 2003. 'Enhancement of alpha2-adrenoceptor-mediated vasoconstriction by the thromboxane-mimetic U46619 in the porcine isolated ear artery: role of the ERK-MAP kinase signal transduction cascade', *Br J Pharmacol*, 139: 156-62.

Bleda, S., J. De Haro, A. Florez, C. Varela, L. Esparza, and F. Acin. 2011. 'Long-term pleiotropic effect of statins upon nitric oxide and C-reactive protein levels in patients with peripheral arterial disease', *Heart Asia*, 3: 130-4.

Boehme, A. K., C. Esenwa, and M. S. Elkind. 2017. 'Stroke Risk Factors, Genetics, and Prevention', *Circ Res*, 120: 472-95.

Bogoyevitch, M. A., D. C. Ng, N. W. Court, K. A. Draper, A. Dhillon, and L. Abas. 2000. 'Intact mitochondrial electron transport function is essential for signalling by hydrogen peroxide in cardiac myocytes', *J Mol Cell Cardiol*, 32: 1469-80.

Boitier, E., R. Rea, and M. R. Duchen. 1999. 'Mitochondria exert a negative feedback on the propagation of intracellular Ca2+ waves in rat cortical astrocytes', *J Cell Biol*, 145: 795-808.

Brandt, U., H. Schagger, and G. von Jagow. 1988. 'Characterisation of binding of the methoxyacrylate inhibitors to mitochondrial cytochrome c reductase', *Eur J Biochem*, 173: 499-506.

Broniarek, I., and W. Jarmuszkiewicz. 2016. '[Statins and mitochondria]', *Postepy Biochem*, 62: 77-84.

Brookes, P. S., Y. Yoon, J. L. Robotham, M. W. Anders, and S. S. Sheu. 2004. 'Calcium, ATP, and ROS: a mitochondrial love-hate triangle', *Am J Physiol Cell Physiol*, 287: C817-33.
Brown, G. C., P. L. Lakin-Thomas, and M. D. Brand. 1990. 'Control of respiration and oxidative phosphorylation in isolated rat liver cells', *Eur J Biochem*, 192: 355-62.
Brown, M. S., and J. L. Goldstein. 1986. 'A receptor-mediated pathway for cholesterol homeostasis', *Science*, 232: 34-47.
Brozovich, F. V., C. J. Nicholson, C. V. Degen, Y. Z. Gao, M. Aggarwal, and K. G. Morgan. 2016. 'Mechanisms of Vascular Smooth Muscle Contraction and the Basis for Pharmacologic Treatment of Smooth Muscle Disorders', *Pharmacol Rev*, 68: 476-532.
Bu, D. X., M. Tarrio, N. Grabie, Y. Zhang, H. Yamazaki, G. Stavrakis, E. Maganto-Garcia, Z. Pepper-Cunningham, P. Jarolim, M. Aikawa, G. Garcia-Cardena, and A. H. Lichtman. 2010. 'Statin-induced Kruppel-like factor 2 expression in human and mouse T cells reduces inflammatory and pathogenic responses', *J Clin Invest*, 120: 1961-70.
Busija, D. W., I. Rutkai, S. Dutta, and P. V. Katakam. 2016. 'Role of Mitochondria in Cerebral Vascular Function: Energy Production, Cellular Protection, and Regulation of Vascular Tone', *Compr Physiol*, 6: 1529-48.
Butch, E. R., and K. L. Guan. 1996. 'Characterization of ERK1 activation site mutants and the effect on recognition by MEK1 and MEK2', *J Biol Chem*, 271: 4230-5.
Cadenas, E., and K. J. Davies. 2000. 'Mitochondrial free radical generation, oxidative stress, and aging', *Free Radic Biol Med*, 29: 222-30.
Cai, H. 2005. 'Hydrogen peroxide regulation of endothelial function: origins, mechanisms, and consequences', *Cardiovasc Res*, 68: 26-36.
Cai, J., and D. P. Jones. 1999. 'Mitochondrial redox signaling during apoptosis', *J Bioenerg Biomembr*, 31: 327-34.
Cain, W. J., J. S. Millar, A. S. Himebauch, U. J. Tietge, C. Maugeais, D. Usher, and D. J. Rader. 2005. 'Lipoprotein [a] is cleared from the plasma primarily by the liver in a process mediated by apolipoprotein [a]', *J Lipid Res*, 46: 2681-91.
Camello-Almaraz, C., P. J. Gomez-Pinilla, M. J. Pozo, and P. J. Camello. 2006. 'Mitochondrial reactive oxygen species and Ca2+ signaling', *Am J Physiol Cell Physiol*, 291: C1082-8.
Campbell, J. D., and R. J. Paul. 1992. 'The nature of fuel provision for the Na+,K(+)-ATPase in porcine vascular smooth muscle', *J Physiol*, 447: 67-82.
Campo, M. L., K. W. Kinnally, and H. Tedeschi. 1992. 'The effect of antimycin A on mouse liver inner mitochondrial membrane channel activity', *J Biol Chem*, 267: 8123-7.
Cargnello, M., and P. P. Roux. 2011. 'Activation and function of the MAPKs and their substrates, the MAPK-activated protein kinases', *Microbiol Mol Biol Rev*, 75: 50-83.
Caspersen, C., N. Wang, J. Yao, A. Sosunov, X. Chen, J. W. Lustbader, H. W. Xu, D. Stern, G. McKhann, and S. D. Yan. 2005. 'Mitochondrial Abeta: a potential focal point for neuronal metabolic dysfunction in Alzheimer's disease', *Faseb j*, 19: 2040-1.
Chalmers, S., and J. G. McCarron. 2009. 'Inhibition of mitochondrial calcium uptake rather than efflux impedes calcium release by inositol-1,4,5-trisphosphate-sensitive receptors', *Cell Calcium*, 46: 107-13.
Chalmers, S., M. L. Olson, D. MacMillan, R. D. Rainbow, and J. G. McCarron. 2007. 'Ion channels in smooth muscle: regulation by the sarcoplasmic reticulum and mitochondria', *Cell Calcium*, 42: 447-66.
Chang, D. T., A. S. Honick, and I. J. Reynolds. 2006. 'Mitochondrial trafficking to synapses in cultured primary cortical neurons', *J Neurosci*, 26: 7035-45.
Chen, L. B. 1988. 'Mitochondrial membrane potential in living cells', *Annu Rev Cell Biol*, 4: 155-81.
Chen, Q., E. J. Vazquez, S. Moghaddas, C. L. Hoppel, and E. J. Lesnefsky. 2003. 'Production of reactive oxygen species by mitochondria: central role of complex III', *J Biol Chem*, 278: 36027-31.

Choi, S. L., S. J. Kim, K. T. Lee, J. Kim, J. Mu, M. J. Birnbaum, S. Soo Kim, and J. Ha. 2001. 'The regulation of AMP-activated protein kinase by H(2)O(2)', *Biochem Biophys Res Commun*, 287: 92-7.

Clempus, R. E., and K. K. Griendling. 2006. 'Reactive oxygen species signaling in vascular smooth muscle cells', *Cardiovasc Res*, 71: 216-25.

Cobb, M. H. 1999. 'MAP kinase pathways', *Prog Biophys Mol Biol*, 71: 479-500.

Cogolludo, A., L. Moreno, L. Bosca, J. Tamargo, and F. Perez-Vizcaino. 2003. 'Thromboxane A2-induced inhibition of voltage-gated K+ channels and pulmonary vasoconstriction: role of protein kinase Czeta', *Circ Res*, 93: 656-63.

Collins, T. J., P. Lipp, M. J. Berridge, W. Li, and M. D. Bootman. 2000. 'Inositol 1,4,5-trisphosphate-induced Ca2+ release is inhibited by mitochondrial depolarization', *Biochem J*, 347: 593-600.

Conley, K. E., S. A. Jubrias, and P. C. Esselman. 2000. 'Oxidative capacity and ageing in human muscle', *J Physiol*, 526 Pt 1: 203-10.

Cool, B., B. Zinker, W. Chiou, L. Kifle, N. Cao, M. Perham, R. Dickinson, A. Adler, G. Gagne, R. Iyengar, G. Zhao, K. Marsh, P. Kym, P. Jung, H. S. Camp, and E. Frevert. 2006. 'Identification and characterization of a small molecule AMPK activator that treats key components of type 2 diabetes and the metabolic syndrome', *Cell Metab*, 3: 403-16.

Copley, Scott, John Beltrame, and David Wilson. 2008. 'Acute Simvastatin Treatment Enhances the Efficacy of Rho Kinase Inhibitor Mediated Vasodilatation in Rat Caudal Arteries', *Heart, Lung and Circulation*, 17: S238.

Corpataux, J. M., J. Naik, K. E. Porter, and N. J. London. 2005. 'The effect of six different statins on the proliferation, migration, and invasion of human smooth muscle cells', *J Surg Res*, 129: 52-6.

Covian, R., and R. S. Balaban. 2012. 'Cardiac mitochondrial matrix and respiratory complex protein phosphorylation', *Am J Physiol Heart Circ Physiol*, 303: H940-66.

Criqui, M. H., V. Aboyans, M. A. Allison, J. O. Denenberg, N. Forbang, M. M. McDermott, C. L. Wassel, and N. D. Wong. 2016. 'Peripheral Artery Disease and Aortic Disease', *Glob Heart*, 11: 313-26.

Curry, L., H. Almukhtar, J. Alahmed, R. Roberts, and P. A. Smith. 2019. 'Simvastatin inhibits L-type Ca2+-channel activity through impairment of mitochondrial function', *Toxicol Sci*.

D'Angelo, G., P. Graceffa, C. A. Wang, J. Wrangle, and L. P. Adam. 1999. 'Mammal-specific, ERK-dependent, caldesmon phosphorylation in smooth muscle. Quantitation using novel anti-phosphopeptide antibodies', *J Biol Chem*, 274: 30115-21.

Dallner, G., and P. J. Sindelar. 2000. 'Regulation of ubiquinone metabolism', *Free Radic Biol Med*, 29: 285-94.

Das, S., C. Steenbergen, and E. Murphy. 2012. 'Does the voltage dependent anion channel modulate cardiac ischemia-reperfusion injury?', *Biochim Biophys Acta*, 1818: 1451-6.

Davidson, M. H. 2001. 'Safety profiles for the HMG-CoA reductase inhibitors: treatment and trust', *Drugs*, 61: 197-206.

Davies, S. P., H. Reddy, M. Caivano, and P. Cohen. 2000. 'Specificity and mechanism of action of some commonly used protein kinase inhibitors', *Biochem J*, 351: 95-105.

De Pinieux, G., P. Chariot, M. Ammi-Said, F. Louarn, J. L. Lejonc, A. Astier, B. Jacotot, and R. Gherardi. 1996. 'Lipid-lowering drugs and mitochondrial function: effects of HMG-CoA reductase inhibitors on serum ubiquinone and blood lactate/pyruvate ratio', *Br J Clin Pharmacol*, 42: 333-7.

Deichmann, R., C. Lavie, and S. Andrews. 2010. 'Coenzyme q10 and statin-induced mitochondrial dysfunction', *Ochsner J*, 10: 16-21.

Demaurex, N., D. Poburko, and M. Frieden. 2009. 'Regulation of plasma membrane calcium fluxes by mitochondria', *Biochim Biophys Acta*, 1787: 1383-94.

Dessy, C., I. Kim, C. L. Sougnez, R. Laporte, and K. G. Morgan. 1998. 'A role for MAP kinase in differentiated smooth muscle contraction evoked by alpha-adrenoceptor stimulation', *Am J Physiol*, 275: C1081-6.

Dhingra, R., and R. S. Vasan. 2012. 'Age as a risk factor', *Med Clin North Am*, 96: 87-91.

Diebold, B. A., N. V. Bhagavan, and R. J. Guillory. 1994. 'Influences of lovastatin administration on the respiratory burst of leukocytes and the phosphorylation potential of mitochondria in guinea pigs', *Biochim Biophys Acta*, 1200: 100-8.

Dimitrova, Y., S. Dunoyer-Geindre, G. Reber, F. Mach, E. K. Kruithof, and P. de Moerloose. 2003. 'Effects of statins on adhesion molecule expression in endothelial cells', *J Thromb Haemost*, 1: 2290-9.

Dimopoulos, G. J., S. Semba, K. Kitazawa, M. Eto, and T. Kitazawa. 2007. 'Ca2+-dependent rapid Ca2+ sensitization of contraction in arterial smooth muscle', *Circ Res*, 100: 121-9.

Doeller, J. E., T. S. Isbell, G. Benavides, J. Koenitzer, H. Patel, R. P. Patel, J. R. Lancaster, Jr., V. M. Darley-Usmar, and D. W. Kraus. 2005. 'Polarographic measurement of hydrogen sulfide production and consumption by mammalian tissues', *Anal Biochem*, 341: 40-51.

Dohlmann, T. L., T. Morville, A. B. Kuhlman, K. M. Chrois, J. W. Helge, F. Dela, and S. Larsen. 2019. 'Statin Treatment Decreases Mitochondrial Respiration But Muscle Coenzyme Q10 Levels Are Unaltered: The LIFESTAT Study', *J Clin Endocrinol Metab*, 104: 2501-08.

Drummond, R. M., and F. S. Fay. 1996. 'Mitochondria contribute to Ca2+ removal in smooth muscle cells', *Pflugers Arch*, 431: 473-82.

Drummond, R. M., and R. A. Tuft. 1999a. 'Release of Ca2+ from the sarcoplasmic reticulum increases mitochondrial [Ca2+] in rat pulmonary artery smooth muscle cells', *J Physiol*, 516 (Pt 1): 139-47.

———. 1999b. 'Release of Ca2+ from the sarcoplasmic reticulum increases mitochondrial [Ca2+] in rat pulmonary artery smooth muscle cells', *J Physiol*, 516 (Pt 1): 139-47.

Duchen, M. R. 1999. 'Contributions of mitochondria to animal physiology: from homeostatic sensor to calcium signalling and cell death', *J Physiol*, 516 (Pt 1): 1-17.

———. 2000. 'Mitochondria and calcium: from cell signalling to cell death', *J Physiol*, 529 Pt 1: 57-68.

Dujovne, C. A. 2002. 'Side effects of statins: hepatitis versus "transaminitis"-myositis versus "CPKitis"', *Am J Cardiol*, 89: 1411-3.

Dykens, J. A., and A. K. Stout. 2001. 'Assessment of mitochondrial membrane potential in situ using single potentiometric dyes and a novel fluorescence resonance energy transfer technique', *Methods Cell Biol*, 65: 285-309.

Ekstrand, Mats I., Mügen Terzioglu, Dagmar Galter, Shunwei Zhu, Christoph Hofstetter, Eva Lindqvist, Sebastian Thams, Anita Bergstrand, Fredrik Sterky Hansson, Aleksandra Trifunovic, Barry Hoffer, Staffan Cullheim, Abdul H. Mohammed, Lars Olson, and Nils-Göran Larsson. 2007. 'Progressive parkinsonism in mice with respiratory-chain-deficient dopamine neurons', *Proceedings of the National Academy of Sciences*, 104: 1325-30.

Ellinsworth, David C., Nilima Shukla, Ingrid Fleming, and Jamie Y. Jeremy. 2014. 'Interactions between thromboxane A2, thromboxane/prostaglandin (TP) receptors, and endothelium-derived hyperpolarization', *Cardiovasc Res*, 102: 9-16.

Emaus, R. K., R. Grunwald, and J. J. Lemasters. 1986. 'Rhodamine 123 as a probe of transmembrane potential in isolated rat-liver mitochondria: spectral and metabolic properties', *Biochim Biophys Acta*, 850: 436-48.

Enis, D. R., B. R. Shepherd, Y. Wang, A. Qasim, C. M. Shanahan, P. L. Weissberg, M. Kashgarian, J. S. Pober, and J. S. Schechner. 2005. 'Induction, differentiation, and remodeling of blood vessels after transplantation of Bcl-2-transduced endothelial cells', *Proc Natl Acad Sci U S A*, 102: 425-30.

Escobales, N., M. Castro, P. I. Altieri, and P. Sanabria. 1996. 'Simvastatin releases Ca2+ from a thapsigargin-sensitive pool and inhibits InsP3-dependent Ca2+ mobilization in vascular smooth muscle cells', *J Cardiovasc Pharmacol*, 27: 383-91.

Etienne-Manneville, S., and A. Hall. 2002. 'Rho GTPases in cell biology', *Nature*, 420: 629-35.

Favari, E., A. Chroni, U. J. Tietge, I. Zanotti, J. C. Escola-Gil, and F. Bernini. 2015. 'Cholesterol efflux and reverse cholesterol transport', *Handb Exp Pharmacol*, 224: 181-206.

Feigin, V. L., C. M. Lawes, D. A. Bennett, S. L. Barker-Collo, and V. Parag. 2009. 'Worldwide stroke incidence and early case fatality reported in 56 population-based studies: a systematic review', *Lancet Neurol*, 8: 355-69.

Feng, J., S. M. Damrauer, M. Lee, F. W. Sellke, C. Ferran, and M. R. Abid. 2010. 'Endothelium-dependent coronary vasodilatation requires NADPH oxidase-derived reactive oxygen species', *Arterioscler Thromb Vasc Biol*, 30: 1703-10.

Fink, B. D., J. A. Herlein, M. A. Yorek, A. M. Fenner, R. J. Kerns, and W. I. Sivitz. 2012. 'Bioenergetic effects of mitochondrial-targeted coenzyme Q analogs in endothelial cells', *J Pharmacol Exp Ther*, 342: 709-19.

Fink, B. D., Y. O'Malley, B. L. Dake, N. C. Ross, T. E. Prisinzano, and W. I. Sivitz. 2009. 'Mitochondrial targeted coenzyme Q, superoxide, and fuel selectivity in endothelial cells', *PLoS One*, 4: e4250.

Fisar, Z., J. Hroudova, N. Singh, A. Koprivova, and D. Maceckova. 2016. 'Effect of Simvastatin, Coenzyme Q10, Resveratrol, Acetylcysteine and Acetylcarnitine on Mitochondrial Respiration', *Folia Biol (Praha)*, 62: 53-66.

FitzGerald, G. A., C. Healy, and J. Daugherty. 1987. 'Thromboxane A2 biosynthesis in human disease', *Fed Proc*, 46: 154-8.

Fontaine, E. M., A. Devin, M. Rigoulet, and X. M. Leverve. 1997. 'The yield of oxidative phosphorylation is controlled both by force and flux', *Biochem Biophys Res Commun*, 232: 532-5.

Ford, I., H. Murray, C. J. Packard, J. Shepherd, P. W. Macfarlane, and S. M. Cobbe. 2007. 'Long-term follow-up of the West of Scotland Coronary Prevention Study', *N Engl J Med*, 357: 1477-86.

Fu, X., M. C. Gong, T. Jia, A. V. Somlyo, and A. P. Somlyo. 1998. 'The effects of the Rho-kinase inhibitor Y-27632 on arachidonic acid-, GTPgammaS-, and phorbol ester-induced Ca2+-sensitization of smooth muscle', *FEBS Lett*, 440: 183-7.

Fukata, Y., M. Amano, and K. Kaibuchi. 2001. 'Rho-Rho-kinase pathway in smooth muscle contraction and cytoskeletal reorganization of non-muscle cells', *Trends Pharmacol Sci*, 22: 32-9.

Gabella, G. 2012. 'Cells of visceral smooth muscles', *J Smooth Muscle Res*, 48: 65-95.

Galtier, F., T. Mura, E. Raynaud de Mauverger, H. Chevassus, A. Farret, J. P. Gagnol, F. Costa, A. Dupuy, P. Petit, J. P. Cristol, J. Mercier, and A. Lacampagne. 2012. 'Effect of a high dose of simvastatin on muscle mitochondrial metabolism and calcium signaling in healthy volunteers', *Toxicol Appl Pharmacol*, 263: 281-6.

Gao, L., K. Laude, and H. Cai. 2008. 'Mitochondrial pathophysiology, reactive oxygen species, and cardiovascular diseases', *Vet Clin North Am Small Anim Pract*, 38: 137-55, vi.

Gao, N., J. Huang, W. He, M. Zhu, K. E. Kamm, and J. T. Stull. 2013. 'Signaling through myosin light chain kinase in smooth muscles', *J Biol Chem*, 288: 7596-605.

Garcia, M. J., R. F. Reinoso, A. Sanchez Navarro, and J. R. Prous. 2003. 'Clinical pharmacokinetics of statins', *Methods Find Exp Clin Pharmacol*, 25: 457-81.

Gayard, M., C. Guilluy, A. Rousselle, B. Viollet, D. Henrion, P. Pacaud, G. Loirand, and M. Rolli-Derkinderen. 2011. 'AMPK alpha 1-induced RhoA phosphorylation mediates vasoprotective effect of estradiol', *Arterioscler Thromb Vasc Biol*, 31: 2634-42.

Geng, B., L. Chang, C. Pan, Y. Qi, J. Zhao, Y. Pang, J. Du, and C. Tang. 2004. 'Endogenous hydrogen sulfide regulation of myocardial injury induced by isoproterenol', *Biochem Biophys Res Commun*, 318: 756-63.

Gerencser, A. A., C. Chinopoulos, M. J. Birket, M. Jastroch, C. Vitelli, D. G. Nicholls, and M. D. Brand. 2012. 'Quantitative measurement of mitochondrial membrane potential in cultured cells: calcium-induced de- and hyperpolarization of neuronal mitochondria', *J Physiol*, 590: 2845-71.

Gero, D., R. Torregrossa, A. Perry, A. Waters, S. Le-Trionnaire, J. L. Whatmore, M. Wood, and M. Whiteman. 2016. 'The novel mitochondria-targeted hydrogen sulfide (H2S) donors AP123

and AP39 protect against hyperglycemic injury in microvascular endothelial cells in vitro', *Pharmacol Res*, 113: 186-98.

Gerő, D., R. Torregrossa, A. Perry, A. Waters, S. Le-Trionnaire, J. L. Whatmore, M. Wood, and M. Whiteman. 2016. 'The novel mitochondria-targeted hydrogen sulfide (H(2)S) donors AP123 and AP39 protect against hyperglycemic injury in microvascular endothelial cells in vitro', *Pharmacol Res*, 113: 186-98.

Ghirlanda, G., A. Oradei, A. Manto, S. Lippa, L. Uccioli, S. Caputo, A. V. Greco, and G. P. Littarru. 1993. 'Evidence of plasma CoQ10-lowering effect by HMG-CoA reductase inhibitors: a double-blind, placebo-controlled study', *J Clin Pharmacol*, 33: 226-9.

Ghosh, D., A. U. Syed, M. P. Prada, M. A. Nystoriak, L. F. Santana, M. Nieves-Cintrón, and M. F. Navedo. 2017. 'Calcium Channels in Vascular Smooth Muscle', *Adv Pharmacol*, 78: 49-87.

Ginsberg, H. N., N. A. Le, M. P. Short, R. Ramakrishnan, and R. J. Desnick. 1987. 'Suppression of apolipoprotein B production during treatment of cholesteryl ester storage disease with lovastatin. Implications for regulation of apolipoprotein B synthesis', *J Clin Invest*, 80: 1692-7.

Goglia, F., and V. P. Skulachev. 2003. 'A function for novel uncoupling proteins: antioxidant defense of mitochondrial matrix by translocating fatty acid peroxides from the inner to the outer membrane leaflet', *Faseb j*, 17: 1585-91.

Goirand, F., M. Solar, Y. Athea, B. Viollet, P. Mateo, D. Fortin, J. Leclerc, J. Hoerter, R. Ventura-Clapier, and A. Garnier. 2007. 'Activation of AMP kinase alpha1 subunit induces aortic vasorelaxation in mice', *J Physiol*, 581: 1163-71.

Goldstein, J. L., and M. S. Brown. 1990. 'Regulation of the mevalonate pathway', *Nature*, 343: 425-30.

Gonzalez-Pacheco, F. R., C. Caramelo, M. A. Castilla, J. J. Deudero, J. Arias, S. Yague, S. Jimenez, R. Bragado, and M. V. Alvarez-Arroyo. 2002. 'Mechanism of vascular smooth muscle cells activation by hydrogen peroxide: role of phospholipase C gamma', *Nephrol Dial Transplant*, 17: 392-8.

Görlach, A., K. Bertram, S. Hudecova, and O. Krizanova. 2015. 'Calcium and ROS: A mutual interplay', *Redox Biol*, 6: 260-71.

Gotto, A. M., Jr., and J. Moon. 2010. 'Pitavastatin for the treatment of primary hyperlipidemia and mixed dyslipidemia', *Expert Rev Cardiovasc Ther*, 8: 1079-90.

Goubern, M., M. Andriamihaja, T. Nubel, F. Blachier, and F. Bouillaud. 2007. 'Sulfide, the first inorganic substrate for human cells', *Faseb j*, 21: 1699-706.

Gowans, G. J., S. A. Hawley, F. A. Ross, and D. G. Hardie. 2013. 'AMP is a true physiological regulator of AMP-activated protein kinase by both allosteric activation and enhancing net phosphorylation', *Cell Metab*, 18: 556-66.

Grann, M., S. Comerma-Steffensen, D. D. Arcanjo, and U. Simonsen. 2016. 'Mechanisms Involved in Thromboxane A2 -induced Vasoconstriction of Rat Intracavernous Small Penile Arteries', *Basic Clin Pharmacol Toxicol*, 119 Suppl 3: 86-95.

Green, K. N., and C. Peers. 2002. 'Divergent pathways account for two distinct effects of amyloid beta peptides on exocytosis and Ca(2+) currents: involvement of ROS and NF-kappaB', *J Neurochem*, 81: 1043-51.

Griffiths, E. J., and G. A. Rutter. 2009. 'Mitochondrial calcium as a key regulator of mitochondrial ATP production in mammalian cells', *Biochim Biophys Acta*, 1787: 1324-33.

Grundy, S. M. 1998. 'Consensus statement: Role of therapy with "statins" in patients with hypertriglyceridemia', *Am J Cardiol*, 81: 1b-6b.

Gutterman, D. D., H. Miura, and Y. Liu. 2005. 'Redox modulation of vascular tone: focus of potassium channel mechanisms of dilation', *Arterioscler Thromb Vasc Biol*, 25: 671-8.

Guyton, K. Z., Y. Liu, M. Gorospe, Q. Xu, and N. J. Holbrook. 1996. 'Activation of mitogen-activated protein kinase by H2O2. Role in cell survival following oxidant injury', *J Biol Chem*, 271: 4138-42.

Hafner, R. P., G. C. Brown, and M. D. Brand. 1990. 'Analysis of the control of respiration rate, phosphorylation rate, proton leak rate and protonmotive force in isolated mitochondria using the 'top-down' approach of metabolic control theory', *Eur J Biochem*, 188: 313-9.
Hajnoczky, G., G. Csordas, S. Das, C. Garcia-Perez, M. Saotome, S. Sinha Roy, and M. Yi. 2006. 'Mitochondrial calcium signalling and cell death: approaches for assessing the role of mitochondrial Ca2+ uptake in apoptosis', *Cell Calcium*, 40: 553-60.
Hajnoczky, G., R. Hager, and A. P. Thomas. 1999. 'Mitochondria suppress local feedback activation of inositol 1,4, 5-trisphosphate receptors by Ca2+', *J Biol Chem*, 274: 14157-62.
Halestrap, A. P. 2009. 'What is the mitochondrial permeability transition pore?', *J Mol Cell Cardiol*, 46: 821-31.
Hall, A. 1998. 'Rho GTPases and the actin cytoskeleton', *Science*, 279: 509-14.
Halliwell, B. 2000. 'Lipid peroxidation, antioxidants and cardiovascular disease: how should we move forward?', *Cardiovasc Res*, 47: 410-8.
Hansford, R. G., B. A. Hogue, and V. Mildaziene. 1997. 'Dependence of H2O2 formation by rat heart mitochondria on substrate availability and donor age', *J Bioenerg Biomembr*, 29: 89-95.
Hardie, D. G., D. Carling, and M. Carlson. 1998. 'The AMP-activated/SNF1 protein kinase subfamily: metabolic sensors of the eukaryotic cell?', *Annu Rev Biochem*, 67: 821-55.
Hatefi, Y. 1985. 'The mitochondrial electron transport and oxidative phosphorylation system', *Annu Rev Biochem*, 54: 1015-69.
Hawley, S. A., A. E. Gadalla, G. S. Olsen, and D. G. Hardie. 2002. 'The antidiabetic drug metformin activates the AMP-activated protein kinase cascade via an adenine nucleotide-independent mechanism', *Diabetes*, 51: 2420-5.
Heo, J., K. W. Raines, V. Mocanu, and S. L. Campbell. 2006. 'Redox regulation of RhoA', *Biochemistry*, 45: 14481-9.
Hernandez-Mijares, A., C. Banuls, S. Rovira-Llopis, N. Diaz-Morales, I. Escribano-Lopez, C. de Pablo, A. Alvarez, S. Veses, M. Rocha, and V. M. Victor. 2016. 'Effects of simvastatin, ezetimibe and simvastatin/ezetimibe on mitochondrial function and leukocyte/endothelial cell interactions in patients with hypercholesterolemia', *Atherosclerosis*, 247: 40-7.
Herrero-Martin, G., and A. Lopez-Rivas. 2008. 'Statins activate a mitochondria-operated pathway of apoptosis in breast tumor cells by a mechanism regulated by ErbB2 and dependent on the prenylation of proteins', *FEBS Lett*, 582: 2589-94.
Herrero, A., and G. Barja. 1997. 'Sites and mechanisms responsible for the low rate of free radical production of heart mitochondria in the long-lived pigeon', *Mech Ageing Dev*, 98: 95-111.
Herrington, J., Y. B. Park, D. F. Babcock, and B. Hille. 1996. 'Dominant role of mitochondria in clearance of large Ca2+ loads from rat adrenal chromaffin cells', *Neuron*, 16: 219-28.
Hogan, Q. H., C. Sprick, Y. Guo, S. Mueller, M. Bienengraeber, B. Pan, and H. E. Wu. 2014. 'Divergent effects of painful nerve injury on mitochondrial Ca(2+) buffering in axotomized and adjacent sensory neurons', *Brain Res*, 1589: 112-25.
Holtzman, D., and C. L. Moore. 1973. 'Oxidative phosphorylation in immature rat brain mitochondria', *Biol Neonate*, 22: 230-42.
———. 1975. 'Respiration in immature rat brain mitochondria', *J Neurochem*, 24: 1011-5.
Horman, S., N. Morel, D. Vertommen, N. Hussain, D. Neumann, C. Beauloye, N. El Najjar, C. Forcet, B. Viollet, M. P. Walsh, L. Hue, and M. H. Rider. 2008. 'AMP-activated protein kinase phosphorylates and desensitizes smooth muscle myosin light chain kinase', *J Biol Chem*, 283: 18505-12.
Hoth, M., C. M. Fanger, and R. S. Lewis. 1997. 'Mitochondrial regulation of store-operated calcium signaling in T lymphocytes', *J Cell Biol*, 137: 633-48.
Hung, C. Y., Y. C. Hsieh, K. Y. Wang, J. L. Huang, W. Loh el, C. H. Lin, and T. J. Wu. 2013. 'Efficacy of different statins for primary prevention of atrial fibrillation in male and female patients: a nationwide population-based cohort study', *Int J Cardiol*, 168: 4367-9.

Ichiki, T., K. Takeda, T. Tokunou, N. Iino, K. Egashira, H. Shimokawa, K. Hirano, H. Kanaide, and A. Takeshita. 2001. 'Downregulation of angiotensin II type 1 receptor by hydrophobic 3-hydroxy-3-methylglutaryl coenzyme A reductase inhibitors in vascular smooth muscle cells', *Arterioscler Thromb Vasc Biol*, 21: 1896-901.

Iglesias, A., M. Arranz, J. J. Alvarez, J. Perales, J. Villar, E. Herrera, and M. A. Lasuncion. 1996. 'Cholesteryl ester transfer activity in liver disease and cholestasis, and its relation with fatty acid composition of lipoprotein lipids', *Clin Chim Acta*, 248: 157-74.

Im, I., M. J. Jang, S. J. Park, S. H. Lee, J. H. Choi, H. W. Yoo, S. Kim, and Y. M. Han. 2015. 'Mitochondrial Respiratory Defect Causes Dysfunctional Lactate Turnover via AMP-activated Protein Kinase Activation in Human-induced Pluripotent Stem Cell-derived Hepatocytes', *J Biol Chem*, 290: 29493-505.

Ishihata, A., K. Tasaki, and Y. Katano. 2002. 'Involvement of p44/42 mitogen-activated protein kinases in regulating angiotensin II- and endothelin-1-induced contraction of rat thoracic aorta', *Eur J Pharmacol*, 445: 247-56.

Istvan, E. S., and J. Deisenhofer. 2001. 'Structural mechanism for statin inhibition of HMG-CoA reductase', *Science*, 292: 1160-4.

Jackson, J. B., and D. G. Nicholls. 1986. 'Methods for the determination of membrane potential in bioenergetic systems', *Methods Enzymol*, 127: 557-77.

Javadov, S., S. Jang, and B. Agostini. 2014. 'Crosstalk between mitogen-activated protein kinases and mitochondria in cardiac diseases: therapeutic perspectives', *Pharmacol Ther*, 144: 202-25.

Jiang, S., D. W. Park, W. S. Stigler, J. Creighton, S. Ravi, V. Darley-Usmar, and J. W. Zmijewski. 2013. 'Mitochondria and AMP-activated protein kinase-dependent mechanism of efferocytosis', *J Biol Chem*, 288: 26013-26.

Johnson, L. V., M. L. Walsh, B. J. Bockus, and L. B. Chen. 1981. 'Monitoring of relative mitochondrial membrane potential in living cells by fluorescence microscopy', *J Cell Biol*, 88: 526-35.

Johnson, L. V., M. L. Walsh, and L. B. Chen. 1980. 'Localization of mitochondria in living cells with rhodamine 123', *Proc Natl Acad Sci U S A*, 77: 990-4.

Jones, S. P., Y. Teshima, M. Akao, and E. Marban. 2003. 'Simvastatin attenuates oxidant-induced mitochondrial dysfunction in cardiac myocytes', *Circ Res*, 93: 697-9.

Joyal, J. L., T. Hagen, and J. R. Aprille. 1995. 'Intramitochondrial protein synthesis is regulated by matrix adenine nucleotide content and requires calcium', *Arch Biochem Biophys*, 319: 322-30.

Jukema, J. W., C. P. Cannon, A. J. de Craen, R. G. Westendorp, and S. Trompet. 2012. 'The controversies of statin therapy: weighing the evidence', *J Am Coll Cardiol*, 60: 875-81.

Junemann, S., P. Heathcote, and P. R. Rich. 1998. 'On the mechanism of quinol oxidation in the bc1 complex', *J Biol Chem*, 273: 21603-7.

Kadenbach, Bernhard. 2003. 'Intrinsic and extrinsic uncoupling of oxidative phosphorylation', *Biochimica et Biophysica Acta (BBA) - Bioenergetics*, 1604: 77-94.

Kahn, B. B., T. Alquier, D. Carling, and D. G. Hardie. 2005. 'AMP-activated protein kinase: ancient energy gauge provides clues to modern understanding of metabolism', *Cell Metab*, 1: 15-25.

Kajinami, K., H. Mabuchi, and Y. Saito. 2000. 'NK-104: a novel synthetic HMG-CoA reductase inhibitor', *Expert Opin Investig Drugs*, 9: 2653-61.

Kamakura, S., T. Moriguchi, and E. Nishida. 1999. 'Activation of the protein kinase ERK5/BMK1 by receptor tyrosine kinases. Identification and characterization of a signaling pathway to the nucleus', *J Biol Chem*, 274: 26563-71.

Kang, S., H. H. Woo, K. Kim, K. M. Lim, J. Y. Noh, M. Y. Lee, Y. M. Bae, O. N. Bae, and J. H. Chung. 2014. 'Dysfunction of vascular smooth muscle and vascular remodeling by simvastatin', *Toxicol Sci*, 138: 446-556.

Karwi, Q. G., J. Bornbaum, K. Boengler, R. Torregrossa, M. Whiteman, M. E. Wood, R. Schulz, and G. F. Baxter. 2017a. 'AP39, a mitochondria-targeting hydrogen sulfide (H2 S) donor, protects

against myocardial reperfusion injury independently of salvage kinase signalling', *Br J Pharmacol*, 174: 287-301.

———. 2017b. 'AP39, a mitochondria-targeting hydrogen sulfide (H(2) S) donor, protects against myocardial reperfusion injury independently of salvage kinase signalling', *Br J Pharmacol*, 174: 287-301.

Kearney, A. S., L. F. Crawford, S. C. Mehta, and G. W. Radebaugh. 1993. 'The interconversion kinetics, equilibrium, and solubilities of the lactone and hydroxyacid forms of the HMG-CoA reductase inhibitor, CI-981', *Pharm Res*, 10: 1461-5.

Kelso, G. F., C. M. Porteous, G. Hughes, E. C. Ledgerwood, A. M. Gane, R. A. Smith, and M. P. Murphy. 2002. 'Prevention of mitochondrial oxidative damage using targeted antioxidants', *Ann N Y Acad Sci*, 959: 263-74.

Keskitalo, J. E., M. K. Pasanen, P. J. Neuvonen, and M. Niemi. 2009. 'Different effects of the ABCG2 c.421C>A SNP on the pharmacokinetics of fluvastatin, pravastatin and simvastatin', *Pharmacogenomics*, 10: 1617-24.

Kharbanda, S., S. Saxena, K. Yoshida, P. Pandey, M. Kaneki, Q. Wang, K. Cheng, Y. N. Chen, A. Campbell, T. Sudha, Z. M. Yuan, J. Narula, R. Weichselbaum, C. Nalin, and D. Kufe. 2000. 'Translocation of SAPK/JNK to mitochondria and interaction with Bcl-x(L) in response to DNA damage', *J Biol Chem*, 275: 322-7.

Kieler-Jensen, N., S. Lundin, and S. E. Ricksten. 1995. 'Vasodilator therapy after heart transplantation: effects of inhaled nitric oxide and intravenous prostacyclin, prostaglandin E1, and sodium nitroprusside', *J Heart Lung Transplant*, 14: 436-43.

Kim, Hoeon, Lothar Esser, M. Bilayet Hossain, Di Xia, Chang-An Yu, Josep Rizo, Dick van der Helm, and Johann Deisenhofer. 1999. 'Structure of Antimycin A1, a Specific Electron Transfer Inhibitor of Ubiquinol−Cytochrome c Oxidoreductase', *Journal of the American Chemical Society*, 121: 4902-03.

Kimura, H., N. Shibuya, and Y. Kimura. 2012. 'Hydrogen sulfide is a signaling molecule and a cytoprotectant', *Antioxid Redox Signal*, 17: 45-57.

Kimura, K., M. Ito, M. Amano, K. Chihara, Y. Fukata, M. Nakafuku, B. Yamamori, J. Feng, T. Nakano, K. Okawa, A. Iwamatsu, and K. Kaibuchi. 1996. 'Regulation of myosin phosphatase by Rho and Rho-associated kinase (Rho-kinase)', *Science*, 273: 245-8.

Kitajima, S., H. Ozaki, and H. Karaki. 1993. 'The effects of ATP and alpha,beta-methylene-ATP on cytosolic Ca2+ level and force in rat isolated aorta', *Br J Pharmacol*, 110: 263-8.

Kitazawa, T., M. Eto, T. P. Woodsome, and M. Khalequzzaman. 2003. 'Phosphorylation of the myosin phosphatase targeting subunit and CPI-17 during Ca2+ sensitization in rabbit smooth muscle', *J Physiol*, 546: 879-89.

Kizub, I. V., O. O. Pavlova, C. D. Johnson, A. I. Soloviev, and A. V. Zholos. 2010. 'Rho kinase and protein kinase C involvement in vascular smooth muscle myofilament calcium sensitization in arteries from diabetic rats', *Br J Pharmacol*, 159: 1724-31.

Klemke, R. L., S. Cai, A. L. Giannini, P. J. Gallagher, P. de Lanerolle, and D. A. Cheresh. 1997. 'Regulation of cell motility by mitogen-activated protein kinase', *J Cell Biol*, 137: 481-92.

Koga, Y., and M. Ikebe. 2008. 'A novel regulatory mechanism of myosin light chain phosphorylation via binding of 14-3-3 to myosin phosphatase', *Mol Biol Cell*, 19: 1062-71.

Koh, K. K. 2000. 'Effects of statins on vascular wall: vasomotor function, inflammation, and plaque stability', *Cardiovasc Res*, 47: 648-57.

Kostis, W. J., J. Q. Cheng, J. M. Dobrzynski, J. Cabrera, and J. B. Kostis. 2012. 'Meta-analysis of statin effects in women versus men', *J Am Coll Cardiol*, 59: 572-82.

Kotlikoff, M. I., G. Herrera, and M. T. Nelson. 1999. 'Calcium permeant ion channels in smooth muscle', *Rev Physiol Biochem Pharmacol*, 134: 147-99.

Kumar, A., H. Kaur, P. Devi, and V. Mohan. 2009. 'Role of coenzyme Q10 (CoQ10) in cardiac disease, hypertension and Meniere-like syndrome', *Pharmacol Ther*, 124: 259-68.

Kuznetsov, A. V., M. Hermann, V. Saks, P. Hengster, and R. Margreiter. 2009. 'The cell-type specificity of mitochondrial dynamics', *Int J Biochem Cell Biol*, 41: 1928-39.

Kwak, B. R., and F. Mach. 2001. 'Statins inhibit leukocyte recruitment: new evidence for their anti-inflammatory properties', *Arterioscler Thromb Vasc Biol*, 21: 1256-8.

Kwak, H. B., A. Thalacker-Mercer, E. J. Anderson, C. T. Lin, D. A. Kane, N. S. Lee, R. N. Cortright, M. M. Bamman, and P. D. Neufer. 2012. 'Simvastatin impairs ADP-stimulated respiration and increases mitochondrial oxidative stress in primary human skeletal myotubes', *Free Radic Biol Med*, 52: 198-207.

Laaksonen, R., K. Jokelainen, J. Laakso, T. Sahi, M. Harkonen, M. J. Tikkanen, and J. J. Himberg. 1996. 'The effect of simvastatin treatment on natural antioxidants in low-density lipoproteins and high-energy phosphates and ubiquinone in skeletal muscle', *Am J Cardiol*, 77: 851-4.

Lagaud, G., N. Gaudreault, E. D. Moore, C. Van Breemen, and I. Laher. 2002. 'Pressure-dependent myogenic constriction of cerebral arteries occurs independently of voltage-dependent activation', *Am J Physiol Heart Circ Physiol*, 283: H2187-95.

Lai, B., L. Zhang, L. Y. Dong, Y. H. Zhu, F. Y. Sun, and P. Zheng. 2005. 'Inhibition of Qi site of mitochondrial complex III with antimycin A decreases persistent and transient sodium currents via reactive oxygen species and protein kinase C in rat hippocampal CA1 cells', *Exp Neurol*, 194: 484-94.

———. 2006. 'Impact of inhibition of Qo site of mitochondrial complex III with myxothiazol on persistent sodium currents via superoxide and protein kinase C in rat hippocampal CA1 cells', *Neurobiol Dis*, 21: 206-16.

Lampl, T., J. A. Crum, T. A. Davis, C. Milligan, and V. Del Gaizo Moore. 2015. 'Isolation and functional analysis of mitochondria from cultured cells and mouse tissue', *J Vis Exp*.

Laufs, U., and J. K. Liao. 2000. 'Direct vascular effects of HMG-CoA reductase inhibitors', *Trends Cardiovasc Med*, 10: 143-8.

Laufs, U., D. Marra, K. Node, and J. K. Liao. 1999. '3-Hydroxy-3-methylglutaryl-CoA reductase inhibitors attenuate vascular smooth muscle proliferation by preventing rho GTPase-induced down-regulation of p27(Kip1)', *J Biol Chem*, 274: 21926-31.

Lee, C. W., and H. B. Peng. 2008. 'The function of mitochondria in presynaptic development at the neuromuscular junction', *Mol Biol Cell*, 19: 150-8.

Lee, K. Y., and H. C. Choi. 2013. 'Acetylcholine-induced AMP-activated protein kinase activation attenuates vasoconstriction through an LKB1-dependent mechanism in rat aorta', *Vascul Pharmacol*, 59: 96-102.

Lenaz, G., G. D. Daves, Jr., and K. Kfolkers. 1968. 'Organic structural specificity and sites of coenzyme Q in succinoxidase and DPNH-oxidase systems', *Arch Biochem Biophys*, 123: 539-50.

Lesnefsky, E. J., D. He, S. Moghaddas, and C. L. Hoppel. 2006. 'Reversal of mitochondrial defects before ischemia protects the aged heart', *Faseb j*, 20: 1543-5.

Lewington, S., G. Whitlock, R. Clarke, P. Sherliker, J. Emberson, J. Halsey, N. Qizilbash, R. Peto, and R. Collins. 2007. 'Blood cholesterol and vascular mortality by age, sex, and blood pressure: a meta-analysis of individual data from 61 prospective studies with 55,000 vascular deaths', *Lancet*, 370: 1829-39.

Li, C. B., X. X. Li, Y. G. Chen, H. Q. Gao, M. C. Bao, J. Zhang, P. L. Bu, Y. Zhang, and X. P. Ji. 2012. 'Simvastatin exerts cardioprotective effects and inhibits the activity of Rho-associated protein kinase in rats with metabolic syndrome', *Clin Exp Pharmacol Physiol*, 39: 759-64.

Li, N., K. Ragheb, G. Lawler, J. Sturgis, B. Rajwa, J. A. Melendez, and J. P. Robinson. 2003. 'Mitochondrial complex I inhibitor rotenone induces apoptosis through enhancing mitochondrial reactive oxygen species production', *J Biol Chem*, 278: 8516-25.

Li, Z., K. Okamoto, Y. Hayashi, and M. Sheng. 2004. 'The importance of dendritic mitochondria in the morphogenesis and plasticity of spines and synapses', *Cell*, 119: 873-87.

Libby, P. 2001. 'Current concepts of the pathogenesis of the acute coronary syndromes', *Circulation*, 104: 365-72.

Lindsay, D. P., A. K. Camara, D. F. Stowe, R. Lubbe, and M. Aldakkak. 2015. 'Differential effects of buffer pH on Ca(2+)-induced ROS emission with inhibited mitochondrial complexes I and III', *Front Physiol*, 6: 58.

Littarru, G. P., and P. Langsjoen. 2007. 'Coenzyme Q10 and statins: biochemical and clinical implications', *Mitochondrion*, 7 Suppl: S168-74.

Littarru, G. P., and L. Tiano. 2007. 'Bioenergetic and antioxidant properties of coenzyme Q10: recent developments', *Mol Biotechnol*, 37: 31-7.

Liu, M. Y., and M. Colombini. 1992. 'Regulation of mitochondrial respiration by controlling the permeability of the outer membrane through the mitochondrial channel, VDAC', *Biochim Biophys Acta*, 1098: 255-60.

Liu, X., R. R. Chhipa, I. Nakano, and B. Dasgupta. 2014. 'The AMPK inhibitor compound C is a potent AMPK-independent antiglioma agent', *Mol Cancer Ther*, 13: 596-605.

Lopez-Jimenez, F., V. Simha, R. J. Thomas, T. G. Allison, A. Basu, R. Fernandes, R. T. Hurst, S. L. Kopecky, I. J. Kullo, S. L. Mulvagh, W. G. Thompson, J. F. Trejo-Gutierrez, and R. S. Wright. 2014. 'A summary and critical assessment of the 2013 ACC/AHA guideline on the treatment of blood cholesterol to reduce atherosclerotic cardiovascular disease risk in adults: filling the gaps', *Mayo Clin Proc*, 89: 1257-78.

Lozano, R., M. Naghavi, K. Foreman, S. Lim, K. Shibuya, V. Aboyans, J. Abraham, T. Adair, R. Aggarwal, S. Y. Ahn, M. Alvarado, H. R. Anderson, L. M. Anderson, K. G. Andrews, C. Atkinson, L. M. Baddour, S. Barker-Collo, D. H. Bartels, M. L. Bell, E. J. Benjamin, D. Bennett, K. Bhalla, B. Bikbov, A. Bin Abdulhak, G. Birbeck, F. Blyth, I. Bolliger, S. Boufous, C. Bucello, M. Burch, P. Burney, J. Carapetis, H. Chen, D. Chou, S. S. Chugh, L. E. Coffeng, S. D. Colan, S. Colquhoun, K. E. Colson, J. Condon, M. D. Connor, L. T. Cooper, M. Corriere, M. Cortinovis, K. C. de Vaccaro, W. Couser, B. C. Cowie, M. H. Criqui, M. Cross, K. C. Dabhadkar, N. Dahodwala, D. De Leo, L. Degenhardt, A. Delossantos, J. Denenberg, D. C. Des Jarlais, S. D. Dharmaratne, E. R. Dorsey, T. Driscoll, H. Duber, B. Ebel, P. J. Erwin, P. Espindola, M. Ezzati, V. Feigin, A. D. Flaxman, M. H. Forouzanfar, F. G. Fowkes, R. Franklin, M. Fransen, M. K. Freeman, S. E. Gabriel, E. Gakidou, F. Gaspari, R. F. Gillum, D. Gonzalez-Medina, Y. A. Halasa, D. Haring, J. E. Harrison, R. Havmoeller, R. J. Hay, B. Hoen, P. J. Hotez, D. Hoy, K. H. Jacobsen, S. L. James, R. Jasrasaria, S. Jayaraman, N. Johns, G. Karthikeyan, N. Kassebaum, A. Keren, J. P. Khoo, L. M. Knowlton, O. Kobusingye, A. Koranteng, R. Krishnamurthi, M. Lipnick, S. E. Lipshultz, S. L. Ohno, J. Mabweijano, M. F. MacIntyre, L. Mallinger, L. March, G. B. Marks, R. Marks, A. Matsumori, R. Matzopoulos, B. M. Mayosi, J. H. McAnulty, M. M. McDermott, J. McGrath, G. A. Mensah, T. R. Merriman, C. Michaud, M. Miller, T. R. Miller, C. Mock, A. O. Mocumbi, A. A. Mokdad, A. Moran, K. Mulholland, M. N. Nair, L. Naldi, K. M. Narayan, K. Nasseri, P. Norman, M. O'Donnell, S. B. Omer, K. Ortblad, R. Osborne, D. Ozgediz, B. Pahari, J. D. Pandian, A. P. Rivero, R. P. Padilla, F. Perez-Ruiz, N. Perico, D. Phillips, K. Pierce, C. A. Pope, 3rd, E. Porrini, F. Pourmalek, M. Raju, D. Ranganathan, J. T. Rehm, D. B. Rein, G. Remuzzi, F. P. Rivara, T. Roberts, F. R. De Leon, L. C. Rosenfeld, L. Rushton, R. L. Sacco, J. A. Salomon, U. Sampson, E. Sanman, D. C. Schwebel, M. Segui-Gomez, D. S. Shepard, D. Singh, J. Singleton, K. Sliwa, E. Smith, A. Steer, J. A. Taylor, B. Thomas, I. M. Tleyjeh, J. A. Towbin, T. Truelsen, E. A. Undurraga, N. Venketasubramanian, L. Vijayakumar, T. Vos, G. R. Wagner, M. Wang, W. Wang, K. Watt, M. A. Weinstock, R. Weintraub, J. D. Wilkinson, A. D. Woolf, S. Wulf, P. H. Yeh, P. Yip, A. Zabetian, Z. J. Zheng, A. D. Lopez, C. J. Murray, M. A. AlMazroa, and Z. A. Memish. 2012. 'Global and regional mortality from 235 causes of death for 20 age groups in 1990 and 2010: a systematic analysis for the Global Burden of Disease Study 2010', *Lancet*, 380: 2095-128.

Ma, T., Q. H. Qi, J. Xu, Z. L. Dong, and W. X. Yang. 2004. 'Signal pathways involved in emodin-induced contraction of smooth muscle cells from rat colon', *World J Gastroenterol*, 10: 1476-9.

MacKay, C. E., Y. Shaifta, V. V. Snetkov, A. A. Francois, J. P. T. Ward, and G. A. Knock. 2017. 'ROS-dependent activation of RhoA/Rho-kinase in pulmonary artery: Role of Src-family kinases and ARHGEF1', *Free Radic Biol Med*, 110: 316-31.

Madiraju, A. K., D. M. Erion, Y. Rahimi, X. M. Zhang, D. T. Braddock, R. A. Albright, B. J. Prigaro, J. L. Wood, S. Bhanot, M. J. MacDonald, M. J. Jurczak, J. P. Camporez, H. Y. Lee, G. W. Cline, V. T. Samuel, R. G. Kibbey, and G. I. Shulman. 2014. 'Metformin suppresses gluconeogenesis by inhibiting mitochondrial glycerophosphate dehydrogenase', *Nature*, 510: 542-6.

Makowska, A., K. Zablocki, and J. Duszynski. 2000. 'The role of mitochondria in the regulation of calcium influx into Jurkat cells', *Eur J Biochem*, 267: 877-84.

Marcoff, L., and P. D. Thompson. 2007. 'The role of coenzyme Q10 in statin-associated myopathy: a systematic review', *J Am Coll Cardiol*, 49: 2231-7.

Matthews, R. T., L. Yang, S. Browne, M. Baik, and M. F. Beal. 1998. 'Coenzyme Q10 administration increases brain mitochondrial concentrations and exerts neuroprotective effects', *Proc Natl Acad Sci U S A*, 95: 8892-7.

McCarron, J. G., K. N. Bradley, D. MacMillan, S. Chalmers, and T. C. Muir. 2004. 'The sarcoplasmic reticulum, Ca2+ trapping, and wave mechanisms in smooth muscle', *News Physiol Sci*, 19: 138-47.

McCarron, J. G., E. R. Flynn, K. N. Bradley, and T. C. Muir. 2000. 'Two Ca2+ entry pathways mediate InsP3-sensitive store refilling in guinea-pig colonic smooth muscle', *J Physiol*, 525 Pt 1: 113-24.

McCarron, J. G., and T. C. Muir. 1999. 'Mitochondrial regulation of the cytosolic Ca2+ concentration and the InsP3-sensitive Ca2+ store in guinea-pig colonic smooth muscle', *J Physiol*, 516 (Pt 1): 149-61.

McCarron, J. G., M. L. Olson, and S. Chalmers. 2012. 'Mitochondrial regulation of cytosolic Ca(2)(+) signals in smooth muscle', *Pflugers Arch*, 464: 51-62.

McCarron, J. G., M. L. Olson, C. Wilson, M. E. Sandison, and S. Chalmers. 2013. 'Examining the role of mitochondria in Ca^{2+} signaling in native vascular smooth muscle', *Microcirculation*, 20: 317-29.

McFadzean, I., and A. Gibson. 2002. 'The developing relationship between receptor-operated and store-operated calcium channels in smooth muscle', *Br J Pharmacol*, 135: 1-13.

McFarland, A. J., S. Anoopkumar-Dukie, D. S. Arora, G. D. Grant, C. M. McDermott, A. V. Perkins, and A. K. Davey. 2014. 'Molecular mechanisms underlying the effects of statins in the central nervous system', *Int J Mol Sci*, 15: 20607-37.

McKenzie, M., S. C. Lim, and M. R. Duchen. 2017. 'Simultaneous Measurement of Mitochondrial Calcium and Mitochondrial Membrane Potential in Live Cells by Fluorescent Microscopy', *J Vis Exp*.

Mendes, P., P. G. Robles, and S. Mathur. 2014. 'Statin-induced rhabdomyolysis: a comprehensive review of case reports', *Physiother Can*, 66: 124-32.

Michelakis, E. D., I. Rebeyka, X. Wu, A. Nsair, B. Thebaud, K. Hashimoto, J. R. Dyck, A. Haromy, G. Harry, A. Barr, and S. L. Archer. 2002. 'O2 sensing in the human ductus arteriosus: regulation of voltage-gated K+ channels in smooth muscle cells by a mitochondrial redox sensor', *Circ Res*, 91: 478-86.

Mihos, C. G., M. J. Salas, and O. Santana. 2010. 'The pleiotropic effects of the hydroxy-methyl-glutaryl-CoA reductase inhibitors in cardiovascular disease: a comprehensive review', *Cardiol Rev*, 18: 298-304.

Mizuno, Y., E. Isotani, J. Huang, H. Ding, J. T. Stull, and K. E. Kamm. 2008. 'Myosin light chain kinase activation and calcium sensitization in smooth muscle in vivo', *Am J Physiol Cell Physiol*, 295: C358-64.

Modis, K., E. M. Bos, E. Calzia, H. van Goor, C. Coletta, A. Papapetropoulos, M. R. Hellmich, P. Radermacher, F. Bouillaud, and C. Szabo. 2014. 'Regulation of mitochondrial bioenergetic

function by hydrogen sulfide. Part II. Pathophysiological and therapeutic aspects', *Br J Pharmacol*, 171: 2123-46.

Mohaupt, M. G., R. H. Karas, E. B. Babiychuk, V. Sanchez-Freire, K. Monastyrskaya, L. Iyer, H. Hoppeler, F. Breil, and A. Draeger. 2009. 'Association between statin-associated myopathy and skeletal muscle damage', *Cmaj*, 181: E11-8.

Moral-Sanz, J., A. D. Mahmoud, F. A. Ross, J. Eldstrom, D. Fedida, D. G. Hardie, and A. M. Evans. 2016. 'AMP-activated protein kinase inhibits Kv 1.5 channel currents of pulmonary arterial myocytes in response to hypoxia and inhibition of mitochondrial oxidative phosphorylation', *J Physiol*, 594: 4901-15.

Mori, A., E. Ishikawa, T. Amano, K. Sakamoto, and T. Nakahara. 2017. 'Anti-diabetic drug metformin dilates retinal blood vessels through activation of AMP-activated protein kinase in rats', *Eur J Pharmacol*, 798: 66-71.

Mori, M., and H. Tsushima. 2004. 'Vanadate activates Rho A translocation in association with contracting effects in ileal longitudinal smooth muscle of guinea pig', *J Pharmacol Sci*, 95: 443-51.

Moudgil, R., E. D. Michelakis, and S. L. Archer. 2005. 'Hypoxic pulmonary vasoconstriction', *J Appl Physiol (1985)*, 98: 390-403.

Muller, F. L., A. G. Roberts, M. K. Bowman, and D. M. Kramer. 2003. 'Architecture of the Qo site of the cytochrome bc1 complex probed by superoxide production', *Biochemistry*, 42: 6493-9.

Murphy, M. P., and R. A. Smith. 2000. 'Drug delivery to mitochondria: the key to mitochondrial medicine', *Adv Drug Deliv Rev*, 41: 235-50.

Mytilinaiou, M., I. Kyrou, M. Khan, D. K. Grammatopoulos, and H. S. Randeva. 2018. 'Familial Hypercholesterolemia: New Horizons for Diagnosis and Effective Management', *Front Pharmacol*, 9: 707.

Nadanaciva, S., J. A. Dykens, A. Bernal, R. A. Capaldi, and Y. Will. 2007. 'Mitochondrial impairment by PPAR agonists and statins identified via immunocaptured OXPHOS complex activities and respiration', *Toxicol Appl Pharmacol*, 223: 277-87.

Nagata, D., R. Takeda, M. Sata, H. Satonaka, E. Suzuki, T. Nagano, and Y. Hirata. 2004. 'AMP-activated protein kinase inhibits angiotensin II-stimulated vascular smooth muscle cell proliferation', *Circulation*, 110: 444-51.

Nagumo, H., Y. Sasaki, Y. Ono, H. Okamoto, M. Seto, and Y. Takuwa. 2000. 'Rho kinase inhibitor HA-1077 prevents Rho-mediated myosin phosphatase inhibition in smooth muscle cells', *Am J Physiol Cell Physiol*, 278: C57-65.

Nakagawa, H., H. Karaki, K. Murakami, and N. Urakawa. 1985. 'Effects of antimycin A on vascular and intestinal smooth muscle contraction and calcium movements', *Arch Int Pharmacodyn Ther*, 276: 92-105.

Nakayama, K., F. Okamoto, and Y. Harada. 1956. 'Antimycin A: isolation from a new Streptomyces and activity against rice plant blast fungi', *J Antibiot (Tokyo)*, 9: 63-6.

Nangia, R., H. Singh, and K. Kaur. 2016. 'Prevalence of cardiovascular disease (CVD) risk factors', *Med J Armed Forces India*, 72: 315-19.

Nawaz, Muhammad, Claudia Manzl, Veronika Lacher, and Gerhard Krumschnabel. 2006. 'Copper-Induced Stimulation of Extracellular Signal-Regulated Kinase in Trout Hepatocytes: The Role of Reactive Oxygen Species, Ca2+, and Cell Energetics and the Impact of Extracellular Signal-Regulated Kinase Signaling on Apoptosis and Necrosis', *Toxicological Sciences*, 92: 464-75.

Nelson, T. E. 1991. 'Skeletal muscle targets for the action of anesthetic agents', *Adv Exp Med Biol*, 301: 3-8.

Newman, T. B., and S. B. Hulley. 1996. 'Carcinogenicity of lipid-lowering drugs', *Jama*, 275: 55-60.

Newton, J. N., A. D. Briggs, C. J. Murray, D. Dicker, K. J. Foreman, H. Wang, M. Naghavi, M. H. Forouzanfar, S. L. Ohno, R. M. Barber, T. Vos, J. D. Stanaway, J. C. Schmidt, A. J. Hughes, D. F. Fay, R. Ecob, C. Gresser, M. McKee, H. Rutter, I. Abubakar, R. Ali, H. R. Anderson, A. Banerjee, D. A. Bennett, E. Bernabe, K. S. Bhui, S. M. Biryukov, R. R. Bourne, C. E. Brayne, N. G. Bruce, T.

S. Brugha, M. Burch, S. Capewell, D. Casey, R. Chowdhury, M. M. Coates, C. Cooper, J. A. Critchley, P. I. Dargan, M. K. Dherani, P. Elliott, M. Ezzati, K. A. Fenton, M. S. Fraser, T. Furst, F. Greaves, M. A. Green, D. J. Gunnell, B. M. Hannigan, R. J. Hay, S. I. Hay, H. Hemingway, H. J. Larson, K. J. Looker, R. Lunevicius, R. A. Lyons, W. Marcenes, A. J. Mason-Jones, F. E. Matthews, H. Moller, M. E. Murdoch, C. R. Newton, N. Pearce, F. B. Piel, D. Pope, K. Rahimi, A. Rodriguez, P. Scarborough, A. E. Schumacher, I. Shiue, L. Smeeth, A. Tedstone, J. Valabhji, H. C. Williams, C. D. Wolfe, A. D. Woolf, and A. C. Davis. 2015. 'Changes in health in England, with analysis by English regions and areas of deprivation, 1990-2013: a systematic analysis for the Global Burden of Disease Study 2013', *Lancet*, 386: 2257-74.

Ng, L. L., J. E. Davies, and R. J. Wojcikiewicz. 1994. '3-Hydroxy-3-methyl glutaryl coenzyme A reductase inhibition modulates vasopressin-stimulated Ca2+ responses in rat A10 vascular smooth muscle cells', *Circ Res*, 74: 173-81.

Ngai, P. K., and M. P. Walsh. 1984. 'Inhibition of smooth muscle actin-activated myosin Mg2+-ATPase activity by caldesmon', *J Biol Chem*, 259: 13656-9.

Nichols, W. W., C. J. Pepine, E. A. Geiser, and C. R. Conti. 1980. 'Vascular load defined by the aortic input impedance spectrum', *Fed Proc*, 39: 196-201.

O'Flaherty, M., I. Buchan, and S. Capewell. 2013. 'Contributions of treatment and lifestyle to declining CVD mortality: why have CVD mortality rates declined so much since the 1960s?', *Heart*, 99: 159-62.

O'Malley, Y., B. D. Fink, N. C. Ross, T. E. Prisinzano, and W. I. Sivitz. 2006. 'Reactive oxygen and targeted antioxidant administration in endothelial cell mitochondria', *J Biol Chem*, 281: 39766-75.

Oeckler, R. A., P. M. Kaminski, and M. S. Wolin. 2003a. 'Stretch enhances contraction of bovine coronary arteries via an NAD(P)H oxidase-mediated activation of the extracellular signal-regulated kinase mitogen-activated protein kinase cascade', *Circ Res*, 92: 23-31.

Oeckler, Richard A., Pawel M. Kaminski, and Michael S. Wolin. 2003b. 'Stretch Enhances Contraction of Bovine Coronary Arteries via an NAD(P)H Oxidase–Mediated Activation of the Extracellular Signal–Regulated Kinase Mitogen-Activated Protein Kinase Cascade', *Circulation Research*, 92: 23-31.

Ogasahara, S., A. G. Engel, D. Frens, and D. Mack. 1989. 'Muscle coenzyme Q deficiency in familial mitochondrial encephalomyopathy', *Proc Natl Acad Sci U S A*, 86: 2379-82.

Olson, M. L., S. Chalmers, and J. G. McCarron. 2010. 'Mitochondrial Ca2+ uptake increases Ca2+ release from inositol 1,4,5-trisphosphate receptor clusters in smooth muscle cells', *J Biol Chem*, 285: 2040-50.

Orsi, A., O. Sherman, and Z. Woldeselassie. 2001. 'Simvastatin-associated memory loss', *Pharmacotherapy*, 21: 767-9.

Ostrakhovitch, E. A., and M. G. Cherian. 2005. 'Role of p53 and reactive oxygen species in apoptotic response to copper and zinc in epithelial breast cancer cells', *Apoptosis*, 10: 111-21.

Owen, M. R., E. Doran, and A. P. Halestrap. 2000. 'Evidence that metformin exerts its anti-diabetic effects through inhibition of complex 1 of the mitochondrial respiratory chain', *Biochem J*, 348 Pt 3: 607-14.

Paiva, H., K. M. Thelen, R. Van Coster, J. Smet, B. De Paepe, K. M. Mattila, J. Laakso, T. Lehtimaki, K. von Bergmann, D. Lutjohann, and R. Laaksonen. 2005. 'High-dose statins and skeletal muscle metabolism in humans: a randomized, controlled trial', *Clin Pharmacol Ther*, 78: 60-8.

Palizvan, M. R., M. R. Nejad, A. Jand, and M. Rafeie. 2013. 'Cardiovascular physiology misconceptions and the potential of cardiovascular physiology teaching to alleviate these', *Med Teach*, 35: 454-8.

Parekh, A. B., and R. Penner. 1997. 'Store depletion and calcium influx', *Physiol Rev*, 77: 901-30.

Parihar, A., M. S. Parihar, W. J. Zenebe, and P. Ghafourifar. 2012. 'Statins lower calcium-induced oxidative stress in isolated mitochondria', *Hum Exp Toxicol*, 31: 355-63.

Park, M. K., M. C. Ashby, G. Erdemli, O. H. Petersen, and A. V. Tepikin. 2001. 'Perinuclear, perigranular and sub-plasmalemmal mitochondria have distinct functions in the regulation of cellular calcium transport', *Embo j*, 20: 1863-74.
Park, W. H., Y. W. Han, S. H. Kim, and S. Z. Kim. 2007. 'An ROS generator, antimycin A, inhibits the growth of HeLa cells via apoptosis', *J Cell Biochem*, 102: 98-109.
Parker, K. H., C. J. Jones, J. R. Dawson, and D. G. Gibson. 1988. 'What stops the flow of blood from the heart?', *Heart Vessels*, 4: 241-5.
Pearson-Stuttard, Jonathan, Madhavi Bajekal, Shaun Scholes, Martin O'Flaherty, Nathaniel Mark Hawkins, Rosalind Raine, and Simon Capewell. 2012. 'Recent UK trends in the unequal burden of coronary heart disease', *Heart*, 98: 1573-82.
Pedersen, T. R. 2010. 'Pleiotropic effects of statins: evidence against benefits beyond LDL-cholesterol lowering', *Am J Cardiovasc Drugs*, 10 Suppl 1: 10-7.
Pedrini, S., T. L. Carter, G. Prendergast, S. Petanceska, M. E. Ehrlich, and S. Gandy. 2005. 'Modulation of statin-activated shedding of Alzheimer APP ectodomain by ROCK', *PLoS Med*, 2: e18.
Petretta, M., P. Costanzo, P. Perrone-Filardi, and M. Chiariello. 2010. 'Impact of gender in primary prevention of coronary heart disease with statin therapy: a meta-analysis', *Int J Cardiol*, 138: 25-31.
Pham, N. A., B. H. Robinson, and D. W. Hedley. 2000. 'Simultaneous detection of mitochondrial respiratory chain activity and reactive oxygen in digitonin-permeabilized cells using flow cytometry', *Cytometry*, 41: 245-51.
Piomboni, P., R. Focarelli, A. Stendardi, A. Ferramosca, and V. Zara. 2012. 'The role of mitochondria in energy production for human sperm motility', *Int J Androl*, 35: 109-24.
Pitter, J. G., P. Maechler, C. B. Wollheim, and A. Spat. 2002. 'Mitochondria respond to Ca2+ already in the submicromolar range: correlation with redox state', *Cell Calcium*, 31: 97-104.
Pochynyuk, O., J. Medina, N. Gamper, H. Genth, J. D. Stockand, and A. Staruschenko. 2006. 'Rapid translocation and insertion of the epithelial Na+ channel in response to RhoA signaling', *J Biol Chem*, 281: 26520-7.
Prueksaritanont, T., B. Ma, X. Fang, R. Subramanian, J. Yu, and J. H. Lin. 2001. 'beta-Oxidation of simvastatin in mouse liver preparations', *Drug Metab Dispos*, 29: 1251-5.
Prueksaritanont, T., Y. Qiu, L. Mu, K. Michel, J. Brunner, K. M. Richards, and J. H. Lin. 2005. 'Interconversion pharmacokinetics of simvastatin and its hydroxy acid in dogs: effects of gemfibrozil', *Pharm Res*, 22: 1101-9.
Putney, J. W., Jr. 2001. 'Pharmacology of capacitative calcium entry', *Mol Interv*, 1: 84-94.
Quinlan, C. L., A. L. Orr, I. V. Perevoshchikova, J. R. Treberg, B. A. Ackrell, and M. D. Brand. 2012. 'Mitochondrial complex II can generate reactive oxygen species at high rates in both the forward and reverse reactions', *J Biol Chem*, 287: 27255-64.
Quion, J. A., and P. H. Jones. 1994. 'Clinical pharmacokinetics of pravastatin', *Clin Pharmacokinet*, 27: 94-103.
Raha, S., G. E. McEachern, A. T. Myint, and B. H. Robinson. 2000. 'Superoxides from mitochondrial complex III: the role of manganese superoxide dismutase', *Free Radic Biol Med*, 29: 170-80.
Raman, M., W. Chen, and M. H. Cobb. 2007. 'Differential regulation and properties of MAPKs', *Oncogene*, 26: 3100-12.
Ramkumar, S., A. Raghunath, and S. Raghunath. 2016. 'Statin Therapy: Review of Safety and Potential Side Effects', *Acta Cardiol Sin*, 32: 631-39.
Ramos, R., M. Comas-Cufi, R. Marti-Lluch, E. Ballo, A. Ponjoan, L. Alves-Cabratosa, J. Blanch, J. Marrugat, R. Elosua, M. Grau, M. Elosua-Bayes, L. Garcia-Ortiz, and M. Garcia-Gil. 2018. 'Statins for primary prevention of cardiovascular events and mortality in old and very old adults with and without type 2 diabetes: retrospective cohort study', *Bmj*, 362: k3359.
Rapizzi, E., P. Pinton, G. Szabadkai, M. R. Wieckowski, G. Vandecasteele, G. Baird, R. A. Tuft, K. E. Fogarty, and R. Rizzuto. 2002. 'Recombinant expression of the voltage-dependent anion

channel enhances the transfer of Ca2+ microdomains to mitochondria', *J Cell Biol*, 159: 613-24.

Rattan, S. 2010. '3-Hydroxymethyl coenzyme A reductase inhibition attenuates spontaneous smooth muscle tone via RhoA/ROCK pathway regulated by RhoA prenylation', *Am J Physiol Gastrointest Liver Physiol*, 298: G962-9.

Richter, E. A., and M. Hargreaves. 2013. 'Exercise, GLUT4, and skeletal muscle glucose uptake', *Physiol Rev*, 93: 993-1017.

Rikitake, Y., H. H. Kim, Z. Huang, M. Seto, K. Yano, T. Asano, M. A. Moskowitz, and J. K. Liao. 2005. 'Inhibition of Rho kinase (ROCK) leads to increased cerebral blood flow and stroke protection', *Stroke*, 36: 2251-7.

Rikitake, Y., and J. K. Liao. 2005. 'Rho GTPases, statins, and nitric oxide', *Circ Res*, 97: 1232-5.

Rizzuto, R., P. Bernardi, and T. Pozzan. 2000. 'Mitochondria as all-round players of the calcium game', *J Physiol*, 529 Pt 1: 37-47.

Roberts, R. E. 2001. 'Role of the extracellular signal-regulated kinase (Erk) signal transduction cascade in alpha(2) adrenoceptor-mediated vasoconstriction in porcine palmar lateral vein', *Br J Pharmacol*, 133: 859-66.

———. 2004. 'The role of Rho kinase and extracellular regulated kinase-mitogen-activated protein kinase in alpha2-adrenoceptor-mediated vasoconstriction in the porcine palmar lateral vein', *J Pharmacol Exp Ther*, 311: 742-7.

———. 2012. 'The extracellular signal-regulated kinase (ERK) pathway: a potential therapeutic target in hypertension', *J Exp Pharmacol*, 4: 77-83.

Roger, V. L., A. S. Go, D. M. Lloyd-Jones, R. J. Adams, J. D. Berry, T. M. Brown, M. R. Carnethon, S. Dai, G. de Simone, E. S. Ford, C. S. Fox, H. J. Fullerton, C. Gillespie, K. J. Greenlund, S. M. Hailpern, J. A. Heit, P. M. Ho, V. J. Howard, B. M. Kissela, S. J. Kittner, D. T. Lackland, J. H. Lichtman, L. D. Lisabeth, D. M. Makuc, G. M. Marcus, A. Marelli, D. B. Matchar, M. M. McDermott, J. B. Meigs, C. S. Moy, D. Mozaffarian, M. E. Mussolino, G. Nichol, N. P. Paynter, W. D. Rosamond, P. D. Sorlie, R. S. Stafford, T. N. Turan, M. B. Turner, N. D. Wong, and J. Wylie-Rosett. 2011. 'Heart disease and stroke statistics--2011 update: a report from the American Heart Association', *Circulation*, 123: e18-e209.

Rogers, P. A., G. M. Dick, J. D. Knudson, M. Focardi, I. N. Bratz, A. N. Swafford, Jr., S. Saitoh, J. D. Tune, and W. M. Chilian. 2006. 'H2O2-induced redox-sensitive coronary vasodilation is mediated by 4-aminopyridine-sensitive K+ channels', *Am J Physiol Heart Circ Physiol*, 291: H2473-82.

Ronot, X., L. Benel, M. Adolphe, and J. C. Mounolou. 1986. 'Mitochondrial analysis in living cells: the use of rhodamine 123 and flow cytometry', *Biol Cell*, 57: 1-7.

Rosenfeldt, F. L., S. Pepe, R. Ou, J. A. Mariani, M. A. Rowland, P. Nagley, and A. W. Linnane. 1999. 'Coenzyme Q10 improves the tolerance of the senescent myocardium to aerobic and ischemic stress: studies in rats and in human atrial tissue', *Biofactors*, 9: 291-9.

Rossoni, L. V., M. Wareing, C. F. Wenceslau, M. Al-Abri, C. Cobb, and C. Austin. 2011. 'Acute simvastatin increases endothelial nitric oxide synthase phosphorylation via AMP-activated protein kinase and reduces contractility of isolated rat mesenteric resistance arteries', *Clin Sci (Lond)*, 121: 449-58.

Rottenberg, H. 1984. 'Membrane potential and surface potential in mitochondria: uptake and binding of lipophilic cations', *J Membr Biol*, 81: 127-38.

Roux, E., and M. Marhl. 2004. 'Role of sarcoplasmic reticulum and mitochondria in Ca2+ removal in airway myocytes', *Biophys J*, 86: 2583-95.

Rundek, T., A. Naini, R. Sacco, K. Coates, and S. DiMauro. 2004. 'Atorvastatin decreases the coenzyme Q10 level in the blood of patients at risk for cardiovascular disease and stroke', *Arch Neurol*, 61: 889-92.

Rygiel, T. P., A. E. Mertens, K. Strumane, R. van der Kammen, and J. G. Collard. 2008. 'The Rac activator Tiam1 prevents keratinocyte apoptosis by controlling ROS-mediated ERK phosphorylation', *J Cell Sci*, 121: 1183-92.

Sadeghi, M. M., M. Collinge, R. Pardi, and J. R. Bender. 2000. 'Simvastatin modulates cytokine-mediated endothelial cell adhesion molecule induction: involvement of an inhibitory G protein', *J Immunol*, 165: 2712-8.

Sahai, E., and C. J. Marshall. 2002. 'ROCK and Dia have opposing effects on adherens junctions downstream of Rho', *Nat Cell Biol*, 4: 408-15.

Satoh, K., A. Yamato, T. Nakai, K. Hoshi, and K. Ichihara. 1995. 'Effects of 3-hydroxy-3-methylglutaryl coenzyme A reductase inhibitors on mitochondrial respiration in ischaemic dog hearts', *Br J Pharmacol*, 116: 1894-8.

Schachter, M. 2005. 'Chemical, pharmacokinetic and pharmacodynamic properties of statins: an update', *Fundam Clin Pharmacol*, 19: 117-25.

Scheffler, I. E. 2001. 'Mitochondria make a come back', *Adv Drug Deliv Rev*, 49: 3-26.

Schirris, T. J., G. H. Renkema, T. Ritschel, N. C. Voermans, A. Bilos, B. G. van Engelen, U. Brandt, W. J. Koopman, J. D. Beyrath, R. J. Rodenburg, P. H. Willems, J. A. Smeitink, and F. G. Russel. 2015. 'Statin-Induced Myopathy Is Associated with Mitochondrial Complex III Inhibition', *Cell Metab*, 22: 399-407.

Schneider, H., K. M. Schubert, S. Blodow, C. P. Kreutz, S. Erdogmus, M. Wiedenmann, J. Qiu, T. Fey, P. Ruth, L. T. Lubomirov, G. Pfitzer, Y. Schnitzler M. Mederos, D. G. Hardie, T. Gudermann, and U. Pohl. 2015. 'AMPK Dilates Resistance Arteries via Activation of SERCA and BKCa Channels in Smooth Muscle', *Hypertension*, 66: 108-16.

Schultz, B. G., D. K. Patten, and D. J. Berlau. 2018. 'The role of statins in both cognitive impairment and protection against dementia: a tale of two mechanisms', *Transl Neurodegener*, 7: 5.

Scragg, J. L., M. L. Dallas, J. A. Wilkinson, G. Varadi, and C. Peers. 2008. 'Carbon monoxide inhibits L-type Ca2+ channels via redox modulation of key cysteine residues by mitochondrial reactive oxygen species', *J Biol Chem*, 283: 24412-9.

Searcy, D. G. 2001. 'Sulfide oxidation coupled to ATP synthesis in chicken liver mitochondria', *Comp Biochem Physiol B Biochem Mol Biol*, 129: 129-37.

Seto, S. W., A. L. Au, T. Y. Lam, S. S. Chim, S. M. Lee, S. Wan, D. C. Tjiu, N. Shigemura, A. P. Yim, S. W. Chan, S. K. Tsui, G. P. Leung, and Y. W. Kwan. 2007. 'Modulation by simvastatin of iberiotoxin-sensitive, Ca2+-activated K+ channels of porcine coronary artery smooth muscle cells', *Br J Pharmacol*, 151: 987-97.

Seto, S. W., A. L. Au, C. C. Poon, Q. Zhang, R. W. Li, J. H. Yeung, S. K. Kong, S. M. Ngai, S. Wan, H. P. Ho, S. M. Lee, M. P. Hoi, S. W. Chan, G. P. Leung, and Y. W. Kwan. 2013. 'Acute simvastatin inhibits K ATP channels of porcine coronary artery myocytes', *PLoS One*, 8: e66404.

Sever, P. S., B. Dahlof, N. R. Poulter, H. Wedel, G. Beevers, M. Caulfield, R. Collins, S. E. Kjeldsen, A. Kristinsson, G. T. McInnes, J. Mehlsen, M. Nieminen, E. O'Brien, and J. Ostergren. 2003. 'Prevention of coronary and stroke events with atorvastatin in hypertensive patients who have average or lower-than-average cholesterol concentrations, in the Anglo-Scandinavian Cardiac Outcomes Trial--Lipid Lowering Arm (ASCOT-LLA): a multicentre randomised controlled trial', *Lancet*, 361: 1149-58.

Shcheglovitov, A., T. Zhelay, Y. Vitko, V. Osipenko, E. Perez-Reyes, P. Kostyuk, and Y. Shuba. 2005. 'Contrasting the effects of nifedipine on subtypes of endogenous and recombinant T-type Ca2+ channels', *Biochem Pharmacol*, 69: 841-54.

Shepherd, J., S. M. Cobbe, I. Ford, C. G. Isles, A. R. Lorimer, P. W. MacFarlane, J. H. McKillop, and C. J. Packard. 1995. 'Prevention of coronary heart disease with pravastatin in men with hypercholesterolemia. West of Scotland Coronary Prevention Study Group', *N Engl J Med*, 333: 1301-7.

Short, Kevin R., Maureen L. Bigelow, Jane Kahl, Ravinder Singh, Jill Coenen-Schimke, Sreekumar Raghavakaimal, and K. Sreekumaran Nair. 2005. 'Decline in skeletal muscle mitochondrial function with aging in humans', *Proc Natl Acad Sci U S A*, 102: 5618-23.

Siasos, G., V. Tsigkou, M. Kosmopoulos, D. Theodosiadis, S. Simantiris, N. M. Tagkou, A. Tsimpiktsioglou, P. K. Stampouloglou, E. Oikonomou, K. Mourouzis, A. Philippou, M.

Vavuranakis, C. Stefanadis, D. Tousoulis, and A. G. Papavassiliou. 2018. 'Mitochondria and cardiovascular diseases-from pathophysiology to treatment', *Ann Transl Med*, 6: 256.
Siciliano, G., L. Volpi, S. Piazza, G. Ricci, M. Mancuso, and L. Murri. 2007. 'Functional diagnostics in mitochondrial diseases', *Biosci Rep*, 27: 53-67.
Siragusa, M., and I. Fleming. 2016. 'The eNOS signalosome and its link to endothelial dysfunction', *Pflugers Arch*, 468: 1125-37.
Sirvent, P., J. Mercier, G. Vassort, and A. Lacampagne. 2005. 'Simvastatin triggers mitochondria-induced Ca2+ signaling alteration in skeletal muscle', *Biochem Biophys Res Commun*, 329: 1067-75.
Smith, I. F., L. D. Plant, J. P. Boyle, R. A. Skinner, H. A. Pearson, and C. Peers. 2003. 'Chronic hypoxia potentiates capacitative Ca2+ entry in type-I cortical astrocytes', *J Neurochem*, 85: 1109-16.
Smith, J. C. 1990. 'Potential-sensitive molecular probes in membranes of bioenergetic relevance', *Biochim Biophys Acta*, 1016: 1-28.
Smith, M. H., K. R. Denninghoff, L. W. Hillman, and R. A. Chipman. 1998. 'Oxygen Saturation Measurements of Blood in Retinal Vessels during Blood Loss', *J Biomed Opt*, 3: 296-303.
Snetkov, V. A., G. A. Knock, L. Baxter, G. D. Thomas, J. P. Ward, and P. I. Aaronson. 2006. 'Mechanisms of the prostaglandin F2alpha-induced rise in [Ca2+]i in rat intrapulmonary arteries', *J Physiol*, 571: 147-63.
Soedamah-Muthu, S. S., S. J. Livingstone, V. Charlton-Menys, D. J. Betteridge, G. A. Hitman, H. A. Neil, W. Bao, D. A. DeMicco, G. M. Preston, J. H. Fuller, C. D. Stehouwer, C. G. Schalkwijk, P. N. Durrington, and H. M. Colhoun. 2015. 'Effect of atorvastatin on C-reactive protein and benefits for cardiovascular disease in patients with type 2 diabetes: analyses from the Collaborative Atorvastatin Diabetes Trial', *Diabetologia*, 58: 1494-502.
Somlyo, A. P., and A. V. Somlyo. 1994. 'Signal transduction and regulation in smooth muscle', *Nature*, 372: 231-6.
———. 2000. 'Signal transduction by G-proteins, rho-kinase and protein phosphatase to smooth muscle and non-muscle myosin II', *J Physiol*, 522 Pt 2: 177-85.
———. 2003. 'Ca2+ sensitivity of smooth muscle and nonmuscle myosin II: modulated by G proteins, kinases, and myosin phosphatase', *Physiol Rev*, 83: 1325-58.
Sonmez Uydes-Dogan, B., G. Topal, S. Takir, F. Ilkay Alp, D. Kaleli, and O. Ozdemir. 2005. 'Relaxant effects of pravastatin, atorvastatin and cerivastatin on isolated rat aortic rings', *Life Sci*, 76: 1771-86.
Sotnikova, R. 1998. 'Investigation of the mechanisms underlying H2O2-evoked contraction in the isolated rat aorta', *Gen Pharmacol*, 31: 115-9.
St-Pierre, J., J. A. Buckingham, S. J. Roebuck, and M. D. Brand. 2002. 'Topology of superoxide production from different sites in the mitochondrial electron transport chain', *J Biol Chem*, 277: 44784-90.
Starkov, A. A., and G. Fiskum. 2001. 'Myxothiazol induces H(2)O(2) production from mitochondrial respiratory chain', *Biochem Biophys Res Commun*, 281: 645-50.
———. 2003. 'Regulation of brain mitochondrial H2O2 production by membrane potential and NAD(P)H redox state', *J Neurochem*, 86: 1101-7.
Stegemann, J. P., H. Hong, and R. M. Nerem. 2005. 'Mechanical, biochemical, and extracellular matrix effects on vascular smooth muscle cell phenotype', *J Appl Physiol (1985)*, 98: 2321-7.
Stofega, M. R., C. L. Yu, J. Wu, and R. Jove. 1997. 'Activation of extracellular signal-regulated kinase (ERK) by mitogenic stimuli is repressed in v-Src-transformed cells', *Cell Growth Differ*, 8: 113-9.
Stubbs, E. B., Jr., and C. L. Von Zee. 2012. 'Prenylation of Rho G-proteins: a novel mechanism regulating gene expression and protein stability in human trabecular meshwork cells', *Mol Neurobiol*, 46: 28-40.

Su, B., S. Mitra, H. Gregg, S. Flavahan, M. A. Chotani, K. R. Clark, P. J. Goldschmidt-Clermont, and N. A. Flavahan. 2001. 'Redox regulation of vascular smooth muscle cell differentiation', *Circ Res*, 89: 39-46.

Sun, H., Y. Yuan, P. Wang, R. Cai, W. Xia, R. Huang, and S. Wang. 2015. 'Intensified low-density lipoprotein-cholesterol target of statin therapy and cancer risk: a meta-analysis', *Lipids Health Dis*, 14: 140.

Sun, W., T. S. Lee, M. Zhu, C. Gu, Y. Wang, Y. Zhu, and J. Y. Shyy. 2006. 'Statins activate AMP-activated protein kinase in vitro and in vivo', *Circulation*, 114: 2655-62.

Sun, Y. V., S. M. Damrauer, Q. Hui, T. L. Assimes, Y. L. Ho, P. Natarajan, D. Klarin, J. Huang, J. Lynch, S. L. DuVall, S. Pyarajan, J. P. Honerlaw, J. M. Gaziano, K. Cho, D. J. Rader, C. J. O'Donnell, P. S. Tsao, and P. W. F. Wilson. 2018. 'Effects of Genetic Variants Associated with Familial Hypercholesterolemia on Low-Density Lipoprotein-Cholesterol Levels and Cardiovascular Outcomes in the Million Veteran Program', *Circ Genom Precis Med*, 11.

Sung, J. Y., and H. C. Choi. 2012. 'Nifedipine inhibits vascular smooth muscle cell proliferation and reactive oxygen species production through AMP-activated protein kinase signaling pathway', *Vascul Pharmacol*, 56: 1-8.

Suter, M., U. Riek, R. Tuerk, U. Schlattner, T. Wallimann, and D. Neumann. 2006. 'Dissecting the role of 5'-AMP for allosteric stimulation, activation, and deactivation of AMP-activated protein kinase', *J Biol Chem*, 281: 32207-16.

Swärd, Karl, Karl Dreja, Anders Lindqvist, Erik Persson, and Per Hellstrand. 2002. 'Influence of Mitochondrial Inhibition on Global and Local [Ca 2+] in Rat Tail Artery', *Circulation Research*, 90: 792-99.

Szabo, C., C. Ransy, K. Modis, M. Andriamihaja, B. Murghes, C. Coletta, G. Olah, K. Yanagi, and F. Bouillaud. 2014. 'Regulation of mitochondrial bioenergetic function by hydrogen sulfide. Part I. Biochemical and physiological mechanisms', *Br J Pharmacol*, 171: 2099-122.

Szabo, C., C. Ransy, K. Módis, M. Andriamihaja, B. Murghes, C. Coletta, G. Olah, K. Yanagi, and F. Bouillaud. 2014. 'Regulation of mitochondrial bioenergetic function by hydrogen sulfide. Part I. Biochemical and physiological mechanisms', *Br J Pharmacol*, 171: 2099-122.

Szendroedi, Julia, Albrecht I. Schmid, Marek Chmelik, Christian Toth, Attila Brehm, Martin Krssak, Peter Nowotny, Michael Wolzt, Werner Waldhausl, and Michael Roden. 2007. 'Muscle Mitochondrial ATP Synthesis and Glucose Transport/Phosphorylation in Type 2 Diabetes', *PLoS Med*, 4: e154.

Tai, I. C., Y. H. Wang, C. H. Chen, S. C. Chuang, J. K. Chang, and M. L. Ho. 2015. 'Simvastatin enhances Rho/actin/cell rigidity pathway contributing to mesenchymal stem cells' osteogenic differentiation', *Int J Nanomedicine*, 10: 5881-94.

Takai, Y., T. Sasaki, and T. Matozaki. 2001. 'Small GTP-binding proteins', *Physiol Rev*, 81: 153-208.

Takemoto, M., K. Node, H. Nakagami, Y. Liao, M. Grimm, Y. Takemoto, M. Kitakaze, and J. K. Liao. 2001. 'Statins as antioxidant therapy for preventing cardiac myocyte hypertrophy', *J Clin Invest*, 108: 1429-37.

Takemoto, M., J. Sun, J. Hiroki, H. Shimokawa, and J. K. Liao. 2002. 'Rho-kinase mediates hypoxia-induced downregulation of endothelial nitric oxide synthase', *Circulation*, 106: 57-62.

Tasaki, K., M. Hori, H. Ozaki, H. Karaki, and I. Wakabayashi. 2003. 'Difference in signal transduction mechanisms involved in 5-hydroxytryptamine- and U46619-induced vasoconstrictions', *J Smooth Muscle Res*, 39: 107-17.

Taverne, Y. J., A. J. Bogers, D. J. Duncker, and D. Merkus. 2013. 'Reactive oxygen species and the cardiovascular system', *Oxid Med Cell Longev*, 2013: 862423.

Tavintharan, S., C. N. Ong, K. Jeyaseelan, M. Sivakumar, S. C. Lim, and C. F. Sum. 2007a. 'Reduced mitochondrial coenzyme Q10 levels in HepG2 cells treated with high-dose simvastatin: a possible role in statin-induced hepatotoxicity?', *Toxicol Appl Pharmacol*, 223: 173-9.

———. 2007b. 'Reduced mitochondrial coenzyme Q10 levels in HepG2 cells treated with high-dose simvastatin: A possible role in statin-induced hepatotoxicity?', *Toxicol Appl Pharmacol*, 223: 173-79.
Taylor, F., M. D. Huffman, A. F. Macedo, T. H. Moore, M. Burke, G. Davey Smith, K. Ward, and S. Ebrahim. 2013. 'Statins for the primary prevention of cardiovascular disease', *Cochrane Database Syst Rev*: Cd004816.
Terada, H. 1990. 'Uncouplers of oxidative phosphorylation', *Environ Health Perspect*, 87: 213-8.
Tesfamariam, B., B. H. Frohlich, and R. E. Gregg. 1999. 'Differential effects of pravastatin, simvastatin, and atorvastatin on Ca2+ release and vascular reactivity', *J Cardiovasc Pharmacol*, 34: 95-101.
Thengchaisri, N., and L. Kuo. 2003. 'Hydrogen peroxide induces endothelium-dependent and -independent coronary arteriolar dilation: role of cyclooxygenase and potassium channels', *Am J Physiol Heart Circ Physiol*, 285: H2255-63.
To, M. S., E. C. Aromataris, J. Castro, M. L. Roberts, G. J. Barritt, and G. Y. Rychkov. 2010. 'Mitochondrial uncoupler FCCP activates proton conductance but does not block store-operated Ca(2+) current in liver cells', *Arch Biochem Biophys*, 495: 152-8.
Touchberry, C. D., N. Silswal, V. Tchikrizov, C. J. Elmore, S. Srinivas, A. S. Akthar, H. K. Swan, L. A. Wetmore, and M. J. Wacker. 2014. 'Cardiac thromboxane A2 receptor activation does not directly induce cardiomyocyte hypertrophy but does cause cell death that is prevented with gentamicin and 2-APB', *BMC Pharmacol Toxicol*, 15: 73.
Turrens, J. F. 1997. 'Superoxide production by the mitochondrial respiratory chain', *Biosci Rep*, 17: 3-8.
———. 2003. 'Mitochondrial formation of reactive oxygen species', *J Physiol*, 552: 335-44.
Turrens, J. F., and A. Boveris. 1980. 'Generation of superoxide anion by the NADH dehydrogenase of bovine heart mitochondria', *Biochem J*, 191: 421-7.
Uehata, M., T. Ishizaki, H. Satoh, T. Ono, T. Kawahara, T. Morishita, H. Tamakawa, K. Yamagami, J. Inui, M. Maekawa, and S. Narumiya. 1997. 'Calcium sensitization of smooth muscle mediated by a Rho-associated protein kinase in hypertension', *Nature*, 389: 990-4.
Vafai, Scott B., and Vamsi K. Mootha. 2012. 'Mitochondrial disorders as windows into an ancient organelle', *Nature*, 491: 374.
Vaishnavi, S. N., A. G. Vlassenko, M. M. Rundle, A. Z. Snyder, M. A. Mintun, and M. E. Raichle. 2010. 'Regional aerobic glycolysis in the human brain', *Proc Natl Acad Sci U S A*, 107: 17757-62.
Van Aelst, L., and C. D'Souza-Schorey. 1997. 'Rho GTPases and signaling networks', *Genes Dev*, 11: 2295-322.
Van Hemelrijck, M., Y. Folkvaljon, J. Adolfsson, O. Akre, L. Holmberg, H. Garmo, and P. Stattin. 2016. 'Causes of death in men with localized prostate cancer: a nationwide, population-based study', *BJU Int*, 117: 507-14.
VanBavel, E., E. T. van der Meulen, and J. A. Spaan. 2001. 'Role of Rho-associated protein kinase in tone and calcium sensitivity of cannulated rat mesenteric small arteries', *Exp Physiol*, 86: 585-92.
Vandiver, M., and S. H. Snyder. 2012. 'Hydrogen sulfide: a gasotransmitter of clinical relevance', *J Mol Med (Berl)*, 90: 255-63.
Velho, J. A., H. Okanobo, G. R. Degasperi, M. Y. Matsumoto, L. C. Alberici, R. G. Cosso, H. C. Oliveira, and A. E. Vercesi. 2006. 'Statins induce calcium-dependent mitochondrial permeability transition', *Toxicology*, 219: 124-32.
Villalba, N., E. Stankevicius, U. Simonsen, and D. Prieto. 2008. 'Rho kinase is involved in Ca2+ entry of rat penile small arteries', *Am J Physiol Heart Circ Physiol*, 294: H1923-32.
Volkel, S., and M. K. Grieshaber. 1996. 'Mitochondrial sulfide oxidation in Arenicola marina. Evidence for alternative electron pathways', *Eur J Biochem*, 235: 231-7.

Vosper, J., A. Masuccio, M. Kullmann, C. Ploner, S. Geley, and L. Hengst. 2015. 'Statin-induced depletion of geranylgeranyl pyrophosphate inhibits cell proliferation by a novel pathway of Skp2 degradation', *Oncotarget*, 6: 2889-902.

Vrancken Peeters, M. P., A. C. Gittenberger-de Groot, M. M. Mentink, and R. E. Poelmann. 1999. 'Smooth muscle cells and fibroblasts of the coronary arteries derive from epithelial-mesenchymal transformation of the epicardium', *Anat Embryol (Berl)*, 199: 367-78.

Wall, J. A., J. Wei, M. Ly, P. Belmont, J. J. Martindale, D. Tran, J. Sun, W. J. Chen, W. Yu, P. Oeller, S. Briggs, A. B. Gustafsson, M. R. Sayen, R. A. Gottlieb, and C. C. Glembotski. 2006. 'Alterations in oxidative phosphorylation complex proteins in the hearts of transgenic mice that overexpress the p38 MAP kinase activator, MAP kinase kinase 6', *Am J Physiol Heart Circ Physiol*, 291: H2462-72.

Wang, Q. S., Y. M. Zheng, L. Dong, Y. S. Ho, Z. Guo, and Y. X. Wang. 2007. 'Role of mitochondrial reactive oxygen species in hypoxia-dependent increase in intracellular calcium in pulmonary artery myocytes', *Free Radic Biol Med*, 42: 642-53.

Wang, S., B. Liang, B. Viollet, and M. H. Zou. 2011. 'Inhibition of the AMP-activated protein kinase-alpha2 accentuates agonist-induced vascular smooth muscle contraction and high blood pressure in mice', *Hypertension*, 57: 1010-7.

Wang, Y., D. Oxer, and S. Hekimi. 2015. 'Mitochondrial function and lifespan of mice with controlled ubiquinone biosynthesis', *Nat Commun*, 6: 6393.

Waypa, G. B., R. Guzy, P. T. Mungai, M. M. Mack, J. D. Marks, M. W. Roe, and P. T. Schumacker. 2006. 'Increases in mitochondrial reactive oxygen species trigger hypoxia-induced calcium responses in pulmonary artery smooth muscle cells', *Circ Res*, 99: 970-8.

Waypa, G. B., J. D. Marks, M. M. Mack, C. Boriboun, P. T. Mungai, and P. T. Schumacker. 2002. 'Mitochondrial reactive oxygen species trigger calcium increases during hypoxia in pulmonary arterial myocytes', *Circ Res*, 91: 719-26.

Werner, M., J. Sacher, and M. Hohenegger. 2004. 'Mutual amplification of apoptosis by statin-induced mitochondrial stress and doxorubicin toxicity in human rhabdomyosarcoma cells', *Br J Pharmacol*, 143: 715-24.

Whelchel, A., J. Evans, and J. Posada. 1997. 'Inhibition of ERK activation attenuates endothelin-stimulated airway smooth muscle cell proliferation', *Am J Respir Cell Mol Biol*, 16: 589-96.

White, R. E., J. P. Kryman, A. M. El-Mowafy, G. Han, and G. O. Carrier. 2000. 'cAMP-dependent vasodilators cross-activate the cGMP-dependent protein kinase to stimulate BK(Ca) channel activity in coronary artery smooth muscle cells', *Circ Res*, 86: 897-905.

Whiteman, M., S. Le Trionnaire, M. Chopra, B. Fox, and J. Whatmore. 2011. 'Emerging role of hydrogen sulfide in health and disease: critical appraisal of biomarkers and pharmacological tools', *Clin Sci (Lond)*, 121: 459-88.

Wilden, P. A., Y. M. Agazie, R. Kaufman, and S. P. Halenda. 1998. 'ATP-stimulated smooth muscle cell proliferation requires independent ERK and PI3K signaling pathways', *Am J Physiol*, 275: H1209-15.

Will, M., A. C. Qin, W. Toy, Z. Yao, V. Rodrik-Outmezguine, C. Schneider, X. Huang, P. Monian, X. Jiang, E. de Stanchina, J. Baselga, N. Liu, S. Chandarlapaty, and N. Rosen. 2014. 'Rapid induction of apoptosis by PI3K inhibitors is dependent upon their transient inhibition of RAS-ERK signaling', *Cancer Discov*, 4: 334-47.

Williams, George S. B., Liron Boyman, Aristide C. Chikando, Ramzi J. Khairallah, and W. J. Lederer. 2013. 'Mitochondrial calcium uptake', *Proceedings of the National Academy of Sciences*, 110: 10479-86.

Wu, P. Y., B. Lai, Y. Dong, Z. M. Wang, Z. C. Li, and P. Zheng. 2010. 'Different oxidants and PKC isozymes mediate the opposite effect of inhibition of Q(i) and Q(o) site of mitochondrial complex III on calcium currents in rat cortical neurons', *Biochim Biophys Acta*, 1803: 1072-82.

Xi, Q., S. Y. Cheranov, and J. H. Jaggar. 2005. 'Mitochondria-derived reactive oxygen species dilate cerebral arteries by activating Ca2+ sparks', *Circ Res*, 97: 354-62.

Xia, D., L. Esser, W. K. Tang, F. Zhou, Y. Zhou, L. Yu, and C. A. Yu. 2013. 'Structural analysis of cytochrome bc1 complexes: implications to the mechanism of function', *Biochim Biophys Acta*, 1827: 1278-94.

Xiao, D., W. J. Pearce, L. D. Longo, and L. Zhang. 2004. 'ERK-mediated uterine artery contraction: role of thick and thin filament regulatory pathways', *Am J Physiol Heart Circ Physiol*, 286: H1615-22.

Xu, Z., J. Sun, Q. Tong, Q. Lin, L. Qian, Y. Park, and Y. Zheng. 2016. 'The Role of ERK1/2 in the Development of Diabetic Cardiomyopathy', *Int J Mol Sci*, 17.

Yada, T., M. Nakata, T. Shiraishi, and M. Kakei. 1999. 'Inhibition by simvastatin, but not pravastatin, of glucose-induced cytosolic Ca2+ signalling and insulin secretion due to blockade of L-type Ca2+ channels in rat islet beta-cells', *Br J Pharmacol*, 126: 1205-13.

Yadav, V. R., T. Song, L. Joseph, L. Mei, Y. M. Zheng, and Y. X. Wang. 2013. 'Important role of PLC-gamma1 in hypoxic increase in intracellular calcium in pulmonary arterial smooth muscle cells', *Am J Physiol Lung Cell Mol Physiol*, 304: L143-51.

Yong, R., and D. G. Searcy. 2001. 'Sulfide oxidation coupled to ATP synthesis in chicken liver mitochondria', *Comp Biochem Physiol B Biochem Mol Biol*, 129: 129-37.

Young, T. A., C. C. Cunningham, and S. M. Bailey. 2002. 'Reactive oxygen species production by the mitochondrial respiratory chain in isolated rat hepatocytes and liver mitochondria: studies using myxothiazol', *Arch Biochem Biophys*, 405: 65-72.

Yu, K. C., and A. D. Cooper. 2001. 'Postprandial lipoproteins and atherosclerosis', *Front Biosci*, 6: D332-54.

Zalewski, A., Y. Shi, and A. G. Johnson. 2002. 'Diverse origin of intimal cells: smooth muscle cells, myofibroblasts, fibroblasts, and beyond?', *Circ Res*, 91: 652-5.

Zarate, A., L. Manuel-Apolinar, L. Basurto, E. De la Chesnaye, and I. Saldivar. 2016. '[Cholesterol and atherosclerosis. Historical considerations and treatment]', *Arch Cardiol Mex*, 86: 163-9.

Zhang, D. X., and D. D. Gutterman. 2007. 'Mitochondrial reactive oxygen species-mediated signaling in endothelial cells', *Am J Physiol Heart Circ Physiol*, 292: H2023-31.

Zhang, H., B. Weir, L. S. Marton, R. L. Macdonald, V. Bindokas, R. J. Miller, and J. R. Brorson. 1995. 'Mechanisms of hemolysate-induced [Ca2+]i elevation in cerebral smooth muscle cells', *Am J Physiol*, 269: H1874-90.

Zhang, M., Y. Dong, J. Xu, Z. Xie, Y. Wu, P. Song, M. Guzman, J. Wu, and M. H. Zou. 2008. 'Thromboxane receptor activates the AMP-activated protein kinase in vascular smooth muscle cells via hydrogen peroxide', *Circ Res*, 102: 328-37.

Zhang, W., J. Wu, L. Zhou, H. Y. Xie, and S. S. Zheng. 2010. 'Fluvastatin, a lipophilic statin, induces apoptosis in human hepatocellular carcinoma cells through mitochondria-operated pathway', *Indian J Exp Biol*, 48: 1167-74.

Zhou, W., K. H. Chen, W. Cao, J. Zeng, H. Liao, L. Zhao, and X. Guo. 2010. 'Mutation of the protein kinase A phosphorylation site influences the anti-proliferative activity of mitofusin 2', *Atherosclerosis*, 211: 216-23.

Zorov, D. B., M. Juhaszova, and S. J. Sollott. 2014. 'Mitochondrial reactive oxygen species (ROS) and ROS-induced ROS release', *Physiol Rev*, 94: 909-50.

Zou, M. H., S. S. Kirkpatrick, B. J. Davis, J. S. Nelson, W. G. th Wiles, U. Schlattner, D. Neumann, M. Brownlee, M. B. Freeman, and M. H. Goldman. 2004. 'Activation of the AMP-activated protein kinase by the anti-diabetic drug metformin in vivo. Role of mitochondrial reactive nitrogen species', *J Biol Chem*, 279: 43940-51.

Zsurka, Gábor, and Wolfram S. Kunz. 2010. 'Mitochondrial dysfunction in neurological disorders with epileptic phenotypes', *J Bioenerg Biomembr*, 42: 443-48.